Radiothérapie adaptative morphologique et métabolique des cancers ORL

Joël Castelli

THÈSE / UNIVERSITÉ DE RENNES 1
sous le sceau de l'Université Bretagne Loire

pour le grade de

DOCTEUR DE L'UNIVERSITÉ DE RENNES 1

Mention : Biologie et sciences de la santé

Ecole doctorale Biologie Santé

présentée par

Joël Castelli

Préparée à l'unité de recherche LTSI-INSERM, U1099
Laboratoire Traitement du Signal et de l'Image
ISTIC UFR Informatique et Électronique

Intitulé de la thèse : Radiothérapie adaptative morphologique et métabolique des cancers ORL

Thèse soutenue à Rennes le 11 décembre 2017

devant le jury composé de :

Juliette THARIAT
PU-PH Centre François Baclesse / *rapporteur*

Nicolas BOUSSION
Physicien médical CHU Brest / *rapporteur*

Jean BOURHIS
PU-PH CHUV Lausanne / *examinateur*

Adrien DEPEURSINGE
PU HES-SO/EPFL / *examinateur*

Robin GARCIA
Physicien médical Institut Sainte Catherine / *examinateur*

Caroline LAFOND
Physicien médical INSERM U1099 / *co-directeur de thèse*

Antoine SIMON
MCU Université de Rennes 1 / *co-directeur de thèse*

Renaud DE CREVOISIER
PU-PH Centre Eugene Marquis / *directeur de thèse*

Remerciements

A Monsieur le Professeur Renaud de Crevoisier

Je vous remercie d'avoir accepté de diriger ce travail. Votre niveau d'exigence vis-à-vis de vous-même, votre disponibilité et vos valeurs humaines sont un modèle pour moi. J'espère que la suite de ma carrière fera honneur à la confiance que vous m'avez accordée.

A Madame la Docteur Caroline Lafond

Je te suis reconnaissant d'avoir accepté d'encadrer ce travail. Tes conseils et remarques au cours de cette thèse ont permis d'améliorer sa qualité. C'est un plaisir de travailler au quotidien avec toi, autant sur le versant clinique que scientifique.

A Monsieur le Docteur Antoine Simon

Je te remercie pour ton encadrement, tes conseils et ta bienveillance, non seulement au cours de ce travail de thèse mais aussi depuis le début de mon parcours scientifique. J'espère pouvoir continuer à bénéficier de ton expérience pour la suite de mes travaux.

A Madame la Professeur Juliette Thariat

J'ai eu le plaisir de te rencontrer lors de mon internat à Nice. Déjà à l'époque, j'avais été impressionné par ton niveau de production scientifique, et c'est en toute logique que tu as été nommée PU-PH à Caen. Je te remercie de l'honneur que tu me fais en acceptant de juger ce travail.

A Monsieur le Docteur Nicolas Boussion

Vous me faites l'honneur d'accepter de juger cette thèse, et je vous en remercie. Votre connaissance des problématiques en radiothérapie et votre expertise en TEP justifie pleinement votre place dans ce jury.

A Monsieur le Professeur Jean Bourhis

Mon année de mobilité à vos côtés à Lausanne a été une expérience enrichissante. J'ai pu profiter de votre « instinct » concernant les voies de recherches prometteuses, tout en bénéficiant de votre grande expérience en radiothérapie ORL. Je suis ravi d'avoir des projets avec vous au travers du GORTEC, et j'espère pouvoir continuer à bénéficier de vos précieux conseils.

A Monsieur le Professeur Adrien Depeursinge

Ce fut un vrai plaisir de travailler avec toi durant cette année en Suisse. Tu as su me faire profiter de ton expérience, de tes connaissances, avec patience et pédagogie. Je te remercie de participer à ce jury de thèse et j'espère que nous aurons l'occasion de poursuivre notre collaboration.

A Monsieur le Docteur Robin Garcia

Vous avez réactivé avec succès le groupe physique médical au sein du GORTEC, contribuant ainsi à la dynamique indispensable de notre groupe. Une de vos premières actions a été d'initier une évaluation de la radiothérapie adaptative et des outils qui s'y rapportent. Votre présence au sein de ce jury était donc une évidence pour moi, et je vous remercie d'avoir accepté de juger mon travail.

A Madame la Docteur Elisabeth le Prisé

Je vous remercie pour votre soutien depuis mon arrivée à Rennes. Vos connaissances en radiothérapie, votre dynamisme et votre motivation au quotidien m'impressionnent toujours autant. J'espère être digne de votre département de radiothérapie.

Aux membres du laboratoire du traitement du signal et de l'image

Je tiens à remercie Monsieur Lotfi Senhadji de m'avoir accueilli au sein de son unité de recherche.

Je remercie également Oscar Acosta pour sa présence et ses conseils.

Je remercie Bastien Rigaud pour tous nos échanges, et pour son aide tout au long de cette thèse.

Enfin, je souhaite exprimer à l'ensemble des membres du LTSI ma profonde reconnaissance pour l'accueil et le temps qu'ils m'ont accordé.

Aux membres du Centre Eugene Marquis, du Centre Hospitalier Universitaire Vaudois et du service d'ORL du CHU de Rennes

A travers votre implication dans la prise en charge des patients inclus dans les protocoles de recherche, vous avez contribué à la réalisation de ce travail et je vous en remercie.

A ma famille

A mes parents, qui m'ont toujours soutenu et qui sont mes modèles. Merci pour tout.
A Cécilia, ma sœur, désormais aussi dans le soin mais aussi avec talent dans l'écriture.
A mes grands-parents, qui m'ont tant apporté.
A ma fille, Anaïs, merci pour le bonheur que tu m'apportes depuis bientôt 9 ans.
A ma femme, Marjory, merci pour ton amour. Tu me donnes la force d'avancer au quotidien. Ce travail est aussi le tien car il n'aurait pas été possible sans ton soutien.

Liste des abréviations

AJCC :	*American Joint Committee on Cancer*
CBCT :	*Cone-Beam Computed Tomography*
CT :	*Computed Tomography*
CTV :	*Clinical Target Volume*
GORTEC :	Groupe d'oncologie radiothérapie tête et cou
GTV :	*Gross Tumor Volume*
Gy :	Gray
MTV :	*Metabolic tumor volume*
MVCT :	*Mega Voltage Computed Tomography*
ORL :	Oto-rhino-laryngologie
PTV :	*Planning Target Volume*
RCMI :	Radiothérapie conformationnelle par modulation d'intensité
SUV :	*Standard uptake value*
TEP :	Tomographie par émission de positons
UH :	Unité Hounsfield
VADS :	Voies aéro-digestives supérieures

Table des matières

Tables des figures (hors articles)

Table des tableaux (hors articles)

Introduction

Le traitement des cancers des voies aéro-digestives supérieures (VADS) repose sur une approche multidisciplinaire, combinant la chirurgie, la radiothérapie et la chimiothérapie. La radiothérapie se fonde sur l'utilisation de rayonnements ionisants dont l'objectif est de provoquer la mort des cellules tumorales. La planification du traitement de radiothérapie est réalisée à partir d'un scanner réalisé avant le début de traitement. Le radiothérapeute va délinéer sur ce scanner les volumes cibles (tumeur primitive et ganglions) ainsi que les organes sains à protéger. Après la mise en place des faisceaux de traitement, le calcul de la dose est réalisé en utilisant l'information de densité électronique fournie par le scanner. La difficulté de cette étape de dosimétrie est d'atteindre une dose élevée dans la tumeur pour essayer d'obtenir la guérison du patient, tout en limitant la dose dans les tissus sains, pour limiter la toxicité, en particulier pour les parotides. En effet, le principal effet secondaire de la radiothérapie est la xérostomie (entrainant des difficultés de parole, d'alimentation et des troubles dentaires), liée à l'irradiation des parotides. Les techniques récentes de radiothérapie telle que la modulation d'intensité ont permis d'augmenter la conformation de la dose, limitant de ce fait la toxicité. Ces techniques ont permis d'atteindre un taux de contrôle loco-régional à 2 ans d'environ 80% et un taux de xérostomie à 1 an d'environ 40% [1-5]. Cependant une faiblesse de la radiothérapie est liée au fait que tout le traitement (durant 7 semaines) repose sur une planification unique, ne prenant pas en compte les modifications anatomiques qui peuvent survenir pendant le traitement, par exemple liées à un amaigrissement du patient. Du fait de ces modifications anatomiques, la dose délivrée peut ne pas correspondre à la dose planifiée, avec un risque de surdosage des tissus sains (risque majoré de toxicité) et/ou de sous dosage de la tumeur (risque de récidive). La réalisation d'un nouveau plan de traitement devient alors nécessaire afin de corriger ces variations anatomiques. Ce processus de replanification en cours de traitement est appelé radiothérapie adaptative. Il s'agit d'une approche récente, qui suscite de nombreuses interrogations, notamment au regard de la charge de travail représentée par chaque replanification. Ainsi l'objectif de la radiothérapie adaptative est-il de diminuer la toxicité, d'augmenter le contrôle local ou les deux à la fois ? Est-ce que tous les patients ont besoin d'une approche de radiothérapie adaptative ? Les

replanifications doivent elle être réalisées selon un schéma pré déterminé ou bien guidées par des paramètres anatomiques et/ou dosimétriques ? A quelle fréquence et quand faut-il replanifier ? Faut-il replanifier *de novo* ou bien en prenant en considération la dose précédemment délivrée ? Et enfin, est ce que le bénéfice individuel pour le patient contrebalance l'investissement humain et économique nécessaire à sa mise place. Son évaluation pose le problème de l'estimation de la dose reçue séance après séance dans des structures déformables, spécialement pour les cancers des VADS. Cette estimation de la dose cumulée fait appel à des méthodes de recalage élastique, ce qui pose le problème de leur évaluation, en particulier pour ce qui concerne leur précision.

La mise en œuvre dans une pratique clinique quotidienne d'une radiothérapie adaptative nécessitera donc plusieurs étapes. La première est d'estimer son bénéfice, à la fois en termes de diminution de la dose aux organes sains (dans un objectif de diminution de la toxicité) et de couverture du volume tumoral (dans un objectif de contrôle local). Ensuite le développement d'outils d'identification des patients bons candidats permettra de limiter cette approche aux patients pouvant en tirer un réel bénéfice. Enfin, l'identification du schéma optimal en termes de nombre et de fréquence de replanification permettra d'obtenir le maximum de bénéfice de la technique tout en évitant une charge de travail inutile.

La première partie de ce manuscrit décrit le contexte et la problématique médico-scientifique de la radiothérapie adaptative en ORL, et est suivie des objectifs de cette thèse. Les travaux menés sont ensuite décrits, tout d'abord dans un objectif d'épargne des glandes parotides pour réduire la xérostomie, puis pour l'amélioration de la couverture du volume cible.

Les résultats de cette thèse apparaissent sous forme de différents articles écrits en anglais, introduits et conclus en français. Ce document se termine par une synthèse et une conclusion en français.

1 Contexte et problématique médico-scientifique

Après une brève description des cancers des voies aéro-digestives supérieures (VADS), les principes de la radiothérapie et ses récentes évolutions seront détaillées. Les limites de la radiothérapie pour prendre en compte les variations anatomiques seront exposées, limites justifiant d'une radiothérapie adaptative dont les principes seront abordés. Enfin la place prépondérante de l'imagerie dans la radiothérapie adaptative sera détaillée.

1.1 Cancers des voies aéro-digestives supérieures

1.1.1 Epidémiologie

Les cancers des voies aéro-digestives supérieures (VADS), également appelés cancers de la sphère Oto-rhino-laryngologique (ORL) représentent le 5^{éme} cancer en termes d'incidence au niveau mondial [6]. Il existe un lien majeur entre l'apparition de ces cancers et le mode de vie, les ¾ des cas étant liés au tabac et à l'alcool [7]. Les autres facteurs de risque sont l'exposition aux radiations ou à des agents chimiques carcinogènes, et à certains virus (virus d'Eptsein Barr, papillomavirus humain) [8]. L'âge moyen de survenue est d'environ 60-65 ans avec une incidence plus élevée chez l'homme (10 hommes pour 1 femme) [9].

1.1.2 Classification

L'anatomie des VADS est complexe et peut être divisée en plusieurs sous localisations que sont la cavité buccale, le nasopharynx, l'oropharynx, l'hypopharynx et le larynx (Figure 1). Cette distinction anatomique est importante à la fois en termes de pronostic et de thérapeutique.

Le drainage lymphatique au niveau des VADS est très important, expliquant qu'environ 50% des patients ont une atteinte ganglionnaire lors du diagnostic [10]. L'extension des cancers des VADS s'évalue en fonction du stade TNM (*Tumor Node Metastasis*) de l'*American Joint Committee on Cancer* (AJCC):

- Le stade T (*tumor*, de 0 à 4) correspond à la taille et à l'extension de la tumeur primitive,

- Le stade N (*node*, de 0 à 3) décrit l'extension ganglionnaire régionale,

- Le stade M (*metastasis*, 0 ou 1) correspond à la présence ou non de métastases à distance.

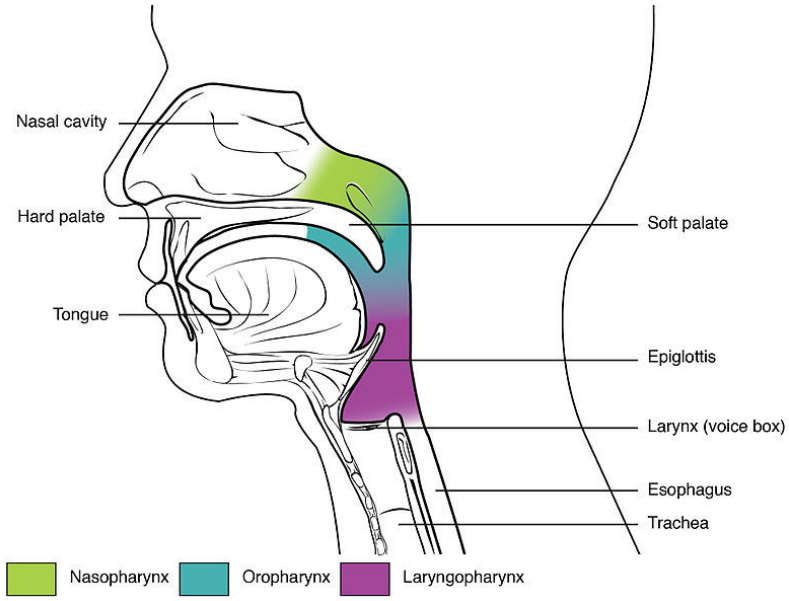

Figure 1 : Anatomie des voies aéro-digestives supérieures

La classification en stade des cancers de VADS est illustrée

Table 1.

Table 1 : Regroupement en stade des cancers des VADS [11].

	T stage	N Stage	M Stage	Historic 5-year survival[a]	Treatment goal	
Stage 0	Tis	N0	M0	N/A	Curative	
Stage I	T1	N0	M0	56–68.1%	Curative	30–40% of cases
Stage II	T2	N0	M0	45.4–52.9%	Curative	
Stage III[b]	T3	N0	M0	36.3–56.3%	Curative	
	T1-3	N1	M0		Curative	
Stage IV A	T4a	N0 or N1	M0	26.5–38.9%	Curative	>50% of cases
	T1-4a	N2	M0		Curative	
Stage IV B	T4b	Any N	M0		Curative	
	Any T	N3	M0		Curative	
Stage IV C	Any T	Any N	M1		Palliative	10% of cases

1.1.3 Principes thérapeutiques

Le traitement des cancers localement avancés des VADS repose sur une approche pluridisciplinaire, impliquant les chirurgiens, les oncologues radiothérapeutes et les oncologues médicaux. Pour les tumeurs non accessibles à une chirurgie, le traitement consiste en une association d'une radiothérapie avec un traitement médical (chimiothérapie à base de sels de platine ou thérapie ciblée (cetuximab) [12-14]). La radiothérapie est une méthode de traitement locorégional des cancers, utilisant des rayonnements ionisants pour détruire les cellules tumorales. L'unité de dose utilisé est le Gray (Gy), 1 Gy correspondant à un dépôt d'énergie de 1 Joule dans 1 Kg de matière. L'irradiation peut entrainer indirectement des lésions de l'ADN, par radiolyse de l'eau contenue dans la cellule, radiolyse produisant ensuite des radicaux libres hautement toxiques pour la cellule. Un effet direct du rayonnement, moins fréquent, sur l'ADN de la cellule est également possible. Ces effets directs ou indirects vont produire des lésions de l'ADN, qui, si elles sont sévères ou si elles dépassent les capacités de réparation de la cellule, vont conduire à la mort cellulaire. Les rayonnements produisent donc un effet biologique aussi bien sur la tumeur que le tissu sain. Cependant la capacité de réparation des tissus sains est supérieure à celle de la tumeur. Cet effet différentiel entre le tissu sain et la tumeur permet de limiter la toxicité en fractionnant la dose de rayonnement sur plusieurs jours. Ainsi, pour les cancers des VADS localement avancés, la dose classique de traitement est de 66 à 74 Gy, délivrée à raison de 1,8 à 2,2 Gy par jour, 5 jours par semaine pendant 5 à 7 semaines. L'objectif de la radiothérapie est donc de délivrer la dose la plus élevée dans le volume cible (tumeur primitive et adénopathies) afin de guérir le patient, tout en évitant autant que possible d'irradier les tissus sains, qui peuvent être très proche de la tumeur. La chimiothérapie est combinée avec la radiothérapie afin d'essayer d'augmenter le taux de contrôle local et la survie de ces patients. Le bénéfice en terme de survie globale de l'ajout d'une chimiothérapie à base de sels de platine a été estimée à 6% à 5 ans dans une méta-analyse [15]. Le taux de rechute locale, qui conditionne en grande partie le pronostic de ces patients, est élevé, de l'ordre de 20 à 40 % à 2 ans [1-5]. Les effets secondaires de la radiothérapie vont dépendre du niveau d'irradiation des organes à risque. Il peut s'agir d'effets secondaires aigus, survenant dans les 3 mois post traitement ou de toxicités tardives, qui vont persister plusieurs mois ou années après la fin du traitement. Une des principales toxicités

de la radiothérapie est représentée par la xérostomie (sensation de bouche sèche liée à une diminution du flux salivaire), qui va entrainer des complications au niveau alimentaire, de la parole et dentaire. La xérostomie est causée par une irradiation des glandes salivaires, parotides et sous maxillaires, notamment. Les parotides ont un rôle crucial, contribuant à la majorité de la sécrétion salivaire alors que les glandes sous maxillaires ont un rôle plus marginal [16]. L'irradiation des deux parotides à une dose supérieure à 40 Gy entraine ainsi une perte définitive de la fonction salivaire [17]. Au cours d'une radiothérapie pour un cancer ORL, il existe donc un double défi thérapeutique et technologique portant sur la guérison et de qualité de vie, tenant à l'optimisation du ciblage de la radiothérapie. Les grandes évolutions techniques de la radiothérapie réalisées au cours des dernières années ont cherché à répondre à cette problématique, afin d'améliorer encore l'efficacité et la tolérance de la radiothérapie.

1.2 Radiothérapie des cancers ORL

Au cours de la radiothérapie, le patient est allongé sur la table de la machine de traitement qui va délivrer le faisceau d'irradiation (Figure 2).

Figure 2 : Patient installé sur la table de traitement, sous l'accélérateur linéaire de particules.

Afin d'assurer l'efficacité du traitement, il est nécessaire que chaque séance de traitement se déroule dans les mêmes conditions que celle prévue lors de la planification du traitement. Plusieurs avancées technologiques ont été réalisées afin de répondre à cet objectif de ciblage de

la dose, que ce soit au niveau de la balistique de la dose ou des dispositifs d'imagerie permettant le positionnement du patient.

1.2.1 De la radiothérapie "2D" conventionnelle à la radiothérapie 3D avec modulation d'intensité (RCMI)

Historiquement (avant les années 2000), des clichés radiographiques standards étaient utilisés pour déterminer les volumes de traitement. Au cours de cette radiothérapie 2D conventionnelle, la mise en place des faisceaux de traitement était assez simple, les plans de traitement consistant le plus souvent en 2 faisceaux latéraux opposés ou 4 faisceaux en « boîte ». En raison de la grande incertitude sur la position réelle de la tumeur, cette technique impliquait un large champ d'irradiation, entrainant de ce fait une importante irradiation du tissu sain.

L'intégration de la tomodensitométrie (ou scanner) dans les années 1990-2000 à l'étape de la planification correspond au développement de la radiothérapie 3D. Cette technique représente une avancée majeure de la radiothérapie, permettant de prendre en compte l'anatomie en coupe axiale, et de réaliser la délinéation de volumes complexes (tumeur ou organes sains) en 3D de façon précise. L'intégration des collimateurs multi lames dans les accélérateurs de particules (Multi leaf collimator (MLC)) (Figure 3) a permis d'adapter le faisceau de traitement à la forme de la cible de traitement.

Figure 3 : Un collimateur multi-lames, utilisé pour conformer la forme du faisceau au volume de traitement

La modulation d'intensité (RCMI), développée dans les années 2000 représente la dernière génération de radiothérapie conformationnelle 3D. Cette technique présente deux avantages majeurs par rapport à la radiothérapie 3D standard :

- Un profil d'intensité du faisceau modulé (Figure 4). La RCMI permet de moduler à la fois le nombre de champs et l'intensité de l'irradiation dans chaque champ. Cette modulation permet d'obtenir une infinité de distributions de doses, capables de s'adapter à la forme du volume cible tout en limitant la dose aux organes à risque.
- La planification inverse par ordinateur. L'opérateur fournit au système les contraintes de dose correspondant aux niveaux minimaux et/ou maximaux de dose à délivrer aux volumes-cibles tumoraux et aux organes sains à risque. C'est ensuite le logiciel de planification qui va, grâce à un processus itératif, déterminer la balistique, la contribution de chaque champ et la modulation de l'intensité de l'irradiation permettant de respecter au mieux les objectifs.

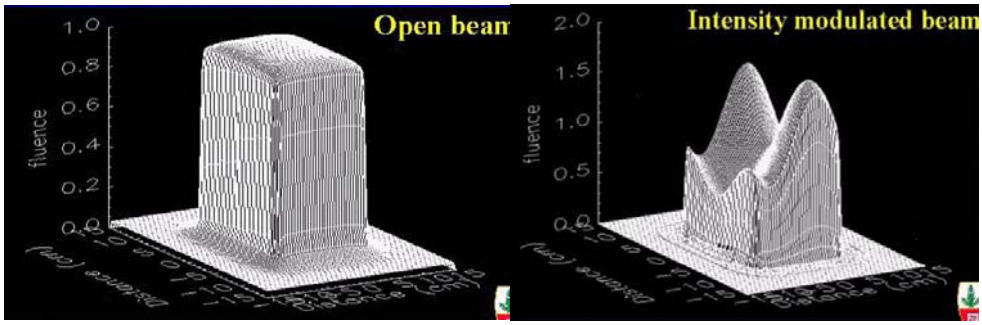

Figure 4 : Différence entre radiothérapie 3D et modulation d'intensité

A gauche: Répartition homogène de la dose au sein du champ d'irradiation en radiothérapie 3D standard.
A droite: Répartition hétérogène de la dose dans un champ de traitement en RCMI.

La RCMI permet ainsi de délivrer une dose hautement conformationnelle dans des structures anatomiques complexes tout en préservant les tissus sains. Ainsi, pour les cancers des VADS, trois études randomisées ont démontré une meilleure épargne des glandes parotides en utilisant la RCMI par rapport à une technique sans RCMI, permettant un meilleur flux salivaire et une diminution du risque de xérostomie [1-3].

1.2.2 Traitement standard actuel par radiothérapie

La radiothérapie standard des cancers ORL est donc actuellement une radiothérapie par modulation d'intensité, avec guidage par l'image au minimum hebdomadaire pour assurer un bon repositionnement de la cible. Le processus global d'un traitement par radiothérapie est illustré Figure 5.

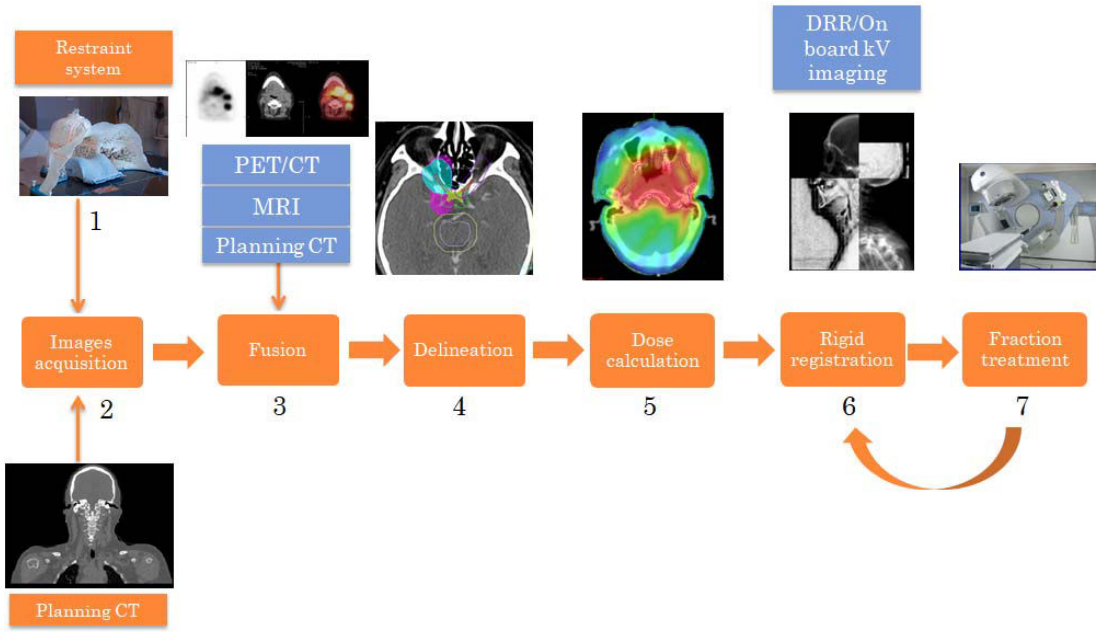

Figure 5 : Processus global d'un traitement par radiothérapie avec modulation d'intensité guidée par l'image résumé en 7 étapes.

DRR : Digital reconstructed radiography.

1.2.2.1 Scanner de planification et délinéation des volumes d'intérêt

Lors de l'étape de planification, un masque thermoformé personnalisé est réalisé afin d'assurer l'immobilisation du patient dans la même position durant toute la durée du traitement (étape 1). Une acquisition scanner est ensuite réalisée (étape 2). Une étape optionnelle de fusion d'images (TEP et/ou IRM) peut être réalisée afin d'aider à la définition des volumes tumoraux (étape 3). Le radiothérapeute va ensuite délinéer les différents volumes sur le scanner de planification (étape 4). Le volume tumoral macroscopique (*gross tumor volume* (GTV)) correspond à la tumeur visible à l'examen et/ou sur les différents examens d'imagerie. Le volume cible clinique (*clinical target volume* (CTV)) correspond à une marge supplémentaire autour du GTV pour prendre en compte le risque d'envahissement microscopique. Il dépend essentiellement de la localisation tumorale en fonction des barrières anatomiques ou des zones de faiblesse. Un volume cible interne (*internal target volume* (ITV)) peut être ajouté autour du CTV pour prendre en compte les mouvements physiologiques et les variations de taille. Ce volume est surtout utile au cours d'une irradiation thoracique pour prendre en compte les mouvements respiratoires, et n'est que très rarement utilisé lors d'une radiothérapie des VADS. Classiquement, 5 mm de marges sont ajoutés autour du CTV, définissant ainsi le volume final de traitement (*planning target volume* (PTV)). Cette marge permet de prendre en compte les déplacements et éventuelles déformations du volume cible, et les incertitudes liées à la position du patient sous l'appareil de traitement. La dose totale de traitement sera délivrée dans le PTV. Le radiothérapeute va également délinéer les organes sains à risque de toxicité.

1.2.2.2 Dosimétrie par planification inverse

L'étape de dosimétrie (étape 5) va consister à déterminer le plan de traitement en fonction des volumes cibles et des organes à risque. Après définition des objectifs de doses aux volumes cibles et aux organes à risque, les paramètres de traitement sont optimisés par un processus de planification inverse qui va agir sur la forme et l'intensité de chaque faisceau de traitement. Ce processus va permettre d'obtenir une dose hautement conformée aux volumes cibles, épargnant autant que possible les organes sains. Un exemple de dosimétrie pour un cancer du nasopharynx est illustré Figure 6.

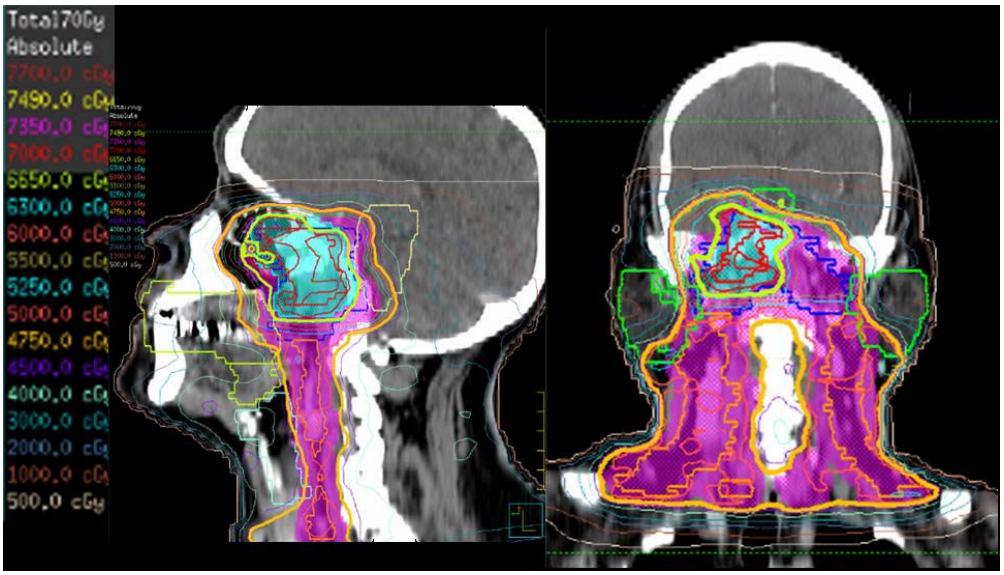

Figure 6 : Dosimétrie pour un cancer du nasopharynx en vue sagittale et coronale.

Le *planning target volume* (PTV) est représenté en violet et bleu clair, les parotides sont en vert. Le trait orange représente l'isodose 95% (66,5 Gy) de la dose de prescription (70 Gy). La haute dose au délivrée au niveau du PTV tout en épargnant les parotides.

1.2.2.3 Radiothérapie guidée par l'image

Dans ce contexte de très haute conformation de la dose, une très faible variation de position peut entraîner un sous-dosage du volume cible et/ou un surdosage des organes à risque en particulier de la moelle [18]. Un masque plastique thermoformé avec cinq points d'attache est généralement utilisé pour immobiliser le patient. Même si un tel système de contention permet de limiter les erreurs de positionnement, les repères utilisés pour positionner le patient sous l'accélérateur sont sur la surface externe du patient voire sur le masque, et non pas dans le volume cible. Des déplacements importants peuvent de ce fait être observés. En moyenne dans la littérature, les erreurs systématiques et aléatoires varient de 1,6 à 4,6 mm et 1,1 à 2,5 mm respectivement [19, 20]. Au vu de ces erreurs de positionnement, la marge de 5 mm classiquement admise pour le volume cible prévisionnel peut s'avérer insuffisante. Dans une série de 15 patients traités par tomothérapie, Houghton *et al.* ont ainsi observé des erreurs de position de plus de 5 mm pour près de 25 % des séances de traitement [21]. De très fortes variations existent par ailleurs en fonction des sous-régions considérées, pouvant aller jusqu'à près de 9 mm pour la mandibule [22, 23].

Des systèmes de guidage par l'image ont donc été développés pour repositionner le patient, non plus en fonction de marqueurs externes, mais suivant des structures anatomiques (étape 6). Les accélérateurs de particules utilisés pour le traitement sont ainsi équipés de système d'imagerie, utilisant des tubes à rayons X. Cette imagerie peut être de type 2D (2 images kV perpendiculaires) ou 3D, en utilisant plusieurs images 2D dans différentes projections (400 à 600) pour reconstruire une image volumique (*cone beam CT* (CBCT) en cas d'imagerie kV ou *mega voltage CT* (MVCT) en cas d'imagerie MV).

Le guidage par l'image standard, reposant sur une imagerie 2D, consiste en un recalage osseux, avec deux approches possibles, l'une différée (*offline*) et l'autre en direct (*online*), c'est-à-dire réalisée en début de fraction de traitement. Le guidage par l'image différé, basé sur l'analyse de plusieurs séances d'irradiation, permet de diminuer l'erreur systématique de 1,6–2,1 mm à 1,1–1,2 mm mais n'a pas d'effet sur l'erreur aléatoire, au contraire du guidage en temps réel qui est la référence [20, 22, 24-26]. D'un point de vue dosimétrique, la réalisation d'un guidage par l'image sur les structures osseuses permet d'éviter un surdosage au niveau des parotides, du canal médullaire, de la cochlée et des structures impliquées dans la déglutition [25-30]. La démonstration du bénéfice clinique de ce recalage est plus difficile, mais celui-ci semble conduire à un gain en termes de qualité de vie (xérostomie et trouble de la déglutition) [28, 30].

Pour ce qui concerne la fréquence des contrôles, la réalisation d'une imagerie quotidienne apparaît supérieure à une approche hebdomadaire, même dans le cas de marge entre les volumes cibles prévisionnel et anatomo-clinique de 5 mm [21-23, 31-33]. Den *et al.* ont même suggéré qu'une tomographie conique quotidienne pourrait permettre de diminuer les marges à 3 mm dans certaines localisations et certaines directions [34]. À noter cependant que malgré une imagerie quotidienne (CBCT ou 2D), près de 11 % des séances présentent des erreurs sur le positionnement de plus de 5 mm [35]. Une grande prudence reste aussi nécessaire pour les régions anatomiques fortement mobiles (oropharynx, larynx). En pratique, le *National Health Service* préconise depuis 2012 une imagerie bidimensionnelle orthogonale quotidienne avec recalage osseux à la place de l'imagerie hebdomadaire conseillée auparavant [36]. Les derniers essais du Groupe d'oncologie radiothérapie tête et cou (Gortec) intègrent également de plus en

plus une imagerie au minimum bihebdomadaire, voire quotidienne. La réalisation d'une imagerie lors des trois à cinq premières séances de traitement avec mesures correctives suivie d'une imagerie hebdomadaire apparaît donc comme le minimum requis lors d'une RCMI ORL [35]. En cas de nécessité d'assurer le maximum de précision du traitement, une imagerie quotidienne avec repositionnement est clairement indispensable. Compte tenu des imprécisions de positionnement malgré un guidage par l'image quotidienne et du fait des hautes doses délivrées, un volume prévisionnel des organes à risque est également considéré dès l'étape de planification. Ce volume correspond à l'addition de marges comprises entre 3 et 5 mm autour de ces organes à risque dit « en série » (moelle, tronc cérébral, larynx, nerf optique).

Au vu de la variabilité de mouvements des différentes sous-régions, la définition d'un sous-volume anatomique pour le repositionnement peut s'avérer nécessaire. Dans ce cas, la région la plus souvent utilisée est le rachis cervical entre C1-C3, afin d'assurer le repositionnement de la moelle, organe le plus critique [23]. Le choix de ce sous-volume reste naturellement dépendant de la localisation traitée. L'utilisation d'une imagerie volumique (tomographie conique) ne semble pas apporter de bénéfice supplémentaire en termes de précision du repositionnement par rapport à une imagerie bidimensionnelle. Cette imagerie peut cependant s'avérer utile pour essayer de prendre en compte la variabilité de mouvements des différentes sous-régions anatomiques entre elles. Ainsi certains auteurs proposent un recalage moyen basé sur les déplacements de plusieurs sous-régions d'intérêt [37]. Cette approche permet potentiellement une diminution du nombre de séances comportant des erreurs de positionnement de plus de 5 mm.

Une fois cette étape de recalage du volume cible dans une position la plus proche possible que celle défini à la planification (étape 1), le traitement peut être réalisé (étape 7).

1.2.3 Variations anatomiques en cours de traitement des cancers des VADS

Pour les tumeurs localement avancées, des modifications morphologiques majeures et complexes, autres qu'un mauvais positionnement du patient, peuvent survenir au cours des sept semaines de traitement telles qu'un amaigrissement du patient, une diminution du volume des

parotides (Table 2) et une fonte tumorale (Table 3). Pour les glandes parotides, toutes les études montrent une diminution du volume entre 5 et 32 % à mi traitement et entre 13 et 41,5% à la fin du traitement, correspondant à une diminution de 1% par jour [38]. Il existe également un déplacement médian de 2 à 5 mm. La parotide controlatérale (par rapport à la tumeur) semble moins, voire ne pas du tout, se déplacer comparativement à la parotide homolatérale [38]. Pour le volume cible, les données sont plus hétérogènes, certaines études rapportant des données sur le volume tumoral macroscopique (GTV), d'autres sur le volume cible clinique (CTV). La fonte tumorale (GTV) a été estimée entre 17 et 93% à mi traitement et à plus de la moitié à la fin (21-75%), correspondant à une diminution de 1,8% à 3,2% par jour. La fonte tumorale semble être asymétrique au cours de la radiothérapie [39]. Ces variations anatomiques entraînent des modifications de la distribution de dose avec un risque de surdosage des organes à risque, en particulier des parotides. Ces modifications interviennent à deux niveaux. Tout d'abord la distribution de dose en elle-même est susceptible d'être modifiée, notamment en cas de modifications du contour externe du patient, voire des voies aériennes. Ces modifications anatomiques entraînent un changement, par rapport à la planification, des interactions particules-matières et donc des doses absorbées localement. Par ailleurs, les tissus subissant des variations anatomiques sont soumis à un déplacement au sein de la distribution de dose. La dose reçue par les tissus peut alors varier. Un simple repositionnement rigide ne pourra pas compenser ces variations dosimétriques. En effet, le repositionnement rigide ne permet de mettre en œuvre, dans le meilleur des cas, qu'un compromis global entre ciblage de la tumeur et épargne des différents tissus sains.

Table 2 : Variation anatomiques des glandes parotides au cours d'une RCMI pour un cancer des VADS

Auteur	***Nb pts***	***Méthode d'évaluation***		***Variations anatomiques par rapport à la planification***	
		Type	***Moment***	***Diminution de volume (%)***	***Déplacement médial (mm)***
Ahn [40]	23	CT	11^{eme}, 22^{eme} et 33^{eme} fr	24	-
Ajani [41]	14	CT	S 2 4 6	37,3	-
Barker [39]	14	CT	3 /semaine	28	3,2
Beltran [42]	15	CT	15^{eme} et 25^{eme} fr	30	-
Berwouts [43]	10	PET/CT	8^{eme} et 18^{th} fr	32	-
Bhide [44]	20	CT	S 2 3 4 5	14,2 à S2	-
Broggi [45]	87	MVCT ou KVCT	1er et dernier jour de RT	26	-
Capelle [46]	20	CT	S3	17,5	-
Castadot [38]	10	CT	1/semaine	1 par jour	3,4
Dewan [47]	30	CT	40 Gy	32	-
Duprez [48]	21	TEP/CT	8^{eme} fr	10 (à la 8^{eme} fr)	-
Hansen [49]	13	CT	19^{eme} fr	18	-
Height [50]	10	CT	40-50 Gy	21	2
Ho [51]	10	CBCT	1/semaine	29	-
Jensen [52]	72	CT	1/semaine	40	-
Loo [53]	5	MVCT	1/semaine	CL : 17.5 HL : 30	-
Marzi [54]	15	CT	1/semaine	41.5	-
Nishi [55]	20	CT	S3 ou S4	-	4,2
Reali [56]	10	CT	S3 5 7	-	de -0,7 à 0,6
Robar [57]	15	CT	1/semaine	-	2,3
Sanguineti [58]	85	CT	1/semaine	32	-
Schwartz [59]	24	CT	1/jour	24	-
Vasquez-Osorio [60]	10	CT	S2	HL : 17 CL : 5	-
Wu [61]	11	CT	1/semaine	13	-
Yip [62]	15	CBCT	1/semaine	4 - 23	-

- = Données non disponible, Nbr pts= nombre de patients, S= semaine de traitement, CBCT= Cone Beam Computed Tomography, CL= controlateral, HL = homolateral, MVCT = Mega Voltage Computed Tomography, fr= fraction, RT = radiotherapie

Table 3 : Variation anatomiques du volume cible au cours d'une RCMI pour un cancer des VADS

Auteur	***Nb pts***	***Méthode d'évaluation***		***Diminution de volume in %***	
		Type	***Moment***	***GTV***	***CTV***
Ahn [40]	23	CT	11^{eme}, 22^{eme} et 33^{eme} fr	17	-
Bando [63]	10	CT	1/semaine	28	-
Barker [39]	14	CT	3/semaine	1,8 (/jour)	-
Belli [64]	30	MVCT	1/semaine	75	-
Berwouts [43]	10	PET/CT	8^{eme} and 18^{eme} fr	75	-
Capelle [46]	20	CT	S3	28	-
Castadot [38]	10	CT	1/semaine	3,2 (/jour)	-
Dewan [47]	30	CT	40 Gy	47	-
Hansen [49]	13	CT	19eme fr	-	7,5
Height [50]	10	CT	40-50 Gy	49	-
Kataria [65]	36	CT	23^{eme} fr	34	-
Marzi [54]	15	CT	1/semaine	74,5	-
Nishi [55]	20	CT	S 3 or 4	37	-
Olteanu [66]	10	PET/CT	8^{eme} et 18^{eme} fr	19 % à 93 % (à la 18^{eme} fr)	-
Schwartz [67]	24	CT	Daily	-	10,3
Simone [68]	10	CT	3^{rd} S	53	-
Surucu [69]	48	CT	5^{eme} S	21	-
Vasquez-Osorio [60]	10	CT	S 2	25	-
Wu [61]	11	CT	1/semaine	-	8
Yip [62]	15	CBCT	1/semaine	-	1 to 6

- = Données non disponible, Nbr pts= nombre de patients, S= semaine de traitement, CBCT= Cone Beam Computed Tomography, CL= controlateral, HL = homolateral, MVCT = Mega Voltage Computed Tomography, fr= fraction, RT = radiotherapie

1.2.4 Principe de la radiothérapie adaptative des cancers des VADS

La radiothérapie adaptative (*adaptive radiation therapy*, ART) consiste à utiliser non plus un unique plan de traitement, comme dans la radiothérapie classique, mais plusieurs plans de traitement [70, 71]. Ces différents plans de traitement permettent d'adapter le traitement à l'évolution individuelle de chaque patient, allant donc vers une meilleure personnalisation de la thérapie. Cette évolution individuelle peut intégrer des aspects anatomiques, mais aussi

métaboliques [72]. Dans le cas d'une prise en compte des modifications anatomiques, la radiothérapie adaptative peut se définir comme une boucle de rétroaction corrective afin d'assurer l'adéquation entre la dose planifiée et la dose délivrée. Trois types de stratégies d'ART sont possibles. L'adaptation peut se faire en direct, pendant la séance, lorsque le patient est sur la table de traitement [73]. La modification est appliquée soit juste avant la séance soit pendant la délivrance de la dose. Cette méthode de radiothérapie adaptative corrige les erreurs systématiques et les erreurs aléatoires. Elle est cependant lourde en ressources humaines et contraintes de temps et nécessite des solutions technologiques, telles que la possibilité de recalculer la distribution de dose en temps réel, actuellement non implémentées. Une seconde approche consiste à anticiper sur les déformations potentielles survenant en cours de traitement. Cette stratégie, utilisée notamment, à travers la génération de bibliothèques de plans de traitement, pour le traitement des cancers du col de l'utérus [74] paraît complexe à mettre en œuvre en ORL où les déformations sont plus difficilement prédictibles. Une troisième approche, dite différée, consiste en une adaptation du plan, en l'absence du patient, à partir d'une image acquise au cours des semaines de traitement. Le calcul d'un nouveau plan est alors réalisé entre les séances de traitement. Cette méthode permet de corriger des variations systématiques et/ou progressives. Du fait du caractère progressif des modifications anatomiques au cours d'une radiothérapie pour un cancer des VADS, cette approche différée semble la plus adaptée.

1.2.5 Place de l'imagerie dans la radiothérapie adaptative des cancers des VADS (article)

1.2.5.1 Introduction

L'imagerie occupe une place majeure dans le processus de la radiothérapie adaptative. L'imagerie (embarquée (CBCT ou MVCT) ou par la réalisation d'une nouvelle acquisition scanner) va ainsi permettre de détecter des variations anatomiques pouvant avoir un impact sur la dose délivrée. Elle va également servir au calcul de la dose à la fraction ou bien dans une approche de cumul de dose par recalage élastique, permettant de guider le déclenchement d'une stratégie de radiothérapie adaptative. Le recalage élastique peut également être utilisé pour propager les contours depuis le scanner de planification vers l'imagerie acquise en cours de traitement, évitant ainsi une longue étape de re-délinéation. Par ailleurs, l'imagerie métabolique, habituellement

réalisée en pré thérapeutique, pourrait aussi trouver sa place en per thérapeutique afin de guider la décision de déclencher une replanification.

L'intégration de l'imagerie sous ses différentes modalités dans un processus de radiothérapie adaptative est discutée dans l'article suivant publié dans la revue IRBM en février 2014.

The role of imaging in adaptive radiotherapy for head and neck cancer

The role of imaging in adaptive radiotherapy for head and neck cancer

IRBM, 2014 Feb

J.Castelli[1*], A.Simon[2, 3], O.Acosta[2, 3], P.Haigron[2, 3], M.Nassef[2, 3], O.Henry[1], E.Chajon[1], R. de Crevoisier[1, 2, 3]

[1]. Centre Eugene Marquis, département des radiations, Rennes, France

[2]. INSERM, U1099, Campus de Beaulieu, Rennes, F-35000, France

3. Université de Rennes 1, LTSI, Campus de Beaulieu, Rennes, F-35000, France

Disponible en ligne sur
ScienceDirect
www.sciencedirect.com
Elsevier Masson France
EM|consulte
www.em-consulte.com
IRBM
IRBM 35 (2014) 33–40

Biomedical image segmentation using variational and statistical approaches

The role of imaging in adaptive radiotherapy for head and neck cancer

J. Castelli [a,*], A. Simon [b,c], O. Acosta [b,c], P. Haigron [b,c], M. Nassef [b,c], O. Henry [a], E. Chajon [a], R. de Crevoisier [a,b,c]

[a] *Département des radiations, centre Eugène-Marquis, Rennes, France*
[b] *U1099, Inserm, campus de Beaulieu, 35000 Rennes, France*
[c] *Campus de Beaulieu, université de Rennes 1, LTSI, 35000 Rennes, France*

Received 19 July 2013; received in revised form 7 November 2013; accepted 5 December 2013
Available online 28 January 2014

Abstract

Radiotherapy (RT), alone or combined with surgery and/or chemotherapy is given to almost all head and neck cancer (HNC). The goal of RT is to increase as much as possible the dose in the tumor to cure the patient, while limiting the dose in the organs at risk, mainly the parotids gland to limit the xerostomia. HNC RT appears particularly challenging due to the complexity of the shape of the anatomical structures, which also changes during the 7 weeks of treatment. Advances in imaging-modalities, -processing and -integration at the different RT steps have been crucial to develop a new image and dose-guided adaptive RT (ART) strategy. Moreover, the integration of functional imaging such as FDG-PET (performed before and during the treatment) leads to an even more highly targeted and dose-escalated ART. This article is an overview of the place and role of imaging at the different steps of HNCART, from a medical point of view.

1. Introduction

Radiotherapy (RT), alone or combined with surgery and/or chemotherapy is the treatment for almost all head and neck cancers. The goal of radiotherapy is to deliver a maximum dose to the tumor target volume, thereby curing the patient, while diminishing the dose to the organs at risk, thus decreasing the risk of toxicity. Recent improvements in radiation techniques have allowed for a reduction in toxicity, particularly the xerostomia by limiting the dose to the parotid gland [1–3]. This progress has been realized thanks to the combined improvement of imaging, computer science and technology of linear accelerators. Imaging plays indeed a crucial role in the three main radiotherapy improvement axis: delineation of the tumor, dose distribution thanks to the use of intensity-modulated RT (IMRT) and tumor localization at the time of the treatment providing a way forward to the new image guided radiotherapy (IGRT) strategies.

The RT reference imaging modality is X-ray Computed Tomography (CT), since the computation of dose distribution is based on electron density maps assessed by the Hounsfield units of the CT image. Reference imaging for tumor visualization is, however, MRI and becoming increasingly used in the 18-Fluoro-deoxy-glucose (FDG)-positron-emission tomography (PET), thus implying the need for multimodal imaging fusion tools for accurate tumor delineation. Moreover, morphological variations can occur during the 7 weeks treatment course, so that the pre-treatment planned dose may not correspond to the actual delivered dose [4,5]. Adaptive radiotherapy (ART) is a new IGRT based strategy aimed at correcting these inters course morphological variations, by re-generating one or more plannings during the treatment course.

The adaptive RT is a new RT strategy that is still at a feasibility level and the first clinical results are not even yet available. Indeed, the presented head and neck adaptive RT workflow comprises different level of complexity, corresponding to the use of both constructor based and homemade software. The treatment (re-) planning are performed by using “standard” IMRT treatment planning system, and the daily bone rigid registration are performed using the LINAC based registration system (grey gradient based algorithm). The cumulative dose monitoring is not yet fully validated and is mostly performed by homemade software, when tested/evaluated by different teams.

* Corresponding author.
E-mail address: j.castelli@rennes.unicancer.fr (J. Castelli).

1959-0318/$ – see front matter © 2013 Elsevier Masson SAS. All rights reserved.
http://dx.doi.org/10.1016/j.irbm.2013.12.003

Head and neck cancer (HNC) is the main tumor site for ART. This article is an overview of the place of imaging at the different steps of HNC ART from a medical point of view.

2. Imaging for treatment

The general overview of image modalities and processing in HNC ART workflow is showed on Fig. 1. Twelve steps have been identified and will be described below. The specific adaptive RT loop (in green, steps 8 to 12) is based on a more standard IMRT workflow (in orange, steps 1 to 7), from the patient immobilization device realization to the fraction treatment.

2.1. Images acquisition, delineation and 3D reconstructions (Step 1–4)

Custom-fitted thermoplastic masks are first realized to immobilize the neck in the same position during the full treatment (step 1). In a standard RT treatment, only one CT acquisition is performed for the planning (step 2). Several target volumes will be consecutively delineated and defined on this planning CT (step 4): the GTV (gross tumor volume) corresponds to the macroscopic visible tumor on clinical examination and/or on different imaging, the clinical target volume (CTV) is the GTV plus a margin corresponding to the sub-clinical microscopic tumor spread. This CTV cannot therefore be fully imaged and mostly depends on the natural history of HNC. Five-millimeter margins are then classically added all around the CTV to define a planning target volume (PTV), taking into account both the anatomical structures displacement and deformations under the mask and the patient position uncertainty under the linear accelerator. The total dose of RT will be finally delivered within this PTV. Organs at risk of toxicity (OAR) are also delineated on the CT. All these volumes are manually segmented by the radiotherapist (Fig. 2).

Manual segmentation in HNC is particularly complex implying a rather large knowledge of both HNC anatomy and natural history of HNC spreading, and is also time consuming (up to 3 hours per patient) [5]. Significant inter- and intra-observer variations in CT-based target delineation have been moreover shown due to the limit of the CT for accurate tumor visualization. MRI (T1 weighted with contrast imaging) presents a superior soft tissue differentiation than CT, without dental artefacts. In comparison with CT, MRI-based GTV has been shown to be smaller and with less interobserver variation than CT-based GTV [6]. Due to the necessity of electron density map, image co-registration between MRI and CT is necessary (step 3), leading potentially to new uncertainties. If the dosimetry should be calculated on CT due to the necessity to take account of electronic density, the dream of the radiation oncologist in head and neck, as in almost all tumor localization, is to use straightly and exclusively the MRI for both the planning and the tumor localization at the time of the treatment. Ongoing works aim to make MRI-based dose distribution feasible [7,8] and first results are encouraging, especially for the pelvis. Only one study was focused on intracranial lesions with very little difference between CT-based plans and MRI-based plans [9]. The integration of the MRI within the LINAC appears particularly complex. However, prototypes already exist and first results were published [10,11]. PET imaging is also particularly helpful in HNC delineation, for both the primary tumor and the lymph node [12].

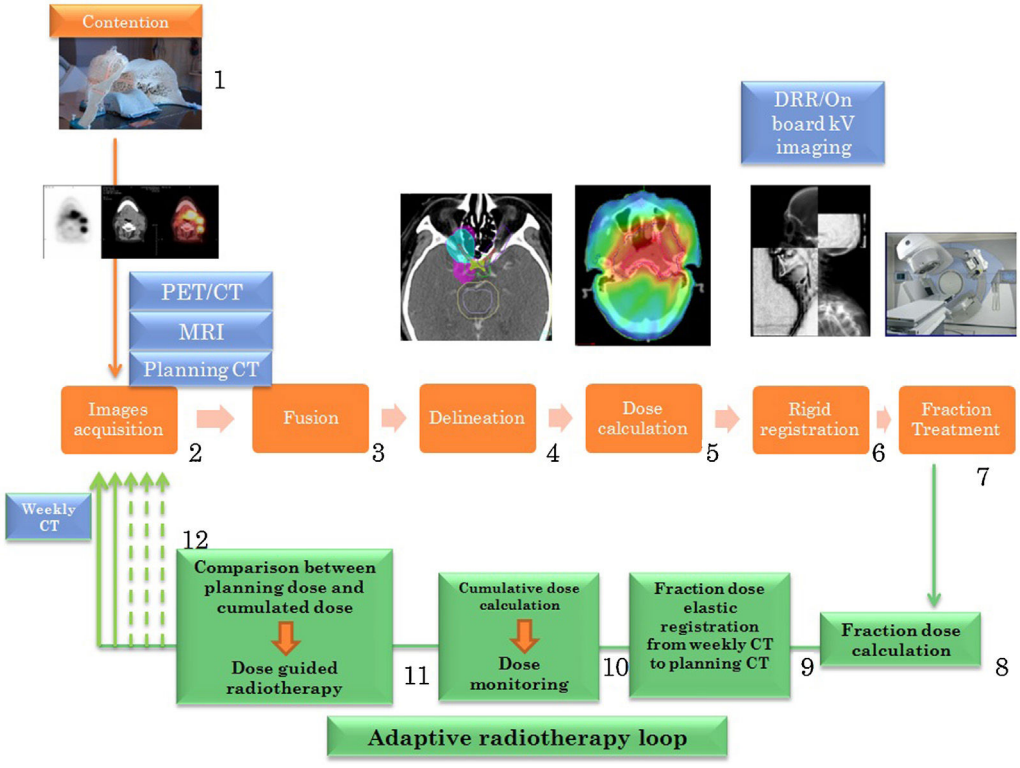

Fig. 1. Overview of image modalities and processing in head and neck adaptive radiotherapy. A total of 12 steps are individualized. In orange: the "standard" RT treatment workflow. In green: the specific adaptive and dose-guided radiotherapy workflow. DRR: digital reconstructed radiograph.

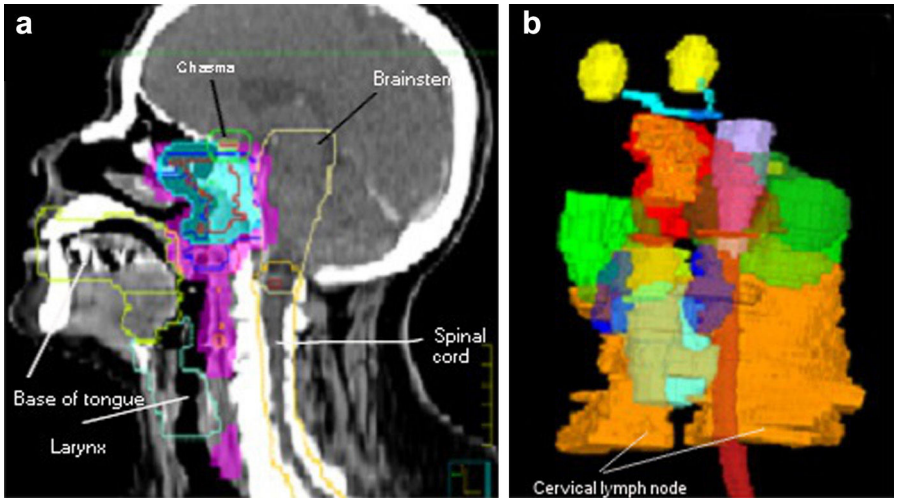

Fig. 2. a and b: anatomical structure delineation (CT imaging) and 3D reconstruction in case of a nasopharynx carcinoma (light blue on the left). The pink color represents the "low risk" Planning Target Volume (PTV). The different organs at risk are shown in Fig. 2b: parotids (green), spinal cord (red) eyes (yellow), optic nerve (light blue).

Geets et al. [13] showed that using PET for segmentation permits to decrease the target volume and therefore the toxicity. For laryngeal tumors, Daisne et al. [14] compared tumor delineation using CT, MRI and PET with the "gold standard" pathological specimen. The best correlation was found with the use of PET. The PET based GTV was smaller than those based on CT or MRI. However, there is a lack of validation for PET segmentations. A simple visual method can lead to major variations in segmentation [15]. Different automatic methods have been tested, by using a percentage of the maximal SUV (Standard Uptake Value) [14,16], a threshold value of SUV [15,17], or a signal/noise ratio [14,18,19]. The use of PET based segmentation must remain however cautious, due to the risk of increasing the recurrence by an inappropriate volume decrease. And, as with MRI, co-registration is necessary on CT in order to compute dose distribution, with a risk of uncertainties during this step (Fig. 3).

2.2. CT-based inverse planning and dose calculation (step 5)

The planning step aims to determine the treatment plan, based on the target and OAR delineations. Number of beams, angulations of beams and rotation of the collimator is previously set by the user. Considering dosimetric constraints, parameters of the treatment (shape of the treatment fields and number of segment by beams) are optimized by an inverse planning dose calculation approach based on objectives of dose on target volume and OAR. IMRT aims to modulate the shape and intensity of the beams of radiation to highly conform the dose distribution to the complex shape of the tumor, avoiding the OARs. The clinical benefit of IMRT over non-IMRT techniques has been clearly demonstrated in HNC. Indeed, 3 randomized studies have shown a better parotid sparing with IMRT [1–3], leading to a better salivary flow and a decreased risk of xerostomia. The

Fig. 3. In a routine practice of head and neck RT, PET imaging is recommended at the planning to identify involved nodes. However, PET imaging should be used prudently for a straight tumor delineation. On the left: PET imaging in treatment position before the planning, showing tumor and two lymph nodes (duration of acquisition = 45 min). In the middle: CT modality in the same treatment position at the same time (duration of acquisition = 1 min) On the right: PET co-registered with CT. The mismatch is visible on the posterior lymph node, explained by the different acquisition duration.

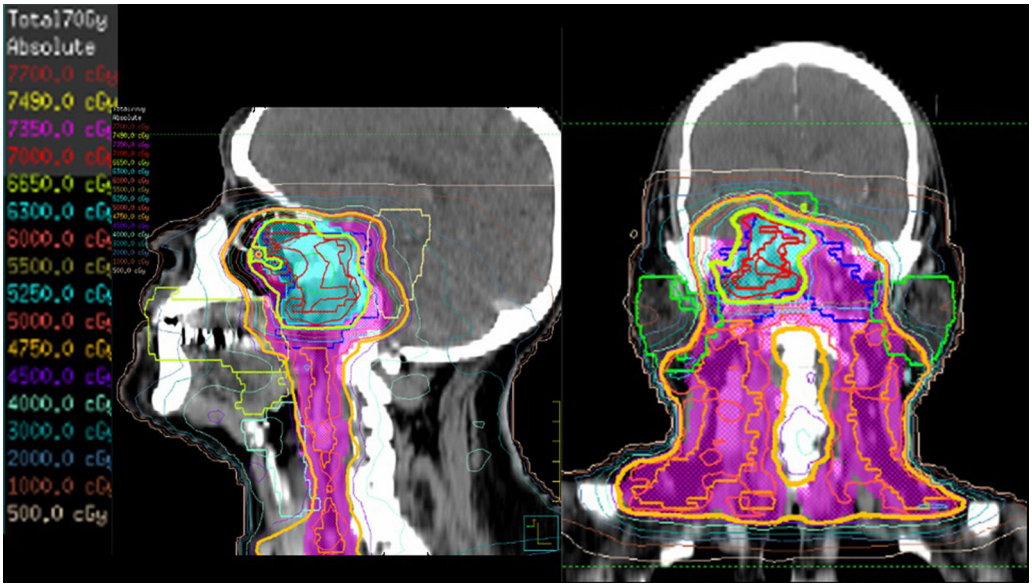

Fig. 4. Sagital and coronal view (CT imaging). Dose distribution for a nasopharynx cancer. In purple and light blue: primary and lymph nodes target volume (PTV). In green: parotids. High dose are delivered within the PTV, with a relatively efficient sparing of the parotids. In orange: 95% (66.5 Gy) of the prescription isodose (70 Gy).

narrow gradient of dose provided by IMRT all around the target requires however a particularly accurate segmentation of all the anatomical structures. An example of IMRT dose distribution sparing the parotid glands is shown on Fig. 4.

2.3. Per-treatment kiloVolt (kV) imaging and CB-CT for rigid registration (step 6)

Controlling the tumor position appears particularly crucial during the 7 weeks of RT, being the main goal of IGRT. The new generations of linear accelerators provide adequate embedded imaging for patient repositioning by a rigid registration. The onboard imaging corresponds to the use of an X-ray tube. This imaging may be 2D (2 perpendiculars kV imaging) or 400 to 600 2D projections for a 3D imaging reconstruction (Cone Beam CT). Setup corrections can be performed by using either bone (2D method) or soft tissue (3D) rigid registration (Fig. 5). This rigid registration leads to a residual setup errors up to 3.6 mm [6]. Under these conditions IGRT doesn't compensate however for shape and volume variations. These changes (tumor

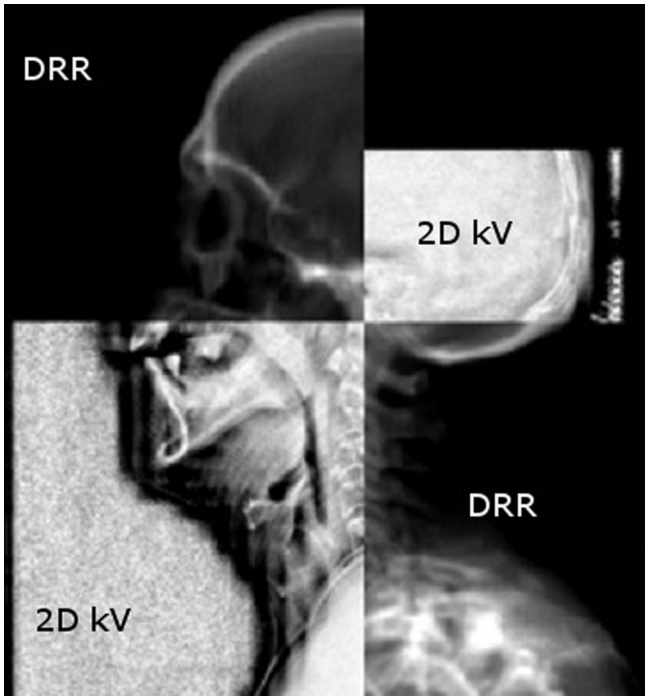

Fig. 5. Mosaic imaging showing a daily bone registration between 2 perpendicular kV imaging acquired before the fraction and the pre-treatment digitally reconstructed radiography (DRR).

regression, alterations of normal tissues, weight loss) may be particularly important during the treatment course [20,21], leading for instance to an increased dose in the parotids [22].

2.4. Adaptive radiotherapy loop (steps 8–12)

ART aims to correct the morphological variations during the course of treatment by generating new periodic plannings. Very few studies suggest that ART allows for the mean parotids dose to be decreased, thereby likely decreasing toxicity [22,23]. The change of anatomy (shrinking of both the tumor and the healthy parotids) modifies the position shape and electron map density of the organs and modifies therefore the dose distribution leading to parotid over irradiation compared to the initial planning dose. A dose distribution can be calculated at the fraction by using the CB-CT (step 8). The cumulative dose can be calculated by applying to the dose at the fraction the same elastic transformation than the anatomical variation between the image at the fraction and the planning CT (step 9) for a cumulative dose monitoring (step 10), as detailed in Fig. 6. The cumulative dose can be compared with the planning dose, in a dose-guided perspective (step 11). The re-planning loop can be repeated as long as the delivered dose differs from the planning dose (step 12). Two theoretical ART strategies may be discussed. In the on-line method, a re-planning is performed immediately after a new CT acquisition, and a new planning is immediately generated. Contouring is time consuming and required a high level of expertise in the field of head and neck tumor imaging (help of the radiologist). New commercial software are particularly helpful to propagate the contours from the planning CT to the per-treatment re-planning C. If their performance appears high for the OARs, their use for the CTV delineation needs absolutely to be validated by the radiation oncologist, in a semi-automatic process. This method appears to be not realistic since the patient remains still on table during the complex segmentation and the full calculation duration of the new plan. Moreover, specific highly expensive equipment is required (CT on rail). In the offline method, a new plan is generated with a delay of few days, enabling also to proceed to the clinical quality assessment process. This method appears feasible with a lower machine-occupation and equipment availability (standard CT). The offline contour propagation from the planning CT to the weekly CT, based on non-rigid image registration (Demons' method, applied to intensities or to distance maps of the delineated organs) [24,25], can save time, however being not fully validated in a routine practice. Another complex issue is the validation of a cumulated dose guided RT strategy (DGRT), so that the new planning could be decided on a cumulative dose monitoring. CB-CT should be used for dose calculation, without needing any CT imaging. But the first issue is the poor image quality of the CB-CT for an accurate tumor and OAR delineation. The second issue is the need of matching CT values and density in CB-CT images. Such tables are specific for an anatomical region and depend of the CB-CT image acquisition parameter [26].

The goal of head and neck ART is at least to maintain the same parotid gland sparing during treatment as the planning. It's even likely that re-planning could even more reduce the dose in these salivary glands compared to the planning due to the anatomical variations, for a subset of patients. Preliminary results suggest for a series of 11 patients that a weekly re-planning can benefit significantly to one third of the PGs (and 50% of the pts), leading to decrease the absolute risk of xerostomia of at least 13%

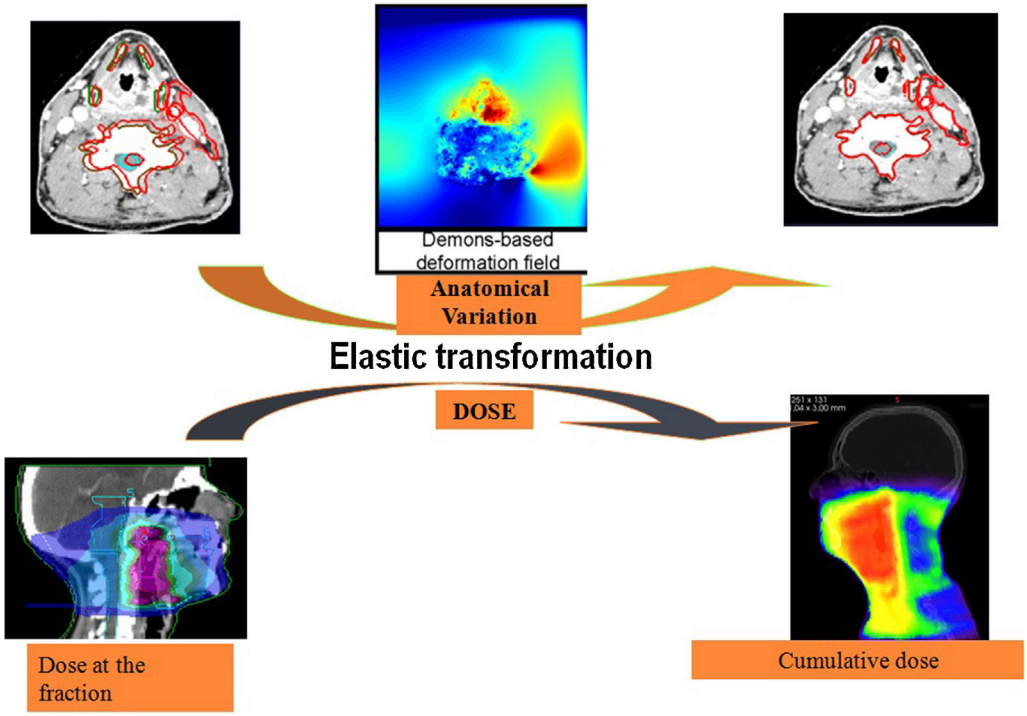

Fig. 6. The cumulative dose can be calculated by applying to the dose at the fraction the same elastic transformation than the anatomical variation between the image at the fraction and the planning CT for a cumulative dose monitoring.

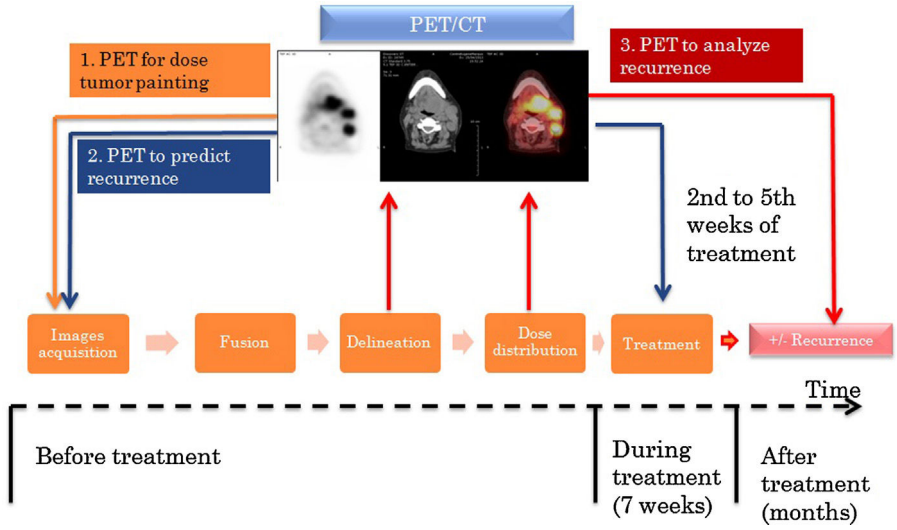

Fig. 7. Three roles of PET imaging in head and neck radiotherapy. 1: Hypermetabolic tumor (FDG) or radioresistant (F-miso) volumes can be identified by PET, allowing a "dose-tumor painting" approach. 2. Metabolic activity assessed before or during the treatment may be a predictor of the recurrence. The analysis of the recurrence is crucial to improve the efficiency of the treatment: is the recurrence mostly fully inside the initial target volume suggesting to increase the dose, or in the border or outside this target volume suggesting to increase this volume?

[27]. The clinical benefit is not yet established and should be demonstrated by ongoing randomized trials.

3. PET for dose tumor painting and for patient outcome prediction

Functional imaging plays an increasing role in RT. Indeed, two main axes of research may be identified in HNC RT: dose tumor painting and prediction/analysis of cancer recurrence. (Fig. 7).

3.1. PET for dose tumor painting

Nowadays, target volumes are considered as a homogeneous risk area. Thus a homogeneous dose is delivered within the whole volume. However, it is well established that tumors are heterogeneous, and constituted of multiples sub-volumes of variable aggressivity. Dose painting aims at producing inhomogeneous dose distributions within the tumor volume adapted to radioresistant areas defined by functional imaging [5] and PET may provide such information. Thus, it became possible to increase doses in the most aggressive regions, without increasing the dose to organs at risk (Fig. 8).

3.2. PET to predict and analyze recurrence

PET has a major role in the evaluation of treatment response. Results at three months after the treatment have suggested a predictive value for relapse [28–30]. A few studies have been focused on correlation between PET before or during treatment and patient outcome [31,32] (Fig. 9). The modifications of the SUV in the tumour during the treatment course are particularly complex to interpret since they can be related to tumour evolution or inflammatory reaction. However, several studies suggest that FDG-PET performed at 20 Gy or 40 Gy [31,32] can be good predictor of tumor recurrence or patient death. These preliminary results are however limited, with a small number of patient and monocentric.

Currently, no evidence has been clearly built for defining the subgroups of different prognoses but several ongoing studies exist, yet. Some studies are ongoing to deal with this question. Thus, most of the locoregional failures occur within the high dose region, confirming the interest of dose painting [33].

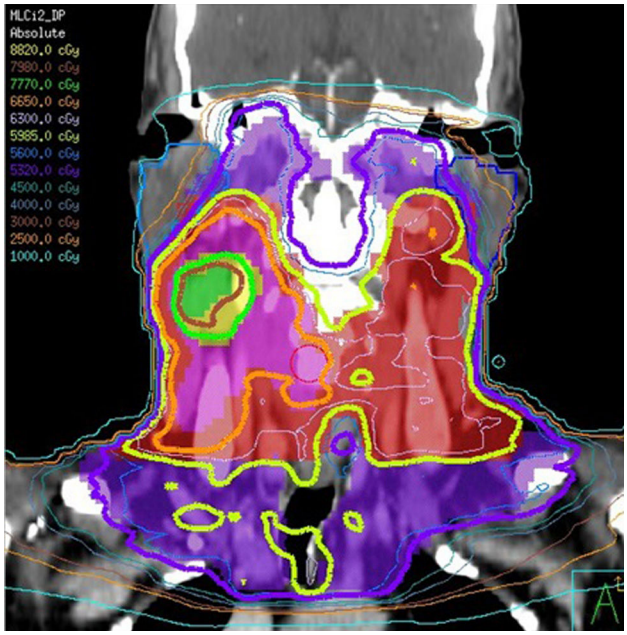

Fig. 8. Dose tumor painting. High doses (yellow and green) are delivered on sub-volumes of the tumor without increasing the dose outside the tumor. The main limitation of such approach is still the validation of the tumor segmentation methods. Each colorwash corresponds to different target volume (depending on the tumor aggressivity). Each color line corresponding to different radiation doses (isodose curves).

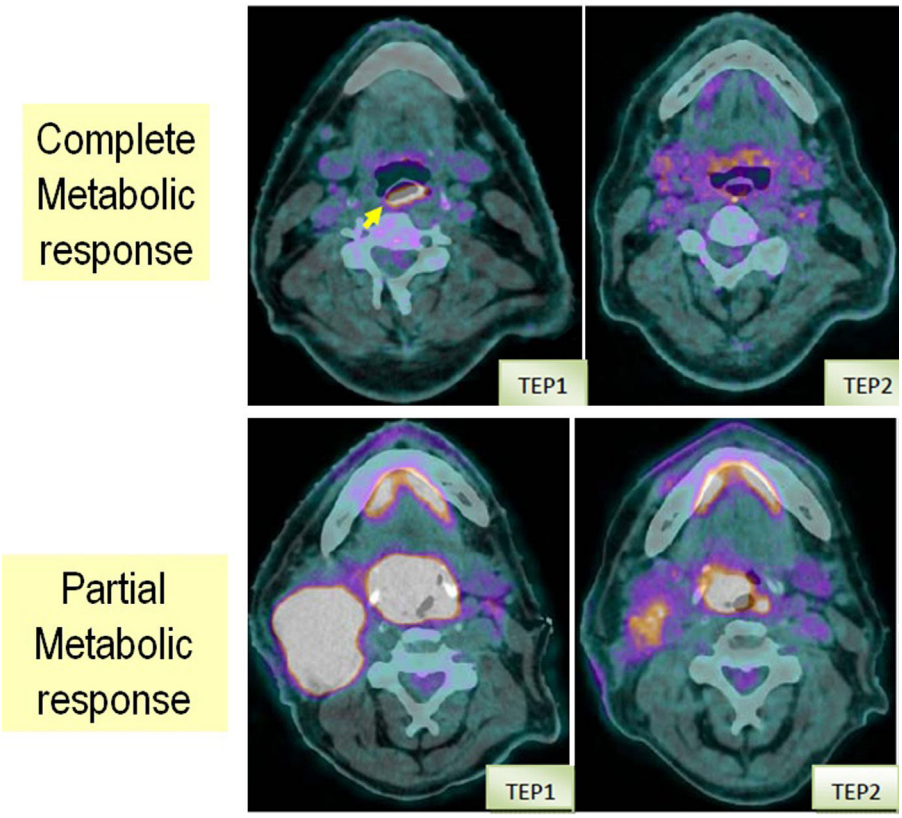

Fig. 9. PET before (left) and during treatment (right), with complete response (up) and partial response (bottom).

4. Conclusion

Imaging plays a major role in the development of radiotherapy and improvement in patient outcome. IGRT aims to reduce setup errors during treatment, by integrating a rigid registration step, nevertheless with a lack of morphological variation consideration. Adaptive radiotherapy aims to correct these morphological variations by realizing one or more plans during the treatment course. Imaging is used to detect these variations, thereby deciding on a potential re-planning. If justified, the re-planning is particularly heavy and complex, implying to segment again all the volumes of interest and to recalculate optimized dose distribution. Contours propagation by non-rigid image registration is a promising alternative to tackle these issues. The combination of PET imaging with the ART workflow open the news field of high escalation dose thanks to a dose tumor painting or sculpting strategy. Moreover, PET may be an important tool for early evaluation of tumor response, likely leading to an increased dose for non-responder patients in an adaptive framework. Ongoing prospective studies aim to demonstrating the benefit of ART (ARTIX) and to confirm the predictive value of PET during treatment (TEmPORaL) in HNC RT.

Acknowledgments

PAIR VADS program (INCA, ARC and Ligue contre le cancer).

References

[1] Kam MK, Leung SF, Zee B, Chau RM, Suen JJ, Mo F, et al. Prospective randomized study of intensity-modulated radiotherapy on salivary gland function in early-stage nasopharyngeal carcinoma patients. J Clin Oncol 2007;25(31):4873–9.

[2] Nutting CM, Morden JP, Harrington KJ, Urbano TG, Bhide SA, Clark C, et al. Parotid-sparing intensity modulated versus conventional radiotherapy in head and neck cancer (PARSPORT): a phase 3 multicentre randomised controlled trial. Lancet Oncol 2011;12(2):127–36.

[3] Pow EH, Kwong DL, McMillan AS, Wong MC, Sham JS, Leung LH, et al. Xerostomia and quality of life after intensity-modulated radiotherapy vs. conventional radiotherapy for early-stage nasopharyngeal carcinoma: initial report on a randomized controlled clinical trial. Int J Radiat Oncol Biol Phys 2006;66(4):981–91.

[4] Barker Jr JL, Garden AS, Ang KK, O'Daniel JC, Wang H, Court LE, et al. Quantification of volumetric and geometric changes occurring during fractionated radiotherapy for head-and-neck cancer using an integrated CT/linear accelerator system. Int J Radiat Oncol Biol Phys 2004;59(4):960–70.

[5] Berwouts D, Olteanu LA, Duprez F, Vercauteren T, De Gersem W, De Neve W, et al. Three-phase adaptive dose-painting-by-numbers for head-and-neck cancer: initial results of the phase I clinical trial. Radiother Oncol 2013.

[6] Rasch C, Steenbakkers R, van Herk M. Target definition in prostate, head, and neck. Semin Radiat Oncol 2005;15(3):136–45.

[7] Dowling JA, Lambert J, Parker J, Salvado O, Fripp J, Capp A, et al. An atlas-based electron density mapping method for magnetic resonance imaging (MRI)-alone treatment planning and adaptive MRI-based prostate radiation therapy. Int J Radiat Oncol Biol Phys 2012;83(1):e5–11.

[8] Lambert J, Greer PB, Menk F, Patterson J, Parker J, Dahl K, et al. MRI-guided prostate radiation therapy planning: Investigation of dosimetric accuracy of MRI-based dose planning. Radiother Oncol 2011;98(3):330–4.

[9] Stanescu T, Jans HS, Pervez N, Stavrev P, Fallone BG. A study on the magnetic resonance imaging (MRI)-based radiation treatment planning of intracranial lesions. Phys Med Biol 2008;53(13):3579–93.
[10] Freyhardt P, Hartwig T, De Bucourt M, Maurer M, Renz D, Gebauer B, et al. MR-guided facet joint injection therapy using an open 1.0-T MRI system: an outcome study. Eur Radiol 2013.
[11] van Heijst TC, den Hartogh MD, Lagendijk JJ, van den Bongard HJ, van Asselen B. MR-guided breast radiotherapy: feasibility and magnetic-field impact on skin dose. Phys Med Biol 2013;58(17):5917–30.
[12] Kubicek GJ, Champ C, Fogh S, Wang F, Reddy E, Intenzo C, et al. FDG-PET staging and importance of lymph node SUV in head and neck cancer. Head Neck Oncol 2010;2:19.
[13] Geets X, Daisne JF, Tomsej M, Duprez T, Lonneux M, Gregoire V. Impact of the type of imaging modality on target volumes delineation and dose distribution in pharyngo-laryngeal squamous cell carcinoma: comparison between pre- and per-treatment studies. Radiother Oncol 2006;78(3):291–7.
[14] Daisne JF, Duprez T, Weynand B, Lonneux M, Hamoir M, Reychler H, et al. Tumor volume in pharyngolaryngeal squamous cell carcinoma: comparison at CT, MR imaging, and FDG PET and validation with surgical specimen. Radiology 2004;233(1):93–100.
[15] Riegel AC, Berson AM, Destian S, Ng T, Tena LB, Mitnick RJ, et al. Variability of gross tumor volume delineation in head-and-neck cancer using CT and PET/CT fusion. Int J Radiat Oncol Biol Phys 2006;65(3):726–32.
[16] Paulino AC, Koshy M, Howell R, Schuster D, Davis LW. Comparison of CT- and FDG-PET-defined gross tumor volume in intensity-modulated radiotherapy for head-and-neck cancer. Int J Radiat Oncol Biol Phys 2005;61(5):1385–92.
[17] Hong R, Halama J, Bova D, Sethi A, Emami B. Correlation of PET standard uptake value and CT window-level thresholds for target delineation in CT-based radiation treatment planning. Int J Radiat Oncol Biol Phys 2007;67(3):720–6.
[18] Perez-Romasanta LA, Bellon-Guardia M, Torres-Donaire J, Lozano-Martin E, Sanz-Martin M, Velasco-Jimenez J. Tumor volume delineation in head and neck cancer with 18-fluor-fluorodeoxiglucose positron emission tomography: adaptive thresholding method applied to primary tumors and metastatic lymph nodes. Clin Transl Oncol 2013;15(4):283–93.
[19] Henriques de Figueiredo B, Barret O, Demeaux H, Lagarde P, De-Mones-Del-Pujol E, Kantor G, et al. Comparison between CT- and FDG-PET-defined target volumes for radiotherapy planning in head-and-neck cancers. Radiother Oncol 2009;93(3):479–82.
[20] Li H, Zhu XR, Zhang L, Dong L, Tung S, Ahamad A, et al. Comparison of 2D radiographic images and 3D cone beam computed tomography for positioning head-and-neck radiotherapy patients. Int J Radiat Oncol Biol Phys 2008;71(3):916–25.
[21] van Kranen S, van Beek S, Rasch C, van Herk M, Sonke JJ. Setup uncertainties of anatomical sub-regions in head-and-neck cancer patients after offline CBCT guidance. Int J Radiat Oncol Biol Phys 2009;73(5):1566–73.
[22] Schwartz DL, Garden AS, Shah SJ, Chronowski G, Sejpal S, Rosenthal DI, et al. Adaptive radiotherapy for head and neck cancer–dosimetric results from a prospective clinical trial. Radiother Oncol 2013;106(1):80–4.
[23] Wu Q, Chi Y, Chen PY, Krauss DJ, Yan D, Martinez A. Adaptive replanning strategies accounting for shrinkage in head and neck IMRT. Int J Radiat Oncol Biol Phys 2009;75(3):924–32.
[24] Castadot P, Lee JA, Parraga A, Geets X, Macq B, Gregoire V. Comparison of 12 deformable registration strategies in adaptive radiation therapy for the treatment of head and neck tumors. Radiother Oncol 2008;89(1):1–12.
[25] Thirion JP. Image matching as a diffusion process: an analogy with Maxwell's demons. Med Image Anal 1998;2(3):243–60.
[26] Richter A, Hu Q, Steglich D, Baier K, Wilbert J, Guckenberger M, et al. Investigation of the usability of conebeam CT data sets for dose calculation. Radiat Oncol 2008;3:42.
[27] Castelli J, Simon A, Henry O, Chajon E, Nassef M, Louvel G, et al. Do we need adaptive radiotherapy in head and neck cancer to decrease xerostomia?; 2013 [Poster ESMO, Available from: http://www.poster-submission.com/board/].
[28] Sherriff JM, Ogunremi B, Colley S, Sanghera P, Hartley A. The role of positron emission tomography/CT imaging in head and neck cancer patients after radical chemoradiotherapy. Br J Radiol 2012;85:e1120–6.
[29] Ceulemans G, Voordeckers M, Farrag A, Verdries D, Storme G, Everaert H. Can 18-FDG-PET during radiotherapy replace post-therapy scanning for detection/demonstration of tumor response in head-and-neck cancer? Int J Radiat Oncol Biol Phys 2011;81(4):938–42.
[30] Castaldi P, Rufini V, Bussu F, Micciche F, Dinapoli N, Autorino R, et al. Can "early" and "late"18F-FDG PET-CT be used as prognostic factors for the clinical outcome of patients with locally advanced head and neck cancer treated with radio-chemotherapy? Radiother Oncol 2012;103(1):63–8.
[31] Farrag A, Ceulemans G, Voordeckers M, Everaert H, Storme G. Can 18F-FDG-PET response during radiotherapy be used as a predictive factor for the outcome of head and neck cancer patients? Nucl Med Commun 2010;31(6):495–501.
[32] Hentschel M, Appold S, Schreiber A, Abolmaali N, Abramyuk A, Dorr W, et al. Early FDG PET at 10 or 20 Gy under chemoradiotherapy is prognostic for locoregional control and overall survival in patients with head and neck cancer. Eur J Nucl Med Mol Imaging 2011;38(7):1203–11.
[33] Chajon E, Lafond C, Louvel G, Castelli J, Williaume D, Henry O, et al. Salivary gland-sparing other than parotid-sparing in definitive head-and-neck intensity-modulated radiotherapy does not seem to jeopardize local control. Radiat Oncol 2013;8(1):132.

1.2.5.2 Place de l'imagerie en radiothérapie : conclusion

L'imagerie occupe une place centrale dans la radiothérapie adaptative. Les systèmes d'imagerie embarqués permettent une évaluation des variations anatomiques pouvant survenir en cours de traitement. Idéalement, cette imagerie pourrait servir à estimer en direct la dose délivrée et ainsi la comparer à la dose planifiée. Cette comparaison permettrait de déclencher une stratégie de radiothérapie adaptative dans un processus de radiothérapie guidée par la dose.

Cependant plusieurs questions demeurent sur les modalités d'imagerie (CBCT ou scanner) à utiliser, la qualité actuelle des CBCT rendant difficile la délinéation des volumes d'intérêts. La place de l'imagerie fonctionnelle (TEP ou IRM) reste également à définir, notamment en termes d'objectifs (amélioration du contrôle local en identifiant les patients mauvais répondeur ? Diminution de la toxicité en identifiant des modifications fonctionnelles précoces prédictives d'une toxicité ?). L'intégration de ces informations morphologiques et fonctionnelles dans le processus de replanification reste imprécise. La décision de replanification doit-elle reposer sur la détection d'une déviation sur l'imagerie du jour (évaluation à la séance) ou dans un contexte plus global sur l'ensemble des séances déjà réalisées, nécessitant alors une opération de cumul de dose ? Lorsque la décision de replanification, faut-il replanifier *de novo* en utilisant l'imagerie du jour ou bien faut-il prendre en compte la dose précédemment délivrée ?

1.3 Problématiques méthodologiques

1.3.1 Quels sont les objectifs thérapeutiques de la radiothérapie adaptative ?

La radiothérapie adaptative vise à corriger les variations quotidiennes de la tumeur et des tissus sains par une modification (en direct ou en différé) du plan de traitement initial. C'est une approche qui peut être assimilée à une technique de contrôle par retour d'information. Elle repose sur la détection de modifications (morphologiques, métaboliques ou dosimétrique) et le choix de réaliser une intervention suite à ces variations, le tout dans un objectif clinique global. Le niveau le plus simple de la radiothérapie adaptative serait d'assurer l'adéquation entre la dose planifiée et la dose délivrée, afin d'assurer l'épargne des tissus sains (en particulier les parotides), tout en maintenant la dose prescrite dans la tumeur. Une approche plus ambitieuse pourrait être d'utiliser le bénéfice dosimétrique de la radiothérapie adaptative pour réaliser une escalade de dose dans la tumeur afin d'augmenter encore le contrôle local. Cette approche pourrait se réaliser en utilisant des techniques de *dose painting* pour des patients identifiés comme étant à haut risque de récidive. Une autre approche serait d'identifier les patients à risque de toxicité, afin de leur proposer une stratégie de replanification pour diminuer autant que possible la dose dans les tissus sains. Enfin, dans une perspective de radiothérapie adaptative quotidienne en direct, une diminution voire une suppression des marges de traitement pourrait s'envisager, permettant ainsi de diminuer encore la toxicité. La radiothérapie adaptative pourrait ainsi répondre à un double objectif de diminuer la toxicité (en particulier la xérostomie) tout en améliorant le contrôle local.

1.3.2 Evaluation et simulation de traitements standards et de stratégies adaptatives

L'évaluation des différentes stratégies de radiothérapie (avec ou sans replanification) peut se faire par différents critères de jugement. Il est possible de réaliser une évaluation purement géométrique des variations anatomiques, sans critères dosimétriques. Une autre possibilité est une évaluation dosimétrique bidimensionnelle, sans information spatiale (analyse des histogrammes dose volumes (HDV)) ou tridimensionnelle (analyse des matrices de dose). La simulation des différentes stratégies peut alors se faire à la séance ou bien en cumulant la dose

séance après séance, grâce à des méthodes de recalage élastique (voir ci-après). Enfin l'utilisation de modèles de prédiction de résultats cliniques (*tumor control probability* (TCP) ou *normal tissue complication probability* (NTCP)) représente un autre niveau d'évaluation. La vérité terrain reste cependant représentée par les évènements cliniques réellement observés, nécessitant la réalisation d'essais thérapeutiques, idéalement de phase III.

Ces critères de jugement impliquent par ailleurs des méthodes d'analyses statistiques de complexités variables (test non paramétrique, modèle linéaire généralisée mixte, modèle de Cox, méthode d'apprentissage automatique (*machine learning),*…) afin de pouvoir les comparer.

1.3.3 Nécessité de développer des approches adaptées pour cumuler la dose : recalage déformable

a) Impossibilité d'additionner les HDV correspondant aux différentes séances

Il n'est, d'une façon générale, pas adapté d'additionner les histogrammes dose-volume (HDV) correspondant à différentes fractions de traitement. En effet, de par les déformations des tissus, les différentes « entrées » (*bins*) de l'histogramme peuvent ne pas correspondre aux mêmes tissus. Les doses correspondantes ne peuvent donc pas être simplement additionnées. L'exemple ci-dessous (Figure 7) illustre cette impossibilité de cumuler les HDV pour estimer la dose cumulée reçue par la vessie au cours d'une irradiation prostatique. La démonstration est faite à l'aide d'un fantôme numérique qui permet de quantifier effectivement la dose totale cumulée [75].

a) Cumul de dose par recalage déformable

Le recalage d'image consiste en la détermination d'une transformation géométrique permettant de mettre en correspondance les points d'un objet dans une vue donnée avec les points correspondants dans une autre vue du même objet ou d'un objet différent. Le recalage peut être utilisé pour trouver les correspondances entre les différentes images d'un même organe, pour évaluer les déformations d'un organe ou pour propager des contours entre différents patients (pour générer un atlas par exemple). Deux grandes catégories de recalage peuvent être identifiées, selon le type de transformation (rigide ou déformable) utilisée. Le recalage rigide est

global, avec six paramètres au maximum (3 axes de translations, 3 axes de rotations) alors que le recalage déformable est local (voxel à voxel), avec beaucoup plus de degrés de liberté. Le processus global du recalage élastique est illustré

Figure 8. Par un processus itératif, un champ de déformation est affiné suivant une métrique quantifiant la similarité entre les images à recaler.

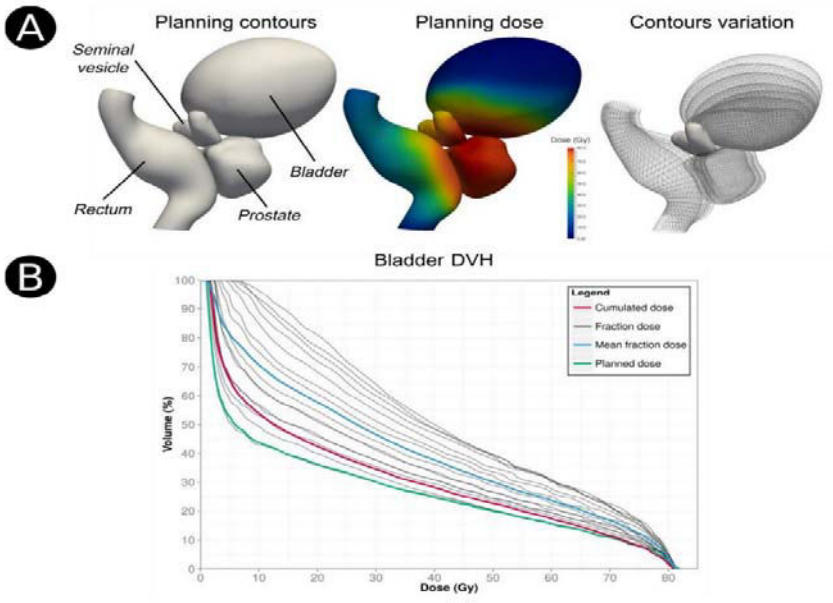

Figure 7 : La moyenne des histogrammes dose volume ne permet pas d'estimer la dose cumulée

DVH: Dose volume histogram

A pelvic numerical phantom [148] was designed (A) to compare dose accumulation using ground truth accumulated dose (in red) and DVH averaging (in blue) in the bladder for prostate cancer irradiation. The fraction dose DVHs are in grey (normalized to the total dose). The ground truth accumulated dose was obtained by propagating the fraction doses to the planning using the reference DVF resulting from biomechanical laws (*cf.* Section 4.4)

The cumulated dose appears superior to the planned dose. The mean fraction dose overestimates the dose received by the bladder

(Source : B. Rigaud, A. Simon, **J. Castelli** *et al*. Deformable image registration for radiation therapy : principle, methods, applications and evaluations. Submitted Acta Oncologica 2017)

Le cumul de dose exploite le recalage pour rapporter à l'anatomie de planification les matrices de dose correspondant à la dose délivrée. Le champ de déformation est estimé entre l'image de la

planification et une image acquise en cours de traitement. Ce champ est ensuite appliqué à la matrice de dose correspondant à la dose délivrée. Ainsi, le recalage élastique permet d'obtenir une dose cumulée au cours du traitement afin de pouvoir comparer la dose délivrée sans ou avec radiothérapie adaptative (Figure 9).

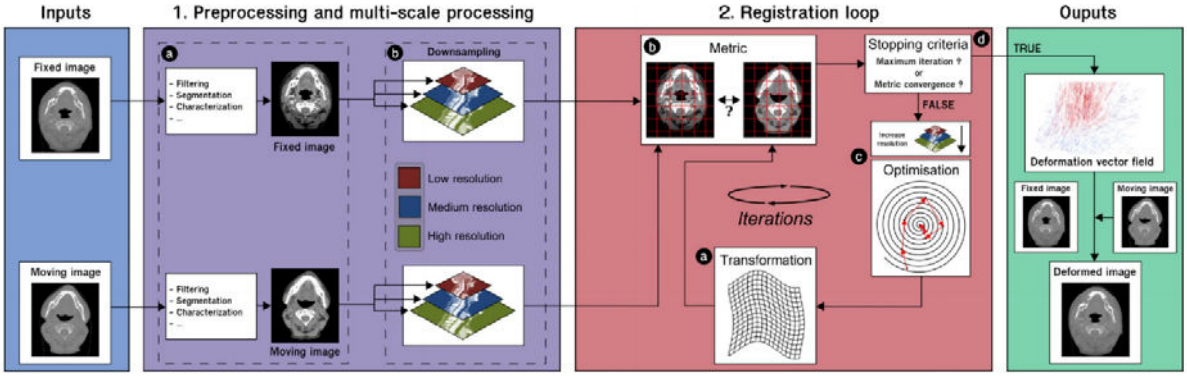

Figure 8 : Processus global pour le recalage déformable d'images

The deformable image registration workflow is divided into two steps:

In the preprocessing step, the input images can be improved either by increasing intensity contrast, segmenting regions of interest or extracting features (*e.g.* salient points, calcification, or metabolic information) (1a). Multi-scale images can be computed with multiple image resolutions downsampled from the original resolution or blurred images by using increasing smoothing filters (1b)

In the second step, the registration loop is launched. At each iteration, the geometric transformation (2a) is updated and the moving image is deformed accordingly. The goal is to find the transformation corresponding to the optimal value of the metric (2b) comparing the fixed image and the transformed moving image. The optimal transformation parameters, obtained by optimization (2c) until the stopping criteria (2d), enable generation of a deformation vector field (DVF) that warps the moving image to match the fixed image

(Source : B. Rigaud, A. Simon, **J. Castelli** *et al*. Deformable image registration for radiation therapy : principle, methods, applications and evaluations. Submitted Acta Oncologica 2017)

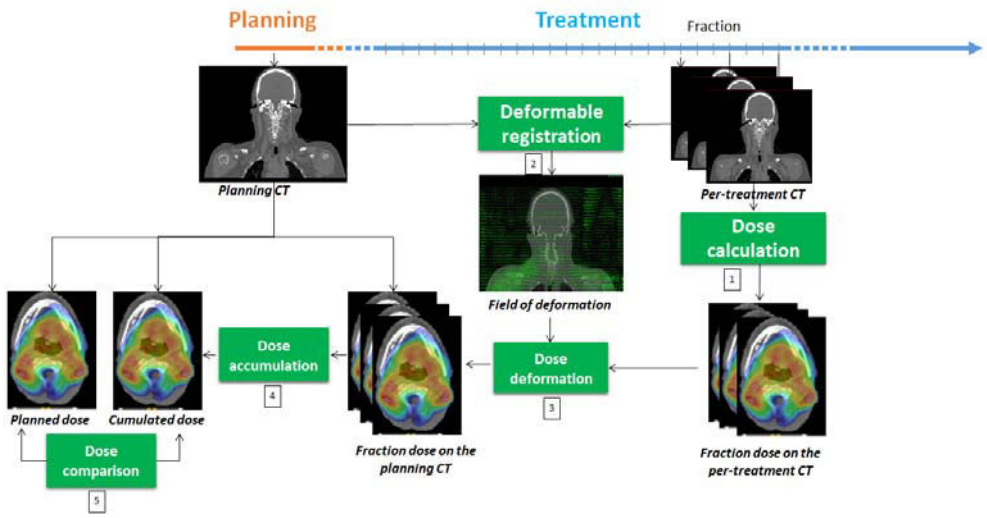

Figure 9 : Le recalage d'image utilisé pour le cumul de dose au cours d'un traitement de radiothérapie

The dose is first calculated at the fraction on the daily image (1), then the planning CT and the daily image are registered using DIR (2). The resulting deformation vector fields are used to propagate the fraction dose to the planning CT (3). The fraction doses are cumulated on the planning CT (4). The cumulated dose can be finally compared to the planned dose (5).

(Source: J.Castelli et al. Adaptive radiotherapy for head and neck cancers. Revision, Acta Oncologica 2017)

Le recalage élastique comporte des limitations à prendre à compte lors de la réalisation d'un cumul de dose. Ces difficultés sont résumées dans la Figure 10, certaines s'appliquant plus que d'autres à l'ORL. Ainsi, en ORL, une des principales limites est liée au fait qu'il est nécessaire d'avoir les mêmes tissus entre les deux images à recaler. Dans le cas contraire, il peut en résulter un champ de déformation erroné, et dans le cas du cumul de dose à des erreurs d'estimation de la dose. C'est pourquoi il paraît erroné de réaliser un cumul de dose par recalage élastique pour la tumeur du fait de la fonte tumorale survenant en cours de traitement. La précision du recalage point à point est également primordiale afin d'assurer un cumul de dose correct.

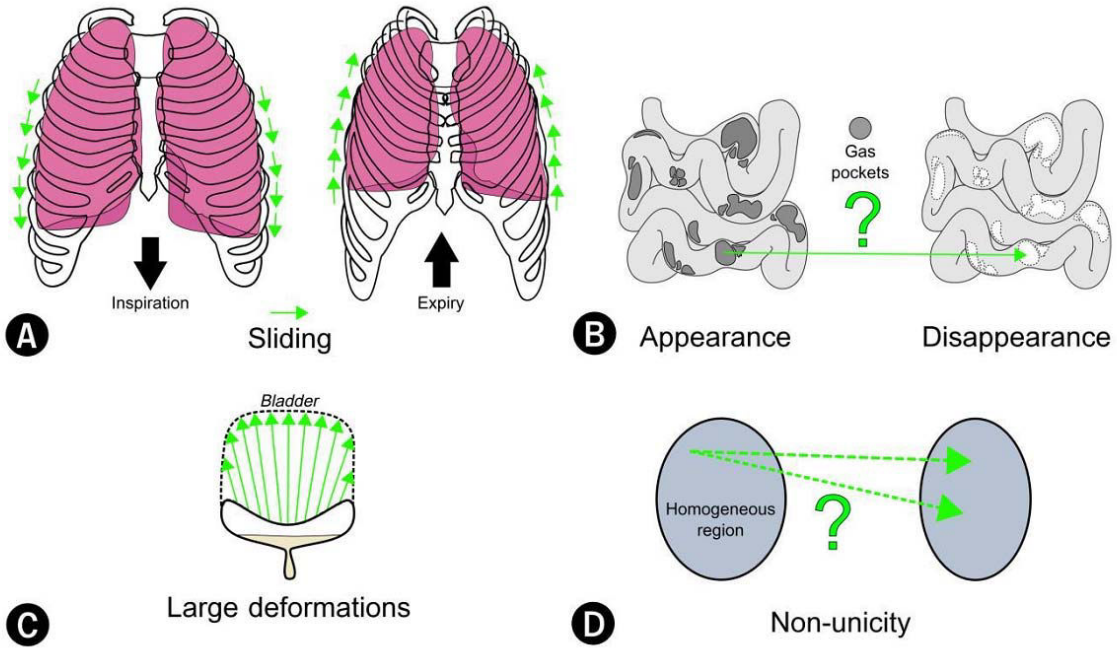

Figure 10 : Illustration des principales difficultés pour le recalage déformable

Organ sliding resulting from deformation vector field (DVF) topology discontinuities (A); Matter appearance/disappearance over time (B); Large local deformations (C); Non-unicity of the DVF where different correspondences can be associated for one point in a homogenous region (D)

(Source : B. Rigaud, A. Simon, **J. Castelli** *et al*. Deformable image registration for radiation therapy : principle, methods, applications and evaluations. Submitted Acta Oncologica 2017)

1.3.4 Tous les patients sont-ils candidats à une radiothérapie adaptative ?

La radiothérapie adaptive est une technique lourde, demandant du temps matériel et humain important [49, 76]. Les données portant sur l'impact dosimétrique sur les tissus sains des variations anatomiques survenant en cours de traitement montrent que tous les patients n'ont pas besoin d'une approche de radiothérapie adaptative (Table 4). Il apparait donc nécessaire d'identifier les patients qui auront un véritable bénéfice dosimétrique et surtout clinique d'une telle stratégie.

Table 4 : Variations de la dose pour les parotides et la moelle au cours d'une radiothérapie standard sans replanification

Auteurs	***Nb pts***	***Parotides Dose moyenne (Gy)***	***Moelle Dose max (Gy)***
Ahn [40]	23	+ 2,5 Gy	+ 3,8 Gy
Bando [63]	10	-	Cumulated dose > 40 Gy for 2 pts
Beltran [42]	15	+ 6 Gy	+ 2,5 Gy
Berwouts [43]	10	-	- 0,1 Gy (D5 %)
Bhide [44]	20	- 1 Gy	+ 2,6 Gy
Capelle [46]	20	-	+ 0.4 Gy (for 11 fr)
Chen [77]	25	-1,1% to -7,2%	+ 1,8-2,7 %
Dewan [47]	30	+3 Gy	+1,63 (D2 %)
Duprez [48]	21	-	No variations
Height [50]	10	-1 Gy	+ 0,5 Gy
Ho [51]	10	+0,2 Gy (D50)	+ 1,1 Gy
Hunter [78]	18	63 % des GP : +2.2 Gy 30 % des GP: -2 Gy	-
Jensen [52]	72	HL: + 4 % CL: + 11 % (Dose médiane)	-
Marzi [54]	15	+1.3 Gy	-
Nishi [55]	20	+ 5 Gy (Dose médiane)	+ 2,1 Gy
O'Daniel [26]	11	HL: + 3 Gy CL: + 1 Gy	No variations
Orban de Xivry [79]	10	< 1 Gy	+ 1,84 Gy (D2 %)
Robar [57]	15	+ 2 %	+ 1,2 %
Yip [62]	15	+ 2 %	-

- = Données non disponible, GP= gland parotide, Gy = Gray, CL= Controlatérale, HL =Homolatérale, fr= fraction, Dx = dose reçue par x% du volume.

En ce qui concerne le contrôle tumoral, près de 30 à 40% des patients traités par radiochimiothérapie vont présenter une récidive, en majorité dans les 2 ans suivant le traitement [5]. Les paramètres morphologiques utilisés dans la classification AJCC ne permettent pas d'identifier correctement ces patients à risque de récidive. L'intégration de nouveaux paramètres, notamment les données de métabolisme fourni par la tomographie par émission de positons (TEP), pourrait apporter une information supplémentaire sur le pronostic des patients. La TEP au ^{18}F-fluorodeoxyglucose (^{18}F-FDG) est devenue un examen de référence pour le bilan d'extension des cancers des VADS localement avancés [80]. Elle est utilisée en routine clinique dans le bilan

d'extension des cancers ORL localement avancés. Elle a montré sa supériorité par rapport au scanner ou à l'IRM notamment dans l'évaluation de l'atteinte ganglionnaire cervicale, la recherche de métastase ou en cas d'adénopathie sans primitif retrouvé [80-85]. Son utilisation en routine clinique est cependant essentiellement qualitative, reposant sur l'interprétation du médecin nucléaire. L'utilisation de paramètres quantitatifs, telle que le volume tumoral métabolique (*metabolic tumor volume* (MTV)) ou la glycolyse totale au sein du volume tumoral (*total lesion glycolysis* (TLG)), fournissant à la fois une information métabolique et de volume pourrait aider à l'identification de ces patients mauvais répondeurs, candidats à une intensification thérapeutique. Ces paramètres nécessitent cependant des opérations de seuillage pour les calculer et sont potentiellement machine dépendant, limitant actuellement leur utilisation en pratique clinique.

L'article suivant, publié dans *Critical Reviews in Oncology/Hematology* en octobre 2016 est une revue systématique de la littérature sur la valeur prédictive de la survie des paramètres TEP quantitatifs pour des patients traités par radiochimiothérapie pour des cancers ORL.

1.3.4.1 Overview of the predictive value of quantitative 18 FDG PET in head and neck cancer treated with chemoradiotherapy (article)

J.Castelli[1,2]; B. De Bari[1]; A.Depeursinge[3,4]; A.Simon[2,5]; A.Devillers[6]; G.Roman Jimenez[2,5,7] ; J.Prior[8] ; R.de Crevoisier[2,5,9]; M.Ozsahin [1], J.Bourhis[1]

Critical Reviews in Oncology/Hematology, 2016 Oct.

1. Radiotherapy Department, CHUV, Lausanne, Suisse
2. INSERM, U1099, Rennes, F-35000, France
3. Ecole Polytechnique Fédérale de Lausanne, CH-1015 Lausanne VD, Switzerland
4. University of Applied Sciences Western Switzerland, 3960 Sierre, Switzerland
5. Université de Rennes 1, LTSI, Rennes, F-35000, France
6. Nuclear Medecine Department, Centre Eugene Marquis, Rennes, F-35000, France
7. Keosys medical imaging, 1 impasse Augustin Fresnel, Saint-herblain, F-44815, France
8. Nuclear Medecine Department, CHUV, Suisse
9. Radiotherapy Department, Centre Eugene Marquis, Rennes, F-35000, France

Critical Reviews in Oncology/Hematology 108 (2016) 40–51

Contents lists available at ScienceDirect

Critical Reviews in Oncology/Hematology

journal homepage: www.elsevier.com/locate/critrevonc

Overview of the predictive value of quantitative 18 FDG PET in head and neck cancer treated with chemoradiotherapy

J. Castelli[a,b,c,*], B. De Bari[a], A. Depeursinge[d,e], A. Simon[b,c], A. Devillers[f], G. Roman Jimenez[b,c,g], J. Prior[h], M. Ozsahin[a], R. de Crevoisier[b,c,i], J. Bourhis[a]

[a] Radiotherapy Department, CHUV, Lausanne, Switzerland
[b] INSERM, U1099, Rennes, F-35000, France
[c] Université de Rennes 1, LTSI, Rennes, F-35000, France
[d] University of Applied Sciences Western Switzerland, 3960 Sierre, Switzerland
[e] Ecole Polytechnique Fédérale de Lausanne, CH-1015 Lausanne VD, Switzerland
[f] Nuclear Medecine Department, Centre Eugene Marquis, Rennes, F-35000, France
[g] Keosys Medical imaging, 1 Impasse Augustin Fresnel, Saint-Herblain, F-44815, France
[h] Nuclear Medecine Department, CHUV, Switzerland
[i] Radiotherapy Department, Centre Eugene Marquis, Rennes, F-35000, France

Contents

ARTICLE INFO

Article history:
Received 27 June 2016
Received in revised form 8 October 2016
Accepted 26 October 2016

Keywords:
PET
Head and neck cancer
Chemoradiotherapy
Clinical outcome

ABSTRACT

18 F-fluorodeoxyglucose (18F-FDG) positron emission tomography/computed tomography (PET/CT) allows to quantify the metabolic activity of a tumor (glycolysis) and has become a reference tool in oncology for the staging, restaging, radiotherapy planning and monitoring response in many cancers. Quantitative analyses have been introduced in order to overcome some of the limits of the visual methods, allowing an easier and more objective comparison of the inter- and intra-patients variations. The aims of this review were to report available evidences on the clinical value of quantitative PET/CT parameters in HNC.

Forty-five studies, for a total of 2928 patients, were analyzed. Most of the data available dealt with the intensity of the metabolism, calculated from the Standard Uptake Value (SUV). Metabolic Tumor Volume (MTV) was well correlated with overall survival and disease free survival, with a higher predictive value than the maximum SUV. Spatial distribution of metabolism and textural analyses seems promising.

1. Introduction

Head and neck cancers are among the most common in the world (5th leading cancer by incidence (Parkin et al., 2005)). The American Joint Committee on Cancer (AJCC) staging is gen-

* Correspondence to: Department of Radiation Oncology, Centre Eugene Marquis avenue de la Bataille Flandre Dunkerque, F–35000 Rennes, France.
E-mail address: j.castelli@rennes.unicancer.fr (J. Castelli).

http://dx.doi.org/10.1016/j.critrevonc.2016.10.009
1040-8428/

erally used to estimate the prognosis and guide therapy (Edge and Compton, 2010). Radio-chemotherapy is a standard treatment of unresectable and/or locally advanced Head and Neck Cancers (Pignon et al., 2000; St Guily et al., 2010). Despite this treatment, the prognosis remains worst and loco-regional recurrence may occur in up to 40% patients, mostly within the first 2-years after treatment (Chajon et al., 2013). ^{18}F-fluorodeoxyglucose (^{18}F-FDG) positron emission tomography/computed tomography (PET/CT) allows to quantify the metabolic activity of a tumor (glycolysis) and has become a reference tool in oncology for the staging, radiotherapy planning and monitoring tumor response in many cancers (Cacicedo et al., 2016; Fletcher et al., 2008). For primary tumor diagnosis, ^{18}F FDG-PET imaging showed a significant better sensitivity (93% vs 65%) and specificity (70% vs 56%) over CT (Gambhir et al., 2001). PET imaging allows a more accurate nodal staging of locally advanced head and neck cancer (Kyzas et al., 2008; Yoo et al., 2013), and could result in changing the therapeutic management in nearly 15% of patients (Lonneux et al., 2010). For patients with cervical node metastases of unknown primary, PET/CT detected a primary tumor in nearly 30% of patients (Rudmik et al., 2011; Wong et al., 2012; Zhu and Wang, 2013).

Thanks to these potential advantages, PET/CT is recommended for the initial staging and for the treatment decision algorithm of advanced head and neck cancer (Yoo et al., 2013). However, in almost all of these studies, only a visual analysis of PET/CT by physician, based on contrast in uptake between normal tissues and potential tumor (i.e. operator dependent), was performed. Visual analysis was sufficient for diagnosis, staging and detection of recurrence, but with the goal of predicting patient' outcome, quantification is necessary. More recently, quantitative analyses have been introduced in order to overcome some of the limits of the visual methods (Table 1). Indeed, quantitative analysis is less operator dependent than visual analysis and can be fully automated, allowing an easier and more objective comparison of the inter- and intra-patient variations. The main goal of the quantification is to obtain parameters reflecting the tumor activity and/or having a prognostic value.

The aims of this review were to report available evidences on the value of quantitative parameters from PET/CT performed at the diagnosis, during treatment and during follow to predict overall- and disease free survival in head and neck cancer and to discuss theirs limits.

2. Materials and methods

We performed a systematic electronic search of articles published in PubMed/MEDLINE from January 2000 to march 2016. Our search was restricted to articles reporting data obtained on humans and to English-written articles dealing with locally advanced head and neck cancer and PET/CT. All the articles which did not report data on the prognostic value of PET/CT-related parameters were excluded as well as all the articles which reported data obtained only from visual analyses. Hence this review was focused on the prognostic value of parameters obtained from quantitative or semi-quantitative analyses. We included all the studies reporting data on PET/CT performed before, during or after exclusive RT +/− CT, excluding those reporting data from surgical series and/or post-operative radio-chemotherapy. The predictive value of PET at diagnosis, during treatment and during follow up was analyzed separately.

3. Results

One hundred and twenty-five studies were identified according to the criteria described above. Seventy-seven studies were excluded since they did not match the inclusion criteria, mainly because they dealt with operated patients (22/77 studies). One retrospective study presenting data on a small population (<20 patients) was also excluded. Finally, 45 studies were included in the analysis, for a total of 2928 patients. Table 2 summarizes the main characteristics of the studies included in this analysis, while Table 3 summarizes the principal results of these studies.

3.1. Predictive value of 18FDG PET before treatment with RT-CT

Forty-two studies investigated the predictive value of quantitative PET parameters at diagnosis (Table 4). The large majority of these studies analyzed parameters based on Standard Uptake Value (SUV), while only 3 studies performed texture or shape analysis.

3.1.1. SUVmax and metabolic tumor volume

Maximum standard uptake value (SUVMax) corresponding to the maximal pixel value in the tumor. Thanks to its ease of use, it was historically the first parameter analyzed. SUVmax was correlated with overall- or disease free survival in 11 studies (Allal et al., 2002; Brun et al., 2002; Castaldi et al., 2012; Chen et al., 2014; Farrag et al., 2010; Higgins et al., 2012; Kitagawa et al., 2003; Machtay et al., 2009; Matoba et al., 2015; Rasmussen et al., 2015; Sanghera et al., 2005). SUVmax allows to identify patients with a high risk of events (death or recurrence). For example, (Rasmussen et al., 2015) analyzed 287 patients with locally advanced head and neck cancers treated with radiotherapy ± chemotherapy. SUVmax showed a higher predictive value for recurrence than T stage, N stage and age. The authors developed a prognostic model of freedom from failure at 2 years, in which including SUVmax significantly increased the predictive value, changing the estimated risk by more than 10% for 23% of the patients. In (Allal et al., 2002), 63 patients treated with RT ± CT were prospectively included. Patients presenting a SUVMax <5.5 g/ml had a 3-year DFS of 79% compared to 42% for those with SUVmax > 5.5 g/ml ($p = 0.005$). However, the range of cutoff values adopted in published studies to define patients at high or low risk of events markedly varied between 3.7 and 9 g/ml (median: 5.8). Noteworthy, also 2 negative studies are available in the literature (Ashamalla et al., 2014; Greven et al., 2001). In (Greven et al., 2001), patients with local recurrence had a mean pretreatment SUV_{Max} of 7.7 g/ml versus 8.2 g/ml for patients without local recurrence. In (Ashamalla et al., 2014), SUVMax was correlated with OS in univariate analysis, but not in multivariate analysis. Only 28 patients were included in this study, which may explain this negative result.

The Metabolic Tumor Volume (MTV), defined as the volume of FDG activity in a tumor assessed by automated volume of interest delineation, and Total Lesion Glycolysis (TLG), defined as MTV x SUVmean, may be more representative of the tumor heterogeneity. The predictive value of MTV was evaluated in 26 studies, with 21 of them also evaluating SUVMax (for a total of 1464 patients). All these studies showed that MTV/TLG were predictive for clinical outcome, with a higher predictive value than SUVmax. In (Chang et al., 2012), 108 patients with nasopharyngeal cancer treated with RT-CT were prospectively included to assess the predictive value of SUVMax, MTV and TLG for DFS and OS. Only Epstein–Barr virus DNA load and TLG of the tumor were significantly correlated with DFS and OS. In particular, patients presenting a TLG value < 65 g showed a 3-year DFS of 79.9% versus 37.4% for other patients ($p < 0.001$), with a hazard ratio of 3.54 ($p = 0.006$) for DFS and of 4.91 ($p = 0.045$) for OS.

In two studies, MTV was found to have a higher predictive value than TNM staging (Kao et al., 2012; Romesser et al., 2014). (Romesser et al., 2014) reported data of 100 oropharyngeal cancer, treated with RT-CT (median follow-up: 49 months). MTV at a cutoff of 9.7 ml was correlated with DFS (80.3% vs 56.7%, $p = 0.015$) and OS

Table 1
Most frequently used quantitative parameters in PET imaging.

Parameters	Definition and method to compute
SUV_{Max}	Maximal pixel value in the tumor
SUV Peak	Average SUV within a small, fixed-size region of interest (ROIpeak) of 1.2 cm diameter, centered on a high-uptake part of the tumor
Metabolic Tumor Volume (MTV)	Sum of the volume of voxels with SUV exceeding a certain threshold value in a tumor
SUV Mean	Average SUV in the ROI (defined by applying a threshold or by visual assessment)
Total Lesion Glycolysis (TLG)	TLG is obtained by multiplying MTV and the mean SUV of the MTV

(84.1% vs 57.8% p = 0.008). In multivariate analysis, only MTV was significant while GTV, T stage and N stage did not.

Noteworthy, the reproducibility of the MTV and/or TLG may be limited by the initial definition of these parameters, which is based on a threshold of SUV, absolute (all pixels with SUV value > x) or relative (all pixels with SUV value > xx% of SUVMax). The choice of the threshold for either method may affect the absolute value of the MTV. Six studies compared the predictive value of MTV and/or TLG computed with different thresholds (Cheng et al., 2015; Kao et al., 2012; Lin et al., 2015; Schinagl et al., 2011; Yabuki et al., 2015). In the study by (Schinagl et al., 2011), 4 thresholds (2.5, 40%, 50% and adaptive threshold based on liver uptake) were compared for 77 patients treated with RT ± CT. MTV 40% was the strongest predictor of DFS and OS. However, even if the predictive value of the other thresholds was slightly lower, they were also correlated with OS and DFS. Same results were reported by the others studies. Based on these results, the use of different thresholds within a reasonable range (between 2 and 3 for an absolute threshold; and between 40 and 50% for a relative threshold) seems to have no major impact on the predictive value of MTV.

3.1.2. Texture and shape analysis

Two different approaches have been used to evaluate tumor heterogeneity, one morphological at macroscopic level (shape of the metabolic area) and the other at pixel level (texture analysis). (Apostolova et al., 2014) used a new parameter to characterize the deviation of the tumor's shape from sphere symmetry (asphericity). The initial assumption of the authors was that "aggressive" tumors are expected to show more irregular shapes, due to necrosis, angiogenesis and extravascular extracellular matrix. In a first study, including patients treated with surgery, radiotherapy or chemotherapy alone, asphericity was correlated with OS and PFS. Based on these results, the authors tried to confirm the predictive value of asphericity in a following study (Hofheinz et al., 2015). Thirty-three patients, with LAHNC treated with RT-CT were included. Using the same cutoff of 20.4 found in (Apostolova et al., 2014), asphericity was correlated with PFS (HR 2.96, p = 0.015) and OS (HR 5.9, p = 0.001).

Two studies evaluated the prognostic value of texture analysis in LAHNC. In the first study (Cheng et al., 2013), including 70 oropharyngeal cancers, TLG and texture uniformity were correlated with OS (HR 5.85 and 0.46 respectively). A 3-point risk scale for DFS and OS was proposed, according to the presence of a uniformity ≤ 0.138 and a TLG > 122.9 g. One point was given for each factor. Clinical outcome (DFS or OS) was significantly different in the 3 risk groups. These findings were confirmed in an independent series of 88 oropharyngeal cancer patients (Cheng et al., 2015).

3.2. Predictive value of quantitative PET parameters during chemoradiotherapy

Early changes in tumor metabolism during radiochemotherapy may be assessed by PET/CT and may be used to tailor treatment. The aims of this adaptive strategy to the treatment' response are to decrease the adverse effect and/or to intensify the treatment, with the final goal to improve the outcome.

Seven studies (374 patients) evaluated the predictive value of PET performed during RT ± CT (Brun et al., 2002; Castaldi et al., 2012; Chen et al., 2014; Farrag et al., 2010; Hentschel et al., 2011; Min et al., 2016, 2015). All but one of them found a correlation between PET parameters RT ± CT and clinical outcome. In a study by Min et al., 100 patients received a PET before and 3 weeks after the beginning of treatment (Min et al., 2016). The authors showed that pre-treatment SUVMax and mid-treatment TLG were correlated with 2-year DFS in multivariate analysis (83% vs 71.4%, p = 0.0019 and 88.4% vs 77.2%, p = 0.012, respectively). Moreover, patients presenting pretreatment TLG < 91 g and a mid-treatment TLG < 9.4 g presented a better 2-year DFS (88.1% vs 61.1%, p = 0.001) and 2-year OS (90% vs 67%, p = 0.012). Other parameter,such as SUVMax and MTV were also correlated to DFS and OS, but TLG was the most predictive one. In (Castaldi et al., 2012), which included 24 patients, no predictive value of PET during treatment was shown. However, the decrease of SUVmax between PET at diagnosis and during treatment was highly correlated with 2-year DFS (100% in case of complete response vs 74% in case of partial response, defined as a reduction of 25% in tumor 18FDG SUV (Young et al., 1999)).

The optimal time to perform PET during treatment is still unclear. Most of the studies performed the PET before the third week to allow time for adapting therapy. A prospective multicentric study (TEMPORAL) (NCT02469922) is undergoing to assess the predictive value of PET at the 2nd and 4th week of chemoradiotherapy. One hundred twenty-three patients are expected to be included.

3.3. Predictive value of 18FDG PET after treatment

After treatment with radiotherapy, PET/CT may be used to identify good responders and avoid useless neck dissection. Twelve studies performed a quantitative or semi quantitative analysis from PET after treatment. All these studies evaluated the SUVMax. A high SUVMax in post treatment was correlated with a poor outcome in 6 studies (Horiuchi et al., 2008; Hoshikawa et al., 2011; Ito et al., 2014; Kim et al., 2016; Kitagawa et al., 2003; Moeller et al., 2010). In (Moeller et al., 2010), 98 patients underwent a PET before and 8 weeks after RT +/− CT. The authors found that a post-treatment SUVMax ≤ 6 g/ml and the variation of SUVMax (in%) between the pre- and post-irradiation PET/CT were predictive for DFS. In (Kim et al., 2016), a PET was performed 3 months after RT-CT. Seventy-eight patients were analyzed. Three-year OS was 87.7% in patients with SUVMax < 4.4 g/ml versus 56.9% (p = 0.002).

A comparison between visual analysis and quantitative parameters was performed by (Hoshikawa et al., 2009). Thirty-five patients underwent PET before and 5 weeks after RT-CT. Patients with a post-treatment SUVMax value > 3 g/ml and decreasing less than 60% compared to the pre-treatment situation presented a higher risk of recurrence (odds ratio = 61.5, p < 0.0001). The overall accuracy for quantitative analysis was 89.9% vs 60.9% for the visual analysis.

Table 2
Main criteria of the 45 studies. * = Mean follow up, CR: Complete Response, LCR: Loco Regional Response, LR: Local Relapse, DSS: Disease Specific Survival, RFS: Recurrence Free Survival, LRFS: Local Relapse Free Survival, DFS: Disease Free Survival, OS: Overall Survival, MTV: Metabolic Tumor Volume, TLG: Total Lesion Glycolysis.

Authors	Year	Subject No.	Study Design	Timing of te PET-CT	Follow up	Localisation	Treatment	End point	Quantitative PET parameters
Greven	2001	45	Prospective	Pre post	N/A	HNC	RT	LR	SUV_{Max}
Allal	2002	63	Prospective	Pre	36	HNC	RT ± CT	DFS OS	SUV_{Max}
Brun	2002	47	Prospective	Pre and per	39.6	HNC	RT ± CT	CR LRC OS	SUV_{Max} Metabolic rate FDG
Kitagawa	2003	20	Prospective	Pre, post	52.8	HNC	CRT	CR	SUV_{Max}
Sanghera	2005	12	Prospective	Pre	24	HNC	RT	OS	SUV_{Max} at 1 and 2 h, SUV_{Max} Difference
Horiuchi	2008	31	Retrospective	Pre and post	N/A	HNC	CRT	LR	SUV_{Max}
Chung	2009	82	Retrospective	Pre	34.8*	Pharynx	RT ± CT	LR DFS OS	SUV_{Max} MTV 2.5
La	2009	85	Retrospective	Pre	20.4*	HNC	RT ± CT	OS DSF LRC	SUV_{Max} MTV 50%
Machtay	2009	60	Retrospective	Pre	N/A	HNC	RT ± CT	OS DFS	SUV_{Max}
Suzuki	2009	45	Retrospective	Pre	24*	HNC	RT	OS DFS	SUV_{Max}
Farrag	2010	43	Prospective	Pre and Per	12.7	HNC	CRT	OS DFS LRRFS	SUV_{Max}
Moeller	2010	98	Prospective	Pre and post	24	HNC	RT ± CT	DFS	SUV_{Max} T Change in SUV_{Max} T
Seol	2010	59	Retrospective	Pre	N/A	HNC	Neo CT ± RT	DFS OS	SUV_{Max} SUVMean MTV 2.5
Deron	2011	22	Retrospective	Pre	20	HNC	RT ± CT	DFS OS	SUV_{Max} MTV 50%
Hentschel	2011	37	Prospective	Pre and per	26	HNC	CRT	DFS OS LRC	SUV_{Max} SUVMean MTV 50%
Hoshikawa	2011	35	Prospective	Pre and post	50	HNC	RT ± CT	Recurrence	SUV_{Max}
Murphy	2011	47	Retrospective	Post	34	HNC	CRT	DFS OS	SUV_{Max} MTV 2, 2.5, 3, 3.5, 4 TLG

Table 2 (*Continued*)

Authors	Year	Subject No.	Study Design	Timing of te PET-CT	Follow up	Localisation	Treatment	End point	Quantitative PET parameters
Schinagl	2011	77	Prospective	Pre	46	HNC	CRT	DFS OS	SUV_{Max} SUVMean MTV 40% 50% MTV 2.5 GTV −PET
Castaldi	2012	24	Prospective	Pre per and post	29.2	HNC	CRT	RFS DSS	SUV_{Max} Change in SUVMax (EORTC criteria)
Chang	2012	108	Prospective	Pre	N/A	Nasopharynx	CRT	OS DFS LRFS	SUV_{Max} MTV 2.5 TLG
Chu	2012	51	Retrospective	Pre	17.5	HNC	RT ± CT	OS DFS	SUV_{Max} MTV50% MTV Velocity
Higgins	2012	88	Retrospective	Pre	15	HNC	RT ± CT	DFS LRC OS	SUV_{Max} SUVMean TLG (manuelly delineated)
Kao	2012	64	Retrospective	Pre	24	Pharynx	RT ± CT	DFS PRFS	MTV 2.5 3.0 40% 50%
Romesser	2012	41	Retrospective	Pre	24.2	HNC	RT ± CT	OS DFS LRFS	SUV_{Max} MTV (Gradient based method)
Tang	2012	83	Retrospective	Pre	20	HNC	CRT	OS DFS	SUV_{Max} MTV 50%
Cheng	2013	70	Retrospective	Pre	>24	Oropharynx	CRT	OS DFS	MTV 2.5 TLG Textural features
Ashamalla	2014	28	Retrospective	Pre and post	36*	HNC	RT ± CT	OS	SUVMax SUVMean Anatomical biological value = SUVMax x greatest tumor diameter
Chen	2014	51	Prospective	Pre and per	23	Pharynx	RT ± CT	OS DFS	SUV_{Max} pre and per SUV reduction ratio
Hanamoto	2014	118	Prospective	Pre	N/A	HNC	CRT	LR	SUV_{Max} SUVMean MTV 2.5 TLG
Ito	2014	36	Retrospective	Post	23.8*	HNC	CRT	OS LC	SUV_{Max}
Romesser	2014	100	Retrospective	Pre	49	Oropharyngeal	CRT	LRC DFS OS	SUV_{Max} MTV 42%
Sager	2014	74	Retrospective	Pre	23	HNC	CRT	DFS OS	SUV_{Max} MTV 50%
Akagunduz	2015	62	Retrospective	Pre	18	HNC	RT ± CT	LRFS DFS OS	SUV_{Max} SULMax MTV (adaptive threshold based)
Cheng	2015	88	Retrospective	Pre	32	Oropharynx	CRT	DFS DSS	MTV 50% 42% 2.5 and adaptive threshold TLG Textural features

Table 2 (*Continued*)

Authors	Year	Subject No.	Study Design	Timing of te PET-CT	Follow up	Localisation	Treatment	End point	Quantitative PET parameters
Hofheinz	2015	37	Prospective	Pre	27*	HNC	CRT	DFS OS	SUV_{Max} SUVMean MTV (adaptive threshold) TLG Asphericity
Lin	2015	91	Retrospective	Pre	18	Pharynx	CRT	OS DFS	SUV_{Max} Nodal MTV2.5 N MTV40% N MTV50% N TLG40% N TLG50% N
Matoba	2015	33	Prospective	Pre and post	N/A	HNC	CRT	LRC DFS OS	SUV_{Max} EORTC Criteria
Min	2015	72	Retrospective	Pre and per	25	HNC	CRT	LRFS DFS MFFS OS	SUV_{Max} MTV 2.5 TLG Percentage reduction between per and pre treatment PET
Moon	2015	44	Retrospective	Pre	34.7	Nasopharynx	CRT	DFS	SUV_{Max} SUVMean MTV (adaptive threshold) TLG
Rasmussen	2015	287	Retrospective	Pre	32	HNC	RT ± CT	Time to failure	SUV_{Max} SUVMean SUVPeak
Schwartz	2015	74	Retrospective	Pre and post	50.4	HNC	CRT	LR DFS OS	SUV_{Max} SUVPeak MTV 40%
Yabuki	2015	118	Retrospective	Pre	36	Larynx	CRT	OS DFS	SUV_{Max} MTV 2, 2.5, 3
Kim	2016	78	Retrospective	Post	52.7	HNC	CRT	DFS OS	SUV_{Max}
Min	2016	100	Retrospective	Pre and per	20	HNC	RT ± CT	LRFS DFS MFFS OS	SUV_{Max} MTV 2.5 TLG Percentage reduction between per and pre treatment PET

Table 3
Correlation between PET quantitative parameters and clinical outcome. CR: Complete Response, LCR: Loco Regional Response, LR: Local Relapse, DSS: Disease Specific Survival, RFS: Recurrence Free Survival, LRFS: Local Relapse Free Survival, DFS: Disease Free Survival, OS: Overall Survival, MTV: Metabolic Tumor Volume, TLG: Total Lesion Glycolysis.

Timing	Authors	Year	End point	Used PET parameters	Significant Prognostic parameters	Threshold	Clinical outcome	Hazard Ratio
Pre and post	Greven	2001	LR	SUVMax	None			
Pre	Allal	2002	DFS OS	SUVMax	SUVMax (DFS)	5.5	3-year DFS 79% vs 42%	N/A
Pre and per	Brun	2002	Complete response (CR) LRC OS	SUVmax Metabolic rate (MR) FDG	Pre Treatment: SUVMax Tumor (CR and LCR) Per Treatment: SUVMax Tumor (CR and LCR), MR Tumor and lymph node (CR and LCR) MR FDG per OS	Pre treatment SUVmaxT = 9 Per trt SUVmaxT = 5	SUVmax pre trt CR 96% vs 64% (p=0.01) LRC 96 vs 57 (p=0.003) MR Tumor per trt CR 96 vs 62% (p=0.007) LRC 96 vs 55% (p = 0.002) OS 72% vs 35% (p = 0.0042) SUVMax per trt LCR 91% vs 62 (p=0.031)	
Pre and post	Kitagawa	2003	Clinical response	SUVMax	SUVMax	N/A	N/A	N/A
Pre	Sanghera	2005	OS	SUVMax at 1 and 2 h, SUVMax Difference	SUV difference	16%	N/A	N/A
Pre and post	Horiuchi	2008	LR	SUVMax	SUVMax Post trt	3.7	N/A	
Pre	Chung	2009	LR DFS OS	SUV Max MTV 2.5	MTV	40		DFS 3.42 (p = 0.04)
Pre	La	2009	OS DFS LRC	SUVMax MTV 50%	MTV50% (OS and DFS)	N/A	N/A	Increase of 17.4 ml of MTV50% = HR 1.9 (first event) and 2.1 (death)
Pre	Machtay	2009	OS DFS	SUVMax	SUVMax	9	2 year DFS 76 vs 37% (p = 0.007) 2 year OS 82% vs 46% (p = 0.016)	DFS: 2.41 (p = 0.03) OS: 2.47 (p = 0.06)
Pre	Suzuki	2009	OS DFS	SUVMax	None	5.5	N/A	N/A
Pre and Per	Farrag	2010	OS DFS LRRFS	SUVMax	Pre: SUVMax (OS) Per SUVmax (OS)	Pre trt: 8.11 Per trt: 4.03	2-year OS SUVmax pre trt 81% vs 50% (p = 0.027) SUVMax Per trt 82 vs 47% (p = 0.026)	N/A
Pre and post	Moeller	2010	DFS	SUVMax T Change in SUVMax T	SUVMax Post Change in SUVMax	6	N/A	N/A
Pre	Seol	2010	DFS OS	SUVMax SUVMean MTV 2.5	MTV	9.3 cm^3	N/A	DFS: 2.19 (p = 0.006) OS: 1.62 (p = 0.051)
Pre	Deron	2011	DFS OS	SUVMax MTV 50%	MTV50(DFS OS)	31 cm^3	N/A	N/A
Pre and per	Hentschel	2011	DFS OS LRC	SUVmax SUVMean MTV 50%	ΔSUVmax10/20 (OS) MTV50 TEP 0 (OS)	ΔSUVmax10/20 50% MTV50% 10.2	2 year OS ΔSUVmax10/20 88% vs 38% (p = 0.02) MTV 50% 83% vs 34% (p = 0.02)	N/A
Pre and post	Hoshikawa	2011	Recurrence	SUVMax	SUVMax Post % change in SUV	60%	N/A	Odds ratio local control 61.5 (p < 0.001)
Post	Murphy	2011	DFS OS	SUVMax MTV 2, 2.5, 3, 3.5, 4 TLG	Post trt: MTV2.0 (DFS OS)	15 cm^3	N/A	Increase of 21 cm^3: 2.5 (DFS) and 2 (OS)
Pre	Schinagl	2011	DFS OS	SUVMax SUVMean MTV 40% 50% MTV 2.5 GTV −PET	GTV PET (LC DFS OS in oral cavity and oropharyngeal cancer) MTV40% (DMFS DFS OS)	N/A	N/A	N/A

Table 3 (*Continued*)

Timing	Authors	Year	End point	Used PET parameters	Significant Prognostic parameters	Threshold	Clinical outcome	Hazard Ratio
Pre per and post	Castaldi	2012	RFS DSS	SUVMax Change in SUVMax (EORTC criteria)	EORTC criteria post	N/A	2 year DSS (late TEP) CR 100% PR 74% PD 33% p=0.009	N/A
Pre	Chang	2012	OS DFS LRFS	SUVMax MTV 2.5 TLG	TLG T (OS DFS)	65 g	3-year DFS 79.9% vs 37.4% (p < 0.001)	DFS: 3.54 OS: 4.9
Pre	Chu	2012	OS DFS	SUVMax MTV50% MTV Velocity (Difference between the 2 pre treatment TEP)	MTV T	N/A	N/A	Increase of 1cc/week = 85% increase of the risk of death
Pre	Higgins	2012	DFS LRC OS	SUVMax SUVMean TLG (manuelly delineated)	SUVMean (DFS)	7 (median)	2 year DFS 82% vs 58% p = 0.03	DFS: 1.14 (p = 0.014)
Pre	Kao	2012	DFS PRFS	MTV 2.5 3.0 40% 50%	MTV 2.5 (DFS PRFS)	13.6 ml	2-year PRFS 72% vs 39% (p = 0.001) 2-year DFS 68% vs 41% (p = 0.008)	DFS HR 2.69 p = 0.011 PRFS HR 3.76 p = 0.003
Pre	Romesser	2012	OS DFS LRFS	SUVMax MTV (Gradient based method)	MTV	7.2	2-year LC 100 vs 54.2% (p = < 0.001) DFS 94.7 vs 39.4% (p = 0.001) OS 94.7 vs 64.2 (p = 0.04)	N/A
Pre	Tang	2012	OS DFS	SUVMax MTV50%	MTV50% T (OS and DFS)	Increase of 17 cm^3 (differencebetweenfirstandthirdquartiles)	N/A	DFS: 2.07 (p = 0.00017) OS: 1.99 (p = 0.0048)
Pre	Cheng	2013	PFS DSS OS	MTV 2.5 TLG Normalized gray-level co-occurence matrix Neighborhood gray-tone difference matrix	TLG (PFS DSS OS) Uniformity (PFS DSS OS)	TLG 121.9 g Uniformity 4 bins 0.138	N/A	PFS TLG: 7.15(p = 0.02) Uniformity: 0.32 (p = 0.001) OS TLG: 5.85 (p = 0.011) Uniformity: 0.46 (p = 0.017)
Pre and post	Ashamalla	2014	OS	SUVMax SUVMean Anatomical biological value = SUVMax X greatest tumor diameter	None	N/A	N/A	N/A
Pre and per	Chen	2014	OS DFS	SUVMax pre et per (T et N) SUV reduction ratio	SUV reduction ratio tumor	3.9	2-year DFS 64% vs 41% (p = 0.045) 2 year OS 66% vs 47% (p = 0.035)	DFS: 2.33 OS: 2.64
Pre	Hanamoto [67]	2014	LR	SUVMax SUVMean MTV 2.5 TLG	For laryngeal and hypopharyngeal cancer, High MTV (> 25 ml) or high TLG (> 144.8 g) = high risk of partial response	N/A	N/A	13.4 (p = 0.003)
Post	Ito	2014	OS LC	SUVMax	SUVMax (OS)	6.1	OS 12.1 vs 44.6 months (p < 0.001)	N/A
Pre	Romesser	2014	LRC PFS OS	SUVMax MTV 42%	MTV (Distant metastasis, Disease progression or death)	9.7	5-year PFS 80.3% vs 56.7% (p = 0.015) 5-year OS 84.1% vs 57.9% (p = 0.008)	PFS: HR2.17 OS: HR 2.37
Pre	Sager	2014	DFS OS	SUVMax MTV 50%	MTV50%	N/A	N/A	DFS: 2.5 OS: 2
Pre	Akagunduz	2015	LRFS DFS OS	SUVMax SULMax MTV (adaptive threshold based)	MTV (treatment response, LR, Disease related death) SULMax (LR)	N/A	3-year (MTV) DFS 75.5% vs 25.3% OS 82.9% vs 55.9%	N/A

Table 3 (*Continued*)

Timing	Authors	Year	End point	Used PET parameters	Significant Prognostic parameters	Threshold	Clinical outcome	Hazard Ratio
Pre	Cheng	2015	PFS DSS	MTV 50% 42% 2.5 and adaptive threshold TLG Grey level run lenght encoding matrix Grey level size zone matrix	Zone size nonuniformity, Uniformity, TLG adaptive threshold (PFS)	N/A	N/A	N/A
Pre	Hofheinz	2015	PFS OS	SUVMax SUVMean MTV (adaptive threshold) TLG Aphericity	TLG MTV ASP	MTV 12.6 TLG 82.6 ASP 22%	N/A	PFS MTV: 2.89 (p = 0.017) TLG: 3.11 (p = 0.02) ASP: 3.09 (p = 0.015) OS MTV: 3.3 (p = 0.018) TLG: 3.32 (p = 0.016) ASP: 5.9 (p = 0.001)
Pre	Lin	2015	Nodal relapse free survival OS DFS	SUVMax Nodal MTV2.5 N MTV40% N MTV50% N TLG40% N TLG50% N	TLG 40% (DFS NRFS)	38g	N/A	DFS: 2.12 (p = 0.02)
Pre and post	Matoba	2015	LRC PFS OS	SUVMax EORTC Criteria	EORTC criteria (OS and PFS)	N/A	N/A	N/A
Pre and per	Min	2015	LRFS DFS MFFS OS	SUVMax MTV 2.5 TLG Percentage reduction between per and pre treatment PET	SUVMax per trt (DFS) MTV Pertrt (DFS) TLG pertrt (LRFS DFS)	SUVMax 4.25 MTV 3.3 TLG 9.4	N/A	N/A
Pre	Moon	2015	DFS	SUVMax SUVMean MTV (adaptive threshold) TLG	TLG	7.6	N/A	DFS: 7.62 (p < 0.001)
Pre	Rasmussen	2015	Time to failure	SUVMax SUVMean SUVPeak	SUVmax	N/A	N/A	Time to failure (for SUVMax increase from 25th to 75th percentile): 1.34 (p = 0.039)
Pre and post	Schwartz	2015	LR PFS OS	SUVMax SUVPeak MTV 40%	Primary MTV 40% (LRR, DM, DFS)	8.76 cm^3	N/A	LRR: 4.01 (p = 0.02) PFS: 2.34 (p = 0.05)
Pre	Yabuki	2015	DFS OS	MTV 2.5 3 (for t and n)	MTV T 2.5 (OS DFS)	4.9 ml	3-year DFS 92.9% vs 38.6% (p < 0.001) 3-year OS 95.35% vs 59.27% (p < 0.001)	DFS: 6.97 (p = 0.001) OS: 1.96 (p = 0.002)
Post	Kim	2016	PFS OS	SUVMax	SUVMax (DFS and OS)	4.4	3-year PFS 81.1% vs 42.9% 3-year OS 87.7% vs 56.9%	PFS: 4.79 (p < 0.001) OS: 4.25 (p = 0.005)
Pre and per	Min	2016	LRFS DFS MFFS OS	SUVMax MTV 2.5 TLG Percentage reduction between per and pre treatment PET	TLG pertrt (DFS) SUVMax per (DFS MFFS) MTV per (DFS OS) TLG per (DFS)	TLG per trt 9.4 SUVMax pre 11.45 and per 4.25 MTV pre 21.95 and per 3.3 TLG pre 91.75 and per 9.4	TLG 2-year DFS 85.9% vs 60.8% (p = 0.005) MTV 2-year DFS 83.2% vs 62.3% (p = 0.018) SUVMax 2-year DFS 82% vs 64.5% (p = 0.025)	TLG DFS: 7.7 MTV DFS: 4.29 SUVMax: 4.18

Table 4
Summary of the results of the 42 studies which analyzed the predictive value of PET before treatment. *: if considering only studies without volumetric PET parameters. DFS: Disease Free Survival, OS: Overall Survival, MTV: Metabolic Tumor Volume, TLG: Total Lesion Glycolysis.

Quantitative parameters	Correlation with DFS/OS	Number of positive studies/total studies	Strength	Weakness
SUV_{Max}	Poorly	14/38 (11/14*)	Ease of use	Poorly reproducible No data concerning heterogeneity
SUV_{Peak}	?	0/2	More robust than SUV_{Max}	May not be representative of nonhomogeneous overall tumor uptake Ideal size of the ROI is still unclear
SUV_{Mean}	No	1/9	–	–
MTV/TLG	Yes	26/26	Represent the heterogeneity of the tumor uptake Ease of use	No clearly segmentation method No data concerning spatial relationships
Shape/ Texture analysis	?	3/3	Represent the heterogeneity of the tumor	No standardized method/Experimental Which correlation with histology?

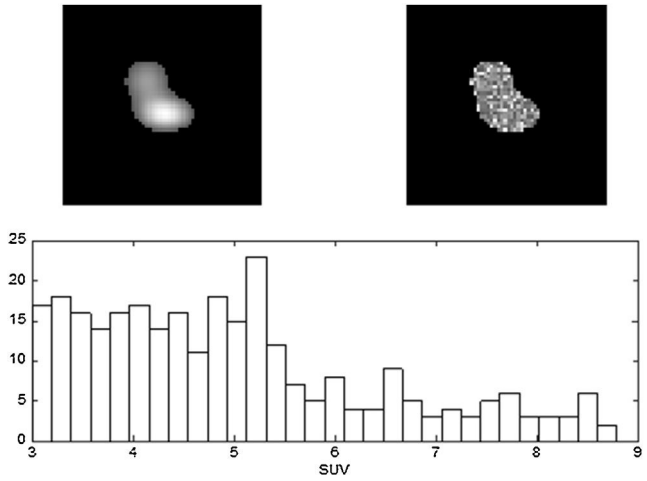

Fig. 1. Heterogeneity measures do not characterize the spatial relationships between voxels. The two tumors in the upper row have identical SUV histograms, although their visual aspect is very dissimilar.

4. Discussion and conclusion

This overview of the available literature shows that MTV and TLG are well correlated with clinical outcome (Local control, Disease Free Survival and overall survical). Most of the available data deal with the intensity of the metabolism, calculated from the SUV, a quantitative parameter used to normalize the uptake of ^{18}F FDG. In practice, SUV is defined as a ratio of tissue radioactivity concentration and the injected dose adjusted by body weight (SUV_{bw} with BW for body weight). Intensity of the metabolism can be analyzed using histogram-based method, which represents the voxel value frequency distribution. This method includes in particular the four histogram moments, i.e., the mean (corresponding to SUVMean), the maximum (corresponding to SUVMax), the median, the skewness (asymmetry of the histogram) and kurtosis (degree of peakedness of a distribution). However, it did not take into account the spatial relationship between voxel values (Fig. 1).

The maximum SUV (SUVMax) corresponds to the maximal pixel value in the tumor. Thanks to its ease of use, it is one of the most used parameters in the clinical practice. However, this value is highly dependent from noise, duration and parameters of acquisition, and so is considered to be poorly reproducible (Boellaard et al., 2004; Nahmias and Wahl, 2008; Nakamoto et al., 2002). This point may explain the wide range of cut-off value for SUVmax reported in the available studies (from 3.7 to 9 g/ml), limiting the generalization of the use of SUVmax for the whole population. Peak SUV (SUV_{Peak}), defined as the average SUV within a small region of interest (1.2 cm of diameter) around the SUV_{Max}, is a more robust alternative to SUV_{Max}. However, SUV_{Peak} may not be representative of nonhomogeneous overall tumor uptake, and the ideal size of the ROI is still unclear (Lee et al., 2007).

Others volumetric parameters like the MTV, the mean SUV within the tumor volume or the TLG are used to represent the heterogeneity of the tumor uptake. The predictive value for clinical outcome of these parameters seems to be higher than SUV_{Max}. However, uptake in PET may be due to inflammatory or infectious reaction. Furthermore, the physiological uptake surrounding organs can also be a source of loss of specificity in the analysis of the signal. A major difficulty in the analysis of PET is to differentiate the tumor signal from the non-tumor signal. PET imaging suffers from a low contrast and spatial resolution, with a high noise background and partial effect volume. Tumor delineation may change depending on the chosen segmentation method. One of the most used automatic method is to use a threshold, between 2 and 3 (absolute value) or 40–50% (relative value of SUVmax).

One important issue concerning the predictive value of MTV is the lack of external validation. Most of the studies were monocentric, using the same PET/CT for all patients. Only two studies performed a validation on an independent dataset (Hofheinz et al., 2015; Tang et al., 2012). The first study (La et al., 2009) included 85 patients and showed that an increase of MTV of 17 cm^3 (from the 25th to 75th percentile) was significantly correlated with an increased risk of death (HR 2.1). The authors validated their results on a dataset of 83 patients treated in the same institution after the original dataset (Tang et al., 2012). Based on (Apostolova et al., 2014), (Hofheinz et al., 2015) used a cutoff of TLG of 58.7 ml. They showed a correlation of TLG only with better DFS (HR 3.01, $p = 0.048$) but not with better OS (HR 2.02, $p = 0.22$). After adjusting the cutoff at a value of 141 ml, TLG was also correlated with OS (HR 3.32, $p = 0.016$). Such methodologies and findings highlight the difficulty in identifying a cutoff which may be tested on external dataset of patients. The use of international guidelines, like the European Association of Nuclear Medecine guidelines for tumor imaging (Boellaard et al., 2015), by harmonizing quantitative FDG PET/CT imaging procedures in multicentre studies and quantitative interpretation criteria, may increases the reproducibility of PET studies.

The spatial relationships between the voxel values within the tumor may be assessed by texture analyses. Texture analyses aim to characterize the internal metabolism morphology of the tumors. From a technical point of view, they characterize the transitions between voxel values. Several approaches exist and they all rely on a quantification of spatial scales organization and directions in images. Most approaches are computing the latter in two dimensions on a slice basis. The most widely used method is the Gray Level Co-occurrence Matrix and consists in calculating matrices count-

Unresolved questions and controversies

1. Reproducibility of PET parameters between different machines and/or centre
2. Which methods (Manually, relative, absolute or adaptive segmentation) and which threshold to compute MTV?
3. When should perform PET during radiotherapy?
4. Which methods for texture and shape analysis?

ing the co-occurrences of two voxels values separated from a set of fixed distances and along set of fixed directions. Several statistics can be computed on these matrices to quantify textural properties (e.g., correlation, contrast, energy). Another popular approach is to apply image filters with various scales and directional properties to continuously quantify transitions between image voxels. One popular example is the isotropic Mexican hat filter (also called Laplacian of Gaussian filter). A comprehensive review of methods for 3-D texture analysis is available in (Depeursinge et al., 2014). This kind of analysis seems promising, but its use should still be considered experimental and limited to clinical studies.

Conflicts of interest

None.

Acknowledgment

The authors wish to thank Ms S.Colombe who assisted in proofreading the manuscript.

References

Allal, A.S., Dulguerov, P., Allaoua, M., Haenggeli, C.A., El-Ghazi el, A., Lehmann, W., Slosman, D.O., 2002. Standardized uptake value of 2-[(18)F] fluoro-2-deoxy-D-glucose in predicting outcome in head and neck carcinomas treated by radiotherapy with or without chemotherapy. J. Clin. Oncol. 20 (5), 1398–1404.

Apostolova, I., Steffen, I.G., Wedel, F., Lougovski, A., Marnitz, S., Derlin, T., Amthauer, H., Buchert, R., Hofheinz, F., Brenner, W., 2014. Asphericity of pretherapeutic tumour FDG uptake provides independent prognostic value in head-and-neck cancer. Eur. Radiol. 24 (9), 2077–2087.

Ashamalla, H., Mattes, M., Guirguis, A., Zaidi, A., Mokhtar, B., Tejwani, A., 2014. The anatomical biological value on pretreatment (18)F-fluorodeoxyglucose positron emission tomography computed tomography predicts response and survival in locally advanced head and neck cancer. World J. Nucl. Med. 13 (2), 102–107.

Boellaard, R., Krak, N.C., Hoekstra, O.S., Lammertsma, A.A., 2004. Effects of noise, image resolution, and ROI definition on the accuracy of standard uptake values: a simulation study. J. Nucl. Med. 45 (9), 1519–1527.

Boellaard, R., Delgado-Bolton, R., Oyen, W.J., Giammarile, F., Tatsch, K., Eschner, W., Verzijlbergen, F.J., Barrington, S.F., Pike, L.C., Weber, W.A., Stroobants, S., Delbeke, D., Donohoe, K.J., Holbrook, S., Graham, M.M., Testanera, G., Hoekstra, O.S., Zijlstra, J., Visser, E., Hoekstra, C.J., Pruim, J., Willemsen, A., Arends, B., Kotzerke, J., Bockisch, A., Beyer, T., Chiti, A., Krause, B.J., European Association of Nuclear, M., 2015. FDG PET/CT: EANM procedure guidelines for tumour imaging: version 2.0. Eur. J. Nucl. Med. Mol. Imaging 42 (2), 328–354.

Brun, E., Kjellen, E., Tennvall, J., Ohlsson, T., Sandell, A., Perfekt, R., Perfekt, R., Wennerberg, J., Strand, S.E., 2002. FDG PET studies during treatment: prediction of therapy outcome in head and neck squamous cell carcinoma. Head Neck 24 (2), 127–135.

Cacicedo, J., Navarro, A., Del Hoyo, O., Gomez-Iturriaga, A., Alongi, F., Medina, J.A., Elicin, O., Skanjeti, A., Giammarile, F., Bilbao, P., Casquero, F., de Bari, B., Dal Pra, A., 2016. Role of fluorine-18 fluorodeoxyglucose PET/CT in head and neck oncology: the point of view of the radiation oncologist. Br. J. Radiol., 20160217.

Castaldi, P., Rufini, V., Bussu, F., Micciche, F., Dinapoli, N., Autorino, R., Lago, M., De Corso, E., Almadori, G., Galli, J., Paludetti, G., Giordano, A., Valentini, V., 2012. Can early and late18F-FDG PET-CT be used as prognostic factors for the clinical outcome of patients with locally advanced head and neck cancer treated with radio-chemotherapy? Radiother. Oncol.: J. Eur. Soc. Ther. Radiol. Oncol. 103 (1), 63–68.

Chajon, E., Lafond, C., Louvel, G., Castelli, J., Williaume, D., Henry, O., Jegoux, F., Vauleon, E., Manens, J.P., Le Prise, E., de Crevoisier, R., 2013. Salivary gland-sparing other than parotid-sparing in definitive head-and-neck intensity-modulated radiotherapy does not seem to jeopardize local control. Radiat. Oncol. 8, 132.

Chang, K.P., Tsang, N.M., Liao, C.T., Hsu, C.L., Chung, M.J., Lo, C.W., Chan, S.C., Ng, S.H., Wang, H.M., Yen, T.C., 2012. Prognostic significance of 18F-FDG PET parameters and plasma Epstein-Barr virus DNA load in patients with nasopharyngeal carcinoma. J. Nucl. Med. 53 (1), 21–28.

Chen, S.W., Hsieh, T.C., Yen, K.Y., Yang, S.N., Wang, Y.C., Chien, C.R., Liang, J.A., Kao, C.H., 2014. Interim FDG PET/CT for predicting the outcome in patients with head and neck cancer. Laryngoscope 124 (12), 2732–2738.

Cheng, N.M., Fang, Y.H., Chang, J.T., Huang, C.G., Tsan, D.L., Ng, S.H., Wang, H.M., Lin, C.Y., Liao, C.T., Yen, T.C., 2013. Textural features of pretreatment 18F-FDG PET/CT images: prognostic significance in patients with advanced T-stage oropharyngeal squamous cell carcinoma. J. Nucl. Med. 54 (10), 1703–1709.

Cheng, N.M., Fang, Y.H., Lee, L.Y., Chang, J.T., Tsan, D.L., Ng, S.H., Wang, H.M., Liao, C.T., Yang, L.Y., Hsu, C.H., Yen, T.C., 2015. Zone-size nonuniformity of 18F-FDG PET regional textural features predicts survival in patients with oropharyngeal cancer. Eur. J. Nucl. Med. Mol. Imaging 42 (3), 419–428.

Depeursinge, A., Foncubierta-Rodriguez, A., Van De Ville, D., Muller, H., 2014. Three-dimensional solid texture analysis in biomedical imaging: review and opportunities. Med. Image Anal. 18 (1), 176–196.

Edge, S.B., Compton, C.C., 2010. The American Joint Committee on Cancer: the 7th edition of the AJCC cancer staging manual and the future of TNM. Ann. Surg. Oncol. 17 (6), 1471–1474.

Farrag, A., Ceulemans, G., Voordeckers, M., Everaert, H., Storme, G., 2010. Can 18F-FDG-PET response during radiotherapy be used as a predictive factor for the outcome of head and neck cancer patients? Nucl. Med. Commun. 31 (6), 495–501.

Fletcher, J.W., Djulbegovic, B., Soares, H.P., Siegel, B.A., Lowe, V.J., Lyman, G.H., Coleman, R.E., Wahl, R., Paschold, J.C., Avril, N., Einhorn, L.H., Suh, W.W., Samson, D., Delbeke, D., Gorman, M., Shields, A.F., 2008. Recommendations on the use of 18F-FDG PET in oncology. J. Nucl. Med. 49 (3), 480–508.

Gambhir, S.S., Czernin, J., Schwimmer, J., Silverman, D.H., Coleman, R.E., Phelps, M.E., 2001. A tabulated summary of the FDG PET literature. J. Nucl. Med. 42 (Suppl. 5), 1S–93S.

Greven, K.M., Williams 3rd, D.W., McGuirt Sr., W.F., Harkness, B.A., D'Agostino Jr., R.B., Keyes Jr., J.W., Watson Jr., N.E., 2001. Serial positron emission tomography scans following radiation therapy of patients with head and neck cancer. Head Neck 23 (11), 942–946.

Hentschel, M., Appold, S., Schreiber, A., Abolmaali, N., Abramyuk, A., Dorr, W., Kotzerke, J., Baumann, M., Zophel, K., 2011. Early FDG PET at 10 or 20 Gy under chemoradiotherapy is prognostic for locoregional control and overall survival in patients with head and neck cancer. Eur. J. Nucl. Med. Mol. Imaging 38 (7), 1203–1211.

Higgins, K.A., Hoang, J.K., Roach, M.C., Chino, J., Yoo, D.S., Turkington, T.G., Brizel, D.M., 2012. Analysis of pretreatment FDG-PET SUV parameters in head-and-neck cancer: tumor SUVmean has superior prognostic value. Int. J. Radiat. Oncol. Biol. Phys. 82 (2), 548–553.

Hofheinz, F., Lougovski, A., Zophel, K., Hentschel, M., Steffen, I.G., Apostolova, I., Wedel, F., Buchert, R., Baumann, M., Brenner, W., Kotzerke, J., van den Hoff, J., 2015. Increased evidence for the prognostic value of primary tumor asphericity in pretherapeutic FDG PET for risk stratification in patients with head and neck cancer. Eur. J. Nucl. Med. Mol. Imaging 42 (3), 429–437.

Horiuchi, C., Taguchi, T., Yoshida, T., Nishimura, G., Kawakami, M., Tanigaki, Y., Matsuda, H., Mikami, Y., Oka, T., Inoue, T., Tsukuda, M., 2008. Early assessment of clinical response to concurrent chemoradiotherapy in head and neck carcinoma using fluoro-2-deoxy-d-glucose positron emission tomography. Auris Nasus Larynx 35 (1), 103–108.

Hoshikawa, H., Mitani, T., Nishiyama, Y., Yamamoto, Y., Ohkawa, M., Mori, N., 2009. Evaluation of the therapeutic effects and recurrence for head and neck cancer after chemoradiotherapy by FDG-PET. Auris Nasus Larynx 36 (2), 192–198.

Hoshikawa, H., Kishino, T., Nishiyama, Y., Yamamoto, Y., Yonezaki, M., Mori, N., 2011. Early prediction of local control in head and neck cancer after chemoradiotherapy by FDG-PET. Nucl. Med. Commun. 32 (8), 684–689.

Ito, K., Shimoji, K., Miyata, Y., Kamiya, K., Minamimoto, R., Kubota, K., Okasaki, M., Morooka, M., Yokoyama, J., 2014. Prognostic value of post-treatment (18)F-FDG PET/CT for advanced head and neck cancer after combined intra-arterial chemotherapy and radiotherapy. Chin. J. Cancer. Res. 26 (1), 30–37.

Kao, C.H., Lin, S.C., Hsieh, T.C., Yen, K.Y., Yang, S.N., Wang, Y.C., Liang, J.A., Hua, C.H., Chen, S.W., 2012. Use of pretreatment metabolic tumour volumes to predict the outcome of pharyngeal cancer treated by definitive radiotherapy. Eur. J. Nucl. Med. Mol. Imaging 39 (8), 1297–1305.

Kim, R., Ock, C.Y., Keam, B., Kim, T.M., Kim, J.H., Paeng, J.C., Kwon, S.K., Hah, J.H., Kwon, T.K., Kim, D.W., Wu, H.G., Sung, M.W., Heo, D.S., 2016. Predictive and prognostic value of PET/CT imaging post-chemoradiotherapy and clinical decision-making consequences in locally advanced head & neck squamous cell carcinoma: a retrospective study. BMC Cancer 16 (1), 116.

Kitagawa, Y., Sano, K., Nishizawa, S., Nakamura, M., Ogasawara, T., Sadato, N., Yonekura, Y., 2003. FDG-PET for prediction of tumour aggressiveness and response to intra-arterial chemotherapy and radiotherapy in head and neck cancer. Eur. J. Nucl. Med. Mol. Imaging 30 (1), 63–71.

Kyzas, P.A., Evangelou, E., Denaxa-Kyza, D., Ioannidis, J.P., 2008. 18F-fluorodeoxyglucose positron emission tomography to evaluate cervical node metastases in patients with head and neck squamous cell carcinoma: a meta-analysis. J. Natl. Cancer Inst. 100 (10), 712–720.

La, T.H., Filion, E.J., Turnbull, B.B., Chu, J.N., Lee, P., Nguyen, K., Maxim, P., Quon, A., Graves, E.E., Loo Jr., B.W., Le, Q.T., 2009. Metabolic tumor volume predicts for

recurrence and death in head-and-neck cancer. Int. J. Radiat. Oncol. Biol. Phys. 74 (5), 1335–1341.
Lee, P., Weerasuriya, D.K., Lavori, P.W., Quon, A., Hara, W., Maxim, P.G., Le, Q.T., Wakelee, H.A., Donington, J.S., Graves, E.E., Loo Jr., B.W., 2007. Metabolic tumor burden predicts for disease progression and death in lung cancer. Int. J. Radiat. Oncol. Biol. Phys. 69 (2), 328–333.
Lin, Y.C., Chen, S.W., Hsieh, T.C., Yen, K.Y., Yang, S.N., Wang, Y.C., Kao, C.H., 2015. Risk stratification of metastatic neck nodes by CT and PET in patients with head and neck cancer receiving definitive radiotherapy. J. Nucl. Med. 56 (2), 183–189.
Lonneux, M., Hamoir, M., Reychler, H., Maingon, P., Duvillard, C., Calais, G., Bridji, B., Digue, L., Toubeau, M., Gregoire, V., 2010. Positron emission tomography with [18F]fluorodeoxyglucose improves staging and patient management in patients with head and neck squamous cell carcinoma: a multicenter prospective study. J. Clin. Oncol. 28 (7), 1190–1195.
Machtay, M., Natwa, M., Andrel, J., Hyslop, T., Anne, P.R., Lavarino, J., Intenzo, C.M., Keane, W., 2009. Pretreatment FDG-PET standardized uptake value as a prognostic factor for outcome in head and neck cancer. Head Neck 31 (2), 195–201.
Matoba, M., Tuji, H., Shimode, Y., Kondo, T., Oota, K., Tonami, H., 2015. Lesion regression rate based on RECIST: prediction of treatment outcome in patients with head and neck cancer treated with chemoradiotherapy compared with FDG PET-CT. J. Radiat. Res. 56 (3), 553–560.
Min, M., Lin, P., Lee, M.T., Shon, I.H., Lin, M., Forstner, D., Bray, V., Chicco, A., Tieu, M.T., Fowler, A., 2015. Prognostic role of metabolic parameters of (18)F-FDG PET-CT scan performed during radiation therapy in locally advanced head and neck squamous cell carcinoma. Eur. J. Nucl. Med. Mol. Imaging 42 (13), 1984–1994.
Min, M., Lin, P., Lee, M., Shon, I.H., Lin, M., Forstner, D., Tieu, M.T., Chicco, A., Bray, V., Fowler, A., 2016. 18F-FDG PET-CT performed before and during radiation therapy of head and neck squamous cell carcinoma: are they independent or complementary to each other? J. Med. Imaging. Radiat. Oncol. 60 (3), 433–440.
Moeller, B.J., Rana, V., Cannon, B.A., Williams, M.D., Sturgis, E.M., Ginsberg, L.E., Macapinlac, H.A., Lee, J.J., Ang, K.K., Chao, K.S., Chronowski, G.M., Frank, S.J., Morrison, W.H., Rosenthal, D.I., Weber, R.S., Garden, A.S., Lippman, S.M., Schwartz, D.L., 2010. Prospective imaging assessment of mortality risk after head-and-neck radiotherapy. Int. J. Radiat. Oncol. Biol. Phys. 78 (3), 667–674.
Murphy, J.D., La, T.H., Chu, K., Quon, A., Fischbein, N.J., Maxim, P.G., Graves, E.E., Loo Jr., B.W., Le, Q.T., 2011. Postradiation metabolic tumor volume predicts outcome in head-and-neck cancer. Int. J. Radiat. Oncol. Biol. Phys. 80 (2), 514–521.
Nahmias, C., Wahl, L.M., 2008. Reproducibility of standardized uptake value measurements determined by 18F-FDG PET in malignant tumors. J. Nucl. Med. 49 (11), 1804–1808.
Nakamoto, Y., Zasadny, K.R., Minn, H., Wahl, R.L., 2002. Reproducibility of common semi-quantitative parameters for evaluating lung cancer glucose metabolism with positron emission tomography using 2-deoxy-2-[18F]fluoro-D-glucose. Mol. Imaging Biol. 4 (2), 171–178.
Parkin, D.M., Bray, F., Ferlay, J., Pisani, P., 2005. Global cancer statistics, 2002. CA Cancer J. Clin. 55 (2), 74–108.
Pignon, J.P., Bourhis, J., Domenge, C., Designe, L., 2000. Chemotherapy added to locoregional treatment for head and neck squamous-cell carcinoma: three meta-analyses of updated individual data. MACH-NC Collaborative Group. Meta-Analysis of Chemotherapy on Head and Neck Cancer. Lancet 355 (9208), 949–955.
Rasmussen, J.H., Vogelius, I.R., Fischer, B.M., Friborg, J., Aznar, M.C., Persson, G.F., Hakansson, K., Kristensen, C.A., Bentzen, S.M., Specht, L., 2015. Prognostic value of 18F-fludeoxyglucose uptake in 287 patients with head and neck squamous cell carcinoma. Head Neck 37 (9), 1274–1281.
Romesser, P.B., Lim, R., Spratt, D.E., Setton, J., Riaz, N., Lok, B., Rao, S., Sherman, E.J., Schoder, H., Lee, N.Y., 2014. The relative prognostic utility of standardized uptake value, gross tumor volume, and metabolic tumor volume in oropharyngeal cancer patients treated with platinum based concurrent chemoradiation with a pre-treatment [(18)F] fluorodeoxyglucose positron emission tomography scan. Oral Oncol. 50 (9), 802–808.
Rudmik, L., Lau, H.Y., Matthews, T.W., Bosch, J.D., Kloiber, R., Molnar, C.P., Dort, J.C., 2011. Clinical utility of PET/CT in the evaluation of head and neck squamous cell carcinoma with an unknown primary: a prospective clinical trial. Head Neck 33 (7), 935–940.
Sanghera, B., Wong, W.L., Lodge, M.A., Hain, S., Stott, D., Lowe, J., Lemon, C., Goodchild, K., Saunders, M., 2005. Potential novel application of dual time point SUV measurements as a predictor of survival in head and neck cancer. Nucl. Med. Commun. 26 (10), 861–867.
Schinagl, D.A., Span, P.N., Oyen, W.J., Kaanders, J.H., 2011. Can FDG PET predict radiation treatment outcome in head and neck cancer? Results of a prospective study. Eur. J. Nucl. Med. Mol. Imaging 38 (8), 1449–1458.
Schwartz, D.L., Harris, J., Yao, M., Rosenthal, D.I., Opanowski, A., Levering, A., Ang, K.K., Trotti, A.M., Garden, A.S., Jones, C.U., Harari, P., Foote, R., Holland, J., Zhang, Q., Le, Q.T., 2015. Metabolic tumor volume as a prognostic imaging-based biomarker for head-and-neck cancer: pilot results from Radiation Therapy Oncology Group protocol 0522. Int. J. Radiat. Oncol. Biol. Phys. 91 (4), 721–729.
St Guily, J.L., Borget, I., Vainchtock, A., Remy, V., Takizawa, C., 2010. Head and neck cancers in France: an analysis of the hospital medical information system (PMSI) database. Head Neck Oncol. 2, 22.
Tang, C., Murphy, J.D., Khong, B., La, T.H., Kong, C., Fischbein, N.J., Colevas, A.D., Iagaru, A.H., Graves, E.E., Loo Jr., B.W., Le, Q.T., 2012. Validation that metabolic tumor volume predicts outcome in head-and-neck cancer. Int. J. Radiat. Oncol. Biol. Phys. 83 (5), 1514–1520.
Wong, W.L., Sonoda, L.I., Gharpurhy, A., Gollub, F., Wellsted, D., Goodchild, K., Lemon, C., Farrell, R., Saunders, M., 2012. 18F-fluorodeoxyglucose positron emission tomography/computed tomography in the assessment of occult primary head and neck cancers?an audit and review of published studies. Clin. Oncol. (R Coll Radiol) 24 (3), 190–195.
Yabuki, K., Shiono, O., Komatsu, M., Sano, D., Nishimura, G., Takahashi, M., Taguchi, T., Inoue, T., Oridate, N., 2015. Predictive and prognostic value of metabolic tumor volume (MTV) in patients with laryngeal carcinoma treated by radiotherapy (RT)/concurrent chemoradiotherapy (CCRT). PLoS One 10 (2), e0117924.
Yoo, J., Henderson, S., Walker-Dilks, C., 2013. Evidence-based guideline recommendations on the use of positron emission tomography imaging in head and neck cancer. Clin. Oncol. (R Coll Radiol) 25 (4), e33–66.
Young, H., Baum, R., Cremerius, U., Herholz, K., Hoekstra, O., Lammertsma, A.A., Pruim, J., Price, P., 1999. Measurement of clinical and subclinical tumour response using [18F]-fluorodeoxyglucose and positron emission tomography: review and 1999 EORTC recommendations. Eur. J. Cancer 35 (13), 1773–1782.
Zhu, L., Wang, N., 2013. 18F-fluorodeoxyglucose positron emission tomography-computed tomography as a diagnostic tool in patients with cervical nodal metastases of unknown primary site: a meta-analysis. Surg. Oncol. 22 (3), 190–194.

1.3.4.2 Conclusion

Les paramètres quantitatifs métaboliques issus de la TEP pré thérapeutique sont corrélés avec la survie et la récidive. Leur valeur prédictive apparait comme supérieure aux paramètres cliniques standards. Une TEP réalisée en cours de traitement pourrait également apporter des renseignements sur la réponse au traitement, mais les données sont actuellement insuffisantes. Une des limites de ces paramètres TEP est liée à leurs caractères potentiellement machine dépendant, la totalité des études étant monocentrique, sans validation externe des paramètres proposés. De plus, le choix du seuillage pour calculer le MTV n'a été évalué que par une seule étude, mais uniquement en utilisant un seuillage en valeur absolu de SUVmax. Enfin le meilleur moment pour réaliser une TEP en cours de traitement doit être précisé. Ces limites soulignent le besoin de réaliser une étude multicentrique avec une validation externe des paramètres TEP à visée de prédiction de la survie.

1.3.5 A quelle fréquence et quand faut-il replanifier ?

La radiothérapie adaptative peut s'envisager sous un mode de nouvelle(s) replanification(s) systématique(s) selon un schéma préétabli, par exemple à la cinquième semaine d'irradiation ou à une fréquence hebdomadaire dans une optique maximaliste. Cette dernière approche non personnalisée n'est cependant pas la plus rentable, car très probablement non nécessaire pour tous les patients. Du fait de la lourdeur du processus de replanifications, la plupart des études de radiothérapie adaptative ont fait le choix d'une à deux replanifications en cours de traitement, soit à un moment préétabli, soit en fonction de la décision du radiothérapeute.

Il est fort possible qu'il n'existe pas un schéma idéal de replanifications, mais plusieurs en fonction notamment des objectifs choisis de la stratégie de radiothérapie adaptative (diminution de la toxicité ou augmentation du contrôle local ?).

2 Objectifs de la thèse

Les objectifs de cette thèse sont de quantifier le bénéfice dosimétrique et de prédire le bénéfice clinique d'une stratégie optimisée de radiothérapie adaptative des cancers des VADS localement avancés.

Ce travail de recherche concernant la radiothérapie adaptative se développe suivant deux axes : l'un concernant l'organe à risque majeur que sont les parotides, et l'autre concernant la cible tumorale. Il vise à :

- L'évaluation de la différence entre dose planifiée et dose délivrée (sans et avec radiothérapie adaptative) et l'estimation du risque de toxicité associé (xérostomie) ;
- L'identification des patients bons candidats à une stratégie de radiothérapie adaptative pour diminuer la toxicité ou augmenter le contrôle local;
- L'identification du meilleur schéma de replanification pour épargner les parotides.

Ces 2 axes sont détaillés dans la Figure 11.

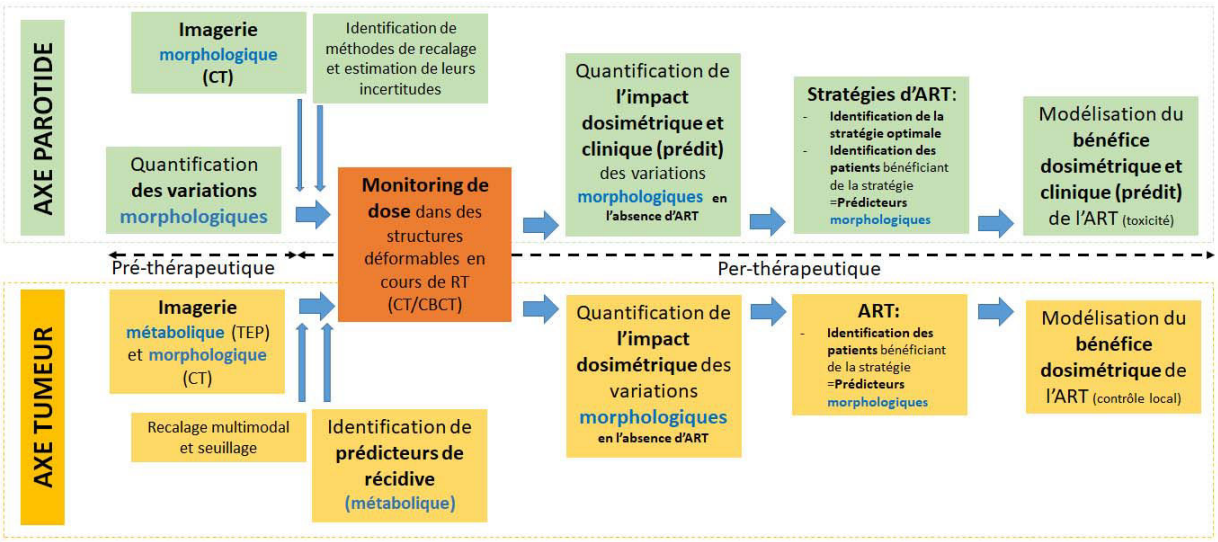

Figure 11 : Objectifs de la thèse

Intégration de l'imagerie morphologique et métabolique pour modéliser le bénéfice dosimétrique et clinique de la radiothérapie adaptative pour diminuer la xérostomie et augmenter le contrôle local

3 Radiothérapie adaptative pour épargner les parotides et diminuer la xérostomie

Par rapport à la radiothérapie standard, la RCMI a initialement montré sa supériorité avec un bénéfice en termes d'épargne des parotides, diminuant le taux de xérostomie à 40 % à 1 an contre 80% en l'absence de RCMI [1, 86]. Cependant, du fait des variations anatomiques précédemment décrites (Table 2 et Table 3), la dose délivrée peut ne pas correspondre à la dose planifiée (Table 4), ce surdosage, en particulier des parotides, pouvant alors entrainer une augmentation du risque de xérostomie. Il apparait donc essentiel d'estimer l'importance et la fréquence de ce surdosage parotidien.

3.1 Modélisation de la RT adaptative en ORL pour épargner les parotides (article)

3.1.1 Introduction

La réalisation d'un scanner hebdomadaire en cours de traitement permet d'estimer le surdosage des parotides au cours d'une RCMI standard sans replanification en réalisant un cumul de dose par recalage élastique. Cette même imagerie scanner permet également de réaliser une modélisation du bénéfice d'une stratégie de radiothérapie adaptative pour épargner les parotides. Un des bénéfices potentiels de la radiothérapie adaptative étant la réduction de la dose reçue par les parotides, ce bénéfice doit aussi être quantifié. Comme évoqué précédemment, différentes combinaisons de fréquences et de moments de replanification peuvent être envisagées. Une stratégie « maximaliste », consistant en des replanifications hebdomadaires, a tout d'abord été considérée pour caractériser le bénéfice maximum potentiel.

L'article reproduit ci-dessous, publié dans la revue *Radiation Oncology* en mai 2015, présente ces travaux.

3.1.2 Impact of head and neck cancer adaptive radiotherapy to spare the parotid glands and decrease the risk of xerostomia

Radiation Oncology, 2015 May

J.Castelli [1,2,3*]; A.Simon [2,3]; G.Louvel [1]; O.Henry [1]; E.Chajon [1]; M.Nassef [2,3]; P.Haigron[2,3]; G.Cazoulat [2,3]; J.D. Ospina [2,3], F.Jegoux [4], K.Benezery [5] and R. de Crevoisier [1,2,3]

[1]. Centre Eugene Marquis, Radiotherapy, Rennes, France

[2]. Rennes University 1, LTSI, Campus de Beaulieu, Rennes, F-35000, France

[3]. INSERM, U1099, Campus de Beaulieu, Rennes, F-35000, France

[4]. CHU Pontchaillou, Rennes, F-35000, France

5. Centre Antoine Lacassagne, Nice, F-06100, France

Castelli et al. Radiation Oncology (2015) 10:6
DOI 10.1186/s13014-014-0318-z

RADIATION ONCOLOGY

RESEARCH Open Access

Impact of head and neck cancer adaptive radiotherapy to spare the parotid glands and decrease the risk of xerostomia

Joel Castelli[1,2,3*], Antoine Simon[2,3], Guillaume Louvel[1], Olivier Henry[1], Enrique Chajon[1], Mohamed Nassef[2,3], Pascal Haigron[2,3], Guillaume Cazoulat[2,3], Juan David Ospina[2,3], Franck Jegoux[4], Karen Benezery[5] and Renaud de Crevoisier[1,2,3]

Abstract

Background: Large anatomical variations occur during the course of intensity-modulated radiation therapy (IMRT) for locally advanced head and neck cancer (LAHNC). The risks are therefore a parotid glands (PG) overdose and a xerostomia increase.
The purposes of the study were to estimate:
- the PG overdose and the xerostomia risk increase during a "standard" IMRT ($IMRT_{std}$);
- the benefits of an adaptive IMRT (ART) with weekly replanning to spare the PGs and limit the risk of xerostomia.

Material and methods: Fifteen patients received radical IMRT (70 Gy) for LAHNC. Weekly CTs were used to estimate the dose distributions delivered during the treatment, corresponding either to the initial planning ($IMRT_{std}$) or to weekly replanning (ART). PGs dose were recalculated at the fraction, from the weekly CTs. PG cumulated doses were then estimated using deformable image registration. The following PG doses were compared: pre-treatment planned dose, per-treatment $IMRT_{std}$ and ART. The corresponding estimated risks of xerostomia were also compared. Correlations between anatomical markers and dose differences were searched.

Results: Compared to the initial planning, a PG overdose was observed during $IMRT_{std}$ for 59% of the PGs, with an average increase of 3.7 Gy (10.0 Gy maximum) for the mean dose, and of 8.2% (23.9% maximum) for the risk of xerostomia. Compared to the initial planning, weekly replanning reduced the PG mean dose for all the patients ($p < 0.05$). In the overirradiated PG group, weekly replanning reduced the mean dose by 5.1 Gy (12.2 Gy maximum) and the absolute risk of xerostomia by 11% ($p < 0.01$) (30% maximum). The PG overdose and the dosimetric benefit of replanning increased with the tumor shrinkage and the neck thickness reduction ($p < 0.001$).

Conclusion: During the course of LAHNC IMRT, around 60% of the PGs are overdosed of 4 Gy. Weekly replanning decreased the PG mean dose by 5 Gy, and therefore by 11% the xerostomia risk.

Keywords: Head and neck cancer, Anatomical variation, Adaptive RT, Xerostomia

* Correspondence: j.castelli@rennes.unicancer.fr
[1]Department of Radiotherapy, Centre Eugene Marquis, Avenue de la bataille Flandre Dunkerque, F-35000 Rennes, France
[2]Rennes University 1, LTSI, Campus de Beaulieu, Rennes F-35000, France
Full list of author information is available at the end of the article

Introduction

The treatment of unresectable Head & Neck Cancer (HNC) consists of a chemoradiotherapy [1,2]. One of the most common toxicity of this treatment is xerostomia, inducing difficulties in swallowing and speaking, loss of taste, and dental caries, with therefore a direct impact on patient quality of life. Xerostomia is mainly caused by radiation induced damage mainly to the parotid glands (PG), and to a lesser extend to the submandibular glands [3]. Intensity modulated radiotherapy (IMRT) permits to deliver highly conformal dose in complex anatomical structures, while sparing critical structures. Indeed, three randomized studies have demonstrated improving (PG) sparing by using IMRT compared to non-IMRT techniques, resulting in better salivary flow and decreased xerostomia risk [4-6]. However, large variations can be observed during the course of IMRT treatment, such as body weight loss [7,8], primary tumor shrinking [7], and PG volume reduction [9]. Due to these anatomical variations and to the tight IMRT dose gradient, the actual administered dose may therefore not correspond to the planned dose, with a risk of radiation overdose to the PGs (Figure 1) [10,11]. This dose difference clearly reduces the expected clinical benefits of IMRT, increasing the risk of xerostomia. Although bone-based image-guided radiation therapy (IGRT) allows for setup error correction, the actual delivered dose to the PGs remains higher than the planned dose [12], due to the fact that IGRT does not take shape/volume variations into account. By performing one or more new planning during the radiotherapy treatment, adaptive radiotherapy (ART) aims to correct such uncertainties. ART has been already shown to decrease the mean PG dose during locally advanced head and neck cancer IMRT [13], but no surrogate of the PG dose difference and of the dosimetric benefit of ART has yet been identified. In the context of IMRT for locally advanced HNC, this study sought to:

- estimate the difference between the planned dose and the actual delivered dose (without replanning) to the PGs, i.e., the PG overdose;
- estimate the PG dose difference with replanning and without replanning to spare the PGs while keeping the same planning target volume (PTV), i.e., the benefit of ART;
- identify anatomical markers correlated with these dose differences (PG overdose and ART benefit).

Materials and methods

Patients and tumors

The study enrolled a total of 15 patients with a mean age of 65 years (ranging from 50 to 87 years). Patient, tumor, and treatment characteristics are provided on Table 1. All tumors were locally advanced (Stage III or IV, AJCC 7th ed). The mean PG volume was 25.3 cc (ranging from 16.6 cc to 52.1 cc, standard deviation (SD): 8.1 cc).

Treatment and planning

All patients underwent IMRT using a total dose of 70 Gy (2 Gy/fraction/day, 35 fractions), with a simultaneous integrated boost technique [14] and concomitant chemotherapy. Planning CTs (CT0) with intravenous contrast agents were acquired with 2 mm slice thickness from the vertex to the carina. A thermoplastic head and shoulder mask with five fixation points was used. PET-CT and MRI co-registration was used for tumor delineation. Three target volumes were generated. Gross tumor volume (GTV) corresponded to the primary tumor along with involved lymph nodes. Clinical target volume 70 Gy (CTV_{70}) was

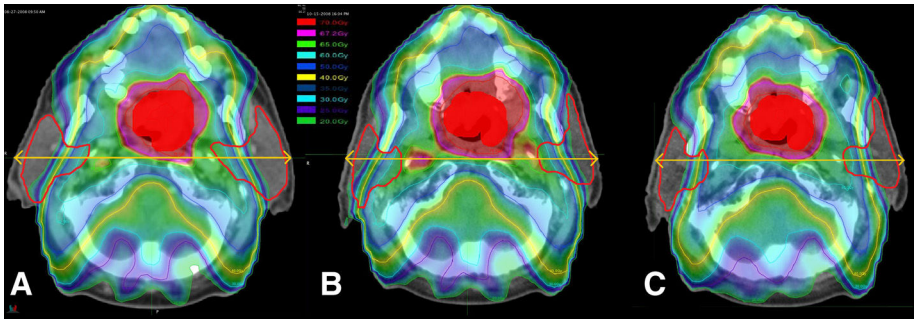

Figure 1 Illustration of the anatomical variations on the dose distribution. IMRT dose distributions at different times for a given patient, showing the PG overdose without replanning **(B)** and the benefit of replanning **(C). A**: Planned dose on the pre-treatment CT (CT0). **B**: Actual delivered dose without replanning during the treatment (Week 3). **C**: Adaptive planned dose with replanning to spare the parotid glands (PG) at the same fraction (Week 3). PGs are shown by the red line. The full red represents the Clinical Target Volume (CTV70). The arrow show the head thickness. Figure 1B and 1C compared to 1A shows that the PGs and the CTV70 volumes and the neck thickness have decreased. These anatomical variations have led to dose hotspots in the neck, close to the internal part of the two PG (Figure 1B). Replanning (Figure 1C) allowed to spare the PG even better than on the planning (Figure 1A).

Table 1 Patient, tumor, and treatment characteristics at the initial planning (CT0)

ID	Gender	Age	Tumor localization	TNM	Volume (cc)			D_{mean} (Gy)		Xerostomia NTCP (%) [21]	
					CTV70	HLP	CLP	HLP	CLP	HLP	CLP
1	M	86	Tonsil	T3N1	45.2	52.1	48.6	30.2	31.1	26.5	28.3
2	F	63	Tonsil	T2Nx	26.3	31.1	27.5	31.4	26	29.0	18.7
3	M	74	Oropharynx	T3N2c	181.5	24.9	20.7	37.9	31.1	44.3	28.4
4	F	66	Oropharynx	T2N2c	107.2	27.8	23.4	32.9	27.9	32.3	22.0
5	M	57	Velum	T3N0	62.4	20.7	18.0	28.1	27.8	22.4	21.7
6	M	67	Oropharynx	T3N2c	156.2	24.5	22.7	30.8	29.4	24.7	21.4
7	M	52	Oropharynx	T4N2	165.1	N/A	21.6	N/A	28.7	N/A	23.4
8	M	67	Trigone	T4N1	139.3	22.0	19.3	30.7	29.2	27.4	24.4
9	F	65	Oropharynx	T3N3	237.5	23.9	20.2	42.4	31.1	55.2	28.2
10	F	65	Oropharynx	T4N3	257.9	N/A	24.5	N/A	35.2	N/A	37.7
11	M	50	Oropharynx	T4N2c	434.5	N/A	17.7	N/A	36.3	N/A	40.3
12	M	53	Oropharynx	T3N0	14.4	16.6	23.3	41.3	24.2	52.9	15.9
13	M	73	Oropharynx	T3N2c	147.0	29.4	29.2	54.6	32.2	81.7	30.7
14	M	56	Larynx	T3N0	14.0	22.8	29.2	19.7	9.2	10.1	2.7
15	M	75	Hypopharynx	T2N2	76.3	20.3	22.4	29.4	29.1	25.0	24.4

M: male; F: female; CT0: initial planning; CTV70: clinical target volume receiving 70 Gy; PGs: parotid glands; HLP: homolateral PGs; CLP: contralateral PGs; Dmean: mean dose at initial planning; N/A: not applicable (PGs included in the CTV), NTCP: normal tissue complication risk of xerostomia defined as a salivary flow ratio <25% of the pretreatment one [21].

equal to GTV plus a 5 mm 3D margin, which was adjusted to exclude air cavities and bone mass without evidence of tumor invasion. CTV_{63} corresponded to the area at high-risk of microscopic spread, while CTV_{56} corresponded to the prophylactic irradiation area. GTV, CTV_{63}, $CTV_{56,}$ and all organs at risk were manually delineated on each CT slice. Adding a 5 mm 3D margin around the CTVs generated the PTVs. PTV expansion was limited to 3 mm from the skin surface in order to avoid the build-up region and to limit skin toxicity [15]. All IMRT plans were generated using Pinnacle V9.2. Seven Coplanar 6-MV photon beams were employed with a step and shoot IMRT technique. The prescribed dose was 70 Gy to PTV_{70}, 63 Gy to $PTV_{63,}$ and 56 Gy to PTV_{56}. The collapsed cone convolution/superposition algorithm was used for dose calculation. The maximum dose within the PTV was 110% (D2%). The minimum PTV volume covered by the 95% isodose line was 95%. Dose constraints were set according to the GORTEC recommendations [16]: a mean dose (D_{mean}) <30 Gy and a median dose <26 Gy for contralateral PGs.

Patients were treated as planned on CT0 and no changes were applied to dose distribution during treatment. During the treatment course, weekly in-room stereoscopic imaging corrected set-up errors >5 mm. All patients signed an informed consent form. The study was approved by the institutional review board (ARTIX study NCT01874587).

Weekly dose estimations, in cases of replanning and without replanning

During the treatment, each patient underwent six weekly CTs (CT1 to CT6) according to the same modalities as CT0, except for the intravenous contrast agents (not systematically used, particularly in case of cisplatin based chemotherapy). For each patient, the anatomical structures were manually segmented on each weekly CT by the same radiation oncologist. In case of complete response, initial macroscopically-involved areas were still included in the CTV_{70}, which was adjusted to exclude any air cavities and bone mass without evidence of initial tumor invasion.

Actual weekly doses (Figure 2, Step 1A) were estimated by calculating the dose distribution on the weekly CT, using treatment parameters and isocenter from CT0. Weekly re-planned doses (Figure 2, Step 1C) were calculated by generating a new IMRT plan on each weekly CT in accordance with the dose constraints described for the initial planning. PTV coverage did not differ between initial planning and weekly re-planned CT. The dose constraints for the organs at risk have respected the GORTEC recommendations at the initial planning and in all replanning.

Total cumulated dose estimations by deformable registration

Cumulated doses were estimated for the two scenarios, with or without replanning (Figure 2 Steps 1B and 1D), according to the following deformable image registration

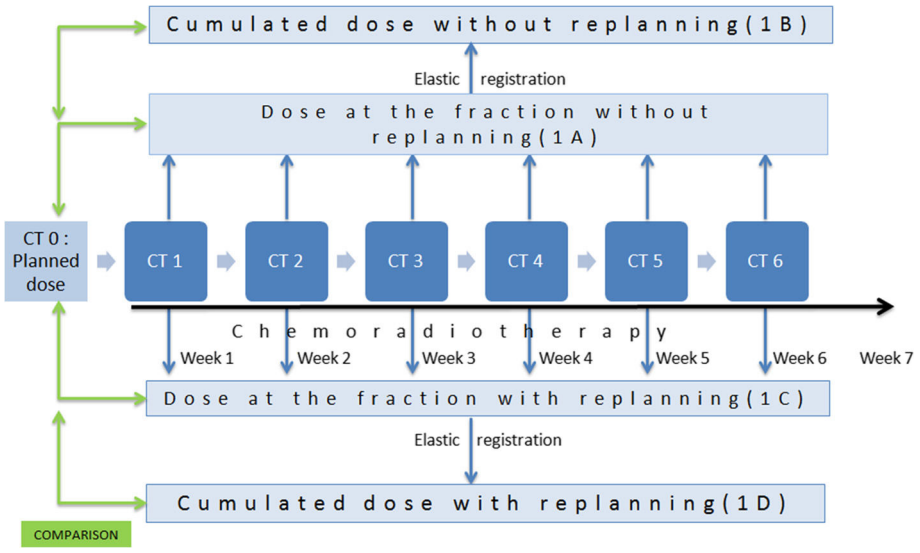

Figure 2 Overall study flow chart. Weekly CT scans were performed during the 7 weeks of treatment. Doses were calculated on each weekly fraction, corresponding either to the initial planning (step 1A) or to a replanning to spare the parotid glands (step 1C). Corresponding cumulated doses were calculated (steps 1B and 1C) using elastic registration. Doses were then compared.

procedure (contour-guided Demons registration algorithm) [17]. For PGs on each CT, a signed distance map was generated to represent the squared Euclidean distance between each voxel and the PG surface. Distance maps of each PG were then registered using the Demons registration algorithm [18]. The resulting deformation fields were employed to map the weekly dose distributions to the planning CT using tri-linear interpolation. Next, the mapped dose distributions were summed to estimate the cumulated dose for each PG. The average Dice score for PG registration, from the weekly CT to each planning CT was computed as followed:

Dice score = $2\times(|A\cap B|)/(|A| + |B|)$, where: A is the delineated PG contour on the weekly CT, B is the planning contour propagated by the registration and |.| denotes the number of voxels encompassed by the contour. The Dice score ranges from 0 (worst case: no match between both contours) to 1 (perfect match) [19]. A 3D dose difference in the PG was calculated between the cumulated dose distribution and planned dose distribution.

Anatomical variation description

Anatomical variations (between CT0 and weekly CTs) were characterized by variations in CTV_{70} and PG volumes, in the distances between PGs and CTV_{70} and in the thickness of the neck (at the level of the geometrical centers of the PGs). The distance between PGs and CTV_{70} corresponded to the minimal distance between the surfaces of the two contours (PG-CTVds), computed using an Euclidean distance map of the first contour, iteratively considering all the points of the second contour and keeping the resulting minimal distance.

Statistical analysis

The impact of the anatomical variations on PG dose was analyzed considering D_{mean} and the full DVH. Their impact on the risk of xerostomia was estimated by using the LKB NTCP model (n = 1, m = 0.4, and TD50 = 39.9) [20,21], the complication being defined as a salivary flow ratio <25% of the pretreatment one [22].

The mean PG dose differences between the weekly doses (with and without replanning) and the planned dose were calculated (Figure 2). The PG overdose was assessed as the difference between the dose without replanning (at the fraction or cumulated) and the dose at the planning. The benefit of weekly replanning was assessed as the difference between the doses with replanning and without replanning (at the fraction or cumulated). Linear mixed-effects models were used to test if the following parameters were correlated with the PG overdose or the benefit of the weekly replanning: initial volumes of the CTV_{70} and of the PGs, decreasing (between the weekly CT and the planning CT) of the volume of the CTV_{70} (in cc and %) and the PGs (in cc and %), shortening of the distance between PGs and CTV_{70}, reduction of the head thickness and the time between the CT0 and the beginning of treatment. All dose and volume comparisons were performed using nonparametric tests (Wilcoxon test). Statistical analysis was carried out using the Statistical Package for the Social Sciences V 20.0.

Results

Since 3 ipsilateral PGs were completely included within the PTV (Patient number 7, 10 and 11), they were excluded from the analysis, resulting in a total of 27 PGs analyzed. The average Dice score [19] for PG registration,

from the weekly CT to each planning CT was 0.92 (from 0.83 to 0.95).

Quantification of anatomical variations during the 7 weeks of treatment

From CT0 to CT6, the PG volumes decreased by a mean value of 28.3% (ranging from 0.0 to 63.4%, SD 18%), corresponding to an average decrease of 1.1 cc/week (ranging from 0.0 to 2.2 cc/week). The CTV_{70} decreased by a mean value of 31% (ranging from 73% to −13%, SD 28%).

The distance between the PGs and the CTV (PG-CTV_{ds}) decreased in 74% of the PGs by 4.3 mm on average (ranging from 0.1 to 12 mm, SD 3.7 mm), whereas it increased in the other 26% of the PGs by 3.2 mm on average (ranging from 1.1 to 6.3 mm, SD 2.1 mm).

The thickness of the neck decreased for 78% of the patients by a mean value of 7.9 mm (ranging from 0.1 to 26.6 mm, SD 6.2 mm).

Dose comparison between planned dose, and doses with or without replanning in PGs

The per-treatment PG doses (with or without replanning) were analyzed, first considering the weekly fractions and then, using the cumulated doses from all weekly fractions, for all the 15 patients. The results are shown in Table 2.

PG dose comparisons at the per-treatment weekly fraction

In order to assess the PG overdose, comparison was first made between the dose at the fraction without replanning (Figure 2 Step 1A) and the planned dose. For 67% of the plans, the D_{mean} increased on average by 4.8 Gy (up to 24.9 Gy, SD 4.6 Gy). In the other 33% of plans, the D_{mean} decreased by 3.9 Gy (up to 10.7 Gy, SD 2.9 Gy). The variation of the mean PG dose during the treatment was showed Figure 3 for two representative patients.

Then, to assess the benefit of replanning, comparison was made between the dose with (Figure 2 step 1C) and without replanning (Figure 2 Step 1A). In 85% of the plans, replanning decreased the D_{mean} on average by 4.6 Gy (up to 23.8 Gy, SD 4.0 Gy).

PG dose comparisons using the cumulated doses and the corresponding estimated xerostomia risks

A PG overdose was reported in 59% (N = 16) of the PGs. Figure 4a shows the D_{mean} difference for each PG of each patients. Ten out of fifteen patients received a higher D_{mean} in at least one PG (6 patients in the 2 PGs), which corresponded to a D_{mean} increase of an average of 3.7 Gy (ranging from 0.4 to 10.0 Gy, SD 2.9 Gy). Figure 5 shows the average planned DVH (red line) and the average cumulated DVH without replanning (blue line).

Figure 4b shows the corresponding difference in the estimated xerostomia risk. The average absolute increased risk of xerostomia was 3% (ranging from −16.7 to 23.9%, SD 2.9%) in all patients, and was 8.2% (ranging from 3.8 to 23.9%, SD 7.1%) among patients with an increased dose to PGs.

Weekly replanning enabled the D_{mean} to be reduced to at least the same value as that of the pre-treatment planning for all over-irradiated PGs (Figure 6). In the subgroup of over-irradiated PGs, the mean D_{mean} difference between the cumulated doses with replanning and without replanning was therefore 5.1 Gy (ranging from 0.6 to 12.2 Gy, SD 3.3 Gy) (p = 0.001). In the subgroup of non-over-irradiated PGs, this mean D_{mean} difference was 1.4 Gy (ranging from 0 to 4.1 Gy, SD 1.7 Gy) (p = 0.001). Figure 5 displays the impact of the replanning to decrease the PG dose, with the average cumulated DVH with replanning (green line) and without replanning (blue line).

In the over-irradiated PG group, the replanning decreased the xerostomia risk by 11% on average (ranging from 1 to 30%, SD 8%) (p < 0.01).

Table 2 Parotid gland overdose and replanning benefit assessments, based on the fraction or the cumulated doses, for all the 15 patients

	D_{mean} (Gy),mean (Min-max;SD)		p-value
	Planned dose (1)	30.9 (9.2-54.6; 7.9)	-
Doses at the fraction	Without replanning (2)	33.0 (7.7-61.2; 9.9)	
	With replanning (3)	29.4 (4.1-51.7; 8.3)	
	PG overdose (4) = (2)-(1)	1.8 (−10.6-24.9; 5.8)	<0,001
	Replanning benefit (5) = (3)-(2)	3.8 (0–23.8; 4.0)	<0,001
Cumulated doses	Without replanning (2)	32.0 (8.7-57.6; 9.3)	-
	With replanning (3)	28.6 (4.6-51.2; 8.4)	
	PG Overdose (4) = (2)-(1)	1.1 (−7.9-10.0; 4.1)	0,1
	Replanning benefit (5) = (3)-(2)	3.6 (0–12.2; 3.3)	<0,001

PGs: parotid glands; Dmean: First, the mean PG dose was calculated for each patient and each week (DmeanWeekly). Then, the mean of the DMeanWeekly was calculated for each patient (DMeanPt). Finally, the mean of the DmeanPt was calculated for the whole population (D(mean)).
p values are calculated using the Wilcoxon test, to test if the Dmean in (1) and (2), and if the Dmean in (2) and (3) are statistically different.

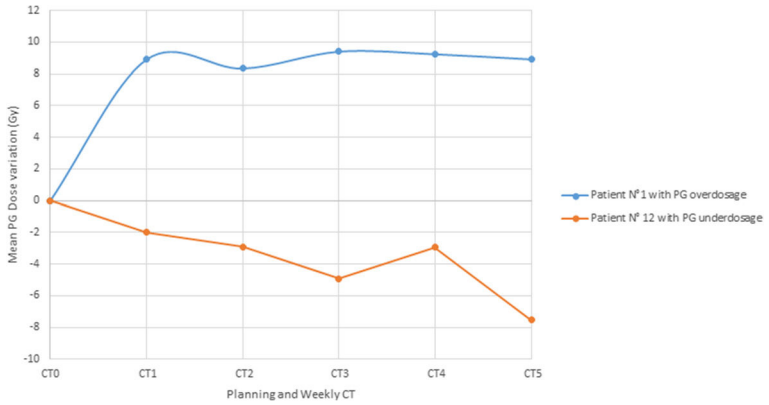

Figure 3 Variation over time of the mean PG dose for two representative patients. Red line corresponding to patient N°1 who presenting an increasing of the mean PG dose cumulated. Blue line corresponding to the patient N°12 who presenting a decreasing of the mean PG dose cumulated.

Anatomical parameters correlated with PG overdose or replanning benefit

PG overdose and replanning benefit (at the fraction or cumulated) increased with the CTV_{70} shrinkage and the reduction of neck thickness ($p < 0.01$). At the fraction, a reduction of 10 cc of the CTV_{70} or of 1 mm of the neck thickness leads to an increase of the mean PG dose of 0.3 Gy. The PG volume variation has no impact on the mean PG dose.

Discussion and conclusion

The main goal of definitive chemoradiotherapy in locally advanced HNC is to improve locoregional control, while

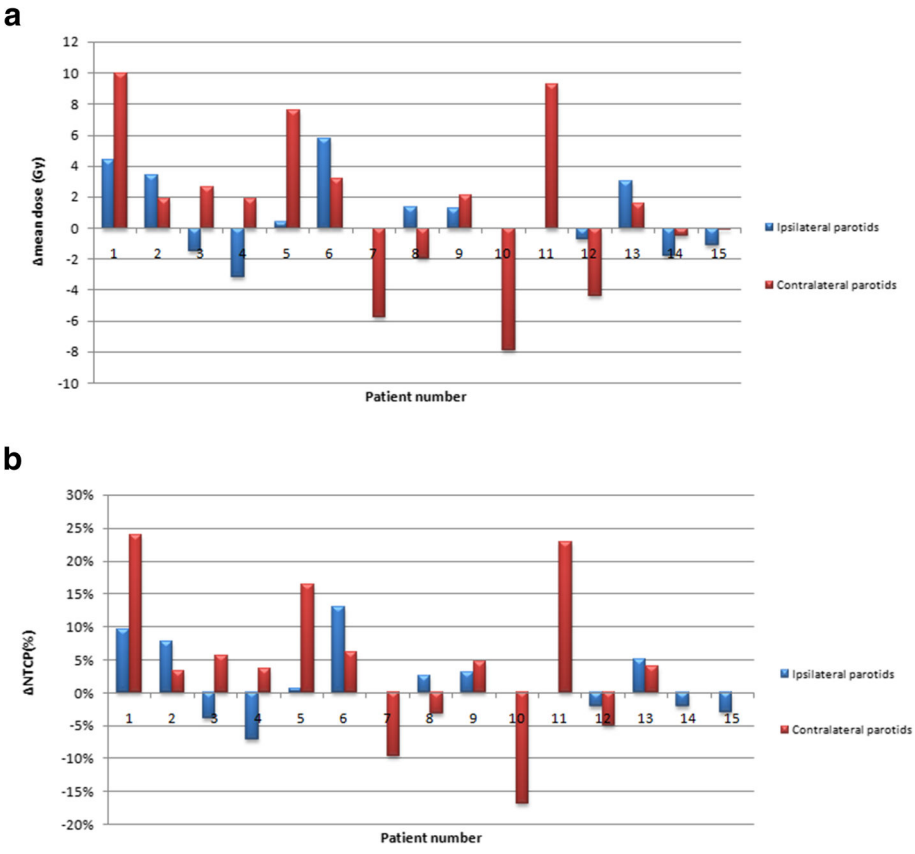

Figure 4 Parotid gland overdose assessment: Difference between the mean cumulated dose (without replanning) and the mean dose at the planning, in each of the parotid gland, for each of the 15 patients (4a). The corresponding impact on the xerostomia risk (%) is presented Figure **4b.** NTCP: normal tissue complication risk of xerostomia defined as a salivary flow ratio <25% of the pretreatment one [21].

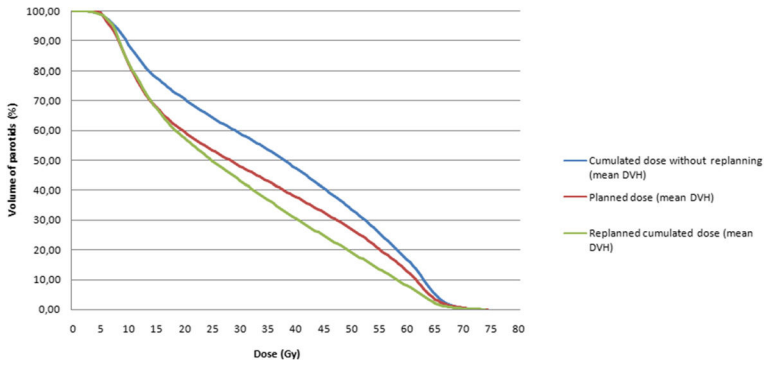

Figure 5 Mean parotid gland dose-volume histograms (DVHs) showing the impact of replanning on the over-irradiated PGs (n = 16).

keeping a high quality of life. Reducing the dose in the PGs during the whole course of IMRT and therefore xerostomia is a major challenge. Indeed, we found the majority of the PGs (59%) being overirradiated of a mean dose of 4 Gy (up to 10 Gy), resulting to an absolute increase risk of xerostomia of 8% (up to 24%). The ART strategy appears to benefit not only to the over-irradiated PG patients, reducing the mean dose of 5 Gy (up to 12 Gy) and the xerostomia risk of 11% (up to 30%), but also to the non-over-irradiated PGs. These results suggest thus a large use of ART for the majority of locally advanced HNC patients. In our study, four patients (N° 4, 7, 10 and 12) have not clear benefit from replanning. These patients were presented a spontaneous decrease of the mean PG dose during the treatment. No more gain was possible with the replanning due to the other constraints (homogeneity,

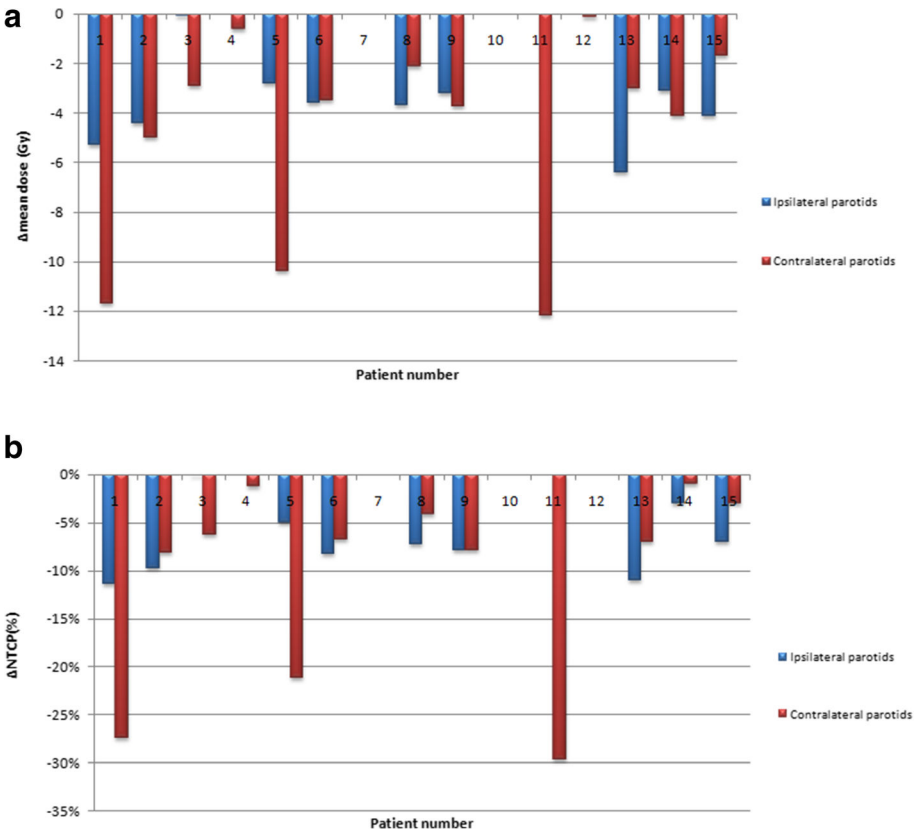

Figure 6 Replanning benefit assessement: cumulated mean dose difference between the dose with replanning and the dose without replanning, in each of the parotid gland (ipsilateral and contralateral), for each of the 15 patients (6a), and corresponding estimated xerostomia risk (%) (6b). NTCP: normal tissue complication risk of xerostomia defined as a salivary flow ratio <25% of the pretreatment one [21].

spinal cord, brainstem …). The GORTEC dose volume constraints has been respected for all the replanning.

The dosimetric benefit of ART has been shown in a limited number of studies, and not exclusively for the PGs. In a series of 22 patients, Schwartz *et al*. evaluated the impact of one and two replanning using daily CT on rails [23]. The mean PG dose was decreased of 3.8% for contralateral PGs and of 9% for ipsilateral PGs, with possible sparing of the oral cavity and larynx. In another series of 20 patients, a single replanning performed at the 3rd or 4th week of treatment decreased the mean PG dose of 10 Gy [9]. On the other hand, Castadot *et al*. didn't show any dosimetric benefits for PGs when using four replanning in a series of 10 patients, however reducing the spinal cord dose and improving the CTV_{56} dose conformation [24].

The optimal number and time of replanning are unclear. Wu *et al*. concluded that one replanning decreased the mean PG dose by 3%, two replanning by 5%, and six replanning by 6% [13]. A "maximalist" weekly replanning strategy was considered feasible in our study, as in an ongoing randomized study (ARTIX) comparing one IMRT based planning to a weekly based IMRT replanning. The benefit of such strategy has to be demonstrated compared to other replanning strategies. Ongoing study (like ART-FORCE trial) test the benefit of only one replanning [24]. The benefit of each supplementary weekly replanning has to be evaluated. A true adaptive RT strategy should be personalized to each patient, ranging potentially from no re-planning to a maximalist weekly replanning. Ideally, replanning decisions may likely be based on either geometrical criteria or cumulated dose monitoring corresponding to the dose-guided RT approach. Replanning is also particularly time-consuming, complete delineation taking up to 2.5 hours in our experience and that of others [25-28]. Deformable image co-registration software can be used to propagate the OAR contours from the initial planning CT to the per-therapeutic planning CT, reducing the delineation time by approximately a factor 3 [26,28]. The CTV delineation should be however carefully checked, to prevent recurrence due to inadequately reduced CTV. Indeed, the goal of ART in our study was to spare the PGs during treatment as they were spared at the planning, while keeping the same appropriate CTV coverage (and not to reduce the CTV coverage).

The analysis of the anatomical variations occurring within the course of IMRT is crucial to understand the overdose of the PGs and to identify early the sub-group of the overdosed PGs (59%). We found that mean volumes decreased by 28% for the PGs and 31% for the CTV, in agreement with the literature reporting values of 15% to 28% for the PGs, 69% for the GTV, and 8% to 51% for the CTV [7,9,13,23,26,29]. We found that the PGs overdose (without replanning) and the dosimetric benefit of replanning increased with the tumor shrinkage and the reduction of head thickness. The last one is likely explained by loss of weight, tumor shrinking and decrease of the PG volume. The reduction of the head thickness leads consequently to the occurrence of dose hotspot in the neck, close or within the PGs (Figure 1). Other studies also found that reduction of the neck diameter increases the risk of over-irradiation [30,31]. The variation of the mean PG dose was more important between the CT0 and the CT1 than between each weekly CT. This difference may be explained by the delay between CT0 and the first weekly CT. In our study, the PG dose differences between the fraction and the initial planning are likely related to both the set-up error (we did not quantified) and the anatomical structures volume/shape variations. Systematic set-up errors may increase the mean PG dose by around 3% by mm of displacement [32]. This point suggests, for a daily practice, to combine both a daily bone registration to correct the set-up errors and replanning to correct the anatomical variations.

Fraction comparison only provides information for a specific moment and there is a need for full treatment dose evaluation and comparison. Deformable registration enables dose fraction accumulation [33]. Since PG shape and volume variations were limited, our study's Dice scores were relatively high (0.92). However, the Dice score does not provide any information regarding the registration's anatomical "point to point" correspondence accuracy. Moreover, the possibility of PG defects observed over the course of radiotherapy [34] should prompt careful consideration of this cumulated dose approach, thereby justifying an independent "fraction to fraction" dose analysis. Our results, based on both weekly fraction and cumulated dose, were consistent. The 3D dose visualization and differential DVH of the dose difference between the cumulated dose and planning dose (Figure 1) revealed moreover the heterogeneity of hotspot distribution in PGs, which may also impact on the xerostomia risk. The cranial part of the PGs seems to be more critical [35,36], maybe due to the presence of an important concentration of salivary gland stem cells at this level [37]. The possible heterogeneity of the radiosensitivity within the PG could be therefore more carefully investigated in order to consider to spare not only the full gland (represented by a mean dose endpoint) but also subparts of the gland. Indeed, relatively small dose (10 Gy) within the PG may cause severe loss of function [38], and dose greater than 20 Gy may cause up to 90% loss of the acinar cells [39]. It seems also that radiation-induced gland dysfunction are due to membrane damage, causing secondarily necrosis of acinar cells and atrophy of the lobules [40].

Our study exhibits limitations. The small patient number did not allow us to analyze the potential impact of

tumor localization. Even if CTs from a single patient were always delineated by the same radiation oncologist, intra-observer variabilities in organ delineation are also potentially responsible for uncertainties. Moreover, the clinical benefit of the weekly replanning has been estimated and was not reported in the study.

In conclusion, an ART strategy combining a daily bone registration and a weekly replanning may be proposed for locally advanced HNC, with an expected benefit to decrease xerostomia. This PG-sparing strategy appears however particularly complex and should be therefore assessed within prospective trials, with a special attention for CTV delineation. The optimal number and time of replanning are unclear. The benefit of a weekly replanning strategy versus other replanning strategies have to been demonstrated.

Competing interests
The authors declare that they have no competing interests.

Authors' contributions
JC, GL, EC, FJ, KB and OH were responsible for patients treatments and care. AS, MN, PH and GC performed the deformable registration and the dose accumulation. JDO, JC, and RdC performed all statistical analysis. JC, AS and RdC wrote the manuscript. All authors helped, read and approved the final manuscript.

Acknowledgements
The authors wish to thank Mr. B.Pitre who assisted in the proof-reading of the manuscript.

Author details
[1]Department of Radiotherapy, Centre Eugene Marquis, Avenue de la bataille Flandre Dunkerque, F-35000 Rennes, France. [2]Rennes University 1, LTSI, Campus de Beaulieu, Rennes F-35000, France. [3]INSERM, U1099, Campus de Beaulieu, Rennes F-35000, France. [4]CHU Pontchaillou, Rennes F-35000, France. [5]Centre Antoine Lacassagne, Nice F-06100, France.

Received: 20 October 2014 Accepted: 22 December 2014
Published online: 09 January 2015

References
1. St Guily JL, Borget I, Vainchtock A, Remy V, Takizawa C. Head and neck cancers in France: an analysis of the hospital medical information system (PMSI) database. Head Neck Oncol. 2010;2:22.
2. Pignon JP, Bourhis J, Domenge C, Designe L. Chemotherapy added to locoregional treatment for head and neck squamous-cell carcinoma: three meta-analyses of updated individual data. MACH-NC Collaborative Group. Meta-Anal Chemother Head Neck Cancer Lancet. 2000;355:949–55.
3. Chambers MS, Rosenthal DI, Weber RS. Radiation-induced xerostomia. Head Neck. 2007;29:58–63.
4. Kam MK, Leung SF, Zee B, Chau RM, Suen JJ, Mo F, et al. Prospective randomized study of intensity-modulated radiotherapy on salivary gland function in early-stage nasopharyngeal carcinoma patients. J Clin Oncol. 2007;25:4873–9.
5. Nutting CM, Morden JP, Harrington KJ, Urbano TG, Bhide SA, Clark C, et al. Parotid-sparing intensity modulated versus conventional radiotherapy in head and neck cancer (PARSPORT): a phase 3 multicentre randomised controlled trial. Lancet Oncol. 2011;12:127–36.
6. Pow EH, Kwong DL, McMillan AS, Wong MC, Sham JS, Leung LH, et al. Xerostomia and quality of life after intensity-modulated radiotherapy vs. conventional radiotherapy for early-stage nasopharyngeal carcinoma: initial report on a randomized controlled clinical trial. Int J Radiat Oncol Biol Phys. 2006;66:981–91.
7. Barker Jr JL, Garden AS, Ang KK, O'Daniel JC, Wang H, Court LE, et al. Quantification of volumetric and geometric changes occurring during fractionated radiotherapy for head-and-neck cancer using an integrated CT/linear accelerator system. Int J Radiat Oncol Biol Phys. 2004;59:960–70.
8. Duma MN, Kampfer S, Schuster T, Winkler C, Geinitz H. Adaptive radiotherapy for soft tissue changes during helical tomotherapy for head and neck cancer. Strahlenther Onkol. 2012;188:243–7.
9. Nishi T, Nishimura Y, Shibata T, Tamura M, Nishigaito N, Okumura M. Volume and dosimetric changes and initial clinical experience of a two-step adaptive intensity modulated radiation therapy (IMRT) scheme for head and neck cancer. Radiother Oncol: J Eur Soc Ther Radiol Oncol. 2013;106:85–9.
10. Hansen EK, Bucci MK, Quivey JM, Weinberg V, Xia P. Repeat CT imaging and replanning during the course of IMRT for head-and-neck cancer. Int J Radiat Oncol Biol Phys. 2006;64:355–62.
11. Lee C, Langen KM, Lu W, Haimerl J, Schnarr E, Ruchala KJ, et al. Assessment of parotid gland dose changes during head and neck cancer radiotherapy using daily megavoltage computed tomography and deformable image registration. Int J Radiat Oncol Biol Phys. 2008;71:1563–71.
12. O'Daniel JC, Garden AS, Schwartz DL, Wang H, Ang KK, Ahamad A, et al. Parotid gland dose in intensity-modulated radiotherapy for head and neck cancer: is what you plan what you get? Int J Radiat Oncol Biol Phys. 2007;69:1290–6.
13. Wu Q, Chi Y, Chen PY, Krauss DJ, Yan D, Martinez A. Adaptive replanning strategies accounting for shrinkage in head and neck IMRT. Int J Radiat Oncol Biol Phys. 2009;75:924–32.
14. Kutcher GJ, Burman C. Calculation of complication probability factors for non-uniform normal tissue irradiation: the effective volume method. Int J Radiat Oncol Biol Phys. 1989;16:1623–30.
15. Mohan R, Wu Q, Manning M, Schmidt-Ullrich R. Radiobiological considerations in the design of fractionation strategies for intensity-modulated radiation therapy of head and neck cancers. Int J Radiat Oncol Biol Phys. 2000;46:619–30.
16. Lee N, Chuang C, Quivey JM, Phillips TL, Akazawa P, Verhey LJ, et al. Skin toxicity due to intensity-modulated radiotherapy for head-and-neck carcinoma. Int J Radiat Oncol Biol Phys. 2002;53:630–7.
17. Gérard JP, Ortholan C, Pointreau Y. Normal tissue tolerance to external beam radiation therapy. Cancer Radiother. 2010;14:227–410.
18. Cazoulat G, Simon A, Dumenil A, Gnep K, de Crevoisier R, Acosta O, et al. Surface-constrained nonrigid registration for dose monitoring in prostate cancer radiotherapy. IEEE Trans Med Imaging. 2014;33:1464–74.
19. Thirion JP. Image matching as a diffusion process: an analogy with Maxwell's demons. Med Image Anal. 1998;2:243–60.
20. Lyman JT. Complication probability as assessed from dose-volume histograms. Radiat Res Suppl. 1985;8:S13–9.
21. Dijkema T, Raaijmakers CP, Ten Haken RK, Roesink JM, Braam PM, Houweling AC, et al. Parotid gland function after radiotherapy: the combined michigan and utrecht experience. Int J Radiat Oncol Biol Phys. 2010;78:449–53.
22. Dice LR. Measures of the amount of ecologic association between species. Ecology. 1945;26:297–302.
23. Schwartz DL, Garden AS, Shah SJ, Chronowski G, Sejpal S, Rosenthal DI, et al. Adaptive radiotherapy for head and neck cancer–dosimetric results from a prospective clinical trial. Radiother Oncol: J Eur Soc Ther Radiol Oncology. 2013;106:80–4.
24. Castadot P, Geets X, Lee JA, Gregoire V. Adaptive functional image-guided IMRT in pharyngo-laryngeal squamous cell carcinoma: is the gain in dose distribution worth the effort? Radiother Oncol: J Eur Soc Ther Radiol Oncol. 2011;101:343–50.
25. Berwouts D, Olteanu LA, Duprez F, Vercauteren T, De Gersem W, De Neve W et al.: Three-phase adaptive dose-painting-by-numbers for head-and-neck cancer: initial results of the phase I clinical trial. Radiotherapy and oncology: journal of the European Society for Therapeutic Radiology and Oncology 2013.
26. Budach W, Bolke E, Fietkau R, Buchali A, Wendt TG, Popp W et al.: Evaluation of time, attendance of medical staff, and resources during radiotherapy for head and neck cancer patients: the DEGRO-QUIRO trial. Strahlenther Onkol, 187:449–460.
27. Daisne JF, Blumhofer A. Atlas-based automatic segmentation of head and neck organs at risk and nodal target volumes: a clinical validation. Radiat Oncol. 2013;8:154.
28. Nishimura Y, Nakamatsu K, Shibata T, Kanamori S, Koike R, Okumura M, et al. Importance of the initial volume of parotid glands in xerostomia for patients with head and neck cancers treated with IMRT. Jpn J Clin Oncol. 2005;35:375–9.

29. Lai YL, Yang SN, Liang JA, Wang YC, Yu CY, Su CH, et al. Impact of body-mass factors on setup displacement in patients with head and neck cancer treated with radiotherapy using daily on-line image guidance. Radiat Oncol. 2014;9:19.
30. You SH, Kim SY, Lee CG, Keum KC, Kim JH, Lee IJ, et al. Is there a clinical benefit to adaptive planning during tomotherapy in patients with head and neck cancer at risk for xerostomia? Am J Clin Oncol. 2012;35:261–6.
31. Delana A, Menegotti L, Bolner A, Tomio L, Valentini A, Lohr F, et al. Impact of residual setup error on parotid gland dose in intensity-modulated radiation therapy with or without planning organ-at-risk margin. Strahlenther Onkol. 2009;185:453–9.
32. Castadot P, Lee JA, Parraga A, Geets X, Macq B, Gregoire V. Comparison of 12 deformable registration strategies in adaptive radiation therapy for the treatment of head and neck tumors. Radiother Oncol: J Eur Soc Ther Radiol Oncol. 2008;89:1–12.
33. Fiorino C, Rizzo G, Scalco E, Broggi S, Belli ML, Dell'Oca I, et al. Density variation of parotid glands during IMRT for head-neck cancer: correlation with treatment and anatomical parameters. Radiother Oncol: J Eur Soc Ther Radiol Oncol. 2012;104:224–9.
34. Konings AWT, Cotteleer F, Faber H, van Luijk P, Meertens H, Coppes RP. Volume effects and region-dependent radiosensitivity of the parotid gland. Int J Radiat Oncol Biol Phys. 2005;62:1090–5.
35. Konings AWT, Faber H, Cotteleer F, Vissink A, Coppes RP. Secondary radiation damage as the main cause for unexpected volume effects: A histopathologic study of the parotid gland. Int J Radiat Oncol Biol Phys. 2006;64:98–105.
36. Lombaert IM, Brunsting JF, Wierenga PK, Faber H, Stokman MA, Kok T, et al. Rescue of salivary gland function after stem cell transplantation in irradiated glands. PLoS One. 2008;3:e2063.
37. Bussels B, Maes A, Flamen P, Lambin P, Erven K, Hermans R, et al. Dose–response relationships within the parotid gland after radiotherapy for head and neck cancer. Radiother Oncol. 2004;73:297–306.
38. Henriksson R, Frojd O, Gustafsson H, Johansson S, Yi-Qing C, Franzen L, et al. Increase in mast cells and hyaluronic acid correlates to radiation-induced damage and loss of serous acinar cells in salivary glands: the parotid and submandibular glands differ in radiation sensitivity. Br J Cancer. 1994;69:320–6.
39. Porter SR, Fedele S, Habbab KM. Xerostomia in head and neck malignancy. Oral Oncol. 2010;46:460–3.
40. Heukelom J, Hamming O, Bartelink H, Hoebers F, Giralt J, Herlestam T, et al. Adaptive and innovative Radiation Treatment FOR improving Cancer treatment outcomE (ARTFORCE); a randomized controlled phase II trial for individualized treatment of head and neck cancer. BMC Cancer. 2013;13:84.

3.1.3 Conclusion

Ce travail de modélisation confirme qu'en cas de RCMI standard sans replanification pour des cancers localement avancés des VADS, environ 2/3 des parotides vont être surdosées de presque 4 Gy par rapport à la dose planifiée, alors que l'autre tiers va présenter un sous dosage spontané. Le surdosage ne concerne donc pas la totalité des parotides, et certains patients pourraient ne pas relever d'une approche de radiothérapie adaptative pour épargner les parotides. Une radiothérapie adaptative hebdomadaire permet de corriger ce surdosage pour la totalité des parotides, voire de diminuer encore la dose par rapport à la dose planifiée. Ce bénéfice est d'autant plus marqué pour les patients ayant un surdosage des parotides en l'absence de radiothérapie adaptative. Dans ce cas, la dose moyenne aux parotides était diminuée de 5 Gy en cas de radiothérapie adaptative par rapport à l'absence de replanification. Cette correction du surdosage pourrait permettre une diminution du risque estimé de xérostomie de 11 %. Concernant les patients avec un sous-dosage des parotides au cours d'une RCMI standard sans replanification, la radiothérapie adaptative apporte un bénéfice mineur, permettant une diminution d'environ 1 Gy de la dose moyenne, avec un bénéfice clinique incertain au vue de la faible variation de dose.

Ces résultats soulignent le besoin de disposer de modèle de prédiction du risque de surdosage des parotides afin de proposer une stratégie de radiothérapie adaptative aux patients qui pourront en retirer un réel bénéfice clinique.

3.2 Identification des bons candidats à une radiothérapie adaptative pour épargner les parotides (article)

3.2.1 Introduction

Si, au cours d'une RCMI standard sans replanification, une majorité de patients vont présenter un surdosage des parotides, certains patients présentent au contraire un sous dosage des parotides. Même si la radiothérapie adaptative permet de diminuer (légèrement) la dose aux parotides chez ces patients, il n'est pas certain que ce gain dosimétrique se traduise par un bénéfice clinique. De plus, du fait de la lourdeur de la radiothérapie adaptative [49, 76], il apparait plus judicieux de concentrer les moyens sur les patients avec un surdosage parotidien, pour lesquels une diminution de plus de 10 % du risque de xérostomie semble possible. Plusieurs articles ont ainsi rapporté une corrélation entre le surdosage des parotides et des paramètres anatomiques tel que la perte de poids [87], la fonte tumorale [55], la diminution du diamètre cervical [40, 46] ou la diminution de volume des parotides [88]. Cependant ces corrélations sont relativement faibles et/ou ont été faites en fin de traitement, ne permettant donc pas d'identifier précocement les patients à risque de surdosage.

Afin de pouvoir guider le radiothérapeute dans le choix de déclencher ou non une stratégie de radiothérapie adaptative, l'utilisation de marqueurs anatomiques et/ou dosimétriques précoces (à la planification ou en début de traitement) prédictifs de l'importance du surdosage des parotides est donc nécessaire. Idéalement ces marqueurs devraient être utilisés non seulement pour identifier les patients à risque de surdosage des parotides, mais aussi pour prédire la sévérité de ce surdosage.

L'article reproduit ci-après, publié dans la revue *Radiation Oncology* en juin 2016, décrit la génération d'un nomogramme permettant une prédiction individualisée du surdosage parotidien.

3.2.2 A nomogram to predict parotid gland overdose in head and neck IMRT

Radiation Oncology, 2016 jun.

J. Castelli[1,2,3*]; A. Simon[2,3]; B. Rigaud[2,3]; C. Lafond[1]; E. Chajon[1]; J.D. Ospina[2,3]; P. Haigron[2,3]; B. Laguerre [4]; A. Ruffier Loubière[5]; K. Benezery[6] and R. de Crevoisier[1,2,3]

[1]. Centre Eugene Marquis, Radiotherapy, Rennes, F-35000

[2]. Rennes University 1, LTSI, Campus de Beaulieu, Rennes, F-35000

[3]. INSERM, U1099, Campus de Beaulieu, Rennes, F-35000

[4]. Centre Eugene Marquis, Medical oncology, Rennes, F-35000

[5]. CHRU de Tours, Radiotherapy, Tours, F-37550

[6]. Centre Antoine Lacassagne, Radiotherapy, Nice, F-06100

Castelli et al. Radiation Oncology (2016) 11:79
DOI 10.1186/s13014-016-0650-6

Radiation Oncology

RESEARCH Open Access

A Nomogram to predict parotid gland overdose in head and neck IMRT

J. Castelli[1,2,3*], A. Simon[2,3], B. Rigaud[2,3], C. Lafond[1], E. Chajon[1], J. D. Ospina[2,3], P. Haigron[2,3], B. Laguerre[4], A. Ruffier Loubière[5], K. Benezery[6] and R. de Crevoisier[1,2,3]

Abstract

Purposes: To generate a nomogram to predict parotid gland (PG) overdose and to quantify the dosimetric benefit of weekly replanning based on its findings, in the context of intensity-modulated radiotherapy (IMRT) for locally-advanced head and neck carcinoma (LAHNC).

Material and methods: Twenty LAHNC patients treated with radical IMRT underwent weekly computed tomography (CT) scans during IMRT. The cumulated PG dose was estimated by elastic registration. Early predictors of PG overdose (cumulated minus planned doses) were identified, enabling a nomogram to be generated from a linear regression model. Its performance was evaluated using a leave-one-out method. The benefit of weekly replanning was then estimated for the nomogram-identified PG overdose patients.

Results: Clinical target volume 70 (CTV70) and the mean PG dose calculated from the planning and first weekly CTs were early predictors of PG overdose, enabling a nomogram to be generated. A mean PG overdose of 2.5Gy was calculated for 16 patients, 14 identified by the nomogram. All patients with PG overdoses >1.5Gy were identified. Compared to the cumulated delivered dose, weekly replanning of these 14 targeted patients enabled a 3.3Gy decrease in the mean PG dose.

Conclusion: Based on the planning and first week CTs, our nomogram allowed the identification of all patients with PG overdoses >2.5Gy to be identified, who then benefitted from a final 4Gy decrease in mean PG overdose by means of weekly replanning.

Keywords: Nomogram, Adaptive radiotherapy, Head and neck, Parotid gland overdose

Introduction

During the course of intensity-modulated radiotherapy (IMRT) for head and neck cancer (HNC), large anatomical variations may result in delivered doses differing from the planned dose [1]. The literature shows that while dose variations in the clinical target volume appear extremely low [2–5], the percentage of patients with estimated PG overdoses ranges widely from 5 to 70 % [1, 5–10]. With the aim of correcting these PG overdoses, an adaptive radiotherapy (ART) strategy involving one or several replannings during treatment has been investigated [1, 2]. These replannings are, however, time-consuming, as a complete delineation can take up to 2.5 h [11–13] and may not be beneficial for all patients. It is therefore crucial to identify patients with PG overdose and evaluate how ART benefits each individual. Ideally, replanning decisions should be based on early and simple anatomical criteria, such as weight loss or decrease in neck diameter, which have been identified as risk factors for over-irradiation [10, 14–17]. However, a clear correlation between these markers and PG overdose has not yet been established [6]. After having identified early predictors of PG overdose, this dosimetric study had two objectives: 1) to generate a nomogram so as to predict PG overdose; 2) to quantify the benefits of weekly replanning, triggered by the nomogram, in terms of dose sparing and decrease in xerostomia risk.

* Correspondence: j.castelli@rennes.unicancer.fr
[1]Centre Eugene Marquis, Radiotherapy, de la Bataille Flandre Dunkerque, F-35000 Rennes, France
[2]Rennes University 1, LTSI, Campus de Beaulieu, Rennes F-35000, France
Full list of author information is available at the end of the article

Materials and methods

Patients and tumors

A total of 20 patients (mean age: 63; range: 50–77) were enrolled in this study. All patients presented with locally-advanced oropharyngeal cancer (Stage III or IV, American Joint Committee on Cancer 7th ed.). Patient, tumor, and treatment characteristics have been provided in Table 1.

Treatment and planning

All patients underwent IMRT with total doses of 70Gy (2Gy/fraction/day, 35 fractions), combined with a simultaneous integrated boost technique [18] and concomitant chemotherapy (cetuximab or platinum). Planning CTs (CT0) were performed with intravenous contrast agents using 2-mm slice thickness, from the vertex to the carina. Three target volumes were generated: $CTV_{70,}$ CTV_{63}, and CTV_{56}. The 70Gy clinical target volume (CTV_{70}) was equal to the gross tumor volume plus a 5-mm 3D margin, adjusted to exclude the air cavities and all bone mass free of tumor invasion. CTV_{63} corresponded to the area at high-risk of microscopic spread, in particular the ipsilateral nodal level II, while CTV_{56} corresponded to the low-risk subclinical area. The planning target volume (PTV) was the CTVs plus a 5-mm 3D margin, limited at 3 mm from the skin surface in order to avoid the build-up region and therefore limit skin toxicity [19]. The minimum PTV covered by the 95 % isodose line was 95 %. Dose constraints were set according to the GORTEC group (the French group of radiation oncology for head and neck cancer) (Table 2).

Parotid sparing was not conducted if considered to the detriment of PTV coverage or other essential organs at risk (OARs).

During the treatment course, set-up errors >5 mm were corrected by weekly in-room stereoscopic kV imaging. Informed consent was obtained from all patients. This study was approved by the institutional review board (ARTIX study NCT01874587).

Weekly dose estimations

Each patient underwent six weekly CTs (CT1-CT6) using the same protocol as CT0 over the treatment course, except for some variations in intravenous contrast agent use, which was not systematically employed,

Table 1 Patient, tumor, and treatment characteristics at initial planning (CT0)

ID	Gender	Age	TNM	Tumor sublocation	Chemotherapy	Volume (cm^3)			Mean planned PG dose (Gy)		Xerostomia NTCP (%) [23, 24]	
						CTV70	ILP	CLP	ILP	CLP	ILP	CLP
1	M	77	T4N0	Tonsil	Cetuximab	45.2	52.1	48.6	30.2	31.1	27.1	28.9
2	F	61	T2N2	Base of tongue	CDDP	26.3	31.1	27.5	31.4	26	29.7	19.1
3	M	70	T3N2c	Oropharynx	CDDP	181.5	24.9	20.7	37.9	31.1	45.1	29.1
4	F	66	T2N2c	Oropharynx	Cetuximab	107.2	27.8	23.4	32.9	27.9	33.1	22.5
5	M	57	T3N0	Velum	CDDP	62.4	20.7	18	28.1	27.8	23	22.3
6	M	67	T3N2c	Base of tongue	CDDP	156.2	24.5	22.7	30.8	29.4	25.4	22.1
7	M	52	T4N2a	Tonsil	Cetuximab	165.1	N/A	21.6	N/A	28.7	N/A	24
8	M	67	T4N1	Base of tongue	CDDP	139.3	22	19.3	30.7	29.2	28	25
9	F	65	T3N3	Base of tongue	CDDP	237.5	23.9	20.2	42.4	31.1	56.1	29
10	F	65	T4N3	Oropharynx	CDDP	257.9	N/A	24.5	N/A	35.2	N/A	38.5
11	M	50	T4N2c	Oropharynx	CDDP	434.5	N/A	17.7	N/A	36.3	N/A	41.1
12	M	53	T3N0	Base of tongue	CDDP	14.4	16.6	23.3	41.3	24.2	53.6	16.3
13	M	73	T3N2c	Oropharynx	Cetuximab	147	29.4	29.2	54.6	32.2	82.1	31.4
14	M	56	T3N0	Epiglottic	Cetuximab	14	22.8	29.2	19.7	9.2	10.3	2.7
15	M	75	T2N2a	Oropharynx	Cetuximab	76.3	20.3	22.4	29.4	29.1	25.6	25
16	M	57	T3N0	Oropharynx	CDDP	46.5	23.8	31.2	32.1	31.2	29.3	31.3
17	M	64	T3N2c	Epiglottic	CDDP	109.8	23.5	15.6	39.6	17.3	49.3	7.8
18	M	55	T1N2b	Tonsil	CDDP	31	20.2	20.8	25.7	23.63	18.7	15.3
19	M	65	T4N0	Velum	CDDP	10.1	23.7	25.3	28.6	28.2	24	23.2
20	M	56	T4N2b	Pharyngeal wall	CDDP	150	32.4	26.8	45	24.4	62.8	16.6

M male, *F* female, *CTV70* clinical target volume receiving 70Gy, *ILP* ipsilateral parotid glands, *CLP* contralateral parotid glands, *CDDP* cisplatin, *NTCP* normal tissue complication, *PG* parotid gland, *N/A* not applicable (PGs included in the CTV)

The NTCP Lyman Kutcher Burman (LKB) model ($n = 1$, $m = 0.4$, and median toxic dose [TD_{50}] = 39.9) [23, 24] defined the risk of xerostomia as a salivary flow ratio <25 % of the pretreatment one

Table 2 Dose constraints according to the GORTEC group (the French group of radiation oncology for head and neck cancer). D2%: Near maximum absorbed dose

Organ at risk	Dose constraint
Spinal cord	D2% < 45Gy
Brainstem	D2% < 54Gy
Optic nerves	D2% < 54Gy
Contralateral parotid	Mean dose < 30Gy, median dose < 26Gy
Ipsilateral parotid	Mean dose: as low as possible
Oral cavity	Mean dose < 30Gy, V30 < 65 %, and V35 < 35 %
Lips	D2% < 30Gy, mean dose < 20Gy

particularly not in the context of cisplatin-based chemotherapy. Anatomical structures were manually segmented on each weekly CT by the same radiation oncologist for each patient. In the event of complete response, the original macroscopically-involved areas were still included in CTV_{70}, which was adjusted to exclude any air cavities and bone mass showing no evidence of original tumor invasion.

Treatment always commenced on Mondays, with each weekly CT performed the following Monday. As patients were treated 5 days per week, each weekly CT corresponded to a 10Gy additional dose to the PTV (CT1 at 10Gy, CT2 at 20Gy, and so on). The actual doses delivered weekly were estimated by calculating the dose distribution on the weekly CTs using treatment parameters and the CT0 isocenter (Fig. 1).

Total cumulated dose estimations using deformable registration

For all patients, the weekly CT images were first registered to the planning CT using a rigid transformation defined by six parameters (three translations and three rotations). The mean squared error was used as a similarity criterion. The cumulated dose estimate relied on deformable image registration, using the free-form deformation (FFD) method. The control points were iteratively displaced according to the considered metric. The dense deformation field was obtained by B-spline interpolation [20]. The mutual information metric was used to handle the modified intensities between CT datasets caused by the presence of contrast agent. The geometric transformation obtained using both rigid and deformable registration was then applied to the weekly dose distributions in order to propagate each one to the planning CT0 dataset. The implementation was provided by the ElastiX library [21].

The average Dice score for PG registration was 0.81 (0.62–0.94). The propagated dose distributions were totaled to compute the cumulated dose on the planning CT, which was finally compared to the planned dose.

Linear regression model and nomogram to predict PG overdose

PG overdose was calculated as the difference between the cumulated mean PG dose and the mean PG dose of the planning CT dataset (CT0).

The following anatomical and dosimetric parameters have previously been described in the literature as correlating with PG overdose [6, 10, 14, 15], and were assessed for this correlation: CTV70 (cm3), PG volume (cm3), neck thickness (mm), PG-to-CTV70 distance, and mean PG dose. The PG-to-CTV70 distance was defined as the minimal Euclidean distance between the surfaces of the two contours. The difference between and ratio of each of these parameters computed from the two CTs (CT0 and each weekly CT, respectively) were also studied. The Pearson correlation was used to assess the correlation between variables significantly correlated with the PG overdose. When high correlation was observed between two variables ($r^2 > 0.5$), only the most significant parameter was included for further analysis. Finally, a linear regression method with backward elimination (coefficient of determination $r^2 > 0.3$, $p < 0.05$) was used to generate a model for PG overdose prediction. Regression was run with and without an intercept. The standard errors were compared to decide whether ordinary least squares or regression through origin provides a superior fit [22]. The model's accuracy was then validated by the quantiles-quantiles plot (QQ-plot) and r^2 for PG overdose prediction. A nomogram was generated based on this model, *i.e.* a chart representing a linear function calculating a predicted value from plotted input data (Fig. 2).

Leave-one-out cross validation was then performed to estimate the model's stability and accuracy. This method consisted in all patients but one ($n = 19$) being used to develop a PG overdose model (difference between cumulated PG dose and planned dose). A PG overdose prediction was then calculated for the one remaining patient using the model. This predicted PG overdose was then compared to the cumulated PG overdose. This step was repeated for each patient. The variance of each model parameters was calculated to estimate the model's stability and identify outliers. The mean squared error of the predicted values was calculated.

Statistical analysis was carried out using the Statistical Package for the Social Sciences V. 20.0, and R language and environment for statistical computing.

Weekly replanning for the patients at risk of PG overdose

Using the nomogram, we identified patients predicted to receive at least one PG overdose, for whom we performed a weekly IMRT replanning on each weekly CT dataset, in accordance with the dose constraints

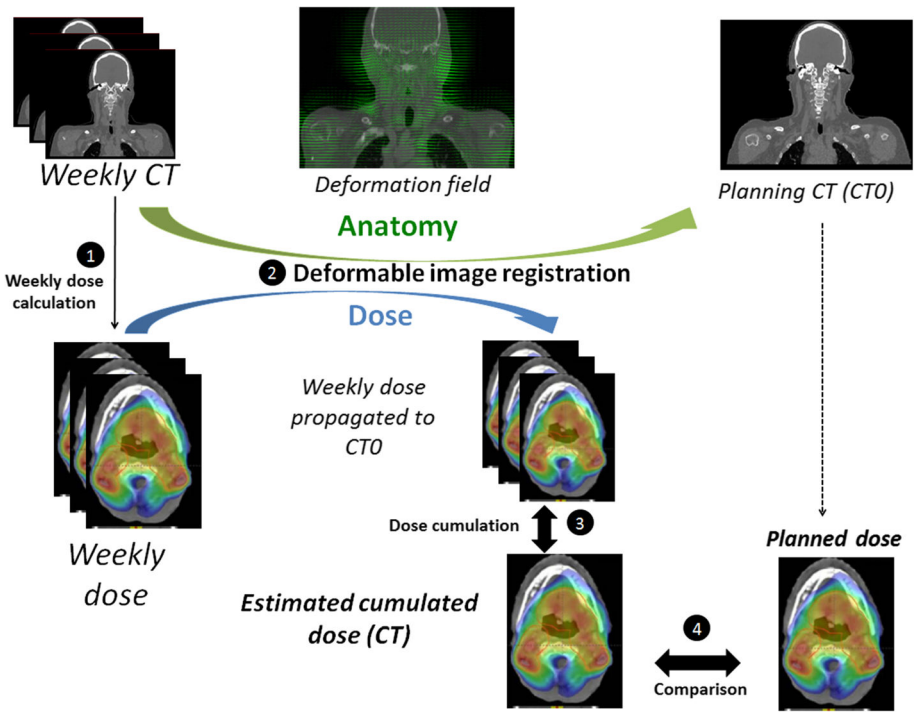

Fig. 1 *Total cumulated dose estimation by deformable image registration in four steps.* Step 1: The weekly delivered doses were calculated from the weekly computed tomography scans (CTs). Step 2: A deformable image registration was applied to the weekly doses according to the deformation field between the weekly and planning CT (CT0). Step 3: The propagated dose distributions were totaled to compute the cumulated dose for the CT0. Step 4: The planned dose was compared with the estimated cumulated dose

described for the initial planning. PTV coverage did not significantly differ between the initial planning and the weekly replanning. The dose constraints specified for the OARs complied with the GORTEC recommendations for all replanning, as for the initial planning. The mean PG cumulated doses with replanning were compared to those without. The impact of the replanning on the risk of xerostomia was estimated by using the Lyman Kutcher Burman (LKB) model of normal tissue complication probability

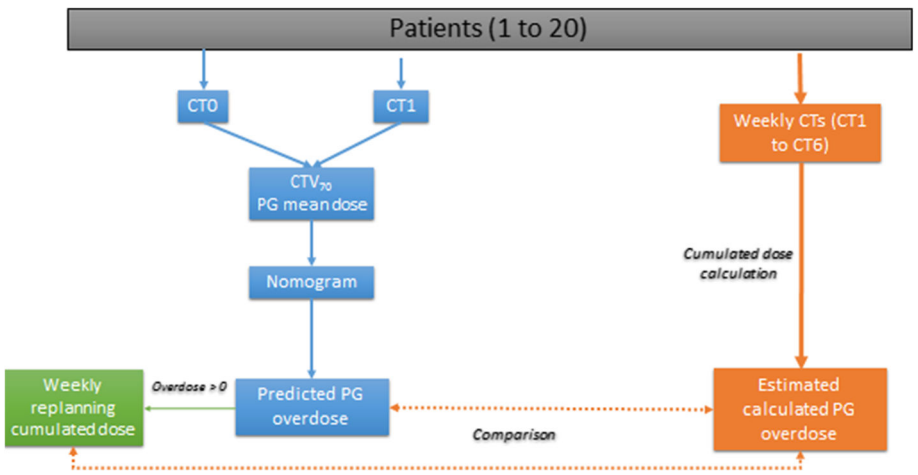

Fig. 2 *Nomogram use to predict parotid gland overdose.* For each patient, the nomogram was used to predict the parotid gland (PG) overdose. In the event of an estimated PG overdose, weekly replanning was performed. The cumulated doses with replanning were compared to those without to quantify the benefit of adaptive radiotherapy (ART). CT: computed tomography; CT0: planning CT; CT: first weekly CT (C1); CTV70: clinical target volume receiving 70Gy

(NTCP) ($n = 1$, m = 0.4, and median toxic dose [TD_{50}] = 39.9) [23, 24], the complication defined as a salivary flow ratio <25 % of the pretreatment one at 12 months.

Results

A total of 37 PGs were analyzed, due to three ipsilateral PGs included within the PTV being excluded from analysis.

Based on the difference between the cumulated and planned PG doses, two PG subgroups were identified (Fig. 3):

- a PG overdose group: 70 % of all the PGs, with a mean dose increase of 2.5Gy (up to 11.7Gy) and 16 patients presenting at least one overdosed PG;
- a PG under-dose group: involving the other 30 % of the PGs, with a mean dose decrease of 1.2Gy (up to 3.1Gy).

When identifying PG overdose predictors, we found the parameters from the first weekly CTs to be the most significant. Two anatomical and three dosimetric parameters were significantly correlated with PG overdose (Table 3).

As the mean PG dose for CT1 and the CT1/planning mean PG dose ratio were highly correlated with the difference between the mean PG doses for CT1 and CT0 (ΔDosePG) ($r^2 = 0.5$ and 0.9, respectively, $p < 0.001$), only the parameter with the highest r^2 was used (mean PG dose difference). The three parameters used for PG overdose prediction were CTV_{70} on the planning CT dataset (CTV_{70_CT0}), the CTV_{70} CT0-to-CT1 difference (ΔCTV_{70}), and the difference between the mean PG doses of CT1 and CT0 (ΔDosePG).

Based on these parameters, the resulting linear regression model for PG overdose prediction, optimized for all patients, was:

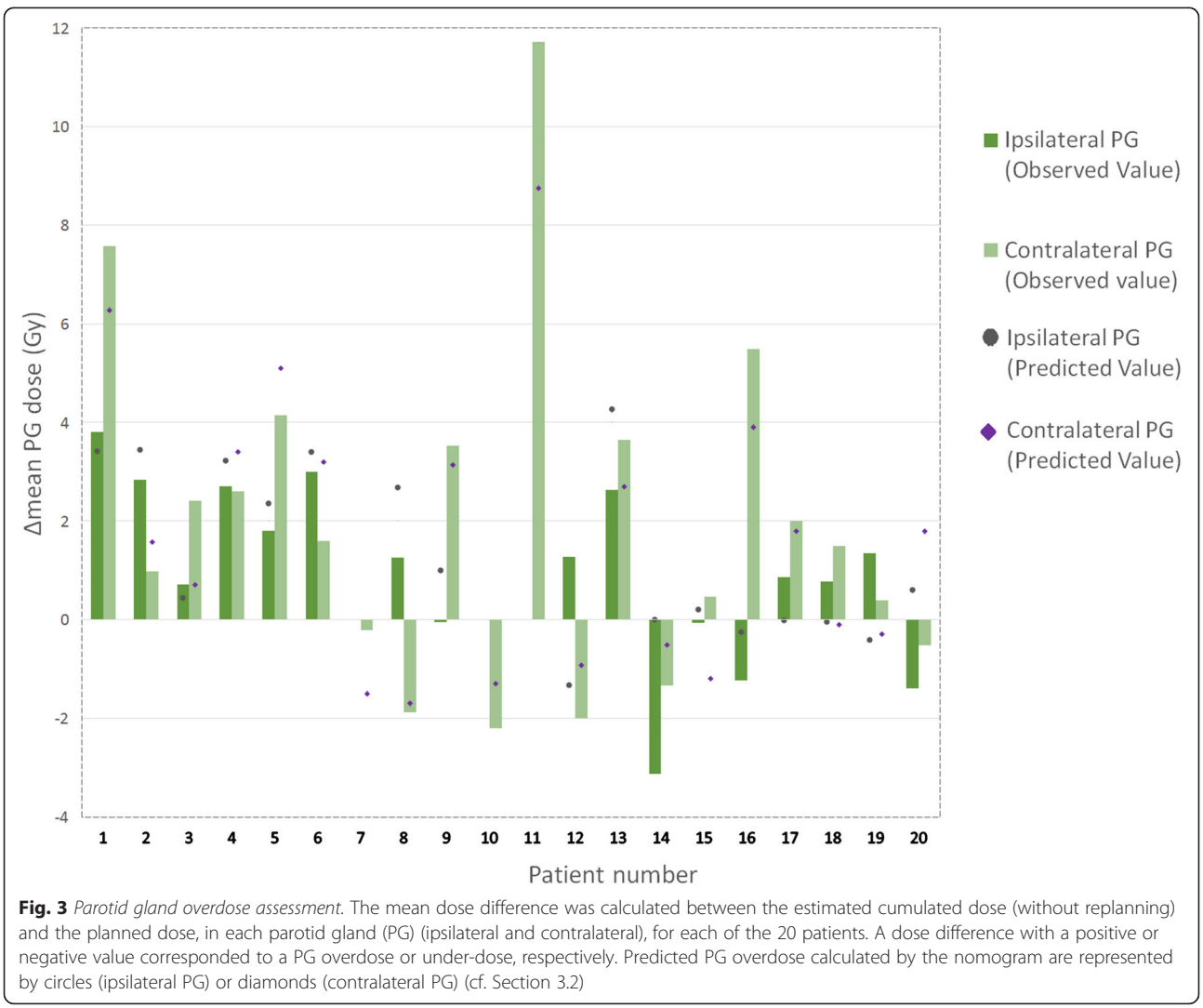

Fig. 3 *Parotid gland overdose assessment.* The mean dose difference was calculated between the estimated cumulated dose (without replanning) and the planned dose, in each parotid gland (PG) (ipsilateral and contralateral), for each of the 20 patients. A dose difference with a positive or negative value corresponded to a PG overdose or under-dose, respectively. Predicted PG overdose calculated by the nomogram are represented by circles (ipsilateral PG) or diamonds (contralateral PG) (cf. Section 3.2)

Table 3 Correlation between the anatomical/dosimetric parameters (calculated on CT0 and CT1) and the PG overdose

Analyzed parameters	r^2	p-value
CTV_{70_CT0}	0.32	0.038
ΔCTV_{70}	−0.46	0.004
ΔDosePG	0.72	<0.001
$DmeanPG_{\_CT1}$	0.49	0.002
$DmeanPG_{\_CT1}/DmeanPG_{\_CT0}$	0.70	<0.001

r^2 = Pearson correlation value, DmeanPG = Mean PG dose (Gy), _CT0 = on the planning CT (CT0), _CT1 = CT at the first week (CT1), Δ = difference of the parameter between CT1 and CT0

$$\mathrm{PGoverdose} = (0.007 \times \mathrm{CTV70_{CTO}}) - (0.045 \times \Delta\mathrm{CTV70}) + (0.509 \times \Delta\mathrm{DosePG})$$

The corresponding nomogram is shown in Fig. 4a. The quantiles-quantiles plot of the nomogram is shown in Fig. 4b.

The correlation between the observed and predicted cumulated PG doses is shown in Fig. 5 ($r^2 = 0.75$).

Dose variations (PG over- or under-doses) were correctly predicted for 25 of the 37 PGs (Fig. 3). Of the 16 patients with at least one overdosed PG, 13 were accurately identified (One patient with an error concerning the side of the PG overdose). In the three patients (Patients 12, 18 and 19) who were inaccurately classified, the mean PG was increased by an average of 1Gy (range: 0.4–1.5Gy).

The model's performance, evaluated using the leave-one-out cross validation, in terms of identifying patients with or without PG overdose achieved sensitivity, specificity, and positive and negative predictive values of 80 %, 60 %, 86 %, and 50 %, respectively. The mean values and standard deviations (SDs) of each coefficient, considering the leave-one-out cross validation, were 0.007 (SD: 0.0006), −0.045 (SD: 0.004), and 0.507 (SD: 0.01), for $\mathrm{CTV70_{CT0}}$, $\Delta CTV70$, and $\Delta DosePG$, respectively. The mean square error for the predicted PG overdose was 2.6 Gy (SD: 1.6 Gy). No significant outliers were extracted from the validation procedure.

For the 14 patients identified by the nomogram as having a predicted PG overdose, the mean PG dose without ART was 34.8Gy (range: 20.9–51.4Gy), corresponding to a mean xerostomia risk of 37 % (20–86 %). The dosimetric benefit of weekly replanning for these 14 patients is shown in Fig. 6. Replanning achieved an average decrease of 3.9Gy in the mean PG dose (range: 0–9.5Gy), representing an average decrease in absolute xerostomia risk of 8 % (0–22 %).

Discussion

We generated a nomogram aimed at predicting PG overdose based on early predictors calculated on the planning CT dataset and on a CT performed in the first week of treatment.

In total, 14 of the 16 patients with a calculated mean PG overdose of 2.5Gy were identified by the nomogram. All patients with a PG overdose >2.5Gy were identified. Weekly replanning of these 14 targeted patients enabled the mean PG dose to be decreased by 3.9Gy compared to the cumulated delivered dose, corresponding to an 8 % decrease in the estimated absolute xerostomia risk.

Due to anatomical variations occurring during the course of IMRT, some PGs can receive doses exceeding the planned dose (overdose). In an attempt to prevent this, ART is designed to take these anatomical variations into account by generating one or several new plannings. An increasing number of studies demonstrate this technique to have dosimetric benefits [1, 2, 4, 25]. The clinical impact of replanning has been evaluated in two studies [5, 26], where it was shown to improve both patient quality of life [26] and localize disease control, yet had no impact on overall survival. Nevertheless, ART is particularly complex and time-consuming [11–13], generating increased workload for all treatment staff. As not all patients may benefit from ART, it is essential to identify early predictors of PG overdose to enable appropriate patient selection. Neck thickness, weight loss, PG volume, initial tumor volume, and decrease in tumor volume were found to correlate with PG overdose [10, 14, 15]. In a recent review [6], these anatomical parameters were identified as selection criteria for ART patient selection, though no clear conclusion was reached due to the heterogeneity of the studies. However, these correlations were mostly primarily identified using parameters calculated at the end of treatment, therefore significantly limiting the possibility of treatment modifications. These parameters were also correlated with each other. Decrease in PG volume, for instance, has been found to correlate with age, body mass index, planned dose to the parotid glands, initial PG volume, and the volume of PG overlapping with lymph node metastases. Decrease in PG volume may be a useful parameter for identifying patients at higher risk of xerostomia [27]. However, neither the Brouwer et al. [6] study nor our own found any clear association between the decrease in PG volume and PG overdose. Other parameters may be indirectly linked to PG overdose. Human papillomavirus (HPV)-positive cancer has demonstrated a higher sensitivity to radiation [28, 29]. As the decrease in the CTV during the first week of treatment was correlated with PG overdose, HPV-status may exert an impact on the risk of PG overdose. Yet our series was not large enough to analyze the impact of this relationship.

Anatomical variations occurring during the first two weeks of treatment may be particularly relevant for PG overdose prediction, and may justify early replanning,

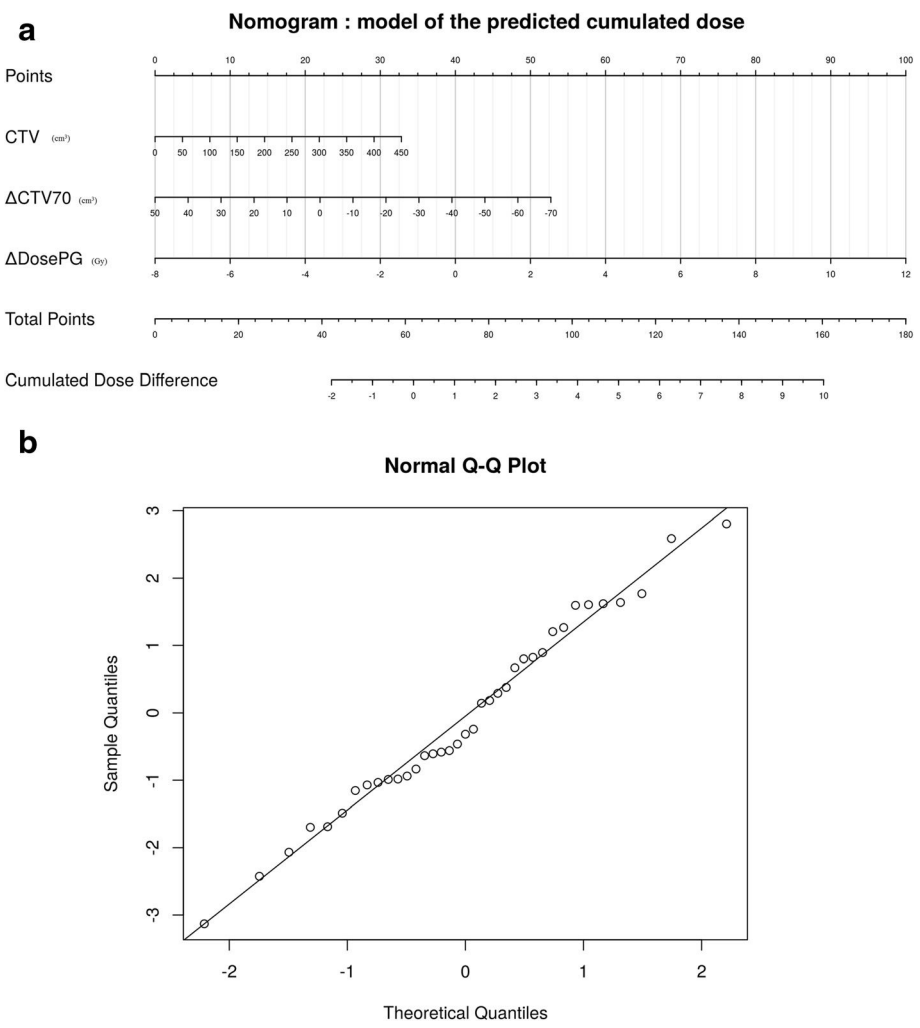

Fig. 4 a Nomogram to predict PG overdose. The nomogram enables easy prediction of the difference between the mean cumulated parotid gland (PG) dose and the mean planned PG dose (in Gy), using three parameters calculated on the planning computed tomography (CT) (CT0) and on a CT performed during the first week of the treatment (CT1). CTV70 (in cm^3): clinical target volume receiving 70Gy; ΔCTV70 (in cm^3): difference between the CTV70 of CT1 and CT0; ΔDosePG (in Gy): mean PG dose difference between CT1 and CT0. **b** Quantiles-quantiles plot (Q-Q plot) of the nomogram. The more accurately the quantile position is aligned, the more linear the model

resulting in significant PG dose sparing [17, 30]. Indeed, in the literature, CTV shrinkage appears to be particularly significant during the first week of radiotherapy [31]. In our study, the only anatomical parameters strongly correlated with PG overdose were CTV_{70} at planning and its decrease in the first week. However, this parameter alone was not sufficient to predict final PG overdose. Indeed, the most relevant parameter in our nomogram was the PG dose difference between the planning CT (CT0) and the first week of treatment CT (CT1). Early PG overdose has also been demonstrated to correlate with the estimated cumulated PG dose by Hunter et al. [8].

In our study, we found that considering the parameters only for the planning CT was not sufficient for PG overdose prediction. The acquisition of a new CT, performed during the first week of treatment with dose calculation, was required to predict the mean cumulated PG dose at the end of treatment. In terms of practical use of ART, replanning decisions can be based solely on anatomical parameters, ideally defined on cone-beam CT (CBCT) performed at the time of the fraction, which is also useful for bone registration to correct for patient set-up. This approach should be explored further, assuming that anatomical parameters alone could be sufficient for PG overdose prediction, and also be visible on the CBCT.

We performed a leave-one-out cross validation to estimate the model's stability and accuracy, which revealed very low variation in each model coefficient. So, the model is not strongly influenced by individual patients, showing that, even if the number of patients is low, the

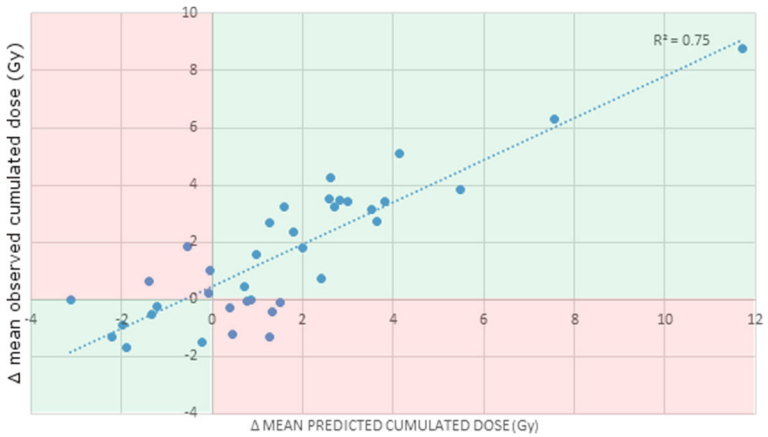

Fig. 5 *Correlation between observed and predicted parotid gland (PG) doses.* Representation of the observed (vertical axis) and predicted (horizontal axis) values of PG dose variation (difference between cumulated and planned PG dose) for each PG. The model included three parameters (CTV_{70} shrinkage at the CT1, mean PG dose difference between the dose delivered at CT1 and the planned dose, and CTV_{70} at the planning). Blue line: regression line ($R^2 = 0.75$). Red areas: wrong predictions (*e.g.* predicted overdose *vs.* observed under-dose). CT: computed tomography; CTV70 (in cm^3): clinical target volume receiving 70Gy; CT1: Week 1 treatment CT

considered population is homogeneous enough for the model to reach stability. No outliers were extracted. These results are proof of the model's good stability and accuracy.

The nomogram's sensitivity was only 80 %, which is insufficient for clinical decision making. The nomogram failed to predict PG overdose for two patients, whom exhibited moderate mean PG dose increases (<1.5Gy). In order to improve the sensitivity and identify other anatomical parameters correlated with PG overdose, a larger patient cohort is required. In addition, an external cohort is needed to validate the nomogram before it can be implemented in routine clinical practice.

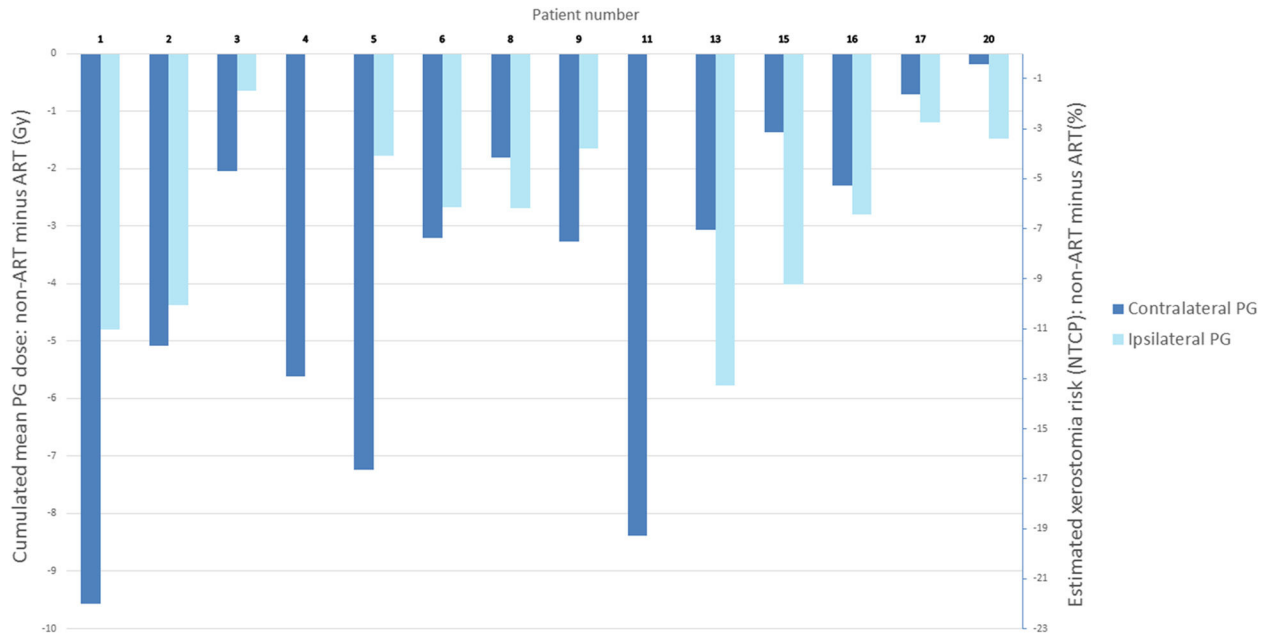

Fig. 6 Benefit of weekly replanning for the 14 parotid gland (PG) overdose patients identified by the nomogram. Cumulated mean dose difference between doses with replanning and those without (left y-axis), in each of the parotid glands (PGs) (ipsilateral and contralateral). The corresponding estimated risk of xerostomia (%), computed using the normal tissue complication (NTCP) Lyman Kutcher Burman (LKB) model (LKB NTCP) (n = 1, m = 0.4, and median toxic dose [TD_{50}] = 39.9) [23, 24] is represented on the right y-axis. Xerostomia was defined as a salivary flow ratio <25 % of the pretreatment one

We attempted to translate the dosimetric benefit from ART to a clinical benefit, based on a xerostomia NTCP model. A strong relation existed between the mean doses to the parotid glands and salivary flow, and the efficacy of these NTCP models proved relatively high (area under the curve: 0.68–0.75) [24, 32–34]. Non-dosimetric patient factors, such as age, tumor stage, baseline xerostomia, and chemotherapy [32, 35–37] may also increase the risk of xerostomia, though this is controversial [32–34]. Using IMRT, severe xerostomia was detected in approximately 40 % of the patients, compared to 80 % using 3D conformal radiotherapy [38, 39]. The dose constraints recently suggested by the QUANTEC group [34] may enable reducing severe xerostomia to under 20 % [33, 37]. However, these dose constraints were only met in a minority of patients. In our study, the estimated xerostomia risk for the cumulated dose without replanning was 37 %, close to the observed xerostomia values in IMRT studies [38, 39]. For the patients predicted to receive overdose by the nomogram (70 % of our population), an ART strategy could enable the xerostomia risk to be reduced to under 30 %.

The key issues affecting ART use include the choice of image registration method to monitor the cumulated dose and thus trigger replanning, within a dose-guided radiotherapy perspective. The PGs are often close to or within a high-dose gradient, and even minor geometrical registration errors can lead to high cumulated-dose errors. A recent study evaluating accuracy for dose accumulation of 10 deformable-image registration methods in HNC [40]. For the most accurate method (FFD with mutual information), a mean cumulated dose point-to-point error of 2.5Gy for the PG was shown. Taking into account these uncertainties, it was possible to correctly identify the overall under- and overdosed PGs. Moreover, potential loss of PG cells during the course of radiotherapy [41] should be carefully considered due to the uncertainty of point-to-point matching between different CTs when using a deformable registration method. In addition, due to the possible heterogeneity of radiosensitivity within the PGs [42–44], local hotspots may also have different impacts on xerostomia risk. In our study, the predicted value of PG overdose was obtained from the estimated cumulated dose using the Dose Index Registry (DIR), and is therefore subject to uncertainty. For all these reasons, and in the interest of clinical justification (correlation between the mean PG dose and xerostomia), we only investigated the mean PG dose. Clearly, more thorough analysis into correlations between the PG cumulated dose and xerostomia, using a larger patient cohort or phantom-based studies evaluating the accuracy of the DIR, need to be carried out in order to validate the dose accumulation method for daily clinical practice.

Conclusion

Based on the planning and first week CTs, our nomogram enabled the identification of all patients with large PG overdoses (≥2.5Gy). Replanning of these targeted patients lead to an eventual 4-Gy decrease in the mean PG overdose, while still respecting the dose-volume constraints in the other OARs and PTV. Other external cohorts are now required to validate this nomogram, as are clinical studies in order to validate the benefit of ART in the aims of decreasing the risk of xerostomia in locally-advanced HNC IMRT.

Abbreviations

ΔCTV_{70}, CTV_{70} CT0-to-CT1 difference; ΔDosePG, difference between the mean PG doses of CT1 and CT0; ART, Adaptive Radiotherapy; CBCT, Cone-beam CT; CTV, Clinical Target Volume; FFD: free-form deformation; GTV, Gross Tumor Volume; LAHNC, locally-advanced head and neck carcinoma; NTCP, normal tissue complication probability; OAR, Organ at risk; PG, Parotid gland; PTV, Planning Target Volume.

Acknowledgments

The authors wish to thank Ms. G. Corrégé PhD who assisted in proofreading the manuscript.

Fundings

This work was funded in part by the French INCa within the PAIR VADS program and by the French ANR within the Investissement d'Avenir program (Labex CAMI) under reference ANR-11-LABX-0004.

Availability of data and materials

This work was a part of an ongoing clinical study. Until the final analysis of this study, the data will not be shared.

Authors' contributions

JC, EC, CL, BL, ARL, and KB were responsible for patients' treatments and care. AS, BG and PH performed the deformable registration and the dose accumulation. JDO, JC, BR and RdC performed all statistical analysis. JC, AS and RdC wrote the manuscript. All authors helped, read and approved the final manuscript.

Competing interests

The authors declare that they have no competing interests.

Consent for publication

Not applicable.

Ethics approval and consent to participate

This study was approved by the institutional review board (ARTIX study NCT01874587).

Author details

[1]Centre Eugene Marquis, Radiotherapy, de la Bataille Flandre Dunkerque, F-35000 Rennes, France. [2]Rennes University 1, LTSI, Campus de Beaulieu, Rennes F-35000, France. [3]INSERM, U1099, Campus de Beaulieu, Rennes F-35000, France. [4]Centre Eugene Marquis, Medical oncology, Rennes F-35000, France. [5]CHRU de Tours, Radiotherapy, Tours F-37550, France. [6]Centre Antoine Lacassagne, Radiotherapy, Nice F-06100, France.

Received: 17 February 2016 Accepted: 17 May 2016
Published online: 08 June 2016

References

1. Castelli J, Simon A, Louvel G, Henry O, Chajon E, Nassef M, Haigron P, Cazoulat G, Ospina J, Jegoux F. Impact of head and neck cancer adaptive radiotherapy to spare the parotid glands and decrease the risk of xerostomia. Radiat Oncol. 2015;10:6.

2. Wu Q, Chi Y, Chen PY, Krauss DJ, Yan D, Martinez A. Adaptive replanning strategies accounting for shrinkage in head and neck IMRT. Int J Radiat Oncol Biol Phys. 2009;75:924–32.
3. Duma MN, Kampfer S, Schuster T, Winkler C, Geinitz H. Adaptive radiotherapy for soft tissue changes during helical tomotherapy for head and neck cancer. Strahlenther Onkol. 2012;188:243–7.
4. Schwartz DL, Garden AS, Shah SJ, Chronowski G, Sejpal S, Rosenthal DI, Chen Y, Zhang Y, Zhang L, Wong PF. Adaptive radiotherapy for head and neck cancer–dosimetric results from a prospective clinical trial. Radiother Oncol. 2013;106:80–4.
5. Chen AM, Daly ME, Cui J, Mathai M, Benedict S, Purdy JA. Clinical outcomes among patients with head and neck cancer treated by intensity-modulated radiotherapy with and without adaptive replanning. Head Neck. 2014;36:1541–6.
6. Brouwer CL, Steenbakkers RJ, Langendijk JA, Sijtsema NM. Identifying patients who may benefit from adaptive radiotherapy: Does the literature on anatomic and dosimetric changes in head and neck organs at risk during radiotherapy provide information to help? Radiother Oncol. 2015; 115(3):285–94.
7. Brown E, Owen R, Harden F, Mengersen K, Oestreich K, Houghton W, Poulsen M, Harris S, Lin C, Porceddu S. Predicting the need for adaptive radiotherapy in head and neck cancer. Radiother Oncol. 2015; 116:57–63.
8. Hunter KU, Fernandes LL, Vineberg KA, McShan D, Antonuk AE, Cornwall C, Feng M, Schipper MJ, Balter JM, Eisbruch A. Parotid glands dose-effect relationships based on their actually delivered doses: implications for adaptive replanning in radiation therapy of head-and-neck cancer. Int J Radiat Oncol Biol Phys. 2013;87:676–82.
9. Lee C, Langen KM, Lu W, Haimerl J, Schnarr E, Ruchala KJ, Olivera GH, Meeks SL, Kupelian PA, Shellenberger TD, Manon RR. Assessment of parotid gland dose changes during head and neck cancer radiotherapy using daily megavoltage computed tomography and deformable image registration. Int J Radiat Oncol Biol Phys. 2008;71:1563–71.
10. Ahn PH, Chen CC, Ahn AI, Hong L, Scripes PG, Shen J, Lee CC, Miller E, Kalnicki S, Garg MK. Adaptive planning in intensity-modulated radiation therapy for head and neck cancers: single-institution experience and clinical implications. Int J Radiat Oncol Biol Phys. 2011;80:677–85.
11. Berwouts D, Olteanu LA, Duprez F, Vercauteren T, De Gersem W, De Neve W, et al. Three-phase adaptive dose-painting-by-numbers for head-and-neck cancer: initial results of the phase I clinical trial. Radiother Oncol. 2013; 107(3):310–6.
12. Budach W, Bolke E, Fietkau R, Buchali A, Wendt TG, Popp W, Matuschek C, Sack H: Evaluation of time, attendance of medical staff, and resources during radiotherapy for head and neck cancer patients: the DEGRO-QUIRO trial. Strahlenther Onkol. 2011;187(8):449–460.
13. Daisne JF, Blumhofer A. Atlas-based automatic segmentation of head and neck organs at risk and nodal target volumes: a clinical validation. Radiat Oncol. 2013;8:154.
14. Lai YL, Yang SN, Liang JA, Wang YC, Yu CY, Su CH, Chen SW. Impact of body-mass factors on setup displacement in patients with head and neck cancer treated with radiotherapy using daily on-line image guidance. Radiat Oncol. 2014;9:19.
15. You SH, Kim SY, Lee CG, Keum KC, Kim JH, Lee IJ, Kim YB, Koom WS, Cho J, Kim SK, Kim GE. Is there a clinical benefit to adaptive planning during tomotherapy in patients with head and neck cancer at risk for xerostomia? Am J Clin Oncol. 2012;35:261–6.
16. Barker Jr JL, Garden AS, Ang KK, O'Daniel JC, Wang H, Court LE, Morrison WH, Rosenthal DI, Chao KS, Tucker SL, et al. Quantification of volumetric and geometric changes occurring during fractionated radiotherapy for head-and-neck cancer using an integrated CT/linear accelerator system. Int J Radiat Oncol Biol Phys. 2004;59:960–70.
17. Sanguineti G, Ricchetti F, Thomas O, Wu B, McNutt T. Pattern and predictors of volumetric change of parotid glands during intensity modulated radiotherapy. Br J Radiol. 2013;86:20130363.
18. Mohan R, Wu Q, Manning M, Schmidt-Ullrich R. Radiobiological considerations in the design of fractionation strategies for intensity-modulated radiation therapy of head and neck cancers. Int J Radiat Oncol Biol Phys. 2000;46:619–30.
19. Lee N, Chuang C, Quivey JM, Phillips TL, Akazawa P, Verhey LJ, Xia P. Skin toxicity due to intensity-modulated radiotherapy for head-and-neck carcinoma. Int J Radiat Oncol Biol Phys. 2002;53:630–7.
20. Rueckert D, Sonoda LI, Hayes C, Hill DL, Leach MO, Hawkes DJ. Nonrigid registration using free-form deformations: application to breast MR images. IEEE Trans Med Imaging. 1999;18:712–21.
21. Klein S, Staring M, Murphy K, Viergever MA. Pluim JP: elastix: a toolbox for intensity-based medical image registration. IEEE Trans Med Imaging. 2010; 29:196–205.
22. Hahn GJ. Fitting regression models with no intercept term. J Quality Technology. 1977;9:56–61.
23. Lyman JT. Complication probability as assessed from dose-volume histograms. Radiat Res Suppl. 1985;8:S13–19.
24. Dijkema T, Raaijmakers CP, Ten Haken RK, Roesink JM, Braam PM, Houweling AC, Moerland MA, Eisbruch A, Terhaard CH. Parotid gland function after radiotherapy: the combined michigan and utrecht experience. Int J Radiat Oncol Biol Phys. 2010;78:449–53.
25. Castadot P, Geets X, Lee JA, Gregoire V. Adaptive functional image-guided IMRT in pharyngo-laryngeal squamous cell carcinoma: is the gain in dose distribution worth the effort? Radiother Oncol. 2011;101:343–50.
26. Yang H, Hu W, Wang W, Chen P, Ding W, Luo W. Replanning during intensity modulated radiation therapy improved quality of life in patients with nasopharyngeal carcinoma. Int J Radiat Oncol Biol Phys. 2013;85:e47–54.
27. Belli ML, Scalco E, Sanguineti G, Fiorino C, Broggi S, Dinapoli N, Ricchetti F, Valentini V, Rizzo G, Cattaneo GM. Early changes of parotid density and volume predict modifications at the end of therapy and intensity of acute xerostomia. Strahlenther Onkol. 2014;190:1001–7.
28. Lassen P, Eriksen JG, Hamilton-Dutoit S, Tramm T, Alsner J, Overgaard J. Effect of HPV-associated p16INK4A expression on response to radiotherapy and survival in squamous cell carcinoma of the head and neck. J Clin Oncol. 2009;27:1992–8.
29. Lassen P, Eriksen JG, Hamilton-Dutoit S, Tramm T, Alsner J, Overgaard J, Danish H. Neck Cancer G: HPV-associated p16-expression and response to hypoxic modification of radiotherapy in head and neck cancer. Radiother Oncol. 2010;94:30–5.
30. Wang ZH, Yan C, Zhang ZY, Zhang CP, Hu HS, Kirwan J, Mendenhall WM. Radiation-induced volume changes in parotid and submandibular glands in patients with head and neck cancer receiving postoperative radiotherapy: a longitudinal study. Laryngoscope. 2009;119:1966–74.
31. Bhide SA, Davies M, Burke K, McNair HA, Hansen V, Barbachano Y, El-Hariry IA, Newbold K, Harrington KJ, Nutting CM. Weekly volume and dosimetric changes during chemoradiotherapy with intensity-modulated radiation therapy for head and neck cancer: a prospective observational study. Int J Radiat Oncol Biol Phys. 2010;76:1360–8.
32. Lee TF, Fang FM. Quantitative analysis of normal tissue effects in the clinic (QUANTEC) guideline validation using quality of life questionnaire datasets for parotid gland constraints to avoid causing xerostomia during head-and-neck radiotherapy. Radiother Oncol. 2013;106:352–8.
33. Moiseenko V, Wu J, Hovan A, Saleh Z, Apte A, Deasy JO, Harrow S, Rabuka C, Muggli A, Thompson A. Treatment planning constraints to avoid xerostomia in head-and-neck radiotherapy: an independent test of QUANTEC criteria using a prospectively collected dataset. Int J Radiat Oncol Biol Phys. 2012;82:1108–14.
34. Deasy JO, Moiseenko V, Marks L, Chao KS, Nam J, Eisbruch A. Radiotherapy dose-volume effects on salivary gland function. Int J Radiat Oncol Biol Phys. 2010;76:S58–63.
35. Lee TF, Liou MH, Huang YJ, Chao PJ, Ting HM, Lee HY, Fang FM. LASSO NTCP predictors for the incidence of xerostomia in patients with head and neck squamous cell carcinoma and nasopharyngeal carcinoma. Sci Rep. 2014;4:6217.
36. Beetz I, Schilstra C, van der Schaaf A, van den Heuvel ER, Doornaert P, van Luijk P, Vissink A, van der Laan BF, Leemans CR, Bijl HP, et al. NTCP models for patient-rated xerostomia and sticky saliva after treatment with intensity modulated radiotherapy for head and neck cancer: the role of dosimetric and clinical factors. Radiother Oncol. 2012;105:101–6.
37. Beetz I, Steenbakkers RJ, Chouvalova O, Leemans CR, Doornaert P, van der Laan BF, Christianen ME, Vissink A, Bijl HP, van Luijk P, Langendijk JA. The QUANTEC criteria for parotid gland dose and their efficacy to prevent moderate to severe patient-rated xerostomia. Acta Oncol. 2014;53:597–604.
38. Kam MK, Leung SF, Zee B, Chau RM, Suen JJ, Mo F, Lai M, Ho R, Cheung KY, Yu BK, et al. Prospective randomized study of intensity-modulated radiotherapy on salivary gland function in early-stage nasopharyngeal carcinoma patients. J Clin Oncol. 2007;25:4873–9.
39. Nutting CM, Morden JP, Harrington KJ, Urbano TG, Bhide SA, Clark C, Miles EA, Miah AB, Newbold K, Tanay M, et al. Parotid-sparing intensity modulated

versus conventional radiotherapy in head and neck cancer (PARSPORT): a phase 3 multicentre randomised controlled trial. Lancet Oncol. 2011;12:127–36.
40. Rigaud B, Simon A, Castelli J, Gobeli M, Ospina Arango JD, Cazoulat G, Henry O, Haigron P, De Crevoisier R. Evaluation of deformable image registration methods for dose monitoring in head and neck radiotherapy. Biomed Res Int. 2015;2015:726268.
41. Fiorino C, Rizzo G, Scalco E, Broggi S, Belli ML, Dell'Oca I, Dinapoli N, Ricchetti F, Rodriguez AM, Di Muzio N, et al. Density variation of parotid glands during IMRT for head-neck cancer: correlation with treatment and anatomical parameters. Radiother Oncol. 2012;104:224–9.
42. Lombaert IM, Brunsting JF, Wierenga PK, Faber H, Stokman MA, Kok T, Visser WH, Kampinga HH, de Haan G, Coppes RP. Rescue of salivary gland function after stem cell transplantation in irradiated glands. PLoS One. 2008;3:e2063.
43. Konings AWT, Cotteleer F, Faber H, van Luijk P, Meertens H, Coppes RP. Volume effects and region-dependent radiosensitivity of the parotid gland. Int J Radiat Oncol Biol Phys. 2005;62:1090–5.
44. Konings AW, Faber H, Cotteleer F, Vissink A, Coppes RP. Secondary radiation damage as the main cause for unexpected volume effects: a histopathologic study of the parotid gland. Int J Radiat Oncol Biol Phys. 2006;64:98–105.

3.2.3 Conclusion

En utilisant des paramètres anatomiques et dosimétrique issus de la planification et du scanner réalisé à la première semaine de traitement, nous avons pu définir un modèle de prédiction du risque de surdosage des parotides. Les patients ayant une tumeur volumineuse, avec une fonte tumorale précoce et présentant un surdosage des parotides à la première semaine de traitement sont les meilleurs candidats à une replanification. Fondé sur ces paramètres, un nomogramme a pu être réalisé afin d'aider à l'estimation du risque de surdosage des parotides. La réalisation d'une replanification chez les patients identifiés par le modèle comme étant à risque de surdosage des parotides permet une diminution de la dose moyenne aux parotides de 4 Gy, ce qui correspond à une diminution du risque estimée de xérostomie de 8 % en valeur absolue.

En raison du nombre limité de patients inclus dans l'étude (20 patients), nous n'avons pas pu réaliser de validation externe. Une validation croisée par *leave-one-out* a cependant été réalisée, permettant d'estimer la sensibilité du nomogramme à 80% et la spécificité à 60%. Ces résultats, qui peuvent s'expliquer par le faible nombre de patients inclus, reste insuffisant pour une utilisation en pratique clinique. Cependant, il est intéressant de noter que le nomogramme permettait d'identifier tous les patients ayant un surdosage de plus de 2,5 Gy, ces patients étant probablement les plus à même de bénéficier d'une radiothérapie adaptative.

Au total, l'utilisation de paramètres anatomiques et dosimétriques simples pourrait permettre l'identification des patients à risque de surdosage des parotides, candidats à une stratégie de replanification hebdomadaire afin de diminuer le risque de xérostomie. Le bénéfice d'une stratégie de radiothérapie adaptative utilisant un nombre moins important de replanification reste cependant à évaluer.

3.3 Stratégie optimale de radiothérapie adaptative pour épargner les parotides

Des résultats précédents, nous avons vu que la radiothérapie adaptative apporte un bénéfice en termes de diminution de la dose aux parotides. Cependant ce bénéfice a été estimé en utilisant une approche systématique de replanification hebdomadaire. Il est possible que cette approche ne soit pas la plus rentable en terme de bénéfice dosimétrique par rapport au temps et à la lourdeur de cette approche. En effet, si une première évaluation portant sur 11 patients avait montré que 6 replanifications permettaient une meilleure épargne des parotides comparée à 2 replanifications [61], ce bénéfice restait modeste. Dans cette étude, seul le nombre de replanifications était variable (1, 2 ou 6). La replanification était réalisée à la troisième semaine de traitement dans le cas d'une replanification unique. Dans le schéma avec 2 replanifications, celles-ci étaient réalisées à la deuxième et quatrième semaine. Enfin la fréquence était hebdomadaire dans le schéma avec 6 replanifications. Une évaluation des différents schémas de replanification (en termes de nombre et de moment de replanification) apparaissait donc comme nécessaire.

Notre équipe a ainsi évalué le bénéfice de l'ensemble des scénarii de replanifications hebdomadaires. En faisant varier la fréquence (de 1 à 6 replanifications) et les semaines de mise en œuvre des replanifications (de la 1^{ière} à la dernière semaine), un total de 63 schémas de replanification ont été comparés (Figure 12). Cette comparaison a reposé sur les mêmes critères que l'article reproduit précédemment (*Impact of head and neck cancer adaptive radiotherapy to spare the parotid glands and decrease the risk of xerostomia*), c'est-à-dire en considérant la dose moyenne reçue par les parotides à partir de la dose cumulée par recalage déformable.

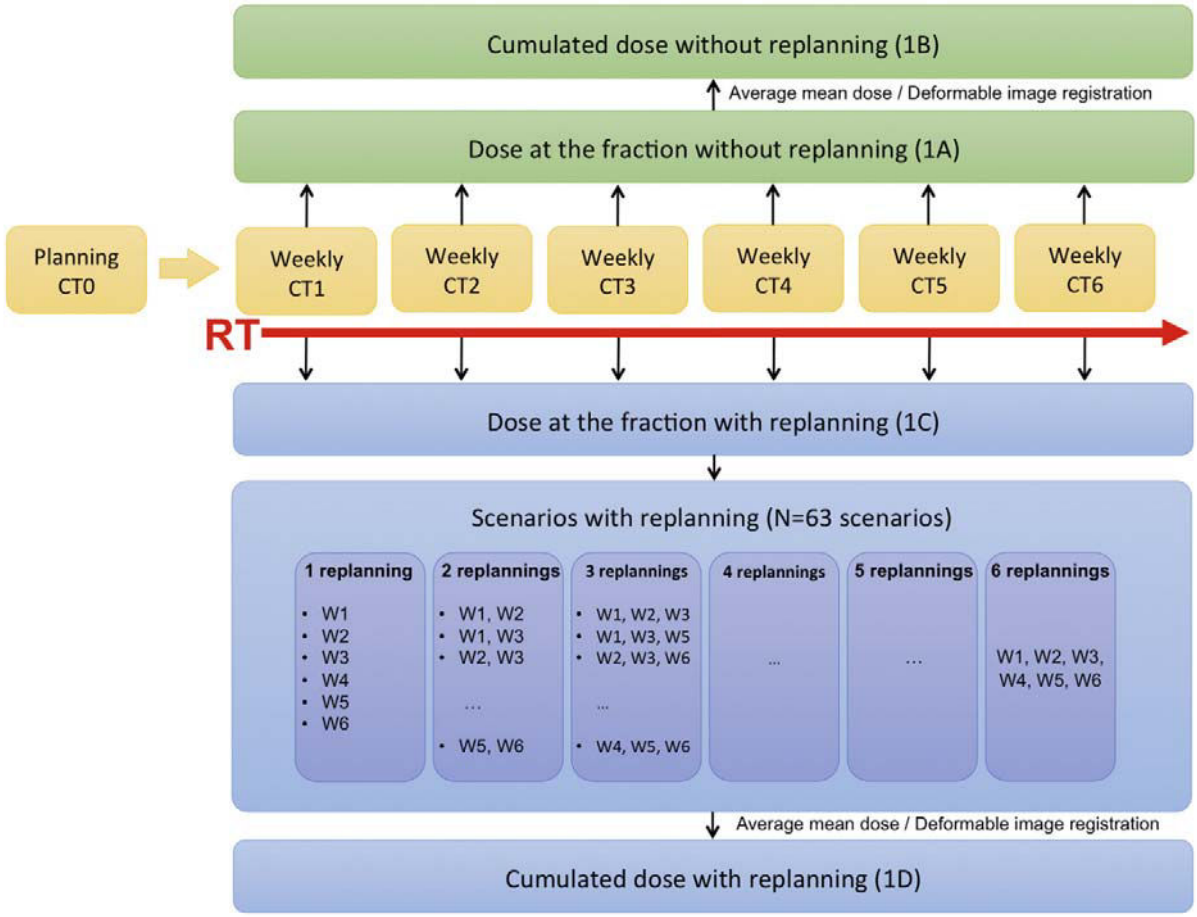

Figure 12 : Schéma de l'étude

CT: *computed tomography*; W: semaine de traitement. Les doses hebdomadaires étaient recalculées sans replanification (step 1A) ou avec (step 1C). Les doses cumulées sans replannification (step 1B) et pour chacun des scénarii (step 1D) ont été calculées en utilisant à la fois la moyenne des doses moyennes et une méthode de recalage élastique, puis ont été comparées avec la dose à la planification.

(Source P.Zhang, A.Simon, B.rigaud, **J.Castelli** *et al.* Radiother. Oncol. 2016)

Les résultats (Figure 13) ont montré que chaque replanification supplémentaire apporte un bénéfice en termes d'épargne des parotides. Cependant, 94 % du bénéfice était atteint avec 3 replanifications à la 1^{ière}, 2^{ième} et 5^{ième} semaine. Un tel schéma de replanification pourrait donc représenter le meilleur compromis en termes de rapport complexité/bénéfice. Ce travail a également permis de souligner que dans le cas où une seule replanification est réalisée, elle doit être faite de façon précoce (dans les 2 premières semaines) pour obtenir le plus de bénéfice sur

l'épargne des parotides. Ce dernier point peut s'expliquer par la survenue précoce des variations anatomiques lors de la radiothérapie. De plus, la réalisation trop tardive d'une replanification n'aura que peu d'impact à l'échelle du traitement du fait du nombre limité de séances auxquelles cette replanification va s'appliquer.

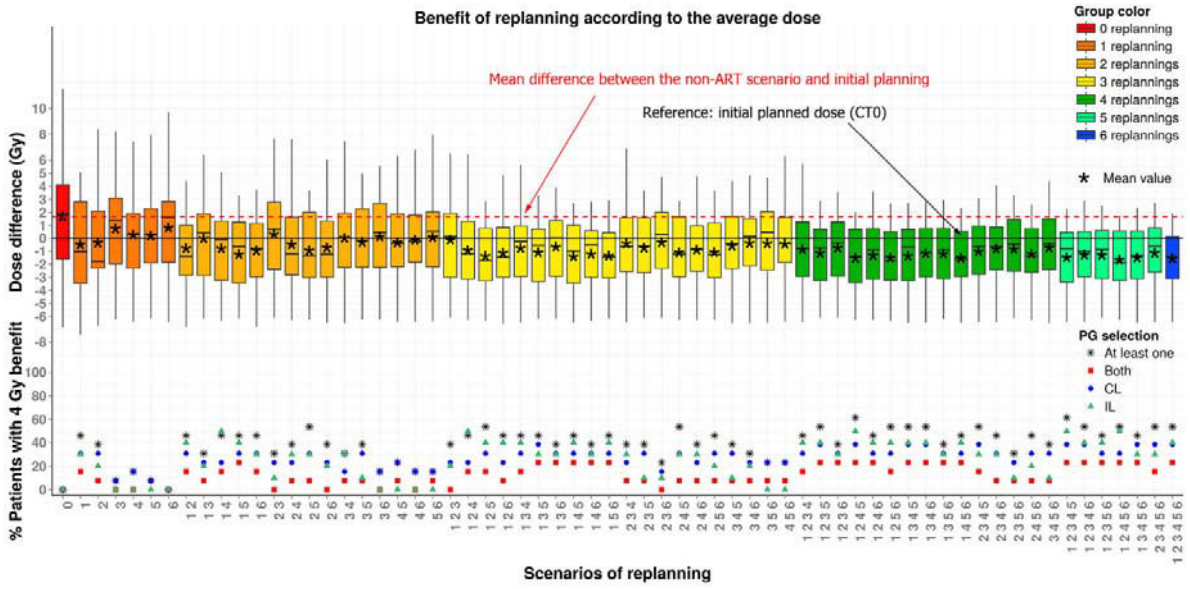

Figure 13 : Bénéfice de la replanification(s) pour épargner les parotides en fonction de chaque scenario, en considérant la moyenne des doses moyenne aux parotides

ART: radiothérapie adaptative; PG: parotide; CL: controlatérale; IL: homolatérale

Chaque boite à moustache représente la différence entre la dose cumulée et la dose planifiée pour chacun des 63 scénarios d'ART. Chaque scenario est identifié par la ou les semaine(s) de replanification, classé par ordre croissant de nombre de replanifications (CT1 to CT6). Les limites de chaque rectangle représentent les 25ieme and 75ieme percentiles, les traits fins verticaux représentent les valeurs extrêmes et la ligne au sein du rectangle correspond à la médiane. Le trait noir horizontal représente la référence pour la différence de dose (dose planifiée sur le scanner initial). La ligne rouge en pointillée correspond à la médiane de la différence de dose pour l'ensemble de la cohorte en l'absence de replanification. Les points en couleur dans la partie inférieure représentent le pourcentage de patient qui ont, pour chaque scénario, un bénéfice de plus de 4 Gy pour les 2 parotides (en noir), au moins une parotide (en vert), seulement pour la parotide homolatérale (en bleu) ou seulement pour la parotide controlatérale (en rouge) comparée à l'absence de replanification.

(Source P.Zhang, A.Simon, B.rigaud, **J.Castelli** *et al.* Radiother. Oncol. 2016)

4 Modélisation de la radiothérapie adaptative des cancers des VADS pour améliorer la couverture du volume cible ou pour l'intensification thérapeutique

La radiothérapie adaptative permet une diminution de la dose reçue par les parotides, et ainsi pourrait permettre de diminuer la toxicité. Elle peut cependant être utilisée aussi pour assurer le maintien d'une couverture tumorale maximale et/ou dans l'optique d'une escalade de dose guidée par l'imagerie (morphologique ou métabolique).

4.1 Quantification du bénéfice de la radiothérapie pour améliorer la couverture du volume cible au cours d'une irradiation d'un cancer des VADS

4.1.1 Introduction

Nous avons vu précédemment que du fait des importantes variations anatomiques survenant en cours de traitement, il existe un surdosage des parotides. Concernant les volumes cibles, il est globalement considéré que l'utilisation d'une marge de traitement autour de la tumeur (*planning treatment volume* (PTV)) devrait limiter le risque de sous dosage du volume cible [61, 89]. Cependant, l'estimation de la dose reçue par la tumeur est un paramètre capital, notamment au regard de la gravité du pronostic des patients traités par radio-chimiothérapie pour un cancer localement avancés des VADS (environ 35 % de récidive locale à 2 ans [5]). Les données disponibles montrent que le sous dosage du volume cible est possible en cours de traitement [40, 44, 77]. Tout comme pour les parotides, ce sous dosage ne semble survenir que pour une partie des patients.

L'évaluation du sous dosage au volume cible pose le problème du cumul de la dose dans la tumeur. En effet, compte tenu de la perte de substance qui va survenir en cours de traitement, il est impossible de réaliser un cumul de dose par recalage élastique. Une approche par la moyenne des doses hebdomadaires a donc été choisis dans l'article suivant (en cours de soumission à la revue Radiotherapy and Oncology en octobre 2017).

4.1.2 Adaptive radiotherapy in head and neck cancer to correct tumor underdose and parotid gland overdose (article)

J.Castelli[1,2,3]; A.Simon[2,3]; B.Rigaud[2,3]; E.Chajon[1]; K.Benezery[4] ; E.Vauleon[5]; F.Jegoux[6]; O.Henry[1]; C.Lafond[1,2,3]; R. de Crevoisier[1,2,3]

Submitted Radiother Oncol (2017 Oct.)

1. Centre Eugene Marquis, Radiotherapy Department, Rennes, F-35000, France
2. Université de Rennes 1, LTSI, Campus de Beaulieu, Rennes, F-35042, France
3. INSERM, U1099, Campus de Beaulieu, Rennes, F-35042, France
4. Centre Antoine Lacassagne, Radiotherapy department, Nice, F-06100, France
5. Centre Eugene Marquis, Department of Oncology, Rennes, F-35000, France
6. CHU Rennes, Head and Neck department, Rennes, F-35000, France

Adaptive radiotherapy in head and neck cancer to correct tumor underdose and parotid gland overdose

J.Castelli[1,2,3]; A.Simon[2,3]; B.Rigaud[2,3]; E.Chajon[1]; K.Benezery[4] ; E.Vauleon[5]; F.Jegoux[6]; O.Henry[1]; C.Lafond[1,2,3]; R. de Crevoisier[1,2,3]

1. Centre Eugene Marquis, Radiotherapy Department, Rennes, F-35000, France

2. Université de Rennes 1, LTSI, Campus de Beaulieu, Rennes, F-35042, France

3. INSERM, U1099, Campus de Beaulieu, Rennes, F-35042, France

4. Centre Antoine Lacassagne, Radiotherapy department, Nice, F-06100, France

5. Centre Eugene Marquis, Department of Oncology, Rennes, F-35000, France

6. CHU Rennes, Head and Neck department, Rennes, F-35000, France

Abstract

Purpose

In the context of locally advanced oropharyngeal cancer (LAOC) treated with definitive radiotherapy (RT) (combined with chemotherapy or cetuximab), the aims of this study were: 1) to estimate the dosimetric impact of anatomical variation on the tumor coverage and the parotid gland; and 2) to estimate the benefit of adaptive radiotherapy for both decrease the mean parotid gland dose and increase tumor coverage.

Materials and methods

Thirty-seven patients with a LAOC treated with IMRT (70 Gy, 2 Gy per fraction) had weekly computed tomography scans during the seven weeks of IMRT. Weekly doses were calculated without or with replanning. The dose delivered to 98% of the CTV (D98_CTV), the nearly maximum dose for the CTV (D2_CTV) and the mean dose of the CTV and the parotid gland were calculated. The delivered dose was estimated as the mean of the weekly dose of each parameters (without or with replanning). The delivered dose without ART was compared to the planned dose, and the delivered dose with ART was compared to the delivered dose without ART. Comparison was performed using median value of each parameter.

Results

The median D98_ CTV delivered without ART was 68 Gy, compared to 69.1 Gy at the planning ($p<0.01$). Ninety-four % of the patients had either CTV underdosage, PG overdose or both. A decrease of the dose to the CTV of more than 2 Gy combined with an increase of the mean PG dose of 2.4 Gy was show for 30% of the patients. Compared to standard IMRT without replanning, ART allowed increasing the D98_ CTV (69.2 Gy compared to 68 Gy, $p<0.01$). In the same time, the D2_CTV with ART was decreased from 74 Gy to 72.85 Gy ($p<0.01$) and the mean CTV dose from 71.4 Gy to 70.9 Gy ($p=0.01$). The mean PG dose was decreased from 27.9 Gy to 25.9 Gy ($p<0.01$).

Conclusion

Thirty % of the patients had a CTV underdose of more than 2 Gy without ART. These patients may be at higher risk of treatment failure. ART allowed increasing treatment homogeneity and correcting both CTV underdose and PG overdose. These dosimetric benefits may allow increasing local control and decreasing toxicity.

1 Introduction

During the course of intensity-modulated radiotherapy (IMRT) for head and neck cancer (HNC), due to large anatomical variations, the delivered dose may differed from the planned dose. Adaptive radiotherapy (ART) using one or several replanning aims to correct these variations and thus optimize the delivered dose distribution to the daily anatomy of the patient. ART was mainly evaluated to decrease the dose to the parotid gland [1-6]. Regarding the dose to the target volume, clinical target volume (CTV) coverage is usually considered more robust to changes, thanks to use of the planning target volume (PTV), combines with a tumor shrinkage. Indeed the analysis of the differences between planned and delivered dose for the GTV, CTV, and PTV showed controversial results. While a majority of the studies found very low dose differences (below 1-2% for the D2% and D95%) [3, 6-12], some reported large dose differences [13-16], of 1.9-Gy underdose to the GTV [16] or of 3 Gy to the PTV (up to 7.4Gy) [15]. However, these studies included a limited numbers of patients (ranging from 10 to 30) and imaging for dose comparison was performed at various time point, mostly only once time [1, 3, 7, 9, 15].

Regarding the benefit of ART to increase tumor coverage, five studies reported an improvement of various dosimetric endpoints, with a more uniform coverage [3, 5, 6] and an increased dose to the tumor compare without ART [4, 6, 15]. However, replanning was performed only time [3, 15] or two time [4-6] for a limited number of patients (10 to 33), while only a subset of patients may have a tumor underdose without ART (REF). Moreover, no data was available regarding the dose variation for both tumor and parotid gland at an individual scale. In particular, the frequency of patients with both a tumor underdose and a parotid gland overdose is not reported.

The aims of this study were to estimate (i) the dosimetric impact of anatomical variations on tumor coverage and parotid gland sparing with a standard IMRT; and (ii) the dosimetric benefit of ART with a weekly systematic replanning, for both correcting the tumor underdose and the parotid gland overdose.

2 Materials and methods

2.1 Patients, tumors and treatment

Thirty-seven patients with a locally advanced oropharyngeal cancer were prospectively included in this study. All tumors were locally advanced, corresponding to T3-4 or N2-3 stage (stage III or IV, AJCC 7th edition).

All patients underwent IMRT with total dose of 70Gy (2Gy/fraction/day, 35 fractions), combined with a simultaneous integrated boost technique [17] and concomitant chemotherapy (cetuximab or platinum). Half of the patient have been treated with a standard one planning based IMRT and half have been treated with a weekly systematic replanning.

All patients had a systematic percutaneous endoscopic gastrostomy for enteral feeding in order to avoid weight loss during the treatment. Informed consent was obtained from all patients. This study was approved by the institutional review board (ARTIX study NCT01874587).

2.2 Planning

Planning CTs (CT0) were performed with intravenous contrast agents using 2-mm slice thickness, from the vertex to the carina. Three target volumes were generated: $CTV_{70,}$ CTV_{63}, and CTV_{56}. The 70Gy clinical target volume (CTV_{70}) was equal to the gross tumor volume plus a 5-mm 3D margin, adjusted to exclude the air cavities and all bone mass free of tumor invasion. CTV_{63} corresponded to the area at high-risk of microscopic spread, in particular the ipsilateral nodal level II, while CTV_{56} corresponded to the low-risk subclinical area. The planning target volume (PTV) was the CTVs plus a 5-mm 3D margin, limited at 3mm from the skin surface in order to avoid the build-up region and therefore limit skin toxicity [18]. The minimum PTV covered by the 95% isodose line was 95%. Dose constraints were set

according to the GORTEC group (the French group of radiation oncology for head and neck cancer) [19]. Parotid sparing was not conducted if considered to the detriment of PTV coverage or other essential organs at risk (OARs).

2.3 Weekly replanning

Each patient underwent six weekly CTs (CT1-CT6) using the same protocol as CT0 over the treatment course, except for some variations in intravenous contrast agent use, which was not systematically employed, particularly not in the context of cisplatin-based chemotherapy. Anatomical structures were propagated from the planning CT to the weekly CT using deformable image registration (MIM Software 6.6©) and were manually corrected by the same radiation oncologist for each patient. In the event of complete response, the original macroscopically-involved areas were still included in CTV_{70}, which was adjusted to exclude any air cavities and bone mass showing no evidence of original tumor invasion. Two weekly dose distributions were performed on each weekly CT dataset, corresponding to two differents situations: standard IMRT without replanning or IMRT with replanning (ART). The standard IMRT without ART dose distribution was computed using treatment parameters and the isocenter from planning after bony registration. Weekly IMRT replanning was performed in accordance with the dose constraints described for the initial planning. The dose constraints specified for the OARs complied with the GORTEC recommendations for all replanning, as for the initial planning.

Treatment always commenced on Mondays, with each weekly CT performed the following Monday. As patients were treated 5 days per week, each weekly CT corresponded to a 10Gy additional dose to the PTV (CT1 at 10Gy, CT2 at 20Gy, and so on).

2.4 Cumulated dose estimations for the CTV and the parotid gland

The dose received by 98% of the CTV_{70} (D98_CTV), the mean CTV_{70} dose, the nearly maximum dose for the CTV (D2_CTV) and the mean parotid gland dose for each scenario (without or with replanning) was calculated. The cumulated dose without or with replanning were estimated using the mean of the

weekly dose for each dosimetric endpoints. Due to the loss of substance of the tumor and potentially of the parotid gland, deformable image registration was not used to cumulate the dose in this two structures.

2.5 Statistical analysis

The endpoints were the cumulated dose for the parotid gland (mean dose) and the CTV (D98, D2 and mean dose). The cumulated dose without ART and with ART were compared with the planned dose using nonparametric tests (Wilcoxon test). The cumulated dose with ART were also compared with the cumulated dose without ART.

3 Results

3.1 Quantification of the CTV underdose and parotid gland overdose with standard IMRT (cumulated dose without ART minus planned dose)

Compared to the planning, when using a standard IMRT without replanning, the median D98_CTV decreased from 69.1 Gy to 68 Gy ($p<0.01$). Twenty-eight (76%) patients had a median decrease of 1.6 Gy of the CTV_D98. Table 1 shows the population repartition based on D98_CTV variations without ART compared with the planned dose. Figure 1 shows the population repartition based on D98_CTV at the planning and cumulated without ART. The median value for the D2_CTV and the mean CTV dose at the planning were 72.8 Gy and 70.9 Gy, compared to a median value without ART of 74 Gy ($p<0.01$) and 71.4 Gy ($p=0.02$) respectively. The median CL PG dose slightly increased without ART compared to the planning (27.9 Gy and 27.8 Gy, respectively ($p<0.01$)). The dose to the CL PG was decreased by a median value of 0.8 Gy for 33% of the patients, while an increased by 2.3 Gy was show for the other 67% of the patients. Table 1 shows the population repartition based on mean parotid gland dose variations without ART compared with the planned dose. Figure 2 shows the population repartition,

for both ipsilateral and contralateral parotid gland, of mean dose at the planning and cumulated without ART.

Ninety-five percent of the patients had either CTV underdosage, CL PG overdose or both. Table 2 shows the population repartition of CTV underdose and parotid gland overdose without ART.

3.2 Quantification of the benefit of ART to correct CTV underdose and parotid gland overdose

Replanning was available for 30 patients. The median D98_CTV was 69.2 Gy with ART, compared to 68 Gy in case of standard IMRT without replanning ($p<0.01$). Compared to standard IMRT without replanning, ART allows to maintain the treatment homogeneity, decreasing the D2_CTV from 74 Gy to 72.85 Gy ($p<0.01$) and the mean CTV dose from 71.4 Gy to 70.9 Gy ($p=0.01$). Figure 1 shows the population repartition of D98_CTV at the planning, cumulated without ART and with ART. No difference between planned dose and cumulated dose with ART was show for the D98_CTV ($p=0.06$), the D2_CTV ($p=0.1$) and the mean CTV dose ($p=0.18$). ART allows also correction of the PG overdose, from 27.9 Gy to 25.9 Gy ($p<0.01$). Figure 2 shows the population repartition of mean PG dose at the planning, cumulated without ART and with ART. The benefit of ART to increase the dose to the CTV and decrease the dose to the parotid gland compared to the planned dose and to cumulated dose without ART is show table 2A and table 2B respectively. The figure 3 shows the individual benefit of ART to correct CTV underdose and PG overdose, compared to the cumulated dose without replanning.

4 Discussion

Our study is the first to report the dosimetric benefit of a maximalist weekly replanning to both increase tumor coverage and decrease mean parotid gland dose during IMRT for head and neck cancer. Nearly half of the patients had a CTV underdose of more than 1 Gy. ART allows also achieving a more uniform coverage of the target volume. Moreover, regarding both contralateral parotid gland and CTV

dose variation, the dose delivered without ART was similarly to the planned dose for only 5 % of the patients.

Thanks to the use of a planning target volume, one can think that the impact of the anatomical variation to the dose delivered to the target volume will be non-significant. However, literature showed controversial results, some studies reported an increase of the dose to the tumor [7, 8], others studies found very low dose differences between planned and delivered dose to the target volume (below 1-2% for the D2% and D95%) [3, 6, 9-12], and finally another studies reported large dose differences [13-16]. However, the tumor localization may also impact on the results, some studies included patients with head and neck cancers without tumor localization criteria [3, 9-12] while others studies included only nasopharynx [14] or oropharynx cancer [6]. The treatment was also different, with definitive or post-operative radiotherapy. All these studies included a limited number of patients (from 10 to 30 patients), while tumor underdose occurred not for all patients but only for a subset, and used a limited number of time points for cumulated the dose. Only five studies cumulated the dose based on at least a weekly imaging [6, 8, 10-12], while the other studies used 1 to 3 time points during the treatment. The method to cumulate the dose may also have a major impact on the results. Deformable image registration to cumulate the dose should not be used for the target volume due to tumor shrinkage. These points may explain the discrepancy between the different studies regarding tumor underdose. In our study, the cumulated dose was estimated by the mean of weekly value. A weekly imaging seems sufficient, as anatomic variations appear progressively over the treatment weeks. The tumor ant treatment homogeneous as all patients included had an oropharynx treated with chemoradiotherapy. We found that nearly 30% of the patients had a decrease of the dose to the CTV of more than 2 Gy, and an increase of the mean PG dose of 2.4 Gy. For these patients, these difference corresponding to one lost fraction to the tumor and to one supplementary fraction to the parotid gland. Such dose differences to the target volume are likely to lead to treatment failure. The impact of the planned dose to the tumor was assessed using quality assurance of radiotherapy for 820 patients included in the TROG 02.02 study. Based on protocol-specified criteria for significant

deviations (Gross disease must receive at least 66.5Gy, no more than 10% of the planning target must receive < 66.5Gy), two subgroups were retrospectively identified. Patients with major deficiencies in their treatment plans had a worse outcome compared with those treatment plans were protocol compliant: 2 years freedom from locoregional failure 54% v 78% respectively ($p<0.001$) [20]. We found that nearly 20% of the patients in our study had a delivered dose without ART to the CTV lower than 66.5Gy. These patients may have a great benefit from an ART strategy, with a potential increase of the local control.

In most of studies, ART was performed with the goal of correcting organs at risk overdose (mostly the parotid glands), allowing a decrease of the mean parotid gland dose (ranging from 0.6 Gy to 4.1 Gy), compared without ART [1, 2, 9, 10]. Regarding the benefit of ART for the tumor coverage, fives studies reported an improvement of the dosimetric endpoints (GTV, CTV, and PTV) with more uniform coverage [3, 5, 6] and increased coverage [4, 6, 15]. Schwartz et al. [6]included 22 patients with an oropharynx cancer. Using one or two replanning, an increase of tumor coverage and dose homogeneity were show. However, these studies used one or two replanning, and included a limited number of patients (from 10 to 30). One study included 30 patients, but only one replanning was performed at 40 Gy and the benefit of ART was estimated for the remaining 30 Gy. Our study is the first to evaluate the benefit of a maximalist weekly replanning for both increase tumor coverage and decrease mean parotid gland dose. In our study, ART allowed to correct CTV underdose for all patients. For the patients with a D98_CTV decrease > 2 Gy, the mean D98_CTV with ART was 68.8 Gy compared to 65.3 Gy without ART and to 68.7 Gy at the planning. This result may explain the better clinical outcome reported for patient treated with ART in two non-randomized studies [21, 22].

Different ART strategies for head and neck cancers were reported in the literature. The majority of the studies suggest that the more replanning are used, the more the PG can be spared, and especially so for oropharyngeal tumors. However, limiting the number of replanning is a crucial issue, given the burden each supplementary replanning entails [15, 23]. This point was addressed in a study investigating the benefit of numerous replanning strategies, defined by various numbers (1 to 6), and

the timings of replanning (at each week of the treatment) with regard to parotid gland sparing for 13 patients with oropharyngeal cancers [24]. Six replannings ensured the best benefits (decrease of 3.3 Gy of the parotid gland mean dose). However, 94% of this benefit was already attained with three replannings at weeks 1, 2, and 5, enabling a decrease of the mean parotid gland dose by 3.1 Gy. In our study, a maximalist number of 6 replanning were used to ensure the maximal benefit of ART. However, a lower number of replanning may be used to decrease the workload while keeping a significant benefit regarding tumor coverage and parotid gland-sparing.

There are two different modalities for ART: online or offline approach. In online ART, the whole process is performed while the patient remains on the treatment couch. This approach enables correction of systematic and random errors, can take into account acute modifications like rapid disease response, and provides small benefit in sparing the parotid gland compared to the off-line approach [10]. On the other hand, due to time constraints, online ART appears unrealistic in today's clinical practice. In the offline approach, a new plan is generated in just a few days, enabling the clinical quality assessment process to be initiated, and using information from previous time point. In clinical practice, offline ART seems more realistic for HNC, as anatomic variations appear progressively over the treatment weeks.

Our study exhibits some limits. Replanning were available only for a subset of patients (30/37). It was not possible to investigate the correlation between CTV underdose and tumor relapse as most of the patients were treated using an ART strategy. The number of patients was limited, even if it was the largest series reporting data of ART for tumor coverage combined with parotid gland sparing. No correlation between CTV underdosage and anatomical parameters were available. To estimate the dose without ART, we used the mean of the weekly CTV_D98 and of the mean PG dose. Such choice may be discussed for the CTV. However, due to tumor shrinkage, dose accumulation using deformable image registration was not possible. To ensure the best benefit of ART, an online approach was simulated in our study, and an offline approach may offer a slightly lower benefit.

5 Conclusion

Compared to the planned dose, nearly half of the patient treated with standard IMRT without ART had a decrease of the dose to 98% of the CTV of more than 1 Gy. Regarding both CTV and PG dose, the delivered dose was similar to the planned dose for only 5% of the patients. A weekly ART corrected both CTV underdose and parotid gland overdose for all patients, and may allowed to increase local control while decreasing toxicity.

Table 1: Population repartition based on D98_CTV variations without ART (Delivered dose without ART minus planned dose)

Dose variations without ART compared to planned dose (Delivered dose without ART minus planned dose)	Nbr of patients (%)
D98_CTV	
> + 1 Gy	1 (3%)
- 1 Gy to + 1 Gy	19 (51%)
< -1 Gy	17 (46%)
Mean parotid gland dose	
> 2 Gy	15 (41%)
-2 Gy to + 2 Gy	19 (51%)
< -2 Gy	3 (8%)

Table 2: Population repartition of CTV underdose and parotid gland overdose without ART (Delivered dose without ART minus planned dose)

	PG$^{\$}$ underdose	PG$^{\$}$ overdose	**Total**
CTV underdose	28% D98_CTV = - 1.2 Gy* PG dose = - 1.1 Gy*	48% D98_CTV = - 2 Gy* PG dose = + 2.3 Gy*	**76%**
CTV overdose	5% D98_CTV = + 0.2 Gy* PG dose = - 0.2 Gy*	19% D98_CTV = + 0.6 Gy* PG dose = + 2.6 Gy*	**24%**
Total	**33%**	**67%**	

*=median, $^{\$}$ = The contralateral parotid gland has been considered only. Number of patients = 37

Table 2A: Population repartition of the benefit of ART to increase the dose to the CTV and decrease the dose to the parotid gland (cumulated dose with ART minus planned dose)

ART compared with the planning	CL PG underdose	CL PG overdose	
CTV underdose	64% D98_CTV = - 0.6 Gy* Mean PG dose = - 2.2 Gy*	3% D98_CTV = - 0.4 Gy* PG dose = 1.1 Gy *	67%
CTV overdose	30% D98_CTV = + 0.7Gy* PG dose = - 1.7Gy*	3% D98_CTV = + 0.2 Gy* Mean PG dose = + 0.9 Gy*	33%
	94%	6%	

*=median, number of patients = 30

2B Population repartition of the benefit of ART to correct the dose to the CTV (underdose/overdose) and decrease the dose to the parotid gland (cumulated dose with ART minus cumulated dose without ART)

ART compared without ART	Correction of the PG overdose	PG dose increase	
Correction of the CTV underdose (D98 increase)	56% D98_CTV = + 1.7Gy* Mean PG dose = - 3.8Gy*	11% D98_CTV = + 2.7Gy* Mean PG dose = + 1.7Gy*	67%
Correction of the CTV overdose (D98 decrease)	33% D98_CTV = - 1Gy* Mean PG dose = - 4.1Gy*	0% D98_CTV = N/A Mean PG dose = N/A	33%
	89%	11%	

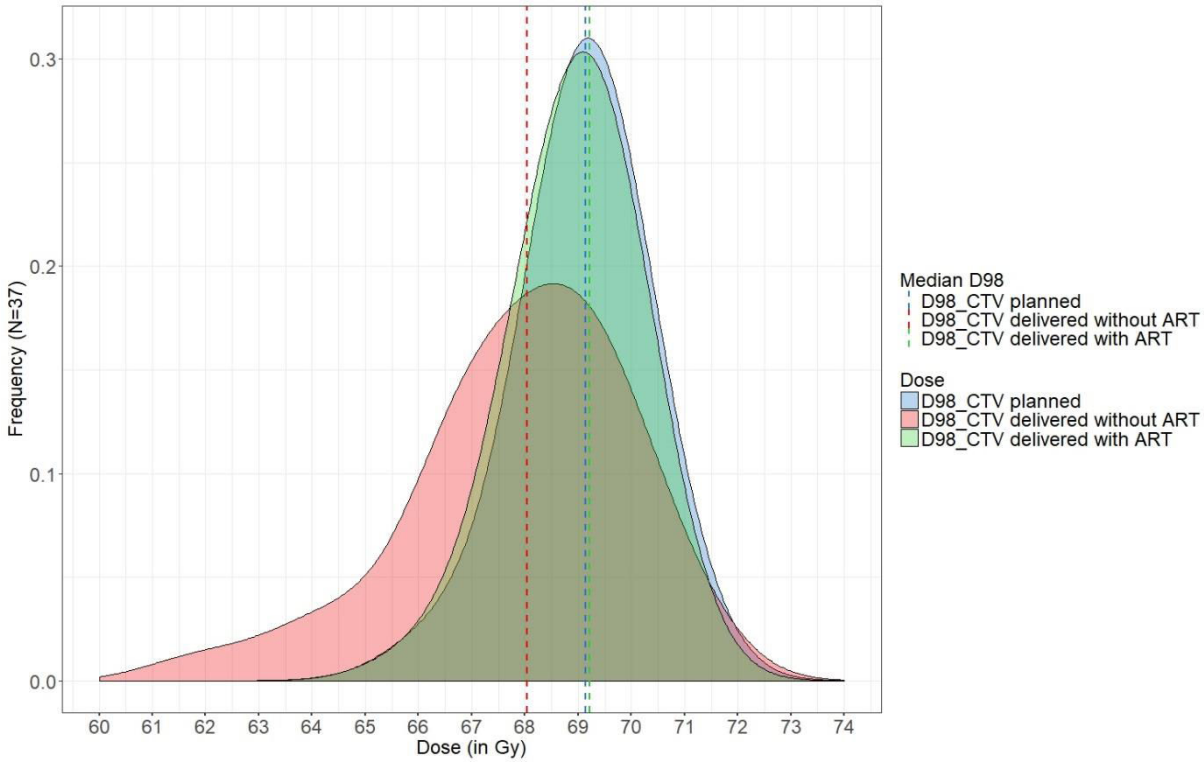

Figure 1: Population repartition of D98 CTV: at the planning, delivered without ART and delivered with ART

The D98_CTV delivered without ART (red area) was decreased compared to the planned dose (blue area). A weekly ART allows correcting tumor underdose (green area).

D98_CTV = Dose delivered to 98% of the CTV.

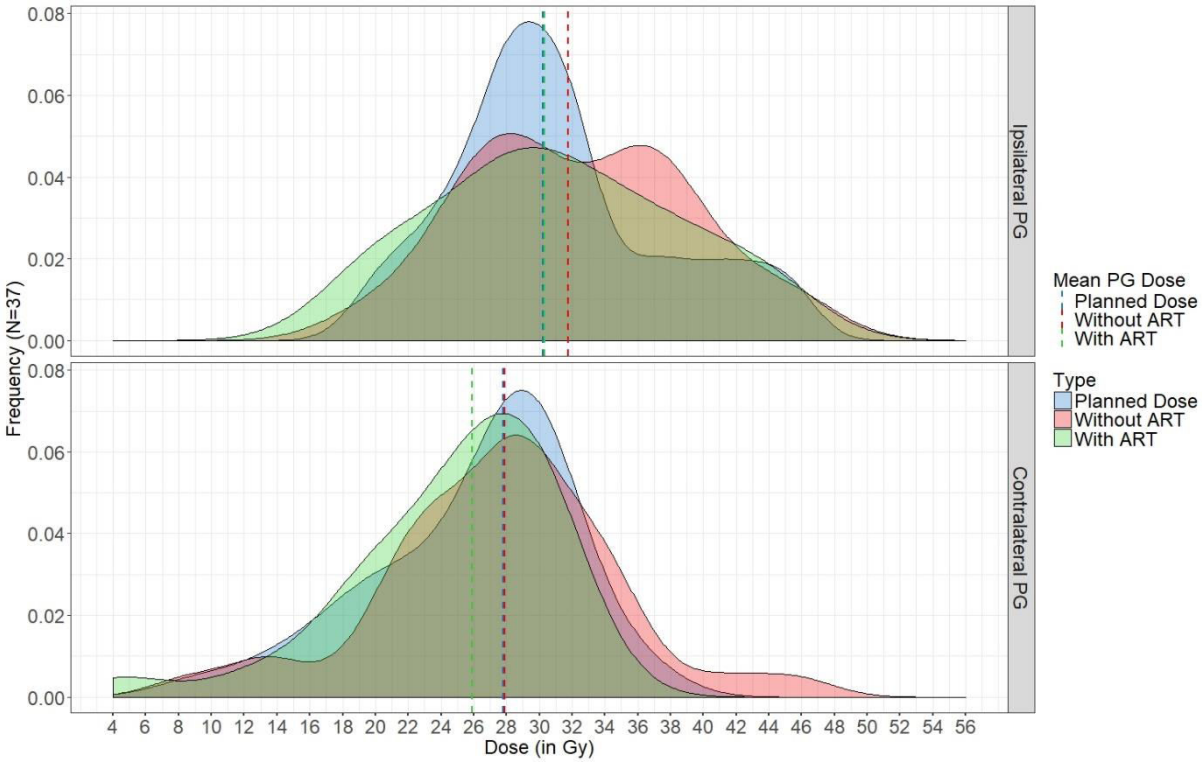

Figure 2: Population repartition of mean PG dose: at the planning, delivered without ART and delivered with ART

Compared to the planned dose (blue area), standard IMRT without ART (red area) leads to an increase of the mean parotid gland dose. A weekly ART (green area) allows correcting this parotid gland overdose.

ART = Adaptive radiotherapy, PG =parotid gland

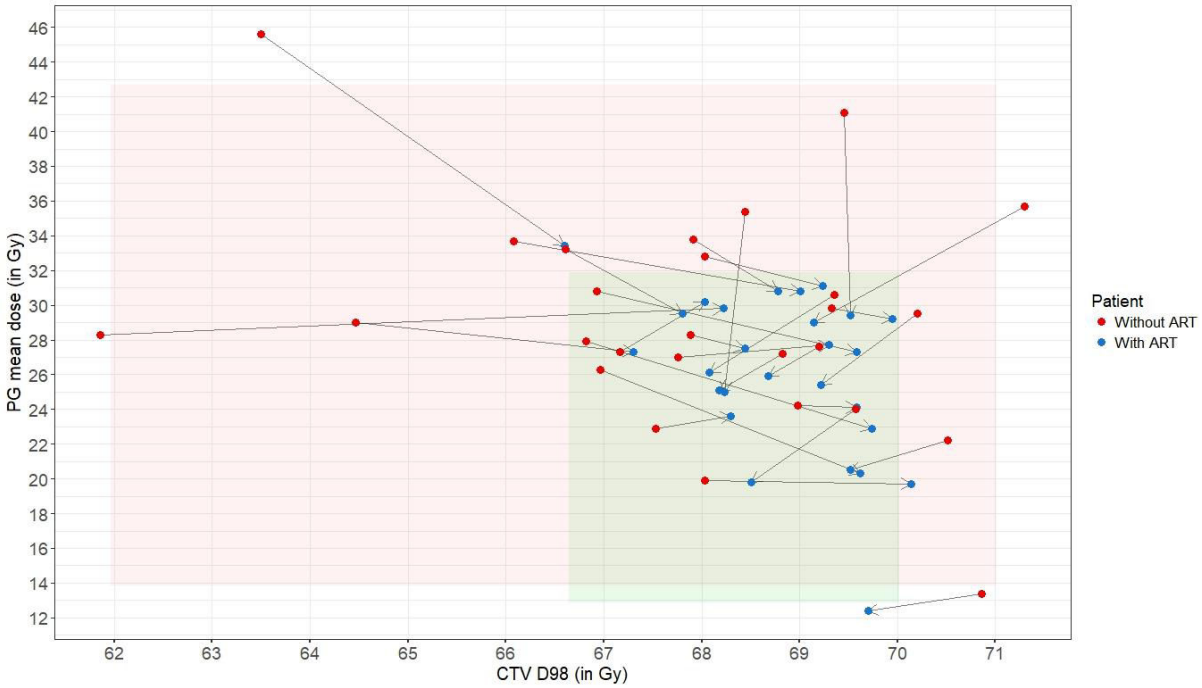

Figure 3: Individual benefit of the ART strategy for both dose to 98% of the Clinical Target Volume high dose and mean contralateral parotid gland

Red and green area corresponding to 95% of the distribution of the patients (N=30) without and with ART respectively. Red and green dots corresponding to the cumulated dose received by 98% of the CTV (D98_CTV) and to the mean parotid gland cumulated dose without or with ART.

7 References

1. Capelle, L., et al., *Adaptive radiotherapy using helical tomotherapy for head and neck cancer in definitive and postoperative settings: initial results.* Clin Oncol (R Coll Radiol), 2012. **24**(3): p. 208-15.
2. Castelli, J., et al., *Impact of head and neck cancer adaptive radiotherapy to spare the parotid glands and decrease the risk of xerostomia.* Radiat Oncol, 2015. **10**(1): p. 6.
3. Dewan, A., et al., *Impact of Adaptive Radiotherapy on Locally Advanced Head and Neck Cancer - A Dosimetric and Volumetric Study.* Asian Pac J Cancer Prev, 2016. **17**(3): p. 985-92.
4. Jensen, A.D., et al., *A clinical concept for interfractional adaptive radiation therapy in the treatment of head and neck cancer.* Int J Radiat Oncol Biol Phys, 2012. **82**(2): p. 590-6.
5. Olteanu, L.A., et al., *Comparative dosimetry of three-phase adaptive and non-adaptive dose-painting IMRT for head-and-neck cancer.* Radiother Oncol, 2014. **111**(3): p. 348-53.
6. Schwartz, D.L., et al., *Adaptive radiotherapy for head and neck cancer--dosimetric results from a prospective clinical trial.* Radiother Oncol, 2013. **106**(1): p. 80-4.
7. Height, R., et al., *The dosimetric consequences of anatomic changes in head and neck radiotherapy patients.* J Med Imaging Radiat Oncol, 2010. **54**(5): p. 497-504.
8. Marzi, S., et al., *Anatomical and dose changes of gross tumour volume and parotid glands for head and neck cancer patients during intensity-modulated radiotherapy: effect on the probability of xerostomia incidence.* Clin Oncol (R Coll Radiol), 2012. **24**(3): p. e54-62.
9. Simone, C.B., 2nd, et al., *Comparison of intensity-modulated radiotherapy, adaptive radiotherapy, proton radiotherapy, and adaptive proton radiotherapy for treatment of locally advanced head and neck cancer.* Radiother Oncol, 2011. **101**(3): p. 376-82.
10. Wu, Q., et al., *Adaptive replanning strategies accounting for shrinkage in head and neck IMRT.* Int J Radiat Oncol Biol Phys, 2009. **75**(3): p. 924-32.
11. Yip, C., et al., *Co-registration of cone beam CT and planning CT in head and neck IMRT dose estimation: a feasible adaptive radiotherapy strategy.* Br J Radiol, 2014. **87**(1034): p. 20130532.
12. O'Daniel, J.C., et al., *Parotid gland dose in intensity-modulated radiotherapy for head and neck cancer: is what you plan what you get?* Int J Radiat Oncol Biol Phys, 2007. **69**(4): p. 1290-6.
13. Bhide, S.A., et al., *Weekly volume and dosimetric changes during chemoradiotherapy with intensity-modulated radiation therapy for head and neck cancer: a prospective observational study.* Int J Radiat Oncol Biol Phys, 2010. **76**(5): p. 1360-8.
14. Chen, C., et al., *Will weight loss cause significant dosimetric changes of target volumes and organs at risk in nasopharyngeal carcinoma treated with intensity-modulated radiation therapy?* Med Dosim, 2014. **39**(1): p. 34-7.
15. Hansen, E.K., et al., *Repeat CT imaging and replanning during the course of IMRT for head-and-neck cancer.* Int J Radiat Oncol Biol Phys, 2006. **64**(2): p. 355-62.
16. Ahn, P.H., et al., *Adaptive planning in intensity-modulated radiation therapy for head and neck cancers: single-institution experience and clinical implications.* Int J Radiat Oncol Biol Phys, 2011. **80**(3): p. 677-85.
17. Mohan, R., et al., *Radiobiological considerations in the design of fractionation strategies for intensity-modulated radiation therapy of head and neck cancers.* Int J Radiat Oncol Biol Phys, 2000. **46**(3): p. 619-30.
18. Lee, N., et al., *Skin toxicity due to intensity-modulated radiotherapy for head-and-neck carcinoma.* Int J Radiat Oncol Biol Phys, 2002. **53**(3): p. 630-7.
19. Castelli, J., et al., *A Nomogram to predict parotid gland overdose in head and neck IMRT.* Radiat Oncol, 2016. **11**: p. 79.

20. Lester J. Peters, B.O.S., Jordi Giralt, Thomas J. Fitzgerald, Andy Trotti, Jacques Bernier, Jean Bourhis, Kally Yuen, Richard Fisher, and Danny Rischin, *Critical Impact of Radiotherapy Protocol Compliance and Quality in the Treatment of Advanced Head and Neck Cancer: Results From TROG 02.02.* JCO, 2010.
21. Yang, H., et al., *Replanning during intensity modulated radiation therapy improved quality of life in patients with nasopharyngeal carcinoma.* Int J Radiat Oncol Biol Phys, 2013. **85**(1): p. e47-54.
22. Lai, Y.L., et al., *Impact of body-mass factors on setup displacement in patients with head and neck cancer treated with radiotherapy using daily on-line image guidance.* Radiat Oncol, 2014. **9**: p. 19.
23. Zhao, L., et al., *The role of replanning in fractionated intensity modulated radiotherapy for nasopharyngeal carcinoma.* Radiother Oncol, 2011. **98**(1): p. 23-7.
24. Zhang, P., et al., *Optimal adaptive IMRT strategy to spare the parotid glands in oropharyngeal cancer.* Radiother Oncol, 2016. **120**(1): p. 41-7.

4.1.3 Conclusion

Au cours d'une radiothérapie standard sans replanification la dose délivrée au volume cible et aux parotides ne correspond à la dose planifiée que pour environ 5 % des patients. Environ la moitié des patients vont présenter un sous dosage de plus de 1 Gy de la tumeur. Ce sous dosage de la tumeur s'associe à un surdosage des glandes parotides de plus de 2 Gy. Il existe donc pour ces patients à la fois un risque d'augmentation de la toxicité (xérostomie) et de récidive tumorale. Une radiothérapie adaptative hebdomadaire permet de corriger à la fois le sous dosage de la tumeur et le surdosage des parotides, permettant d'espérer une augmentation du contrôle local tout en diminuant la toxicité parotidienne. Une replanification hebdomadaire permet également d'améliorer l'homogénéité de la dose au sein du volume cible. Il est cependant difficile d'estimer si ces variations de doses peuvent avoir un impact sur l'efficacité du traitement. En effet, en l'absence de possibilité de réaliser un cumul de dose par recalage élastique, nous avons estimé la dose par la moyenne des doses hebdomadaires. Cette approche ne prend pas en compte l'information spatiale de la dose. Il est donc possible que le sous dosage d'une partie de la tumeur à une semaine donnée du traitement soit compensé lors d'une autre semaine de traitement.

Par ailleurs, tout comme pour les parotides, une partie seulement des patients vont présenter un sous dosage. L'identification précoce de ces patients est donc un objectif majeur dans une optique d'assurer le contrôle local.

4.2 Identification des patients à risque de sous dosage de la tumeur au cours d'une radiothérapie standard sans replanification

4.2.1 Introduction

Comme montré précédemment, environ la moitié des patients vont présenter un sous dosage de la tumeur au cours d'une radiothérapie standard sans replanification. Tout comme pour les parotides, il apparait essentiel d'identifier précocement ces patients afin de leur proposer une stratégie de radiothérapie adaptative avec un objectif de maintien de la couverture tumorale.

4.2.2 Matériels et méthodes

Les paramètres anatomiques et/ou dosimétriques prédictifs de ce sous dosage ont été évalués en utilisant la cohorte de patient précédemment décrite (cf section 4.1.2). Les paramètres anatomiques et dosimétriques suivants ont été analysés dans l'objectif d'évaluer leur corrélation avec le sous dosage tumoral (estimé par la dose reçue par 98% du volume cible clinique D98_CTV)) : CTV70 (cm^3), volume des parotides (cm^3), diamètre du cou (cm), différence entre la D98_CTV planifiée et la D98_CTV à la 1^{ière} semaine, dose moyenne à la parotide à la planification et à la 1^{ière} semaine, et enfin la différence de dose moyenne à la parotide constatée à la 1^{ière} semaine. Un test de corrélation de Pearson a été utilisé pour évaluer la corrélation de ces paramètres entre eux et avec le sous dosage tumoral. Dans le cas de paramètres dépendants entre eux, seul le paramètre avec le coefficient de corrélation le plus élevé a été retenu pour la suite de l'analyse. Un modèle linéaire de régression avec analyse descendante a été réalisé. Une validation croisée par *leave-one-out* a été réalisée pour estimer la précision et la stabilité du modèle.

4.2.3 Résultats

Les résultats du test de corrélation de Pearson entre les paramètres anatomo-dosimétrique et le sous dosage du CTV sont présentés Table 5 .

Table 5 : Correlation between anatomical parameters and variation of the delivered dose for CTV 70

Anatomical parameter	Coefficient of correlation (Spearman)	P value
At the planning		
CTV D98 (in Gy)		0.07
CTV 70 (cm^3)	-0.46	<0.01
Volume of CL PG	0.35	0.04
Volume of HL PG		0.32
Mean CL parotid dose		0.21
Mean HL parotid dose		0.15
T stage		0.47
N stage		0.11
Diameter of the neck		0.47
1st week		
CTV D98 (in Gy)	0.74	<0.01
CTV D98 : Dose difference CT1 – CT0 (in Gy)	0.75	<0.01
CTV 70 (in cm^3)	-0.43	0.01
CTV 70 : Volume difference CT1 – CT0 (in cm^3)		0.33
CL PG (in cm^3)		0.71
CL PG : Volume difference CT1 – CT0 (in cm^3)	-0.37	0.05
HL PG (in cm^3)		0.71
HL PG : Volume difference CT1 – CT0 (in cm^3)		0.08
Diameter of the neck (in cm)		0.88
Diameter of the neck : Difference CT1 – CT0 (in cm)	-0.37	0.03

CTV 70 = Clinical Target Volume; PG = parotid gland

L'analyse en modèle linéaire de régression a retrouvé 2 paramètres significativement corrélés avec le sous dosage de la tumeur. Il s'agissait de la différence de D98_CTV entre la 1ière semaine et la planification et le volume de la tumeur à la planification. A partir de ces 2 paramètres, un modèle de prédiction a été construit selon la formule suivante :

CTV_D98 Variation = (0.70 x ΔCTV_D98_CT1) – (0.004 x CTV70_CT0)

Ce modèle avait un coefficient de détermination ajusté (r^2) de 0.71 ($p<0,001$). L'erreur quadratique moyenne et la précision du modèle, déterminé par la validation croisée était de 1,1

Gy et de 70,5% respectivement (Figure 14). Ce modèle permet de bien classer (sous dosage ou surdosage de la tumeur) 87 % des patients. Les patients avec un sous dosage de plus de 1 Gy sont correctement identifié par le modèle.

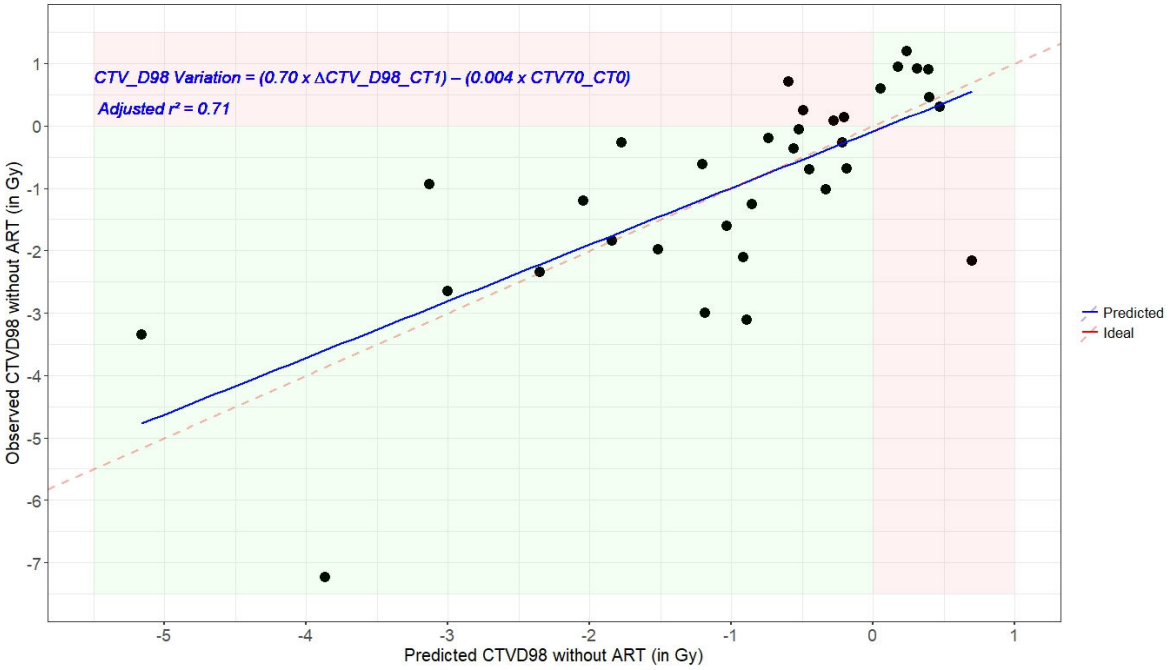

Figure 14 : Correlation between observed and predicted Clinical Tumor Volume (CTV) doses (results of leave-one-out cross validation)

Representation of the observed (vertical axis) and predicted (horizontal axis) values of CTV dose variation (difference between delivered without ART and planned CTV dose) for each patient. The model included two parameters (Mean CTV dose difference between the dose delivered at CT1 and the planned dose, and CTV_{70} at the planning). Blue line: regression line (R^2=0.8), red (dashed) line = perfect fit. Red areas: wrong predictions (*e.g.* predicted underdose *vs.* observed overdose)

CT: computed tomography; CTV70 (in cm^3): clinical target volume receiving 70Gy; CT1: Week 1 treatment CT

4.2.4 Conclusion

Tout comme pour les parotides, il est possible d'identifier précocement (dès la 1ière semaine de traitement) la plupart des patients qui vont présenter un sous dosage de la tumeur, en utilisant des paramètres anatomique et dosimétrique simple. La différence de dose au volume cible à la 1ère semaine de traitement est fortement corrélée à la différence de dose finale. Une corrélation similaire avait été retrouvée pour le modèle de prédiction de surdosage des parotides. Les paramètres anatomiques seuls restent donc insuffisants pour le moment pour prédire le risque de modification de la dose délivrée sans radiothérapie adaptative, que ce soit pour le volume cible ou les parotides.

Au total, la réalisation d'un scanner avec recalcul de dose à la première semaine de traitement permet d'identifier la totalité des patients ayant un sous dosage de la tumeur d'au moins 1 Gy, et dans le même temps les patients ayant un surdosage des parotides de plus de 2,5 Gy. Ces patients pourraient ainsi bénéficier d'une stratégie de radiothérapie adaptative dans l'objectif d'augmenter le contrôle local.

4.3 Identification des patients à haut risque de récidive et nécessitant une couverture tumorale optimale (articles)

4.3.1 Introduction

Environ la moitié des patients présentent un sous dosage de la tumeur de la tumeur d'au moins 1 Gy. Par ailleurs, 30 à 40 % des patients vont présenter une rechute locale, le plus souvent dans les 2 ans suivant la fin du traitement. Même si aucune étude n'est disponible à l'heure actuelle concernant un lien entre ce sous dosage de la tumeur et la récidive locale, il est raisonnable de penser que les patients considérés comme à haut risque de récidive locale devraient être de bons candidats à une stratégie de radiothérapie adaptative dans l'objectif d'assurer une qualité optimale de traitement. Le pronostic de ces patients est estimé globalement en se basant sur la classification AJCC. Cependant cette classification reste insuffisante pour estimer le risque à l'échelle individuelle. La TEP au 18FDG, en fournissant une information sur le métabolisme de la tumeur pourrait permettre d'identifier avant même le début du traitement les patients à haut risque de récidive. Les paramètres de volume métabolique (MTV et TLG) semblent à ce titre prometteur [90]. Cependant ces paramètres nécessitent des opérations de seuillage (en valeur absolu de SUV ou relative par rapport au SUVmax) pour les calculer. La question du choix du seuillage optimal dans une optique de prédiction du risque de récidive n'étant pas résolue à l'heure actuelle. Par ailleurs, aucune étude n'a réalisé de validation externe de ces paramètres issus de la TEP.

Dans ce contexte, nous avons évalué dans un premier travail l'impact du choix de la méthode de seuillage (absolu ou relative) et de son niveau dans un article publié dans Clinical Nuclear Medicine en janvier 2017. Nous avons ensuite évalué la possibilité de réaliser un modèle de prédiction de la survie en utilisant ces paramètres TEP analysés séparément sur la tumeur et les adénopathies. Ce travail est présenté dans un second article publié dans l'European Journal of Cancer en janvier 2017.

4.3.2 Metabolic Tumor Volume and Total Lesion Glycolysis in Oropharyngeal Cancer treated with definitive radiotherapy: Which threshold is the best predictor of local control?

J. Castelli[1,2,3]; A. Depeursinge[4,5]; B. De Bari[1,6]; A. Devillers[7]; R. de Crevoisier[2,3,8]; J. Bourhis[1] ; J.O. Prior[11]

Clinical Nuclear Medicine, 2017 Jan.

1. Department of Radiation Oncology, Lausanne University Hospital, Switzerland
2. INSERM, U1099, Rennes, F-35000, France
3. Université de Rennes 1, LTSI, Rennes, F-35000, France
4. Ecole Polytechnique Fédérale de Lausanne, CH-1015 Lausanne VD, Switzerland
5. University of Applied Sciences Western Switzerland, 3960 Sierre, Switzerland
6. University Hospital Jean Minjoz, INSERM 1098, Besancon, France
7. Nuclear Medecine Department, Centre Eugene Marquis, Rennes, F-35000, France
8. Department of Radiation Oncology, Centre Eugene Marquis, Rennes, F-35000, France
9. Head and Neck department, CHU Rennes, Rennes, F-35000, France
10. Oncology Department, Centre Eugene Marquis, Rennes, F-35000, France
11. Nuclear Medicine and Molecular Imaging Department, Lausanne University Hospital, Switzerland

Metabolic Tumor Volume and Total Lesion Glycolysis in Oropharyngeal Cancer Treated With Definitive Radiotherapy

Which Threshold Is the Best Predictor of Local Control?

Joël Castelli, MD, MSc,†‡ Adrien Depeursinge, PhD,§|| Berardino de Bari, MD,*¶ Anne Devillers, MD,** Renaud de Crevoisier, MD, PhD,†‡†† Jean Bourhis, MD, PhD,* and John O. Prior, MD, PhD‡‡*

Purpose: In the context of oropharyngeal cancer treated with definitive radiotherapy, the aim of this retrospective study was to identify the best threshold value to compute metabolic tumor volume (MTV) and/or total lesion glycolysis to predict local-regional control (LRC) and disease-free survival.

Methods: One hundred twenty patients with a locally advanced oropharyngeal cancer from 2 different institutions treated with definitive radiotherapy underwent FDG PET/CT before treatment. Various MTVs and total lesion glycolysis were defined based on 2 segmentation methods: (i) an absolute threshold of SUV (0–20 g/mL) or (ii) a relative threshold for SUVmax (0%–100%). The parameters' predictive capabilities for disease-free survival and LRC were assessed using the Harrell C-index and Cox regression model.

Results: Relative thresholds between 40% and 68% and absolute threshold between 5.5 and 7 had a similar predictive value for LRC (C-index = 0.65 and 0.64, respectively). Metabolic tumor volume had a higher predictive value than gross tumor volume (C-index = 0.61) and SUVmax (C-index = 0.54). Metabolic tumor volume computed with a relative threshold of 51% of SUVmax was the best predictor of disease-free survival (hazard ratio, 1.23 [per 10 mL], $P = 0.009$) and LRC (hazard ratio: 1.22 [per 10 mL], $P = 0.02$).

Conclusions: The use of different thresholds within a reasonable range (between 5.5 and 7 for an absolute threshold and between 40% and 68% for a relative threshold) seems to have no major impact on the predictive value of MTV. This parameter may be used to identify patient with a high risk of recurrence and who may benefit from treatment intensification.

Key Words: metabolic tumor volume, oropharyngeal cancer, PET, threshold

(*Clin Nucl Med* 2017;42: e281–e285)

^{18}F-FDG PET/CT allows to quantify the metabolic activity of a tumor (glycolysis) and has become a reference tool in oncology for staging, radiotherapy planning, and monitoring tumor response in many cancers.[1,2] Compared with other diagnostic modalities, PET imaging allows a most accurate nodal staging of locally advanced head and neck cancer[3,4] and could result in changing the therapeutic management in nearly 15% of patients.[5]

The SUVmax corresponds to the maximal pixel value in the tumor. Thanks to its ease of use and relative robustness, it is one of the most widely used parameters in clinical practice. However, SUVmax is not representative of nonhomogeneous overall tumor uptake. More recently, volumetric PET parameters—metabolic tumor volume (MTV) and total lesion glycolysis (TLG)—have been correlated with clinical outcome.[6–8] Nonetheless, these parameters require a tumor segmentation that is classically defined by either a percentage of the SUVmax or absolute SUV as the lowest threshold for inclusion. The optimal SUV threshold for clinical outcome prediction in head and neck cancer is not well defined. Few studies have compared different thresholds of MTV and/or TLG,[9–14] and a large majority of studies using the same thresholds of 40% SUVmax[15] or a fixed SUV threshold of greater than 2.5.[16] In the context of oropharyngeal cancer treated with definitive radiotherapy, the aim of this retrospective study was to identify the best threshold value to compute MTV and/or TLG in order to predict clinical outcome.

MATERIALS AND METHODS

All consecutive patients from 1 cancer center and 1 university hospital treated with definitive concurrent chemoradiotherapy or radiotherapy-cetuximab for a locally advanced oropharyngeal carcinoma between January 2010 and December 2015 were retrospectively analyzed. The study enrolled a total of 122 patients. All tumors were locally advanced (stage III or IV, American Joint Committee on Cancer seventh edition).

Treatment and Planning

All patients underwent intensity-modulated radiotherapy using volumetric modulated arc therapy (Rennes) or helical tomotherapy (Lausanne). A total dose of 70 Gy (2 Gy/fraction per day, 35 fractions [Rennes]; or 2.12 Gy/fractions per day, 33 fractions [Lausanne], with a simultaneous integrated boost technique)[17] was delivered combined to concomitant chemotherapy,[18,19] or cetuximab[20] if the patients were not fit for chemotherapy. The modality of planning and treatment were the same as previously described.[21] The study was approved by both institutional ethical committees (NCT02469922).

PET/CT Acquisition

All patients underwent FDG PET/CT for staging before treatment. For (Rennes), the patients lasted at least 4 hours prior to injection of 4 MBq/kg of ^{18}F-FDG (Flucis). Blood glucose levels were checked prior to the injection of ^{18}F-FDG. If not contraindicated, intravenous contrast agents were administered before CT scanning. After a 60-minute uptake period of rest, patients were imaged with

Received for publication October 20, 2016; revision accepted January 15, 2017.
From the *Department of Radiation Oncology, Lausanne University Hospital, Switzerland; †INSERM, U1099, Rennes; ‡Université de Rennes 1, LTSI, Rennes, France; §Ecole Polytechnique Fédérale de Lausanne, Lausanne; and ||University of Applied Sciences Western Switzerland, Sierre, Switzerland; ¶University Hospital Jean Minjoz, INSERM 1098, Besancon; **Nuclear Medicine Department, Centre Eugene Marquis, Rennes; ††Department of Radiation Oncology, Centre Eugene Marquis, Rennes; and ‡‡Nuclear Medicine and Molecular Imaging Department, Lausanne University Hospital, Lausanne, Switzerland.
Conflicts of interest and sources of funding: This work was partly supported by the Swiss National Science Foundation with grant agreement PZ00P2_154891 (to A. Depeursinge). None declared to all other authors.
Correspondence to: Joël Castelli, MD, MSc, Department of Radiation Oncology, Centre Eugene Marquis, avenue de la Bataille Flandre Dunkerque, F-35000 Rennes, France. E-mail: j.castelli@rennes.unicancer.fr.

ISSN: 0363-9762/17/4206–e281
DOI: 10.1097/RLU.0000000000001614

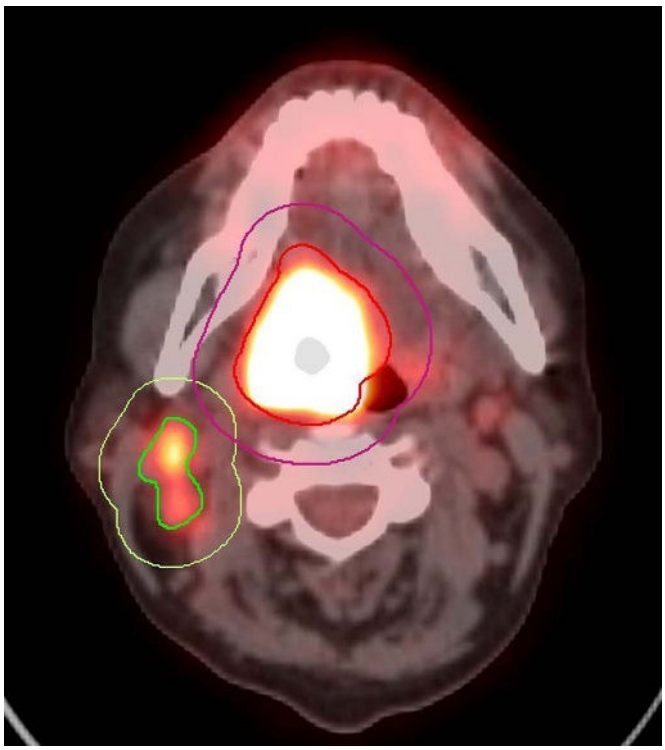

FIGURE 1. Illustration of GTV for the primary tumor (GTV T = red line) and for the lymph nodes (GTV N = green line) delineated by the radiation oncologist, for a patient with a T4 N2 oropharyngeal cancer (SUVmax = 9.4 mg/mL). An ROI was computed by adding 3-dimensional margins of 10 mm to GTV-T (ROI-T = purple line) and GTV-N (ROI-N = yellow line). These 2 ROIs were used to compute MTV at different thresholds.

a PET/CT imaging system Discovery ST (General Electric Medical Systems; General Electric Healthcare, Milwaukee, Wis). First, a CT (120 kV, 80 mA, 0.8-second rotation time, slice thickness 3.75 mm) was performed from the base of the skull to the midthigh. PET scanning was performed immediately after acquisition of the CT. Images were acquired from the base of skull to the midthigh (3 min/bed position). PET images were reconstructed by using an ordered-subset expectation maximization iterative reconstruction (2 iterations, 28 subsets) and an iterative fully 3-dimensional image. CT data were used for attenuation calculation. A similar protocol was used in Lausanne, however, on a slightly more recent system, Discovery D690 TOF PET/CT (General Electric Healthcare), which allowed shorter acquisition (2 min/bed position). PET images were reconstructed after time-of-flight and point-spread-function recovery corrections.

PET Analysis

For each patient, tumor gross tumor volume (GTV-T) and nodal GTV (GTV-N) were manually segmented on each PET/CT by the same radiation oncologist, experienced in head and neck cancer treatments. A region of interest (ROI) was computed by adding 3-dimensional margins of 10 mm to GTV-T and GTV-N (Fig. 1).

A set of quantitative parameters based on SUV histograms was extracted from ROI-T and ROI-N in PET images. SUVmax was first computed from ROI-T as the maximum SUV in the delineated volume. Several metabolic volumes were subsequently defined based on 2 segmentation methods: (i) an absolute threshold of SUV (ranging from 0 to 20 g/mL, 0.5-g/mL steps) or (ii) a relative threshold of SUVmax (0%–100%, 1% steps). Metabolic tumor volume was computed as the metabolic volume of the segmented region in milliliters and TLG as SUVmean × MTV of the corresponding thresholded region.

Statistical Analysis

Patients alive at the time of analysis were censored at the date of last follow-up. Disease-free survival (DFS) was calculated from the first day of radiotherapy (chemoradiotherapy) to the date of first event (local or distant recurrence or death). Locoregional control (LRC) was calculated from the first day of radiotherapy to the date of first recurrence in primary tumor and/or lymph node. Follow-up was calculated using a reverse Kaplan-Meier estimation.[22] Disease-free survival and overall survival (OS) estimations were computed using the Kaplan-Meier method, and 2-sided log-rank test was used to compare groups.

The association of the PET pretreatment parameters with DFS and OS was assessed using univariate Cox analyses. Harrell C-index (C-index) was used to compare different models (C-index ≈ 0.5 → not predictive, C-index ≈ 1 → predictive).[23] The C-index was used to determine the optimal SUV threshold giving the most predictive value for each PET parameter. Factors with significance of $P < 0.1$ and with the highest C-index after univariate analysis

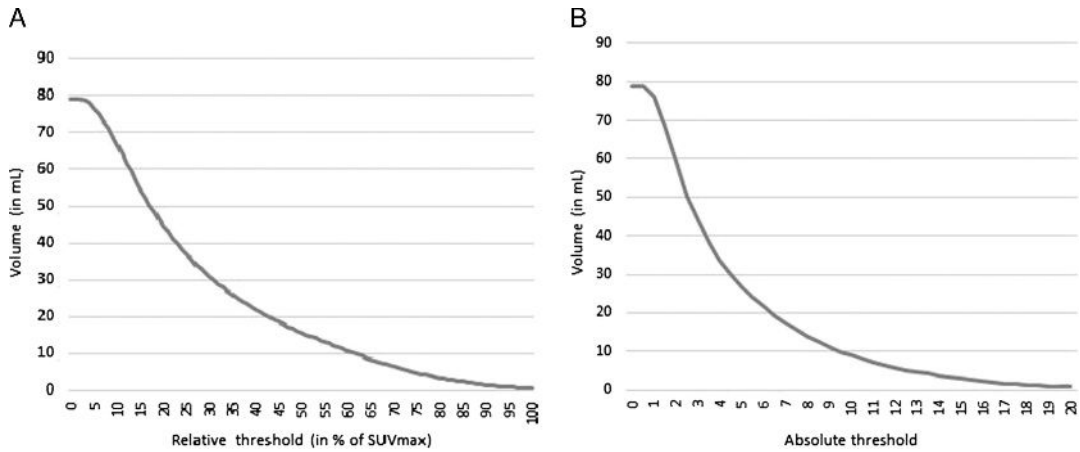

FIGURE 2. Volume in milliliters for each relative (**A**) and absolute threshold (**B**). No impact of the ROI was shown as MTV decreases regularly from 0% to 100% and from 0 to 20 mg/mL.

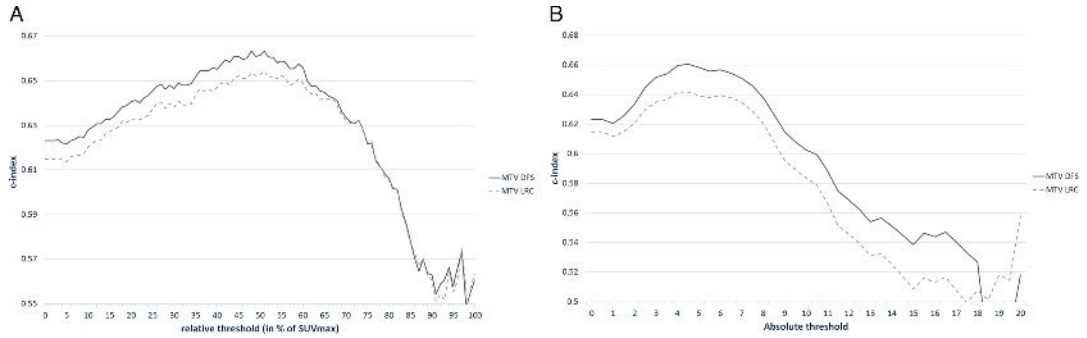

FIGURE 3. C-index values for MTV computed with different relative thresholds (from 0% to 100% of SUVmax) (**A**) or with different absolute thresholds (from 0 to 20 mg/mL) (**B**) to predict DFS and LRC. To estimate the predictive capabilities of PET parameters on survival, Harrell C-index values were calculated (C-index) (C-index ≈ 0.5 → not predictive, C-index ≈ 1 → predictive).[23] The C-index was used to identify the threshold that offered the strongest predictive value for MTV.

were assessed for multivariate Cox regression model using backward elimination. Variables were removed from the model if $P > 0.1$.

Two prognostic risk groups were identified based on the estimated optimal cutoff point by the Hothorn and Lausen[24] method. Kaplan-Meier method was used to evaluate this cutoff.

All analyses were performed using R software 3.2.4 (R Development CoreTeam; http://www.r-project.org).

Follow-up

A clinical evaluation was performed after radiotherapy every 3 months the first 2 years then every 6 months. Database was locked on May 30, 2016.

RESULTS

Clinical Outcome

The median follow-up was 38 months (range, 2–80 months). The 2-year DFS was 56.4% (95% confidence interval [CI], 47.3%–67.3%), and the 2-year LRC was 60.7% (95% CI, 51.6%–71.3%). At the analysis, 44 patients had died, and 47 presented a recurrence (20 with locoregional recurrence, 13 with distant recurrence, and 14 with both locoregional and distant recurrence).

Predictive Parameters

Figure 2 shows the correlation between the volume of MTV and the chosen threshold. No limitation in computation of MTV due to the use of an ROI was found.

SUVmax was not correlated with LRC or DFS (C-index = 0.54, $P = 0.63$). No difference was found between MTV and TLG. All thresholds between 40% and 60% of SUVmax or between 4.5 and 6 mg/mL appear to have a similar predictive value (Fig. 3). Relative thresholds lower than 36% or higher than 84% were not significantly correlated with DFS (Fig. 4). The best threshold to predict OS and DFS was 51% of SUVmax, (C-index = 0.68 for OS [hazard ratio, 1.43 per 10 mL; 1.23–1.65; $P < 0.001$]; and C-index = 0.65 for DFS [hazard ratio, 1.43 per 10 mL; 1.23–1.65; $P = 0.03$]). Gross tumor volume was also correlated with DFS (C-index = 0.66, $P = 0.04$) and LRC (C-index = 0.66, $P = 0.03$). In multivariate analysis, MTV 51% was the only significant parameter.

The estimated cutoff point by the Hothorn and Lausen[24] method for the MTV 51% was 22.7 mL. Based on this cutoff, 2 risk groups were identified. The 2-year DFS and LRC were 63.3% (95% CI, 53.2%–75.5%) and 68% (95% CI, 48%–79.7%) for the group with MTV 51% of less than 22.7 mL versus 32.9% (95% CI, 18.7%–58.1%) ($P < 0.001$) and 35.3% (95% CI, 20.4%–61.2%) ($P < 0.001$) for the group with MTV 51% of 22.7 mL or greater ($P = 0.004$) (Fig. 5), respectively.

DISCUSSION

To the best of our knowledge, our study is the first one addressing the issue of the predictive value of a wide range of different thresholds (from 0 to 20 mg/mL and from 0% to 100% of SUVmax) of MTV and TLG in the specific context of oropharyngeal cancers. Considering both primary tumor and lymph node, we found that a relative threshold of 51% was the best predictor for OS and DFS. However, all thresholds between 40% and 62% of SUVmax or between 4.5 and 6 mg/mL appear to have a similar predictive value. The most predictive threshold was 51%, whereas GTV, SUVmax, and parameters computed from absolute SUV threshold appear less predictive. The use of a relative threshold rather than an absolute

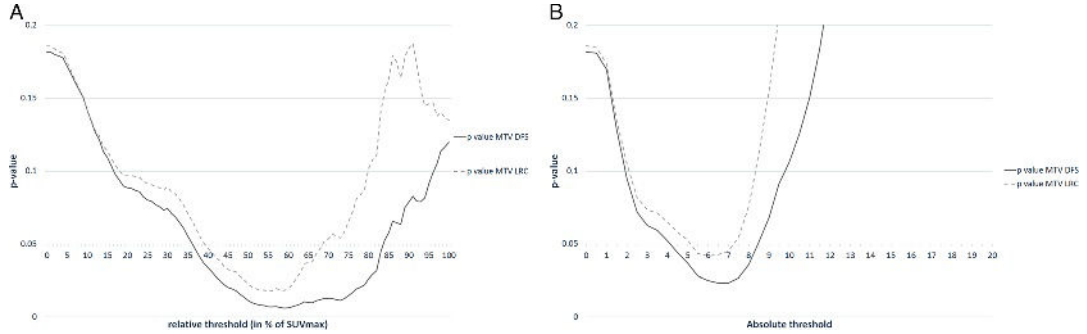

FIGURE 4. *P* values for DFS and LRC of MTV computed with different relative thresholds (from 0% to 100% of SUVmax) (**A**) or with different absolute thresholds (from 0 to 20 mg/mL) (**B**).

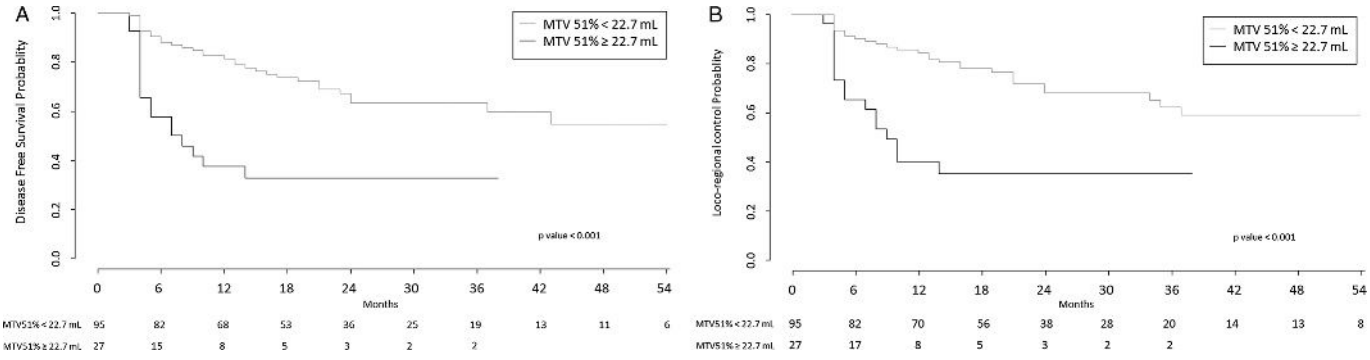

FIGURE 5. Kaplan-Meier curves of DFS (**A**) and LRC (**B**) stratified by MTV computed with a relative threshold of 51% of SUVmax. The population was divided into 2 groups according to the optimal cutoff (Hothorn and Lausen method[24]) of 22.7 mL.

threshold may allow identifying the most metabolic part of the tumor, which may be involved in the recurrence. Relative threshold was also shown to be a better predictor than absolute threshold in a similarly study in cervical cancer.[25] This PET parameter may be used to identify patients with a high risk of recurrence or death, potentially candidates for treatment intensification (eg, dose escalation by dose painting in the MTV).

Several studies also showed a better predictive value of MTV, when compared with GTV and/or American Joint Committee on Cancer staging.[10,26] Noteworthy, the reproducibility of the MTV and/or TLG is limited by the initial definition of these parameters, which is based on a threshold of SUV, absolute (all pixels with SUV value > *x*) or relative (all pixels with SUV value > *xx* % of SUVmax), and most of the studies used only 1 threshold (2.5 or 3 g/mL, or 40%–50%). Six studies compared only 3 or 4 different thresholds of MTV and/or TLG, most often using the same threshold of 40%, 50%, or 2.5 and 3 of absolute SUV.[9–13,27,28] An absolute threshold of 2.5[10,13] and a relative threshold of 40%[9,12] were the best predictors for OS and DFS. However, also, all the other studied thresholds were correlated with OS and DFS but with a lower predictive value. Our study confirms that the use of different relative thresholds within a reasonable range (between 40% and 60%) seems to have no major impact on the predictive value of MTV.

Regarding absolute thresholds, we found a higher value (from 4.5 to 6) than the 2.5 value used routinely.[10,13] However, same result is shown in Abgral et al.[14] This monocentric study compared 14 thresholds (from 2.0 to 7, and 30%, 40%, and 50% of SUVmax) in 80 patients with head and neck cancer treated with surgery and/or radiotherapy. An absolute threshold of 5 was the best one to predict recurrence and death in head and neck cancer. However, the authors computed MTV only for the primary tumor, and not for the lymph nodes.

Another controversial issue is the use of a cutoff value for MTV, which largely varied from 4.9 to 65 mL (median, 13.1 mL).[10,29–32] The use of different thresholds made it difficult to identify the best cutoff to predict clinical outcome. In Abgral et al,[14] a cutoff of 4.9 mL for the MTV 5 was used. However, univariate and multivariate analyses were performed using dichotomized parameters instead of continuous parameters. Dichotomization leads to loss of power, affects the ability to detect relationships, and overestimates the effect size. In our study, in a first step, we used continuous parameters to identify the best threshold (MTV 51%), and in a second step, we used the Hothorn and Lausen[24] method to determine the best cutoff (23 mL).

Our study had some limitations. It was a retrospective analysis, without independent validation. We also calculated MTV with the same threshold for both primary tumor and lymph nodes, instead of using a combination of different thresholds, which may have provided a better predictive value. Despite these limitations, we showed that MTV is an independent prognostic factor, with a higher predictive value than SUVmax and GTV.

CONCLUSIONS

The use of different thresholds within a reasonable range (between 5.5 and 7 for an absolute threshold and between 40% and 68% for a relative threshold) seems to have no major impact on the predictive value of PET parameters. Metabolic tumor volume for both primary tumor and lymph node computed with a relative threshold of 51% of SUV max was the best predictor of OS and DFS. This parameter may be used to identify patients with a high risk of recurrence of death and who may benefit from treatment intensification.

REFERENCES

1. Fletcher JW, Djulbegovic B, Soares HP, et al. Recommendations on the use of ^{18}F-FDG PET in oncology. *J Nucl Med*. 2008;49:480–508.
2. Gambhir SS, Czernin J, Schwimmer J, et al. A tabulated summary of the FDG PET literature. *J Nucl Med*. 2001;42:1S–93S.
3. Kyzas PA, Evangelou E, Denaxa-Kyza D, et al. ^{18}F-fluorodeoxyglucose positron emission tomography to evaluate cervical node metastases in patients with head and neck squamous cell carcinoma+ meta-analysis. *J Natl Cancer Inst*. 2008;100:712–720.
4. Yoo J, Henderson S, Walker-Dilks C. Evidence-based guideline recommendations on the use of positron emission tomography imaging in head and neck cancer. *Clin Oncol (R Coll Radiol)*. 2013;25:e33–e66.
5. Lonneux M, Hamoir M, Reychler H, et al. Positron emission tomography with [^{18}F]fluorodeoxyglucose improves staging and patient management in patients with head and neck squamous cell carcinoma: a multicenter prospective study. *J Clin Oncol*. 2010;28:1190–1195.
6. Schwartz DL, Harris J, Yao M, et al. Metabolic tumor volume as a prognostic imaging-based biomarker for head-and-neck cancer: pilot results from Radiation Therapy Oncology Group protocol 0522. *Int J Radiat Oncol Biol Phys*. 2015;91:721–729.
7. Moon SH, Choi JY, Lee HJ, et al. Prognostic value of volume-based positron emission tomography/computed tomography in patients with nasopharyngeal carcinoma treated with concurrent chemoradiotherapy. *Clin Exp Otorhinolaryngol*. 2015;8:142–148.
8. Cacicedo J, Navarro A, Del Hoyo O, et al. Role of fluorine-18 fluorodeoxyglucose PET/CT in head and neck oncology: the point of view of the radiation oncologist. *Br J Radiol*. 2016;89:20160217.
9. Schinagl DA, Span PN, Oyen WJ, et al. Can FDG PET predict radiation treatment outcome in head and neck cancer? Results of a prospective study. *Eur J Nucl Med Mol Imaging*. 2011;38:1449–1458.
10. Kao CH, Lin SC, Hsieh TC, et al. Use of pretreatment metabolic tumour volumes to predict the outcome of pharyngeal cancer treated by definitive radiotherapy. *Eur J Nucl Med Mol Imaging*. 2012;39:1297–1305.
11. Cheng NM, Fang YH, Lee LY, et al. Zone-size nonuniformity of ^{18}F-FDG PET regional textural features predicts survival in patients with oropharyngeal cancer. *Eur J Nucl Med Mol Imaging*. 2015;42:419–428.

12. Lin YC, Chen SW, Hsieh TC, et al. Risk stratification of metastatic neck nodes by CT and PET in patients with head and neck cancer receiving definitive radiotherapy. *J Nucl Med*. 2015;56:183–189.
13. Yabuki K, Shiono O, Komatsu M, et al. Predictive and prognostic value of metabolic tumor volume (MTV) in patients with laryngeal carcinoma treated by radiotherapy (RT)/concurrent chemoradiotherapy (CCRT). *PLoS One*. 2015;10:e0117924.
14. Abgral R, Keromnes N, Robin P, et al. Prognostic value of volumetric parameters measured by ^{18}F-FDG PET/CT in patients with head and neck squamous cell carcinoma. *Eur J Nucl Med Mol Imaging*. 2014;41:659–667.
15. Abgral R, Valette G, Robin P, et al. Prognostic evaluation of percentage variation of metabolic tumor burden calculated by dual-phase FDG PET-CT imaging in patients with head and neck cancer. *Head Neck*. 2016;38(suppl 1):E600–E606.
16. Park GC, Kim JS, Roh JL, et al. Prognostic value of metabolic tumor volume measured by ^{18}F-FDG PET/CT in advanced-stage squamous cell carcinoma of the larynx and hypopharynx. *Ann Oncol*. 2013;24:208–214.
17. Mohan R, Wu Q, Manning M, et al. Radiobiological considerations in the design of fractionation strategies for intensity-modulated radiation therapy of head and neck cancers. *Int J Radiat Oncol Biol Phys*. 2000;46:619–630.
18. Bernier J, Domenge C, Ozsahin M, et al. Postoperative irradiation with or without concomitant chemotherapy for locally advanced head and neck cancer. *N Engl J Med*. 2004;350:1945–1952.
19. Bourhis J, Sire C, Graff P, et al. Concomitant chemoradiotherapy versus acceleration of radiotherapy with or without concomitant chemotherapy in locally advanced head and neck carcinoma (GORTEC 99-02): an open-label phase 3 randomised trial. *Lancet Oncol*. 2012;13:145–153.
20. Bonner JA, Harari PM, Giralt J, et al. Radiotherapy plus cetuximab for locoregionally advanced head and neck cancer: 5-year survival data from a phase 3 randomised trial, and relation between cetuximab-induced rash and survival. *Lancet Oncol*. 2010;11:21–28.
21. Castelli J, Simon A, Rigaud B, et al. A nomogram to predict parotid gland overdose in head and neck IMRT. *Radiat Oncol*. 2016;11:79.
22. Schemper M, Smith TL. A note on quantifying follow-up in studies of failure time. *Control Clin Trials*. 1996;17:343–346.
23. Harrell FE, Lee KL, Mark DB. Multivariable prognostic models: issues in developing models, evaluating assumptions and adequacy, and measuring and reducing errors. *Stat Med*. 1996;15:361–387.
24. Hothorn T, Lausen B. On the exact distribution of maximally selected rank statistics. *Comput Stat Data Anal*. 2003;43:121–137.
25. Leseur J, Roman-Jimenez G, Devillers A, et al. Pre- and per-treatment ^{18}F-FDG PET/CT parameters to predict recurrence and survival in cervical cancer. *Radiother Oncol*. 2016;120:512–518.
26. Romesser PB, Lim R, Spratt DE, et al. The relative prognostic utility of standardized uptake value, gross tumor volume, and metabolic tumor volume in oropharyngeal cancer patients treated with platinum based concurrent chemoradiation with a pre-treatment [(18)F] fluorodeoxyglucose positron emission tomography scan. *Oral Oncol*. 2014;50:802–808.
27. Murphy JD, La TH, Chu K, et al. Postradiation metabolic tumor volume predicts outcome in head-and-neck cancer. *Int J Radiat Oncol Biol Phys*. 2011; 80:514–521.
28. Moon SH, Choi JY, Lee HJ, et al. Prognostic value of ^{18}F-FDG PET/CT in patients with squamous cell carcinoma of the tonsil: comparisons of volume-based metabolic parameters. *Head Neck*. 2013;35:15–22.
29. Seol YM, Kwon BR, Song MK, et al. Measurement of tumor volume by PET to evaluate prognosis in patients with head and neck cancer treated by chemo-radiation therapy. *Acta Oncol*. 2010;49:201–208.
30. Deron P, Mertens K, Goethals I, et al. Metabolic tumour volume. Prognostic value in locally advanced squamous cell carcinoma of the head and neck. *Nuklearmedizin*. 2011;50:141–146.
31. Hentschel M, Appold S, Schreiber A, et al. Early FDG PET at 10 or 20 Gy under chemoradiotherapy is prognostic for locoregional control and overall survival in patients with head and neck cancer. *Eur J Nucl Med Mol Imaging*. 2011;38:1203–1211.
32. Kikuchi M, Koyasu S, Shinohara S, et al. Prognostic value of pretreatment ^{18}F-fluorodeoxyglucose positron emission tomography/CT volume-based parameters in patients with oropharyngeal squamous cell carcinoma with known p16 and p53 status. *Head Neck*. 2015;37:1524–1531.

4.3.3 A PET-based nomogram for oropharyngeal cancer

J. Castelli[1,2,3]; A. Depeursinge[4,5]; V. Ndoh[6]; J. O. Prior[7]; M. Ozsahin[1]; A. Devillers[8]; H. Bouchaab[1] **;** E. Chajon[6] **;** R. de Crevoisier[6]; N. Scher[1] ; F. Jegoux[9]; B. Laguerre[10]; B. De Bari[1]; J. Bourhis[1]

European Journal of Cancer, 2017 Jan.

1. Radiotherapy Department, Lausanne University Hospital, Switzerland
2. INSERM, U1099, Rennes, F-35000, France
3. Université de Rennes 1, LTSI, Rennes, F-35000, France
4.Ecole Polytechnique Fédérale de Lausanne, CH-1015 Lausanne VD, Switzerland
5. University of Applied Sciences Western Switzerland, 3960 Sierre, Switzerland
6. Radiotherapy Department, Centre Eugene Marquis, Rennes, F-35000, France
7. Nuclear Medicine and Molecular Imaging Department, Lausanne University Hospital, Switzerland
8.Nuclear Medecine Department, Centre Eugene Marquis, Rennes, F-35000, France
9. Head and Neck department, CHU Rennes, Rennes, F-35000, France
10. Oncology Department, Centre Eugene Marquis, Rennes, F-35000, France

European Journal of Cancer 75 (2017) 222–230

Available online at www.sciencedirect.com

ScienceDirect

journal homepage: www.ejcancer.com

Original Research

A PET-based nomogram for oropharyngeal cancers

J. Castelli [a,b,c], A. Depeursinge [d,e], V. Ndoh [f], J.O. Prior [g], M. Ozsahin [a], A. Devillers [h], H. Bouchaab [a], E. Chajon [f], R. de Crevoisier [f], N. Scher [a], F. Jegoux [i], B. Laguerre [j], B. De Bari [a], J. Bourhis [a,*]

[a] *Radiotherapy Department, Lausanne University Hospital, Switzerland*
[b] *INSERM, U1099, Rennes, F-35000, France*
[c] *Université de Rennes 1, LTSI, Rennes, F-35000, France*
[d] *Ecole Polytechnique Fédérale de Lausanne, CH-1015, Lausanne, VD, Switzerland*
[e] *University of Applied Sciences Western Switzerland, 3960, Sierre, Switzerland*
[f] *Radiotherapy Department, Centre Eugene Marquis, Rennes, F-35000, France*
[g] *Nuclear Medicine and Molecular Imaging Department, Lausanne University Hospital, Switzerland*
[h] *Nuclear Medicine Department, Centre Eugene Marquis, Rennes, F-35000, France*
[i] *Head and Neck Department, CHU Rennes, Rennes, F-35000, France*
[j] *Oncology Department, Centre Eugene Marquis, Rennes, F-35000, France*

Received 27 September 2016; received in revised form 28 November 2016; accepted 14 January 2017

KEYWORDS
Oropharyngeal cancer;
Nomogram;
Prognostic score;
PET

Abstract ***Purpose:*** In the context of locally advanced oropharyngeal cancer (LAOC) treated with definitive radiotherapy (RT) (combined with chemotherapy or cetuximab), the aims of this study were: (1) to identify PET-FDG parameters correlated with overall survival (OS) from a first cohort of patients; then (2) to compute a prognostic score; and (3) finally to validate this scoring system in a second independent cohort of patients.
Materials and methods: A total of 76 consecutive patients (training cohort from Rennes) treated with chemoradiotherapy or RT with cetuximab for LAOC were used to build a predictive model of locoregional control (LRC) and OS based on PET-FDG parameters. After internal calibration and validation of this model, a nomogram and a scoring system were developed and tested in a validation cohort of 46 consecutive patients treated with definitive RT for LAOC in Lausanne.
Results: In multivariate analysis, the metabolic tumour volume (MTV) of the primary tumour and the lymph nodes were independent predictive factors for LRC and OS. Internal calibration showed a very good adjustment between the predicted OS and the observed OS at 24 months. Using the predictive score, two risk groups were identified (median OS 42 versus 14 months, $p < 0.001$) and confirmed in the validation cohort from Lausanne (median OS not reached versus 26 months, $p = 0.008$).

* *Corresponding author*: Department of Radiation Oncology, Centre Hospitalier Universitaire Vaudois (CHUV), Bugnon 46, CH-1011, Lausanne, Switzerland. Fax: +41 21 314 46 01.
E-mail address: Jean.Bourhis@chuv.ch (J. Bourhis).

http://dx.doi.org/10.1016/j.ejca.2017.01.018

Conclusions: This is the first report of a PET-based nomogram in oropharyngeal cancer. Interestingly, it appeared stronger than the classical prognostic factors and was validated in independent cohorts markedly diverging in many aspects, which suggest that the observed signal was robust.

1. Introduction

Head and neck cancers (HNC) are among the most common cancers world wide (5th leading cancer by incidence) [1]. The American Joint Committee on Cancer (AJCC) staging, based on the primary tumour extension and nodal spread, is generally used to estimate the prognosis and guide therapy [2]. Based on evidence-based medicine level 1 [3], chemoradiotherapy (CRT) is a standard treatment for non-resected or unresectable locally advanced HNC (LAHNC) [4–6]. Radiotherapy (RT) combined with cetuximab has been established as a potential alternative standard treatment, especially useful when concomitant chemotherapy cannot be used [7]. Despite these treatments, the prognosis of these cancers remains relatively poor and locoregional recurrence can occur in up to 40% patients, mostly occurring in the first 2 years after the treatment [8], suggesting a need to better identify patients with a worse prognosis.

^{18}F-fluorodeoxyglucose (^{18}F-FDG) positron emission tomography/computed tomography (PET/CT) allows to quantify the metabolic activity of a tumour (glycolysis) and has become a reference tool in oncology for staging, RT planning and monitoring tumour response in many cancers [9,10]. PET imaging allows a more accurate nodal staging of LAHNC [11,12] and could result in changing the therapeutic management in nearly 15% of patients [13]. A PET/CT performed at 2–3 months after the end of RT ± chemotherapy allows the identification of good responders and can be useful for decision-making of neck dissection for residual neck disease [14]; however, most of the available studies were based on visual analysis.

The maximum standard uptake value (SUV_{max}) corresponds to the maximal pixel value in the tumour. Thanks to its ease of use and relative robustness, it is one of the most widely used parameters in clinical practice. However, SUV_{max} is not representative of non-homogeneous overall tumour uptake. More recently, volumetric PET parameters, i.e. metabolic tumour volume (MTV) and total lesion glycolysis (TLG), have been correlated with clinical outcome [15–17]. Nonetheless, these parameters require to delineate the tumour. As PET imaging suffers from a low spatial resolution, along with a high noise background and partial volume effect, tumour delineation heavily depends on the chosen segmentation method. One of the most common methods consists of using an automatic threshold, although the threshold value of 42% has been suggested in many studies. However, there are no consistent data for using a specific threshold to compute MTV. Another point is the reproducibility of PET parameters between different scanners and/or institutions, as most of the studies published so far were monocentric.

In this context, the aims of our study were: (1) to identify PET parameters correlated with overall survival (OS) from a first cohort of patients (from Rennes Cancer Center, France); then (2) to create a prognostic scoring system; and (3) finally to validate this scoring system with a second independent cohort of patients (from Lausanne University Hospital, Switzerland).

2. Material and methods

All consecutive patients from Rennes Cancer Center and Lausanne University Hospital treated with definitive concurrent CRT or RT and cetuximab for locally advanced oropharyngeal carcinoma (LAOC) between January 2010 and December 2015 were retrospectively reviewed. Inclusion criteria were an age between 18 and 75 years, T3–4 or N+ stage, no surgery before RT, no history of cancer, a PET performed at least 8 weeks before RT, no metastasis at diagnosis and a minimal follow-up of 6 months.

The study enrolled a total of 122 patients (76 from Rennes and 46 from Lausanne). The main patient, tumour and treatment characteristics are shown in Table 1. All tumours were locally advanced, corresponding to T3–4 or N stage (stage III or IV, AJCC 7th edition).

2.1. Treatment and planning

All patients underwent intensity-modulated RT (IMRT) using volumetric modulated arc therapy (VMAT, Rennes) or helical tomotherapy (Lausanne). A total dose of 70 Gy 2 Gy/fraction/day, 35 fractions (Rennes) or 2.12Gy/fractions/day, 33 fractions (Lausanne) with a simultaneous integrated boost technique [18] was given in combination to concomitant chemotherapy [5,6] or cetuximab [7] if the patients were not fit for chemotherapy. The modality of planning and treatment were the same as previously published [19]. The study was approved by the institutional ethical committees (NCT02469922).

Table 1
Patient characteristics.

Characteristics	Training set cohort—Rennes (N = 76)	External validation set cohort—Lausanne (N = 46)	p-value
Mean age, years (SD)	59.2 (8.6)	63.3 (±9.17)	0.027
Gender, N (%)			0.34
Male	61 (80.3%)	40 (87%)	
Female	15 (19.7%)	6 (13%)	
T-classification, N (%)			0.005
T1	1 (1.4%)	6 (13%)	
T2	20 (26.3%)	16 (34.9%)	
T3	34 (44.7%)	18 (39.1%)	
T4	21 (27.6%)	6 (13%)	
N-classification, N (%)			0.49
N0	11 (14.5%)	3 (6.5%)	
N1	11 (14.5%)	10 (21.7%)	
N2	51 (67.1%)	29 (63.1%)	
N3	3 (3.9%)	4 (8.7%)	
GTV, cm^3	45.8 (±47.7)	25.6 (±26.7)	<0.001
p16			0.001
Positive	15 (19.8%)	17 (37%)	
Negative/ unknown	21 (27.6%)/40 (52.6%)	15(32.6%)/14 (30.4%)	
Chemotherapy, N (%)			0.058
Cisplatin[5]	51 (67.1%)	24 (52.2%)	
Carboplatin − 5FU[6]	9 (11.8%)	4 (8.7%)	
Cetuximab[7]	16 (21.1%)	18 (39.1%)	

GTV = Gross Tumour Volume.

2.2. PET/CT acquisition

All patients underwent FDG PET/CT for staging before treatment. For the training cohort (Rennes), the patients fasted at least 4 h before the injection of 4 Mbq/kg of (^{18}F)-FDG (Flucis). Blood glucose levels were checked before the injection of (^{18}F)-FDG. If not contra-indicated, intravenous contrast agents were administered before CT scanning. After a 60-min uptake period of rest, patients were imaged with the Discovery PET/CT imaging-system (General Electric Medical Systems, Milwaukee, WI, USA). First, a CT (120 kV, 80 mA, 0.8-s rotation time, slice thickness 3.75 mm) was performed from the base of the skull to the mid-thigh. PET scanning was performed immediately after acquisition of the CT. Images were acquired from the base of skull to the mid-thigh (3 min/bed position). PET images were reconstructed by using an ordered-subset expectation maximisation iterative reconstruction (OSEM) (two iterations, 28 subsets) and an iterative fully 3D (Discovery ST). CT data were used for attenuation calculation. A similar protocol was used in Lausanne; however, on a slightly more recent system, Discovery D690 TOF PET/CT (General Electric Healthcare, Milwaukee, WI, USA), which allowed shorter acquisition (2 min/bed position). PET images were reconstructed after time-of-flight and point-spread-function recovery corrections.

2.3. PET analysis

For each patient, gross tumour volume-tumour (GTV-T) and nodal GTV (GTV-N) were manually segmented on each PET/CT by the same radiation oncologist.

A set of quantitative parameters based on SUV histograms were extracted from GTV-T and GTV-N in PET images. SUV_{Max} was first computed from GTV-T as the maximum SUV in the delineated volume. Various metabolic volumes were subsequently defined based on two segmentation methods: (i) an absolute threshold of SUV (ranging from 2.5 g/ml to 8 g/ml, 0.5 g/ml steps) or (ii) a relative threshold of SUV_{Max} (30%, 35%, 40–60 (2% steps), 65% and 70%). Six metabolic intensity parameters were computed using the two segmentation methods at each threshold for both GTV-T and GTV-N. The four statistical moments of the intensity distribution, i.e. SUV_{Mean}, $SUV_{Variance}$, $SUV_{Skewness}$, $SUV_{Kurtosis}$, were computed. The latter are based on the assumption that SUVs are following normal distributions within the metabolic volumes. MTV was computed as the metabolic volume of the segmented region in millilitres. TLG was computed as $SUV_{Mean} \times$ MTV of the corresponding thresholded region. SUV_{Peak} was computed from GTV-T only. The latter was defined as the mean SUV inside a sphere of 1.2 cm centred on the position of SUV_{Max}. The intersection of the sphere and the metabolic region was used when the sphere was not fully included in the metabolic volume.

2.4. Statistical analysis

OS was calculated from the first day of RT to the date of death from any cause. Patients alive at the time of analysis were censored at the date of last follow-up. Locoregional control (LRC) was calculated from the first day of RT to the date of first recurrence in primary tumour and/or lymph node. Follow-up was calculated using a reverse Kaplan–Meier estimation [20]. Both LRC and OS estimations were computed using the Kaplan–Meier method and two-sided log-rank test was used to compare the groups.

The analyses were performed as suggested in the TRIPOD statement [21].

In the first step, the analysis was performed only on the Rennes cohort. The association of the pretreatment parameters with LRC and OS was first assessed using univariate Cox analyses. Harrel's c-index was used to compare different models (c-index $\approx$ 0.5 $\rightarrow$ not predictive, c-index $\approx$ 1 $\rightarrow$ predictive) [22]. The c-index was used to determine the optimal SUV threshold giving the most predictive value for each PET parameter.

Factors with significance of p-value <0.1 and with highest c-index after univariate analyses were assessed

for multivariate Cox regression model using backward elimination. Variables were removed from the model if $p > 0.1$.

An internal validation on the patients from the training cohort (Rennes) was performed by the bootstrap method (1000 datasets constructed by random resampling with replacement from the original) [23]. This method was used to estimate the adjusted c-index and the 95% confidence interval (95% CI) of each parameter. Second, an internal calibration was performed to estimate the accuracy of the final model.

Based on this final model, a nomogram was built to estimate the individual OS probability at 18 and 24 months. β-Coefficient estimations from the final model were used to build a predictive score. Two prognostic risk groups were identified based on the estimated optimal cut-point by Hothorn and Lausen method [24]. Kaplan–Meier method was used to evaluate this score.

Finally, the multivariate Cox model and the prognostic scores were tested in the Lausanne validation cohort. Harrell's concordance index was used for the Cox model and Kaplan–Meier method for the prognostic score.

All analyses were performed using R software 3.2.4 (R Development CoreTeam; http://www.r-project.org).

2.5. Follow-up

A clinical evaluation was performed after RT every 3 months for the first 2 years and then every 6 months. Database was locked on 30th May 2016.

3. Results

3.1. Training cohort (Rennes)

For the training cohort (Rennes), the following parameters were associated with OS in univariate Cox analyses with a $p < 0.1$: N stage, GTV, MTV-N, MTV-T, SUVKurtosis_N, SUVKurtosis_T, SUVMean_N, SUVSkewness_N, SUVSkewness_T, SUVVariance_T, SUVVariance_N, TLG_N and TLG_T (Table 2).

In multivariate Cox analysis, the tumour MTV with a threshold of 35% (MTV_T_35) and the lymph node MTV with a threshold of 44% (MTV_N_44) were the two independent risk factors for OS (Table 3) ($p < 0.001$). The same parameters were also correlated with LRC ($p = 0.03$), with a hazard ratio of 1.01 and 1.043 for MTV_T_35 and MTV_N_44, respectively.

3.2. Internal validation and calibration of the final model for the training cohort

The c-index of the model was 0.69. After internal bootstrap validation, the adjusted c-index was estimated at 0.68. The 95% CI for the coefficient of the parameters

Table 2
Univariate cox analyses for overall survival in the training cohort (Rennes). For PET parameters, data are given only for absolute and relative thresholds with the highest c-index.

Parameters	HR [95% CI]	c-index	p
Gender	0.38 [0.13–1.08]	0.54	0.067
Chemotherapy (Platinum versus Cetuximab)	0.97 [0.67–1.42]	0.49	0.9
PS (0–1 versus 2)	1.56 [0.55–4.44]	0.52	0.39
Age	0.99 [0.95–1.04]	0.49	0.9
Tobacco	2.2 [0.68–7.43]	0.52	0.18
Alcohol	1.65 [0.73–3.79]	0.54	0.22
GTV (as continuous variable)	1.0 [0.99–1.01]	0.6	0.2
T-classification (T1–T2 versus T3–T4)	0.97 [0.47–2.02]	0.49	0.95
N-classification (N0–N1 versus N2–N3)	2.12 [0.95–4.69]	0.56	0.062
AJCC staging (stage III versus IV)	1.71 [0.71–4.11]	0.53	0.19
p16	0.3 [0.04–2.36]	0.53	0.17
SUV_{max}	0.98 [0.92–1.04]	0.52	0.57
MTV-N			
Absolute threshold (SUV = 4.5)	1.02 [1.006–1.03]	0.64	0.004
Relative threshold (SUV = 44%)	1.06 [1.03–1.09]	0.64	<0.001
MTV-T			
Absolute threshold (SUV = 2.5)	1 [0.99–1.02]	0.60	0.14
Relative threshold (SUV = 35%)	1.02 [1.002–1.04]	0.61	0.03
TLG N			
Absolute threshold (SUV = 2.5)	1.002 [1.001–1.004]	0.65	0.003
Relative threshold (SUV = 65%)	1.01 [1–1.01]	0.73	0.004
TLG T			
Absolute threshold (SUV = 2.5)	1 [0.99–1.001]	0.58	0.45
Relative threshold (SUV = 35%)	1 [0.99–1.002]	0.59	0.35
SUV Peak T			
Absolute threshold (SUV = 4.5)	0.98 [0.88–1.09]	0.53	0.8
Relative threshold (SUV = 56%)	0.97 [0.9–1.05]	0.58	0.57
SUV Mean N			
Absolute threshold (SUV = 2.5)	1.24 [1.03–1.49]	0.63	0.06
Relative threshold (SUV = 54%)	1.05 [0.99–1.11]	0.55	0.85
SUV Mean T			
Absolute threshold (SUV = 6.5)	0.98 [0.86–1.11]	0.57	0.79
Relative threshold (SUV = 35%)	0.96 [0.87–1.07]	0.54	0.53
SUV Kurtosis N			
Absolute threshold (SUV = 7)	1.32 [1.06–1.64]	0.58	0.01
Relative threshold (SUV = 60%)	1.27 [1.04–1.57]	0.74	0.02
SUV Kurtosis T			
Absolute threshold (SUV = 2.5)	0.72 [0.48–1.08]	0.57	0.11
Relative threshold (SUV = 70%)	1.07 [0.77–1.43]	0.58	0.6
SUV Skewness N			
Absolute threshold (SUV = 5.5)	0.97 [0.54–1.74]	0.6	0.9
Relative threshold (SUV = 58%)	2.5 [1.32–4.73]	0.65	0.03
SUV Skewness T			
Absolute threshold (SUV = 2.5)	0.35 [0.14–0.85]	0.61	0.02
Relative threshold (SUV = 30%)	0.67 [0.25–1.76]	0.55	0.42
SUV Variance N			
bsolute threshold (SUV = 2.5)	1.1 [1.03–1.18]	0.6	0.004
Relative threshold (SUV = 65%)	1.16 [1.02–1.33]	0.65	0.02
SUV Variance T			
Absolute threshold (SUV = 5.5)	0.97 [0.93–1.02]	0.56	0.24
Relative threshold (SUV = 46%)	0.94 [0.84–1.05]	0.57	0.28

HR = Hazard Ratio, CI = Confidence Interval, GTV = Gross Tumour Volume, SUV = Standard Uptake Value, MTV = Metabolic Tumour Volume, TLG = Total Lesion Glycolysis. Bold values refer to p-values <0.05.

Table 3
Parameters associated with overall survival in multivariate analysis in the training cohort (Rennes).

Parameters	Mean Value (SD) (in cm^3)	HR [95% CI] (per 1 cm^3)	p	95% CI (Bootstrap validation)
MTV_T_35	18 (±15.6)	1.021 [1.000–1.043]	0.052	[1.000–1.056]
MTV_N_44	4.52 (±9.7)	1.057 [1.028–1.087]	<0.001	[1.040–1.094]

HR = hazard ratio, CI = confidence interval, MTV_T_35 = metabolic tumour volume of the tumour computed with a relative threshold at 35% of SUV_{max}, MTV_N_44 = metabolic tumour volume of the lymph node computed with a relative threshold at 44% of SUV_{max}.

of the model are given in Table 3. Internal calibration showed a very good adjustment between the predicted and observed OS at 18 (Fig. 1) and 24 months (Figure E1).

3.3. Nomogram and prognostic score for the training cohort

Based on the final model, a nomogram was computed (Fig. 2). A prognostic score was calculated based on the β-parameter from the Cox model. A normalisation was applied to obtain a score ranging from 0 to 5. The estimated cut-point by Hothorn and Lausen method was 1.33 (Supplementary Figure E2). Based on this cut-off, two risk groups were identified. The median OS was 42 months (95% CI: 20–64) for the low-risk group versus 14 months (95% CI: 5–23) for the high-risk group ($p < 0.001$) (Fig. 3A). The same prognostic score was used to estimate the LRC. The median LRC was not reached for the low-risk group versus 10 months for the high-risk group ($p = 0.009$) (Fig. 3B).

3.4. Comparison between the training and the validation cohort

Median follow-up for the training cohort (Rennes) and validation cohort (Lausanne) were 38 (range, 2–80 months) and 23 months (range, 3–57 months), respectively ($p < 0.001$). The two populations differed notably concerning age (mean 59.2 versus 63.3 years [p = 0.02]), the tumour volume (GTV: 45.8 cm^3 versus 25.6 cm^3 [p < 0.001]) and p16 status (p16+: 18% versus 37%, [$p = 0.001$]) for Rennes and Lausanne, respectively. The use of cetuximab was slightly more frequent in the validation cohort ($p = 0.05$). In both cohorts, most of the patients were smokers (90–95%), with a performance status of 0 or 1.

At time of the analysis, 38 (50%) and six (13%) patients had died, while 26 (34.2%) and 8 (17.3%) patients had a locoregional recurrence for Rennes and Lausanne, respectively. The 2-year OS rate was 58% (95% CI: 46–70%) and 85% [74–99%] for Rennes and Lausanne, respectively ($p = 0.001$).

3.5. Evaluation of the final model and the prognostic score in the validation cohort (Lausanne)

The β-coefficients from the training model were applied to the validation cohort. The c-index was 0.76, higher than in the training cohort (0.69). The prognostic score was calculated for the validation cohort and the cut-off of 1.33 (obtained from the training cohort) was applied. The result confirmed the external validation of the model with a median OS not reached for the low-risk group versus 26 months (95% CI: 22–30) for the high-risk group ($p = 0.008$) (Fig. 3C). For the LRC, the same training model was applied to the validation cohort. The LRC at 18 months for the low-risk and the high-risk group were 96.1% and 63.1%, respectively ($p = 0.009$) (Fig. 3D).

4. Discussion

To our knowledge, this is the first study presenting a PET-based score allowing the prediction of the risk of death in LAOC patients. Even if there are other studies exploring the prognostic values of some PET parameters (SUV, MTV and TLG, etc.) in LAOC, none of them performed an external validation. We found that both MTV-T and MTV-N as continuous variables were major predictors of OS. Noteworthy, the classical clinical variables (T-classification, GTV [T and N], age, gender, etc) were less or not significantly predictive of patient outcome. Other established prognostic parameters (PS, AJCC staging and smoking status) were not significant in our study due to the lack of variability in the distribution of these parameters in both training and validation cohorts (more than 90% of smokers, all patients with PS 0 or 1). One limitation of our study was some missing data concerning p16 status which were available for only half of the patients, as p16 analysis was performed routinely in our centres only since 2013, and hence did not allow a full evaluation of this well-established prognostic parameter in our model. Prevalence of human papilloma virus (HPV) in oropharyngeal cancer was shown to be around 23% in Europe [25], being higher than in our training cohort (19%) and lower than in our validation cohort (37%). The p16 status was found to be highly predictive of treatment outcomes and survival in patients with oropharyngeal cancer [26]. However, smokers with p16-positive tumour seem to have a worse prognosis than those with p16-positive tumour without history of smoking. In our study, most of the patients were smokers which may explain the lack of significance of p16. However, despite the difference in the rate of p16 status (Table 1), the results of the external validation seem confirm that the good

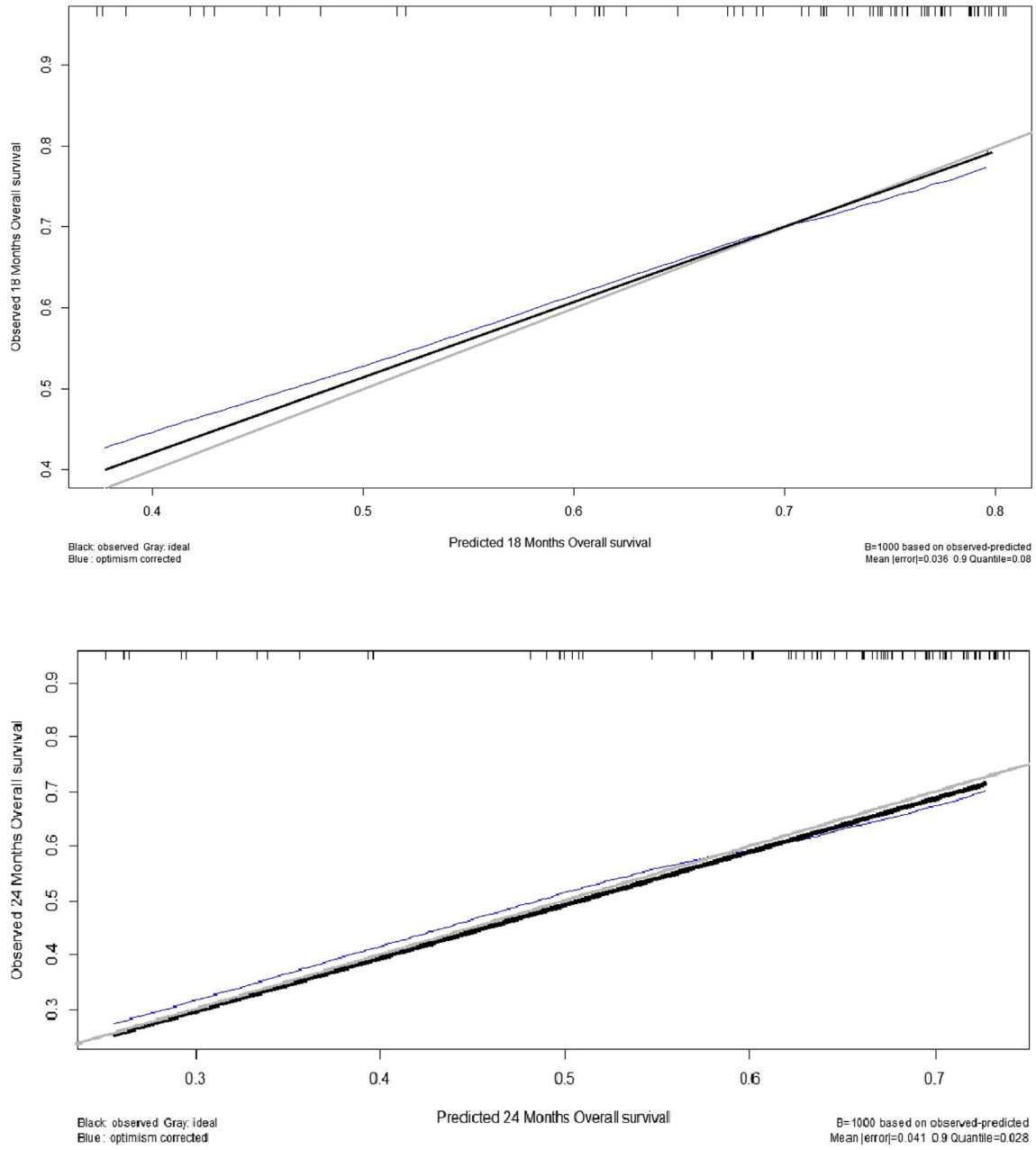

Fig. 1. Internal calibration of the final model for the training cohort (Rennes) at 18 and 24 months. Grey line is the ideal model, black line is the predicted survival and the blue-dotted line is the predicted survival corrected to avoid overfit. Both the 18- and 24-month survivals were nearly perfectly predicted. (For interpretation of the references to colour in this figure legend, the reader is referred to the web version of this article.)

predictive value of our nomogram is not influenced by the p16 status.

The PET-based nomogram obtained from this score allowed the prediction of 18- and 24-month OS in this clinical setting. Three strengths of our study are noteworthy. First, we followed in our study the internationally accepted TRIPOD criteria to build our predicting factors. This is an important quality-assurance issue, reinforcing our results. Second, this is the first study showing the prognostic impact of MTV in an external validation-independent population of oropharyngeal cancer patients. Third, we used continuous parameters instead of dichotomised variables. Dichotomisation leads to loss of power, affects the ability to detect relationships and overestimates the magnitude of the effect.

PET volumetric parameters like MTV or TLG have been used to estimate the heterogeneity of the tumour FDG uptake. Limited data were available but it showed a higher predictive value of MTV compared with more classical parameters (TNM, SUV, GTV…) [27,28], which is consistent with our findings. Only two studies performed a validation on an independent dataset

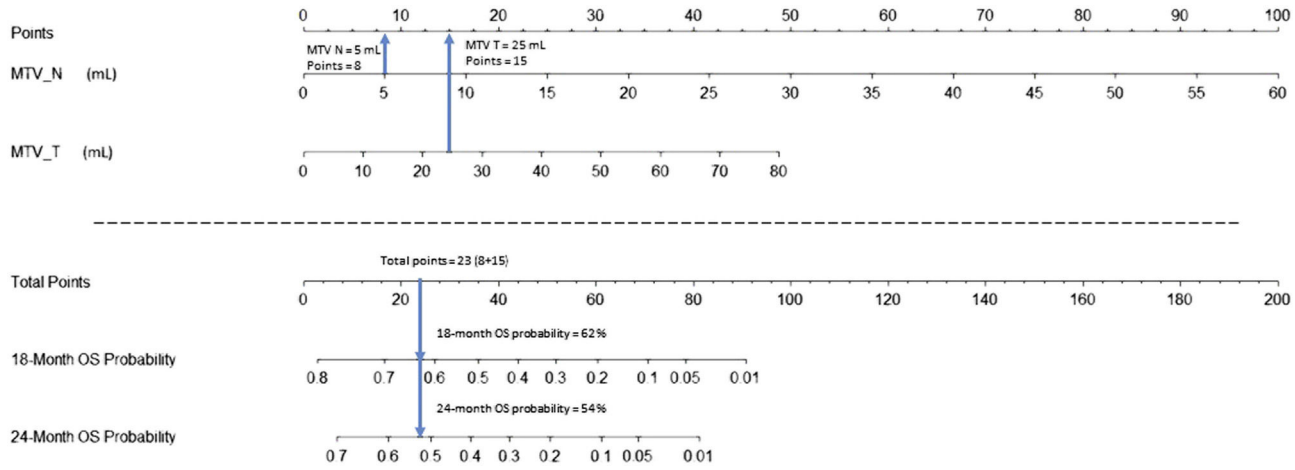

Fig. 2. Nomogram to predict the overall survival (OS) at 18 and 24 months. For each PET parameter, the corresponding points is obtained by drawing a line upward from the corresponding values to the 'Points' line. The total points for each patient is obtained by summing the points for each of the individual factors in the nomogram and is plotted on the 'Total points' line. A line is drawn down to read the corresponding predictions of 18- and 24-month LRC and OS. An example is given: an MTV-T of 25 mL corresponding to 15 points and an MTV-N of 5 mL to 8 points. The total score is 23, corresponding to 18-month and 24-month OS probabilities of 62% and 54%. MTV_N = metabolic tumour volume of the lymph node computed with a threshold = 44% of the SUV_{max}. MTV_T = metabolic tumour volume of the tumour computed with a threshold = 35% of the SUV_{max}.

[29,30]. La *et al.* [31] included 85 patients and showed that an increase of MTV of 17 cm^3 (from the 25th to the 75th percentile) was significantly correlated with an increased risk of death (hazard ratio [HR] 2.1). The authors validated their results on a dataset of 83 patients treated in the same institution after the original dataset [30]. Despite these interesting results, the possibility of adopting their model in the clinical practice is limited by the monocentric nature of their study and by the definition of the cut-off of MTV based on population-dependent characteristics (from the 25th to the 75th percentile). Based on the results of a previous study [32], Hofheinz *et al.* [29] used a cut-off of 58.7 ml for TLG. They showed a correlation of TLG only with better disease-free survival (DFS; HR 3.01, $p = 0.048$) but not with OS (HR 2.02, $p = 0.22$). After adjusting the cut-off at a value of 141 ml, TLG was also correlated with OS (HR 3.32, $p = 0.016$). Such methodologies and findings underline the difficulty in identifying a cut-off, which may be tested and reproducibly validated on an external dataset of patients. In our study, we choose to evaluate the MTV as continuous variables and to perform an external validation without modifying the model and the score obtained from the training dataset. Important differences in age, use of cetuximab, T-classification, p16 status, tumour and nodal volume (GTV) and PET/CT scanner between the training and the validation cohorts were observed. Despite these differences, the very good predictive performance obtained with the training cohort was confirmed (and even higher) for the validation cohort. These data strongly suggest that this new scoring system seem to be robust and could be further proposed and tested for patients' selection in clinical trials to identify patients with a high risk of locoregional failure and death, potentially candidates for treatment intensification, for instance, by dose escalation with dose painting in the MTV.

Noteworthy, the reproducibility of the MTV or TLG is considered to be limited by the initial definition of these parameters, which is based on a threshold of SUV, absolute (all pixel with SUV value > threshold) or relative (all pixel with SUV value > threshold % of SUV_{Max}). In the study by Schinagl *et al.* [33], four thresholds (2.5%, 40%, 50% and an adaptive threshold based on liver uptake) were compared for 77 patients treated by RT with or without chemotherapy. The authors found that 40% MTV was the strongest predictor of DFS and OS. However, also all the other thresholds were correlated with OS and DFS. Same results were reported on a population of 118 patients using three thresholds of MTV (2, 2.5 and 3) [34]. In our study, we evaluated 11 different absolute thresholds (from 2.5 to 8) and 15 relative thresholds (from 30% to 70%). All relative thresholds between 30% and 60% were correlated with OS, confirming the robustness of the MTV as a predictor factor, regardless the threshold chosen. However, based on p-value and c-index, the relative thresholds of 35% for the tumour and 44% for the lymph nodes were the best predictors of OS. The tumour MTV was nearly significant in the final model ($p = 0.052$). However, the final model (combination of both tumour and lymph node MTV) was highly significant ($p < 0.001$) and using tumour MTV increased the c-index of the model to 0.69 versus 0.64 for lymph node MTV alone. The combination of these two parameters probably takes into account the risk of death by local

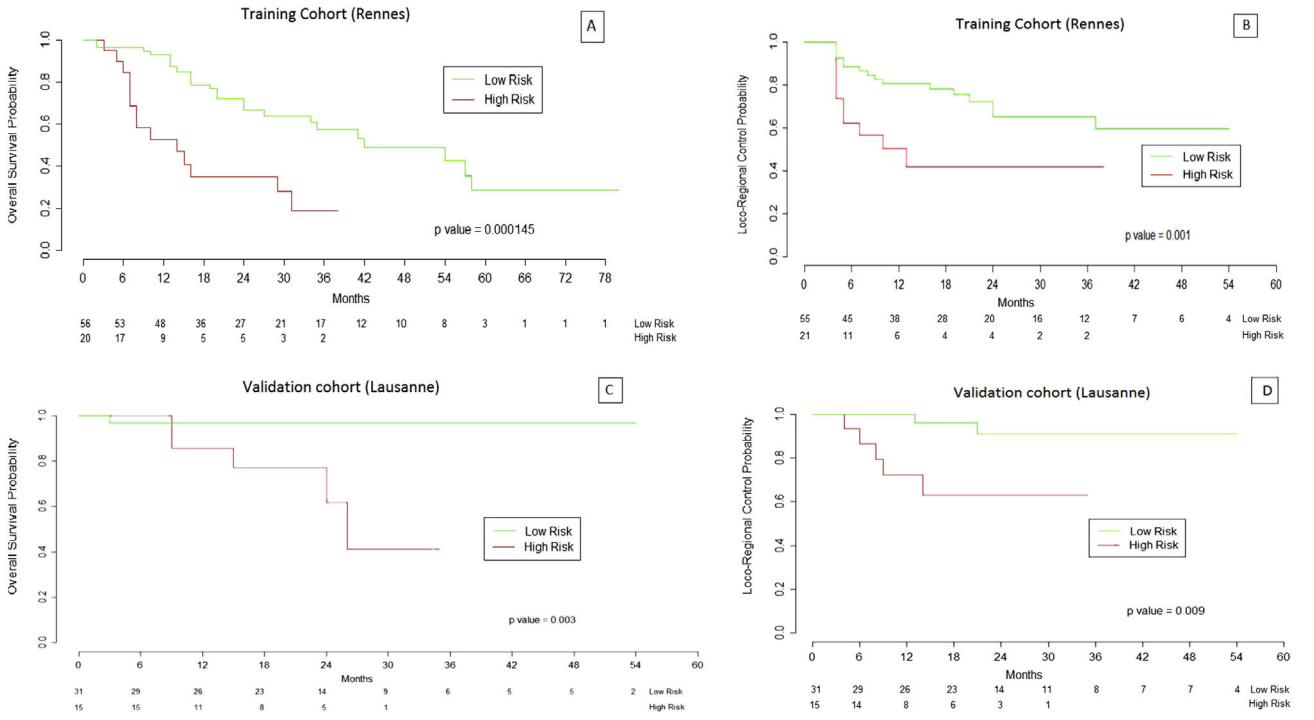

Fig. 3. Kaplan–Meier curves of overall survival and locoregional control for the training cohort (Rennes, A and B) and the validation cohort (Lausanne, C and D) according to the predictive score group (optimal cut-off defined by the Hothorn & Lausen method). High risk: score >1.33, low risk: score ≤1.33. Total score = 5.

relapse (primary tumour) and by metastasis (lymph node), both with a different weight in the final model.

5. Conclusion

MTV as a continuous variable was a strong prognostic factor for OS in LAOC patients treated with CRT or RT + cetuximab. We defined, and successfully validated on an independent dataset, a PET-based predictive score and nomogram that need to be further tested in larger prospective series to define their potential interest for tailoring the therapeutic approach.

Contributors

All authors contributed to the design and concept of the study. JC, EC, AD, MO, JB, HB, FJ, BL and J.O.P were responsible for patients' treatment and care. JC, AD, VN and NS acquired and analysed the data, with all authors contributing to data interpretation. JC and JB drafted and revised the manuscript for content, with all authors contributing to writing the text. All authors approved the final manuscript.

Funding sources

This work was partly supported by the Swiss National Science Foundation with grant agreement PZ00P2_154891 (A. Depeursinge).

Conflict of interest statement

None declared.

Appendix A. Supplementary data

Supplementary data related to this article can be found at http://dx.doi.org/10.1016/j.ejca.2017.01.018.

References

[1] Parkin DM, Bray F, Ferlay J, Pisani P. Global cancer statistics, 2002. CA Cancer J Clin 2005;55(2):74–108.
[2] Edge SB, Compton CC. The American Joint Committee on Cancer: the 7th edition of the AJCC cancer staging manual and the future of TNM. Ann Surg Oncol 2010;17(6):1471–4.
[3] National Comprehensive Cancer Network. Head and neck cancers (Version 1. 2016). In.
[4] Pignon JP, Bourhis J, Domenge C, Designe L. Chemotherapy added to locoregional treatment for head and neck squamous-cell carcinoma: three meta-analyses of updated individual data. MACH-NC Collaborative Group. Meta-Analysis of Chemotherapy on Head and Neck Cancer. Lancet 2000;355(9208):949–55.
[5] Bernier J, Domenge C, Ozsahin M, Matuszewska K, Lefebvre JL, Greiner RH, et al. Postoperative irradiation with or without concomitant chemotherapy for locally advanced head and neck cancer. N Engl J Med 2004;350(19):1945–52.
[6] Bourhis J, Sire C, Graff P, Gregoire V, Maingon P, Calais G, et al. Concomitant chemoradiotherapy versus acceleration of radiotherapy with or without concomitant chemotherapy in locally advanced head and neck carcinoma (GORTEC 99-02): an

open-label phase 3 randomised trial. Lancet Oncol 2012;13(2):145–53.
[7] Bonner JA, Harari PM, Giralt J, Cohen RB, Jones CU, Sur RK, et al. Radiotherapy plus cetuximab for locoregionally advanced head and neck cancer: 5-year survival data from a phase 3 randomised trial, and relation between cetuximab-induced rash and survival. Lancet Oncol 2010;11(1):21–8.
[8] Chajon E, Lafond C, Louvel G, Castelli J, Williaume D, Henry O, et al. Salivary gland-sparing other than parotid-sparing in definitive head-and-neck intensity-modulated radiotherapy does not seem to jeopardize local control. Radiat Oncol 2013;8:132.
[9] Fletcher JW, Djulbegovic B, Soares HP, Siegel BA, Lowe VJ, Lyman GH, et al. Recommendations on the use of ^{18}F-FDG PET in oncology. J Nucl Med 2008;49(3):480–508.
[10] Gambhir SS, Czernin J, Schwimmer J, Silverman DH, Coleman RE, Phelps ME. A tabulated summary of the FDG PET literature. J Nucl Med 2001;42(5 Suppl.):1S–93S.
[11] Kyzas PA, Evangelou E, Denaxa-Kyza D, Ioannidis JP. ^{18}F-fluorodeoxyglucose positron emission tomography to evaluate cervical node metastases in patients with head and neck squamous cell carcinoma: a meta-analysis. J Natl Cancer Inst 2008;100(10):712–20.
[12] Yoo J, Henderson S, Walker-Dilks C. Evidence-based guideline recommendations on the use of positron emission tomography imaging in head and neck cancer. Clin Oncol (R Coll Radiol) 2013;25(4):e33–66.
[13] Lonneux M, Hamoir M, Reychler H, Maingon P, Duvillard C, Calais G, et al. Positron emission tomography with [^{18}F]fluorodeoxyglucose improves staging and patient management in patients with head and neck squamous cell carcinoma: a multicenter prospective study. J Clin Oncol 2010;28(7):1190–5.
[14] Castaldi P, Rufini V, Bussu F, Micciche F, Dinapoli N, Autorino R, et al. Can "early" and "late" ^{18}F-FDG PET-CT be used as prognostic factors for the clinical outcome of patients with locally advanced head and neck cancer treated with radiochemotherapy? Radiother Oncol 2012;103(1):63–8.
[15] Schwartz DL, Harris J, Yao M, Rosenthal DI, Opanowski A, Levering A, et al. Metabolic tumor volume as a prognostic imaging-based biomarker for head-and-neck cancer: pilot results from Radiation Therapy Oncology Group protocol 0522. Int J Radiat Oncol Biol Phys 2015;91(4):721–9.
[16] Moon SH, Choi JY, Lee HJ, Son YI, Baek CH, Ahn YC, et al. Prognostic value of volume-based positron emission tomography/computed tomography in patients with nasopharyngeal carcinoma treated with concurrent chemoradiotherapy. Clin Exp Otorhinolaryngol 2015;8(2):142–8.
[17] Cacicedo J, Navarro A, Del Hoyo O, Gomez-Iturriaga A, Alongi F, Medina JA, et al. Role of [^{18}F] fluorodeoxyglucose PET/CT in head and neck oncology: the point of view of the radiation oncologist. Br J Radiol 2016:20160217.
[18] Mohan R, Wu Q, Manning M, Schmidt-Ullrich R. Radiobiological considerations in the design of fractionation strategies for intensity-modulated radiation therapy of head and neck cancers. Int J Radiat Oncol Biol Phys 2000;46(3):619–30.
[19] Castelli J, Simon A, Rigaud B, Lafond C, Chajon E, Ospina JD, et al. A Nomogram to predict parotid gland overdose in head and neck IMRT. Radiat Oncol 2016;11:79.
[20] Schemper M, Smith TL. A note on quantifying follow-up in studies of failure time. Control Clin Trials 1996;17(4):343–6.
[21] Collins GS, Reitsma JB, Altman DG, Moons KG. Transparent reporting of a multivariable prediction model for individual prognosis or diagnosis (TRIPOD): the TRIPOD statement. Br J Cancer 2015;112(2):251–9.
[22] Harrell FE, Lee KL, Mark DB. Multivariable prognostic models: issues in developing models, evaluating assumptions and adequacy, and measuring and reducing errors. Stat Med 1996;15(4):361–87.
[23] Efron B, Gong G. A leisurely look at the bootstrap, the jackknife, and cross-validation. Am Stat 1983;37(1):36–48.
[24] Hothorn T, Lausen B. On the exact distribution of maximally selected rank statistics. Comput Stat Data Anal 2003;43(2):121–37.
[25] Kreimer AR, Clifford GM, Boyle P, Franceschi S. Human papillomavirus types in head and neck squamous cell carcinomas worldwide: a systematic review. Cancer Epidemiol Biomarkers Prev 2005;14(2):467–75.
[26] Ang KK, Harris J, Wheeler R, Weber R, Rosenthal DI, Nguyen-Tân PF, et al. Human papillomavirus and survival of patients with oropharyngeal cancer. N Engl J Med 2010;363(1):24–35.
[27] Romesser PB, Lim R, Spratt DE, Setton J, Riaz N, Lok B, et al. The relative prognostic utility of standardized uptake value, gross tumor volume, and metabolic tumor volume in oropharyngeal cancer patients treated with platinum based concurrent chemoradiation with a pre-treatment [(18)F] fluorodeoxyglucose positron emission tomography scan. Oral Oncol 2014;50(9):802–8.
[28] Akagunduz OO, Savas R, Yalman D, Kocacelebi K, Esassolak M. Can adaptive threshold-based metabolic tumor volume (MTV) and lean body mass corrected standard uptake value (SUL) predict prognosis in head and neck cancer patients treated with definitive radiotherapy/chemoradiotherapy? Nucl Med Biol 2015;42(11):899–904.
[29] Hofheinz F, Lougovski A, Zophel K, Hentschel M, Steffen IG, Apostolova I, et al. Increased evidence for the prognostic value of primary tumor asphericity in pretherapeutic FDG PET for risk stratification in patients with head and neck cancer. Eur J Nucl Med Mol Imaging 2015;42(3):429–37.
[30] Tang C, Murphy JD, Khong B, La TH, Kong C, Fischbein NJ, et al. Validation that metabolic tumor volume predicts outcome in head-and-neck cancer. Int J Radiat Oncol Biol Phys 2012;83(5):1514–20.
[31] La TH, Filion EJ, Turnbull BB, Chu JN, Lee P, Nguyen K, et al. Metabolic tumor volume predicts for recurrence and death in head-and-neck cancer. Int J Radiat Oncol Biol Phys 2009;74(5):1335–41.
[32] Apostolova I, Steffen IG, Wedel F, Lougovski A, Marnitz S, Derlin T, et al. Asphericity of pretherapeutic tumour FDG uptake provides independent prognostic value in head-and-neck cancer. Eur Radiol 2014;24(9):2077–87.
[33] Schinagl DA, Span PN, Oyen WJ, Kaanders JH. Can FDG PET predict radiation treatment outcome in head and neck cancer? Results of a prospective study. Eur J Nucl Med Mol Imaging 2011;38(8):1449–58.
[34] Yabuki K, Shiono O, Komatsu M, Sano D, Nishimura G, Takahashi M, et al. Predictive and prognostic value of metabolic tumor volume (MTV) in patients with laryngeal carcinoma treated by radiotherapy (RT)/concurrent chemoradiotherapy (CCRT). PLoS One 2015;10(2):e0117924.

4.3.4 Conclusions

Les paramètres TEP de volume (*Metabolic Tumor Volume*) apparaissent nettement supérieurs aux paramètres utilisés en pratique clinique (classification AJCC et au SUVmax). Un seuillage en valeur relative de SUVmax semble supérieur à un seuillage en valeur absolue. La valeur prédictive du MTV reste globalement similaire en cas d'utilisation d'un niveau de seuillage restant compris entre 35 et 55%. L'analyse séparée de l'activité métabolique de la tumeur et des ganglions améliore encore la capacité de prédiction de la survie comparée à une analyse combinée. Cette approche a permis de réaliser un nomogramme identifiant les patients à haut risque de récidive locale et de décès. Une validation externe de ce nomogramme sur une seconde cohorte de patients traités dans un autre centre a pu être réalisée.

Les modalités d'analyse du MTV ganglionnaire restent cependant à mieux définir, notamment par rapport au fait que la référence utilisée pour le seuillage était le SUVmax de la tumeur et non celui des adénopathies. Par ailleurs les zones d'hypoxie, réputées radio-résistantes, ne sont pas hyperfixantes à la TEP au 18FDG.

Au total, une radiothérapie adaptative pourrait être proposée à ces patients à haut risque de rechute avec l'objectif d'assurer une couverture tumorale optimale, et idéalement de leur proposer une intensification thérapeutique. Cependant, le sous volume qui pourrait être à l'origine de la récidive et au sein duquel il serait nécessaire de réaliser une escalade de dose nécessite d'être identifié avant de pouvoir proposer une telle approche.

5 Discussion, synthèse et perspectives

5.1 Radiothérapie adaptative morphologique

L'article suivant synthétise les questions majeures concernant la radiothérapie adaptative des cancers des VADS, et notamment les approches morphologiques de la radiothérapie adaptative. Cette publication est proposée en fin de document de thèse puisque, rédigée en fin de thèse (en révision pour la revue Acta Oncologica en octobre 2017), elle intègre à la fois les données de la littérature et une partie de notre travail (11 articles au total).

5.1.1 Adaptive radiotherapy for head and neck cancer

J. Castelli[a,b,c]*; A. Simon[b,c]; C. Lafond[a,b,c]; N. Perichon[a]; B. Rigaud[b,c]; E. Chajon[a]; B. De Bari[d]; M. Ozsahin[e]; J. Bourhis[e]; R. de Crevoisier[a,b,c]

Revision, Acta Oncologica 2017

[a] Radiotherapy Department, Centre Eugene Marquis, Rennes, F-35000
[b] INSERM, U1099, Rennes, F-35000
[c] Université de Rennes 1, LTSI, Rennes, F-35000
[d] Radiotherapy Department, CHU Jean-Minjoz, Besançon, F-25030
[e] Radiotherapy Department, Lausanne University Hospital, Switzerland

Adaptive radiotherapy for head and neck cancer

J. Castelli[a,b,c]*; A. Simon[b,c]; C. Lafond[a,b,c]; N. Perichon[a]; B. Rigaud[b,c]; E. Chajon[a]; B. De Bari[d]; M. Ozsahin[e]; J. Bourhis[e]; R. de Crevoisier[a,b,c]

[a] *Radiotherapy Department, Centre Eugene Marquis, Rennes, F-35000*

[b] *INSERM, U1099, Rennes, F-35000*

[c] *Université de Rennes 1, LTSI, Rennes, F-35000*

[d] *Radiotherapy Department, CHU Jean-Minjoz, Besançon, F-25030*

[e] *Radiotherapy Department, Lausanne University Hospital, Switzerland*

*Corresponding author: Dr Joël Castelli, Département de radiothérapie, Centre Eugene Marquis, avenue de la Bataille Flandres Dunkerque, FR-35000 Rennes;

Tel.: +33 (0)29 925 30 20, fax: +33 29 925 32 50;

email: j.castelli@rennes.unicancer.fr

Adaptive radiotherapy for head and neck cancer

Introduction: This review, focused on ART in head and neck, aims to (i) identify the various strategies of ART and to (ii) estimate the dosimetric and clinical benefit of these strategies.

Material and methods: We performed an electronic search of articles published in PubMed/MEDLINE and Science Direct from January 2005 to December 2016. Among a total of 134 articles assessed for eligibility, 11 articles only were finally retained for the review.

Results: Eight *in silico* studies tested a various number of replanning, ranging from 1 to 6, aiming mostly to decrease the dose to the parotid glands. The optimal timing for replanning appears early during the first two weeks of treatment. Compared to standard IMRT, ART enables to decrease the dose to the parotid gland from 0.6 to 6 Gy and to the spinal cord from 0.1 to 4 Gy, while improving target coverage and homogeneity in the majorities of the studies. Only five studies report clinical results of ART, three of them included a non-randomized comparison with standard IMRT. These studies show that ART is safe and suggest a benefit of ART to decrease xerostomia, to increase quality of life, and to increase local control. Patients with the largest early anatomical and dose variations are the best candidate for ART.

Conclusion: ART may decrease toxicity and improve local control for locally-advanced head and neck cancer. Randomized trials are, however, necessary to demonstrate the benefit of ART before using the technique in routine practice.

Key words: adaptive radiotherapy, head and neck cancer, parotid gland

1 Introduction

Intensity-modulated radiotherapy (IMRT) is classically based on only one initial planning computed tomography (CT) scan, whereas large anatomical variations can be observed during the treatment course. In case of head and neck IMRT, these variations are body weight loss, primary tumor shrinkage, parotid gland displacement and volume reduction [1-3]. Due to the steep IMRT dose gradient along with the potentials anatomic variations, the actual delivered dose may therefore not correspond to the planned dose. The consequence can be an increase in the doses delivered to the organs at risk (OAR), and/or a decrease in the doses delivered to the tumor, resulting in increased risk of toxicity and recurrence [4, 5] (supplementary table S1 and S2).

The standard approach of image-guided radiotherapy (IGRT) in head and neck cancer consists of rigid registration based on the bony anatomy using planar or Cone Beam CT images. Daily IGRT allows reducing the set-up errors to 1.5 mm [6, 7]. However, the flexibility between rigid bony structures, and the deformations of the target volume and organs at risk may lead to different local misalignments, which are impossible to correct simultaneously with a single couch displacement [8, 9]. Adaptive radiotherapy (ART) using one or several replanning aims to correct these variations and thus optimize the delivered dose distribution to the daily anatomy of the patient. Based on daily CTs, several ART strategies can be designed that potentially require technical and organizational actions, such as dose monitoring based on dose per fraction calculation, cumulated dose during treatment, and replanning. Since the use of ART is very recent, its benefit can be estimated either in silico, using deformable image registration (DIR) for dose accumulation, or clinically, based on a limited number of studies. However, the choice of the optimal algorithm for dose accumulation is particularly complex. The following questions arise also when considering ART's clinical goal: Does it aim to increase local control, decrease toxicity, or both? Do all

patients need ART? What is the optimal number and timing of replanning? Does the gain in patient quality of life counterbalance the human and economic resources required in the whole process?

This review, focused on ART in head and neck, aims to (i) identify the various strategies of ART and to (ii) estimate the dosimetric and clinical benefit of these strategies. The methodological aspects are discussed as well as the identification of the subgroup of patients who are more likely to benefit from ART.

2 Material and methods

We performed an electronic search of articles published in PubMed/MEDLINE and Science Direct, according to PRISMA guidelines [10] from January 2005 to December 2016, using the following keywords: adaptive radiotherapy, anatomical variations, head and neck cancer, parotid glands, target volume. Our search was restricted to articles reporting data obtained from humans written in English and dealing with locally-advanced HNC, and anatomical/dosimetric variation in the context of adaptive radiotherapy. In addition, the references of each study were screened in order to retrieve additional relevant papers. All included studies were reviewed to collect the following data: study design (prospective vs retrospective), number of patients, diagnosis of the included patients, time and modality of evaluation, anatomical and/or dosimetric variations, dosimetric and/or clinical benefit of ART. Retrospective studies with a limited number of patients (<15 patients) were excluded to avoid bias.

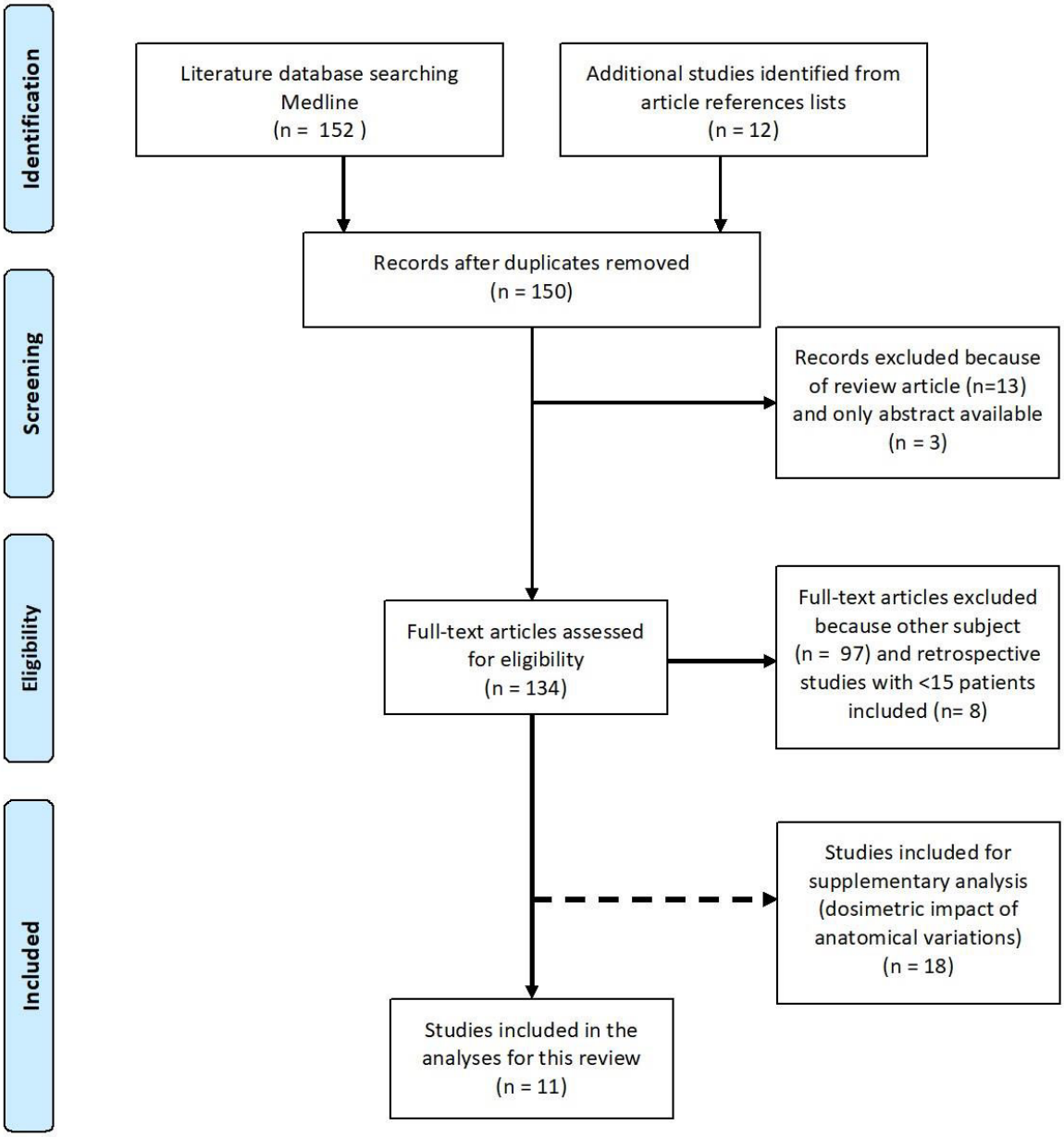

Figure 1: PRISMA flow diagram of the literature search

3 Results

The PRISMA flow diagram of the literature search is show Figure 1. One hundred fifty-two studies were identified from PubMed/MEDLINE. Another twelve studies were identified from references. Three studies was excluded because only the abstract was available and thirteen as they were general reviews. One hundred thirty-four articles were assessed for

eligibility. Ninety-seven studies did not meet the eligibility criteria, as most of them were focused on dose calculation or algorithms for image registration. Eight supplementary studies were excluded due to their retrospective nature with a limited number of patients (<15).

Finally, a total number of eleven studies was included in the analyses for this review, of which 5 reported clinical data. Eighteen other studies were included for supplementary analysis on dosimetric impact of anatomical variations during standard IMRT.

3.1 ART strategies for head and neck cancer in the literature

Eleven studies have been identified as reporting the benefit of ART, either providing dosimetric data (table 1) or clinical results (table 2). These studies included between 10 and 86 patients, treated or simulated with ART. The number of replanning ranged from 1 (72% of the studies) to 6 (10% of the studies), performed in most cases at the 3rd or 4th week of treatment. For comparison between ART and no-ART, two types of approach were used, either by considering another cohort of no-ART patients or by using a single group of patients undergoing treatment simulation with or without ART. The dose comparison could be performed at the fraction or considering the cumulated dose calculated by the mean dose or using DIR (table 1).

Table 1: Dosimetric benefit of ART in head and neck cancer

Author (Year)	*Nb pts*	*Replanning strategies*		*Dosimetric analysis*			*Dosimetric benefit*		
		Nb	*Timing*	*Time point to cumulate the dose*	*Method to cumulate the dose*	*Total dose for the comparison (Gy)*	*Parotid Gland (Dmean)*	*Spinal cord (Dmax)*	*Target Volume (PTV)*
Capelle (2012) [17]	20	1	3th week	2	Average DVH	66	- 0.6 Gy	-0.6 Gy	+0.5 Gy (D1%)
Castelli (2015) [12]	15	6	Weekly	7	DIR	70	- 3.8 Gy	-	-
Dewan (2016) [18]	30	1	40 Gy	2	DVH	30	IL -6 Gy CL -2.2 Gy	-6 Gy	- More uniform coverage - Decrease V110% by 2
Duma (2012) [3]	11	1	16th (9th-21th) Fr	1	DVH	2	No variation	-0.14 Gy	-
Jensen (2012) [23]	15	2 to 4	-	3 to 5	DIR	70	CL: - 11.5 % $ IL: - 3.8 % $	-	Improvement of coverage by 8 %
Olteanu (2014) [22]	10	2	8th and 18th Fr	3	DIR	70	- 6 % $	-	Higher minimum and lower maximum doses
Schwartz (2013) [25]	22	1 or 2	16th and 22th Fr	2 or 3	DIR	70	- 0.7 Gy	-	Increase coverage and dose homogeneity
Zhao (2011) [29]	33	1	15th (+/-5) Fr	2	DVH	37.5 Gy (20-50 Gy)	Decrease mean dose	-	-

$ = Median dose, - = Not assessed, Nb pts = Number of patients, HNC = Head and neck cancer, LAHNC = Locally advanced head and neck cancer, NPC = Nasopharyngeal Carcinoma, Fr= fraction, RT= Radiotherapy, RTCT= Chemoradiotherapy, DVH = Dose Volume Histogram, DIR = Deformable Image Registration, Dmean = Mean dose, Dmax = maximum dose, D1= Dose received by 1 % of the volume, V110% = Percentage of target volume receiving 110 % of the dose prescribed (hot spot), IL = Ipsilateral, CL = Contralateral, PTV = Planning Target Volume

Table 2: Clinical benefit of ART in head and neck cancer

Author (Year)	*Nb pts*		*Tumor site*	*Total dose (Gy)*	*Replanning strategies*		*Follow-up (months)*	*Clinical endpoint*		
	ART	*No ART*			*Nb*	*Timing*		*Loco regional control and survival*	*Acute Toxicity*	*Late toxicity*
Schwartz (2012) [25]¤	22	0	OPC	66-70	1 or 2	16th and 22th Fr	31	2-year LRC = 95 %	- G III mucosal = 100% - G II xerostomia = 55% - G III xerostomia = 5%	Full preservation or functional recovery of speech and eating at 20 months
Kataria (2016) [27]	36	0	LAHNC	70	1	54 Gy	-	- 2-year DFS = 72% - 2-year OS = 75%	G II-III mucosal = 100%	- G II xerostomia = 8% - G II mucosal = 11% - No G III
Yang (2013) [28]¤	86	43	NPC	70-76	1 or 2	15 th and/or 25th Fr	29	2-year LRC: - 97.2% (ART) - 82.2% (No-ART) p=0.04	-	Improvements in quality of life with ART
Chen (2014) [26]	51	266	LAHNC	60* 70µ	1	40 Gy (10-58 Gy)	30	2-year LRC: - 88% (ART) - 79% (No-ART) p=0.01 2-year OS: - 73% (ART) - 79% (No-ART) p=0.55	G III: - 39% (ART) - 30% (No-ART) p=0.45	G III: - 14% (ART) - 19% (No-ART) p=0.71
Zhao (2011) [29]	33	66	NPC	70	1	15th (+/-5) Fr	38	3-year LRFS: - 72.7% (ART) - 68.1% (No-ART) p=0.3	-	No difference except less xerostomia and mucosal with ART for N2 and N3 patients

¤= Prospective studies (non-randomized), *= Adjuvant RT, µ = Definitive RT, Nb pts = Number of patients, LAHNC = Locally advanced head and neck cancer, OPC = oropharynx cancer, NPC = Nasopharyngeal carcinoma, Nb= Number, ART = Adaptive Radiotherapy, Fr= Fraction, LRC = Loco regional control, LRFS = Loco regional free survival, DFS = Disease Free Survival, OS = Overall Survival

3.2 Dosimetric benefit of ART

A total of eight studies reported data on the dosimetric benefit of ART: eight to spare the parotid gland, three for the spinal cord and five to improve the target volume coverage (table 1).

3.2.1 Parotid glands

The difference between mean planned doses and mean delivered doses without ART ranged in the literature from -1 Gy to 6 Gy, with 85% of the studies showing a parotid gland overdosage (supplementary Table S1). Moreover, parotid gland overdose appeared strongly patient-dependent, observed only in 30 to 65% of the patients. Furthermore, a small proportion of patients (10%-30%) were reported to present spontaneous parotid gland underdose [11].

Compared with the mean dose delivered with standard IMRT, ART allowed a dose decrease ranging from 0.6 Gy to 4.1 Gy in all the studies, except one study which did not find a benefit with one replanning only [3]. Surprisingly, the ART strategy has been found to benefit not only to the over-irradiated parotid glands' patients, reducing the mean dose by 5.1 Gy but also to the non-over-irradiated parotid glands, reducing the mean dose by 1.4 Gy [12]. The benefit of ART seems to correlate with the number of replanning. The dosimetric benefit of numerous replanning strategies (63 combinations), defined by various numbers (1 to 6), and timings of replanning (at each week of the treatment), has been investigated in 13 patients with oropharyngeal cancers [13]. Six weekly replanning ensured the best benefits, allowing a decrease of 3.3 Gy of the mean dose. However, 94% of this benefit was already attained with three replanning at weeks 1, 2, and 5, enabling a decrease of the mean dose by 3.1 Gy.

In total, nearly 40% of the patients present a parotid gland overdose (compare to the planned dose) around 2 Gy (up to 6 Gy) when treating with standard IMRT. Compared to the

delivered dose with standard IMRT, ART allows decreasing the mean dose around 4 Gy for all these over-irradiated parotid glands. Moreover, a decrease of dose is also observed for non-overdosed parotid glands, with a dose decrease for the whole population of nearly 2.5 Gy. The dosimetric benefit of ART is improve by increasing the number of replanning. The optimal timing for replanning appears early during the first two weeks of treatment [11, 13, 14].

3.2.2 Spinal cord

Eleven studies reported dose variations for the spinal cord. Compared to the planning and without ART, the maximum dose to the spinal cord increased by a range from -0.1 Gy to 3.8 Gy (supplementary table S1), depending on the patient. However, in most cases, the maximum dose never increased higher than the initial spinal cord dose constraints at the IMRT planning (<45 – 48Gy) [15]. This dose increase correlates with positional variability, yet not with anatomical variation [16].

Three studies reported ART achieved a dosimetric benefit for the spinal cord, decreasing the spinal cord maximum dose by 0.1 Gy to 4 Gy for a number of fractions ranging from 1 to all fractions [3, 17, 18]. The benefit of such dosimetric difference is unclear and may not be translated into a clinical benefit.

In total, for the spinal cord, positional variation is considered as the main cause of dose variation. No strong evidence of the benefit of replanning was show.

Table S1 (supplementary data): Dosimetric impact of anatomical variations for the parotid gland and the spinal cord without ART (difference between delivered and planned dose)

Author	*Nb pts*	*Total prescribed dose*	*Loss of volume (%)**	*Dosimetric analysis*		*Dosimetric impact of anatomical variations**	
				Time point for dose evaluation	*Method to cumulate the dose*	*Parotid glands Dmean (Gy) variation*	*Spinal cord Dmax (Gy) variation*
Ahn (2011) [16]	23	70	24	11th, 22th and 33th fr	Average DVH	+ 2.5 Gy	+ 3.8 Gy
Beltran (2012) [56]	15	70	30	15th and 25th fr	Average DVH	+ 6 Gy	+ 2.5 Gy
Berwouts (2013) [53]	10	70	32	8th and 18th fr	DIR	-	- 0.1 Gy (D5 %)
Bhide (2010) [15]	20	70	14.2 (W2)	Weekly	Comparison of weekly DVH	- 1 Gy	+ 2.6 Gy
Capelle (2012) [17]	20	66	17.5	3rd week	Average DVH	-	+ 0.4 Gy
Castelli (2015) [12]	15	70	28	Weekly	DIR	60 % of PG : + 4 Gy	-
Height (2010) [57]	10	70	21	40-50 Gy	Average DVH	-1 Gy	+ 0.5 Gy
Ho (2012) [58]	10	65	29	Weekly	Average DVH	+ 0.2 Gy (D50)	+ 1.1 Gy
Hunter (2013) [11]	18	70	-	Weekly	Average DVH	63 % of the PG : + 2.2 Gy	-
Jensen (2012) [23]	72	70	40	Weekly	DIR	IL: + 4 % CL: + 11 % $^{\$}$	-
Marzi (2012) [59]	15	70	41.5	Weekly	Average DVH	+ 1.3 Gy	-
Nishi (2013) [2]	20	70	-	3rd or 4th week	Average DVH	+ 5 Gy $^{\$}$	+ 2.1 Gy
O'Daniel (2007) [60]	11	70	-	2/week	DIR	IL: + 3 Gy CL: + 1 Gy	No variations
Orban de Xivry (2010) [61]	10	70	-	Weekly	DIR	< 1 Gy	+ 1.84 Gy (D2 %)
Robar (2007) [62]	15	70	-	Weekly	Average DVH	+ 2 %	+ 1.2 %
Yip (2014) [63]	15	70	4-23	Weekly	Average DVH	+ 2 %	-

*=The loss of volume and dose variations are quantified between the planning CT and the end of treatment, $= Median dose (instead of mean dose), - = Data not assessed, Nb Pts= Number of patients, W= Week, PG= parotid gland, CL= Contralateral, IL = Ipsilateral, D*x*% = Dose delivered to *x* % of the volume

3.2.3 Submandibular glands

Only one study reported an one Gy increase in the submandibular gland mean dose in a small series of 10 patients receiving chemoradiotherapy for laryngeal cancer, undergoing CT scans at the 2nd, 3rd, 4th, and 5th weeks of treatment [19]. No data was available regarding the benefit of ART for the submandibular glands.

Due to the lack of data for the submandibular glands, it is not possible to draw any conclusion.

3.2.4 Target volume (GTV, CTV, and PTV)

The analysis of the differences between planned and delivered dose without ART for the GTV, CTV, and PTV showed controversial results. While a majority of the studies found very low dose differences (below 1-2% for the D2% and D95%), some reported large dose differences [15, 16, 20], of 1.9 Gy underdose to the GTV [16] or a mean reduction of 2 Gy of the minimum dose to the PTV [15] (supplementary table S2).

Five studies reported the dosimetric benefit of ART in increasing the dose to the target volume. All these studies reported improved various dosimetric endpoints (for GTV, CTV, and PTV) with more uniform coverage [18, 21, 22] and increased coverage [21, 23, 24], for instance an increase of 2.1 Gy to the PTV (D95%)[24] (Table 1).

In total, regarding target volume, there is no consensus in the field on how to report target coverage during treatment (coverage index and target volume definition). Only a subset of patients, as for the parotid glands, may need of ART to correct tumor underdose. However, due to the lack of studies and to the variability in endpoints, more data is necessary to draw a conclusion.

Table S2 (supplementary data): Dosimetric impact of anatomical variations for the target volume without ART (Difference between delivered and planned dose)

Author	*Nb pts*	*Total prescribed dose (Gy)*	*Anatomical variations* (average) in %*		*Dosimetric analysis*		*Dosimetric variations (D95%)**		
			GTV	*CTV*	*Time point for dose evaluation*	*Method to cumulate the dose*	*GTV*	*CTV*	*PTV*
Ahn (2011) [16]	23	70	17	-	11th, 22th and 33th Fr	Average DVH	- 1.9 Gy	-	-
Beltran [56]	15	70	-	-	15th and 25th Fr	Average DVH	-	-	-4 %
Bhide [15]	20	70	-	3.2 (W2)	Weekly	Comparison of weekly DVH	-	-	- 2 Gy (*Dmin*)
Capelle [17]	20	66	-	-	3rd week	Average DVH	-	-	- 0.6 Gy
Chen [20]	25	70	-	-		Average DVH	-	-	+ 2 Gy
Height [57]	10	70	49	-	40-50 Gy	Average DVH	+ 0.5 Gy (D99%)	-	-
Marzi [59]	15	70	74.5	-	Weekly	Average DVH	+ 1 Gy	-	-
O'Daniel [60]	11	70	-	-	2/week	DIR	-	No difference	-
Schwartz [21]	24	66-70	-	10.3	16th and 22th Fr	DIR	-	No difference	-
Yip [63]	15	70	-	1 to 6	Weekly	Average DVH	-	No difference	-

*=The loss of volume and dose variations are quantified between the planning CT and the end of treatment, - = Data not assessed, Nb pts = Number of patients, GTV = Gross tumor volume, CTV = Clinical Target Volume, PTV = Planning Target Volume, D*x*% = Dose delivered to *x* % of the volume, Dmin = Dose minimum delivered to the volume

3.3 Clinical benefit of ART

Only five studies reported clinical benefits of ART (Table 2). The number of patients per study ranges from 22 to 86. The median follow-up ranges from 29 to 38 months. The tumors are mostly located in the oropharynx [25-27] and less frequently in the nasopharynx [28, 29]. Three studies report clinical results of ART compared with a no-ART technique [26, 28, 29]. As benchmark from the literature, by treating with standard IMRT, the grade II xerostomia rate at one year is around 40% and the 2-year locoregional control rate is around 80% [30-34].

Each of these 5 studies is described one by one, beginning with the two studies that do not include any comparison group.

Schwartz *et al.* [21, 25] analyzed 22 patients with locally advanced oropharyngeal cancer enrolled in a prospective ART trial. Patients had IMRT using a three-dose level delivered in 30 to 33 daily fractions. Gross disease and high-risk regions received 66 to 70 Gy, immediately adjacent lymph node levels and soft tissues target received 60 to 63 Gy and prophylactic cervical nodal coverage target received 54 to 57 Gy. A 3-4 mm 3D-margins around CTV was used to generate the PTV. All patients received concurrent systemic treatment. A daily online IGRT (in-room CT) was performed. DIR was used to propagate the planning contours to the daily CT for dosimetric evaluation and replanning, when needed. In the event of significant changes (criteria not detailed by the authors), replanning was performed. All patients had at least one replanning (median time at the 16^{th} fraction) and eight had second replanning (median time at the 22^{nd} fraction). With a median follow up of 31 months, the 2-year local-regional control rates was 95%. Regarding acute toxicity, all patients (n=22) had grade III mucositis, 12 had grade II xerostomia, and one patient grade III xerostomia. Quality of life score at 20 months demonstrated full preservation or functional recovery of speech and eating.

Kataria *et al.* [27] included 36 patients with locally-advanced HNC (58% oropharynx), treated with IMRT. The high-risk volume was generated by expanding the gross disease by 1–1.5cm. The low-risk nodal CTV included the remaining nodal levels at risk. A 5mm 3D-margin was used to generate the PTV. All patients received a total dose of 70 Gy in 35 fractions. The dose prescribed to the low-risk nodal volume was not given. All patients underwent a CT after the 23^{rd} fraction (46 Gy), which was used for generating a new dose distribution for the last 8 fractions (16 Gy). Patient received concurrent chemotherapy. Median follow-up was not reported. Regarding toxicities, grade III acute mucositis and

dysphagia were observed in 44% and 18% patients, respectively. No grade III late toxicity was reported. Four recurrences were found within the initial high dose volume. The 2-year disease free survival (DFS) and overall survival (OS) rates were 72% and 75%, respectively.

The study of Zhao *et al.* [29] included 99 patients with Stage II-IV nasopharyngeal carcinoma treated with simultaneous modulated accelerated radiotherapy. GTV was defined as the mass shown in the enhanced CT images, including the nasopharyngeal tumor, the retropharyngeal nodes, and the enlarged neck nodes. Two CTV (high risk and low risk) were defined. A total dose of 70 Gy was prescribed to the high risk CTV (2.5 Gy per fraction), and 56 Gy to the low risk CTV (2 Gy per fraction), delivered in 28 fractions. The margin used for the PTV was not precised. One replanning was performed for 33 patients at various times (ranging from 1st week to 3rd week). The timing of the replanning was decided by the radiation oncologist, based on clinical changes in patient anatomy, as tumor shrinkage (16 patients), weight loss (10 patients) or both (7 patients). After a median follow up of 38 months, the 3-year loco-regional free survival was 72.7% for ART patients (n=33), and 68.1% for no-ART patients (n=66), without significant difference (p=0.3). ART significantly increased 3-year loco-regional free survival for patients with stage T3-T4 only. The 3-year locoregional free survival was 80% for ART patients, compared to 60% for patients without ART (p=0.03). No difference was found for early stage (T1-T2) or in case of large lymph nodes volumes (N2, N3). Regarding late side effects, reported only for 8 patients with ART and 20 patients without ART, no significant difference was observed.

Yang *et al.* analyzed prospectively 129 patients with Stage I-IV nasopharyngeal carcinoma, 86 of them having ART with one or two replanning and 43 refused the replanning [28]. The time for the first replanning was before the 15th fraction for 10 patients, and before the 25th fraction for 53 patients. Twenty-three had two replanning before the 15th and 25th fractions. The PTV were defined by adding a 3-mm margin to the CTV. A total dose of 70 Gy

were delivered to the PTVs of the primary nasopharyngeal tumor and the involved lymph nodes. A total dose of 60 Gy and 56 Gy were delivered to the CTV high risk and low risk respectively. Treatment was delivered in 33 fractions with a simultaneous integrated boost. Stage I patients (n=15) were treated with radiotherapy only, and stage II-IV (n=114) were treated with chemo-radiotherapy. With a median follow-up of 29 months, the 2-year loco-regional control (LRC) rate was significantly improved for the patients with replanning, compared to that of patients without replanning (97.2% *vs.* 92.4%, respectively, p=0.04). The overall survival was not significantly different between the two IMRT strategies (89.8% *vs.* 82.2%, p=0.47). The quality of life scores were, however, significantly better for patients with replanning, while those without replanning reported more complications (for speech, social contact, and teeth).

Similar results were reported by Chen *et al.* in a larger series of 317 primarily oropharyngeal cancer patients, who underwent IMRT with daily IGRT [26]. The median prescribed dose was 60 Gy for patients treated postoperatively (45%), and 70 Gy for patients treated definitively (55%). The PTV margin was 3 to 5 mm around the CTV. One replanning was performed at a median dose of 40 Gy (range: 10-58 Gy), depending on multiple factors (weight loss, nutritional status and tumor shrinkage). With a median follow up of 30 months, the 2-year LRC was 88% for patients treated with ART vs. 79% for those without (p=0.01). There was, however, no significant difference in OS and distant metastasis-free survival between the two treatment groups. No significant difference was demonstrated either in terms of Grade III acute toxicity (39% with ART vs. 30% without ART, p=0.45) or Grade III late toxicity (14% vs. 19%, p=0.71). As the patients with a major tumor shrinkage underwent replanning, the potential advantage of ART exhibited in this study may be due to the selection of tumors with a better prognosis.

Overall, these non-randomized and mostly retrospective studies show that ART is safe and may increase local control, and to a lesser extent, improve quality of life by decreasing toxicity (xerostomia).

4 Discussion

This overview shows that the optimal strategy of ART is a weekly replanning or at least early replanning. ART appears justified to avoid parotid gland overdose [12, 23] and therefore likely decreasing the risk of xerostomia [25]. The benefit of ART for other OARs (submandibular glands, spinal cord) is unclear. ART appears also to correct the target volume underdose for a subset of patients [17, 22, 23] and improves local control in non-randomized studies [26, 28, 29]. The level of evidence of the clinical benefit of ART over non ART is therefore weak. The methods used to demonstrate the dosimetric benefit can be discussed. Moreover, this complex ART technic may be indicated only for a subgroup of patients which need to be identified. Finally, metabolic parameter variation during treatment may also be used to better trigger ART.

4.1 Limitation of the methods to evaluate the benefit of ART

The methods used to evaluate the dosimetric benefit of ART vary according to the type of per-treatment imaging, imaging frequency, methods to evaluate the dose and dosimetric endpoints (table 1). A limited number of patients have been included in each studies (from 10 to 33 patients), decreasing the statistical power of the results. The tumor localization may also impact on the results (oropharynx or nasopharynx). Moreover, per-treatment imaging were performed at different time points and frequencies during IMRT, from just once to each week. Only three studies used more than 2 time points to estimate the cumulated dose. Moreover, the dosimetric impact of anatomical variations was estimated using different dosimetric

endpoints. Indeed, most of the studies reported variations in the mean dose (in Gy or in % compared to prescribed dose), which have been shown to be predictive of xerostomia [35]. Only a few studies also used the normal tissue complication probability (NTCP) model to estimate the increase in xerostomia risk (n=1, m=0.4, and the median toxic dose ([TD_{50}]=39.9 [36, 37]).

The dose comparison could be performed at the fraction [3] or considering the cumulated dose, calculated by the mean dose for only a subset of fractions [18, 29] or for the whole treatment [17]. Dose accumulation could otherwise be estimated using deformable image registration (DIR) [12, 21-23] (supplementary figure S1).

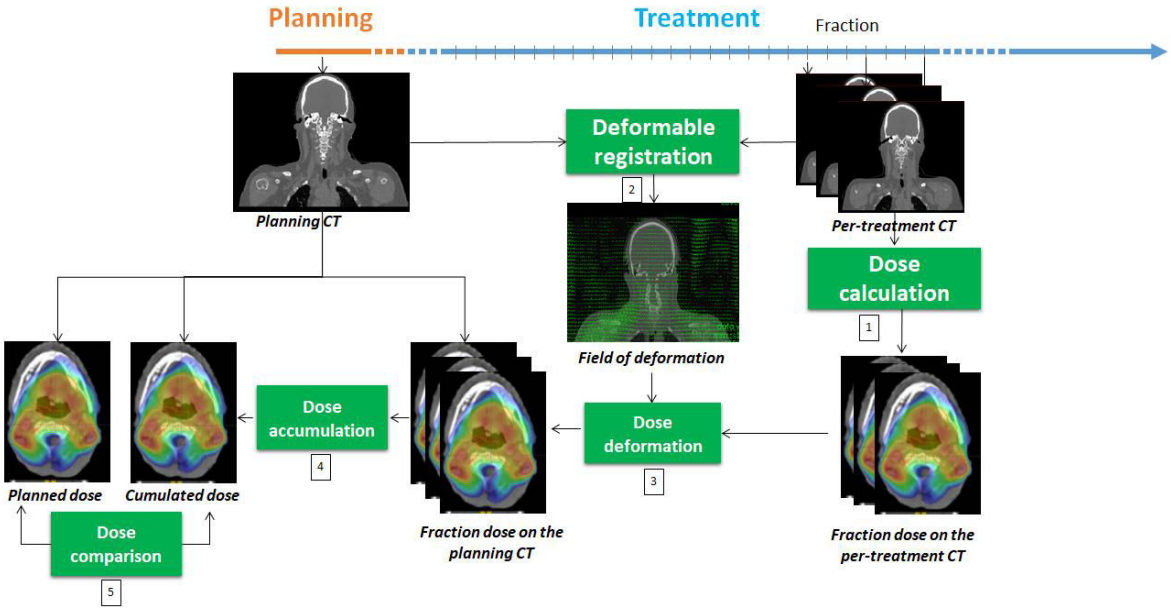

Figure S1 (supplementary): Deformable image registration (DIR) used for both structure propagation and dose accumulation during the course of radiotherapy

The dose is first calculated at the fraction on the daily image (1), then the planning CT and the daily image are registered using DIR (2). The resulting deformation vector fields are used to propagate the fraction dose to the planning CT (3). The fraction doses are cumulated on the planning CT (4). The cumulated dose can be finally compared to the planned dose (5).

The choice of the best method/algorithm for dose accumulation is however particularly complex. The main limitation of the DIR approach is the accuracy of the elastic registration

algorithm, linked to the uncertainty of point-to-point correspondence between the planning CT and the daily imaging. Indeed, the required accuracy of DIR depends strongly on its application, either for dose accumulation or for contour propagation. Dose monitoring for dose accumulation requires a low point-to-point error, especially in case of high dose gradient provided by IMRT (near the parotid gland by example [38]). On the other hand, delineation propagation require only a good correspondence between organ boundaries. Several methods have been therefore described to evaluate the accuracy of DIR algorithms, as visual evaluation [39], similarity indices (Dice similarity for example) [40], point-to-point error [41] or phantom [41, 42]. In practice, DIR can be used routinely for contour propagation since the contours can be visually validated /corrected by the radiation oncologists [43, 44]. However, the analysis of the literature shows that DIR is not yet fully validated in routine practice for dose accumulation. Thereby, due to the variability between the different studies (number of time points and methods to cumulate the dose, accuracy of the DIR methods, doses reported in Gy or in %), it appears difficult to estimate the true benefit of ART to spare the parotid gland and even more to decrease xerostomia.

In this context, studies providing clinical endpoint should be more relevant than *in silico* studies. Only five studies [25-29] reported clinical endpoint. However, these studies were either retrospective [26, 27, 29] or non-randomized [25, 28]. Only one study performed a systematic replanning [28]. For the four others studies, replanning was performed mostly of based on the radiation oncologist decision. As the patients with a major tumor shrinkage underwent more often replanning than patient without tumor response, the potential advantage of ART exhibited in these studies may be due to the selection of tumor with a better prognosis. Regarding toxicities, two studies reported an improvement of the quality of life for patients treated with ART [28, 29]. However, due to the lack of randomisation, the benefit of

ART to reduce toxicity is unclear, due to potential confounding factors (better tumor response, difference at baseline,…).

4.2 Which patients are good candidate for ART?

ART is particularly time-consuming [24, 29], requires many resources, is expensive and carries the risk of error, thus requiring rigorous quality-assurance procedures. Dosimetric and clinical results have demonstrated that ART may not be useful for all patients. It is therefore crucial to target patients with OAR overdose and/or target volume underdose. Ideally, replanning decisions should be based on early and simple anatomical predictors, in a clear objective of parotid gland over dose and/or tumor underdose correction.

In a review evaluating anatomical variations during radiotherapy to identify ART need predictor, no strong conclusion was possible due to the heterogeneity between studies [45]. In another study, Brown *et al.* analyzed 110 patients with oropharyngeal and nasopharyngeal carcinoma, reporting three OAR overdose profiles suitable for ART indication [46]. These three profiles were selected based on tumor location (oropharynx or nasopharynx), disease stage N (N0-2 or N3), initial weight (<or >100 Kg), and initial node size (< or >28 mm). The best candidates for ART were, for oropharyngeal tumor, N3 disease, initial weight > 100 kg and initial node size > 55 mm. For nasopharyngeal tumor, the best candidates were stage N2-3 disease, initial weight > 100 kg and initial node size > 15 mm. In another study with 20 oropharyngeal cancer, a nomogram was built to predict parotid gland overdose (without replanning) based on information from the planning CT and first weekly CT scan. This incorporated the initial volume of the CTV calculated from the planning CT, the shrinkage of the CTV at the first weekly CT, and the difference between the parotid gland mean doses at the first week and planning CTs [14]. The decision of replanning can be also guided by the tumor shrinkage. Indeed, another study proposed selecting good-responder patients for ART

[47]. Two decisions trees were therefore built based on type of chemotherapy, age, primary tumor growth pattern, site, KPS, HPV status, site, initial primary GTV, and total GTV volumes. However, several issues still remains in the issue of patient selection, mainly due to the limited number of patients in the studies [14], the small number of per-treatment imaging [47], unclear criteria to perform replanning [46], and the lack of external validation of the models.

In summary, good candidate for ART are mainly likely those with early tumor shrinkage or early parotid gland overdose. Cross validation studies are, however, necessary to confirm such decision criteria.

4.3 Metabolic ART: adaptive dose painting

Based on the assumption that 18-FDG-avid regions of the tumor are radioresistant and may be at the origin of the recurrence [48], PET can be used to guide dose escalation. In this approach, the dose can be prescribe homogenously inside the 18-FDG-subvolume (dose painting by contour (DPBC)) [49] or heterogeneously for each voxel as the function of the signal intensity of that voxel in the biologic image (dose painting by numbers) [50]. The feasibility of dose escalation based on DPBC in head and neck cancer was evaluated in a phase I [49] which included 41 patients. Based on pre-treatment 18-FDG-PET, the dose was escalated from 72.5 to 77.5 Gy in 32 fractions. One treatment-related death at dose level II (77.5 Gy) halted the study. More than half of the recurrence occurred inside the high dose area, suggesting the potential of 18-FDG-PET to guide dose escalation. However, DPBC is limited by its binary character (inside or outside the target), while dose painting by numbers (DPBN) may allow higher intra tumor doses. Due to anatomical and biological variations of the target volume during treatment [51], anatomical and metabolic ART (with replanning) should be considered to maintain plan quality [52]. However, very few studies addressed this complex strategy [22, 53, 54]. Long-term outcome of adaptive dose painting by numbers (A-

DPBN) was reported in a study having included 72 patients with head and neck cancer [55]. Among these 72 patients, dose escalation was performed using DPBC for 41 patients (without replanning), while 31 patients received 18F-FDG-PET-voxel intensity-based IMRT, adapted to per-treatment changes after 8 fractions (2 phase A-DPBN, 21 patients) or after 8 and 18 fractions (3 phase A-DPBN, 10 patients). Patients were matched to 72 other patients treated with standard IMRT without dose escalation during the same period. The median follow-up was 87.7 months. Patients treated with the 3-phase A-DPBN achieved higher 3-year local control (90%), compared to patient treated with standard IMRT (79%). Regarding late toxicity, no difference was show between A-DPBN and standard IMRT. The authors stated also that A-DPBN allowed to increase the dose to tumor subvolumes, while decreasing the dose to the OARs.

In total, only three prospective studies from the same treatment center (Ghent University Hospital, Belgium) suggest the interest of A-DPBN. Clinical studies, such as the ongoing study NCT01341535 (phase II randomized study comparing adaptive dose escalation to standard IMRT), are necessary to establish the feasibility and to evaluate the benefit of A-DPBN.

5 Conclusion

In summary, anatomical variations during the course of IMRT for locally-advanced head and neck cancer may lead to significant parotid gland and spinal cord overdose, as well as to tumor underdose. The clinical impact of such dose variations justifies the use of performing ART based on weekly or at least early replanning. How frequently should replanning be performed and when is not yet clearly defined, however. Preliminary clinical results suggest that the benefit of ART to decrease toxicity and improve local control nevertheless requires a better identification of the subset of patients that will particularly benefit from the technique. The clinical benefit of ART must compensate for the technique's

high cost, as it requires a high workload for both technicians and equipment. Ongoing randomized trials are, however, necessary to demonstrate the benefit of ART compared to no-ART before using the technique in routine practice in locally-advanced head and neck cancer.

Moreover, the complexity of the technique requires rigorous quality assurance procedures, training, and evaluation, for all the composite steps, including on-board imaging and processing, replanning, and treatment delivery. The new combined MRI/LINAC machines will pave the way for optimized ART.

Conflict of interest statement

None declared

6 REFERENCES

[1] Barker JL, Jr., Garden AS, Ang KK, et al. Quantification of volumetric and geometric changes occurring during fractionated radiotherapy for head-and-neck cancer using an integrated CT/linear accelerator system. Int J Radiat Oncol Biol Phys 2004;59:960-70.

[2] Nishi T, Nishimura Y, Shibata T, et al. Volume and dosimetric changes and initial clinical experience of a two-step adaptive intensity modulated radiation therapy (IMRT) scheme for head and neck cancer. Radiother Oncol 2013;106:85-9.

[3] Duma MN, Kampfer S, Schuster T, et al. Adaptive radiotherapy for soft tissue changes during helical tomotherapy for head and neck cancer. Strahlenther Onkol 2012;188:243-7.

[4] Gregoire V, Jeraj R, Lee JA, et al. Radiotherapy for head and neck tumours in 2012 and beyond: conformal, tailored, and adaptive? Lancet Oncol 2012;13:e292-300.

[5] Schwartz DL. Current progress in adaptive radiation therapy for head and neck cancer. Curr Oncol Rep 2012;14:139-47.

[6] Zeidan OA, Langen KM, Meeks SL, et al. Evaluation of image-guidance protocols in the treatment of head and neck cancers. Int J Radiat Oncol Biol Phys 2007;67:670-7.

[7] Den RB, Doemer A, Kubicek G, et al. Daily image guidance with cone-beam computed tomography for head-and-neck cancer intensity-modulated radiotherapy: a prospective study. Int J Radiat Oncol Biol Phys 2010;76:1353-9.

[8] Djordjevic M, Sjoholm E, Tullgren O, et al. Assessment of residual setup errors for anatomical sub-structures in image-guided head-and-neck cancer radiotherapy. Acta Oncol 2014;53:646-53.

[9] van Kranen S, van Beek S, Mencarelli A, et al. Correction strategies to manage deformations in head-and-neck radiotherapy. Radiother Oncol 2010;94:199-205.

[10] Moher D, Liberati A, Tetzlaff J, et al. Preferred reporting items for systematic reviews and meta-analyses: the PRISMA statement. BMJ 2009;339:b2535.

[11] Hunter KU, Fernandes LL, Vineberg KA, et al. Parotid glands dose-effect relationships based on their actually delivered doses: implications for adaptive replanning in radiation therapy of head-and-neck cancer. Int J Radiat Oncol Biol Phys 2013;87:676-82.

[12] Castelli J, Simon A, Louvel G, et al. Impact of head and neck cancer adaptive radiotherapy to spare the parotid glands and decrease the risk of xerostomia. Radiat Oncol 2015;10:6.

[13] Zhang P, Simon A, Rigaud B, et al. Optimal adaptive IMRT strategy to spare the parotid glands in oropharyngeal cancer. Radiother Oncol 2016;120:41-7.

[14] Castelli J, Simon A, Rigaud B, et al. A Nomogram to predict parotid gland overdose in head and neck IMRT. Radiat Oncol 2016;11:79.

[15] Bhide SA, Davies M, Burke K, et al. Weekly volume and dosimetric changes during chemoradiotherapy with intensity-modulated radiation therapy for head and neck cancer: a prospective observational study. Int J Radiat Oncol Biol Phys 2010;76:1360-8.

[16] Ahn PH, Chen CC, Ahn AI, et al. Adaptive planning in intensity-modulated radiation therapy for head and neck cancers: single-institution experience and clinical implications. Int J Radiat Oncol Biol Phys 2011;80:677-85.

[17] Capelle L, Mackenzie M, Field C, et al. Adaptive radiotherapy using helical tomotherapy for head and neck cancer in definitive and postoperative settings: initial results. Clin Oncol (R Coll Radiol) 2012;24:208-15.

[18] Dewan A, Sharma S, Dewan A, et al. Impact of Adaptive Radiotherapy on Locally Advanced Head and Neck Cancer - A Dosimetric and Volumetric Study. Asian Pac J Cancer Prev 2016;17:985-92.

[19] Castadot P, Geets X, Lee JA, et al. Adaptive functional image-guided IMRT in pharyngo-laryngeal squamous cell carcinoma: is the gain in dose distribution worth the effort? Radiother Oncol 2011;101:343-50.
[20] Chen C, Fei Z, Chen L, et al. Will weight loss cause significant dosimetric changes of target volumes and organs at risk in nasopharyngeal carcinoma treated with intensity-modulated radiation therapy? Med Dosim 2014;39:34-7.
[21] Schwartz DL, Garden AS, Shah SJ, et al. Adaptive radiotherapy for head and neck cancer--dosimetric results from a prospective clinical trial. Radiother Oncol 2013;106:80-4.
[22] Olteanu LA, Berwouts D, Madani I, et al. Comparative dosimetry of three-phase adaptive and non-adaptive dose-painting IMRT for head-and-neck cancer. Radiother Oncol 2014;111:348-53.
[23] Jensen AD, Nill S, Huber PE, et al. A clinical concept for interfractional adaptive radiation therapy in the treatment of head and neck cancer. Int J Radiat Oncol Biol Phys 2012;82:590-6.
[24] Hansen EK, Bucci MK, Quivey JM, et al. Repeat CT imaging and replanning during the course of IMRT for head-and-neck cancer. Int J Radiat Oncol Biol Phys 2006;64:355-62.
[25] Schwartz DL, Garden AS, Thomas J, et al. Adaptive radiotherapy for head-and-neck cancer: initial clinical outcomes from a prospective trial. Int J Radiat Oncol Biol Phys 2012;83:986-93.
[26] Lai YL, Yang SN, Liang JA, et al. Impact of body-mass factors on setup displacement in patients with head and neck cancer treated with radiotherapy using daily on-line image guidance. Radiat Oncol 2014;9:19.
[27] Kataria T, Gupta D, Goyal S, et al. Clinical outcomes of adaptive radiotherapy in head and neck cancers. Br J Radiol 2016;89:20160085.
[28] Yang H, Hu W, Wang W, et al. Replanning during intensity modulated radiation therapy improved quality of life in patients with nasopharyngeal carcinoma. Int J Radiat Oncol Biol Phys 2013;85:e47-54.
[29] Zhao L, Wan Q, Zhou Y, et al. The role of replanning in fractionated intensity modulated radiotherapy for nasopharyngeal carcinoma. Radiother Oncol 2011;98:23-7.
[30] Kam MK, Leung SF, Zee B, et al. Prospective randomized study of intensity-modulated radiotherapy on salivary gland function in early-stage nasopharyngeal carcinoma patients. J Clin Oncol 2007;25:4873-9.
[31] Nutting CM, Morden JP, Harrington KJ, et al. Parotid-sparing intensity modulated versus conventional radiotherapy in head and neck cancer (PARSPORT): a phase 3 multicentre randomised controlled trial. Lancet Oncol 2011;12:127-36.
[32] Pow EH, Kwong DL, McMillan AS, et al. Xerostomia and quality of life after intensity-modulated radiotherapy vs. conventional radiotherapy for early-stage nasopharyngeal carcinoma: initial report on a randomized controlled clinical trial. Int J Radiat Oncol Biol Phys 2006;66:981-91.
[33] Feng FY, Kim HM, Lyden TH, et al. Intensity-modulated chemoradiotherapy aiming to reduce dysphagia in patients with oropharyngeal cancer: clinical and functional results. J Clin Oncol 2010;28:2732-8.
[34] Chajon E, Lafond C, Louvel G, et al. Salivary gland-sparing other than parotid-sparing in definitive head-and-neck intensity-modulated radiotherapy does not seem to jeopardize local control. Radiat Oncol 2013;8:132.
[35] Deasy JO, Moiseenko V, Marks L, et al. Radiotherapy dose-volume effects on salivary gland function. Int J Radiat Oncol Biol Phys 2010;76:S58-63.
[36] Lyman JT. Complication probability as assessed from dose-volume histograms. Radiat Res Suppl 1985;8:S13-9.
[37] Dijkema T, Raaijmakers CP, Ten Haken RK, et al. Parotid gland function after radiotherapy: the combined michigan and utrecht experience. Int J Radiat Oncol Biol Phys 2010;78:449-53.

[38] Rigaud B, Simon A, Castelli J, et al. Evaluation of deformable image registration methods for dose monitoring in head and neck radiotherapy. Biomed Res Int 2015;2015:726268.
[39] Fitzpatrick JM, Hill DL, Shyr Y, et al. Visual assessment of the accuracy of retrospective registration of MR and CT images of the brain. IEEE Trans Med Imaging 1998;17:571-85.
[40] Dice LR. Measures of the amount of ecologic association between species. Ecology 1945;26:297-302.
[41] Graves YJ, Smith AA, McIlvena D, et al. A deformable head and neck phantom with in-vivo dosimetry for adaptive radiotherapy quality assurance. Med Phys 2015;42:1490-7.
[42] Kirby N, Chuang C, Pouliot J. A two-dimensional deformable phantom for quantitatively verifying deformation algorithms. Med Phys 2011;38:4583-6.
[43] Tsuji SY, Hwang A, Weinberg V, et al. Dosimetric evaluation of automatic segmentation for adaptive IMRT for head-and-neck cancer. Int J Radiat Oncol Biol Phys 2010;77:707-14.
[44] Lim JY, Leech M. Use of auto-segmentation in the delineation of target volumes and organs at risk in head and neck. Acta Oncol 2016;55:799-806.
[45] Brouwer CL, Steenbakkers RJ, Langendijk JA, et al. Identifying patients who may benefit from adaptive radiotherapy: Does the literature on anatomic and dosimetric changes in head and neck organs at risk during radiotherapy provide information to help? Radiother Oncol 2015;115:285-94.
[46] Brown E, Owen R, Harden F, et al. Predicting the need for adaptive radiotherapy in head and neck cancer. Radiother Oncol 2015;116:57-63.
[47] Surucu M, Shah KK, Mescioglu I, et al. Decision Trees Predicting Tumor Shrinkage for Head and Neck Cancer: Implications for Adaptive Radiotherapy. Technol Cancer Res Treat 2016;15:139-45.
[48] Pugachev A, Ruan S, Carlin S, et al. Dependence of FDG uptake on tumor microenvironment. Int J Radiat Oncol Biol Phys 2005;62:545-53.
[49] Madani I, Duthoy W, Derie C, et al. Positron emission tomography-guided, focal-dose escalation using intensity-modulated radiotherapy for head and neck cancer. Int J Radiat Oncol Biol Phys 2007;68:126-35.
[50] Vanderstraeten B, De Gersem W, Duthoy W, et al. Implementation of biologically conformal radiation therapy (BCRT) in an algorithmic segmentation-based inverse planning approach. Phys Med Biol 2006;51:N277-86.
[51] Geets X, Tomsej M, Lee JA, et al. Adaptive biological image-guided IMRT with anatomic and functional imaging in pharyngo-laryngeal tumors: impact on target volume delineation and dose distribution using helical tomotherapy. Radiother Oncol 2007;85:105-15.
[52] Differding S, Sterpin E, Janssens G, et al. Methodology for adaptive and robust FDG-PET escalated dose painting by numbers in head and neck tumors. Acta Oncol 2016;55:217-25.
[53] Berwouts D, Olteanu LA, Duprez F, et al. Three-phase adaptive dose-painting-by-numbers for head-and-neck cancer: initial results of the phase I clinical trial. Radiother Oncol 2013;107:310-6.
[54] Duprez F, De Neve W, De Gersem W, et al. Adaptive dose painting by numbers for head-and-neck cancer. Int J Radiat Oncol Biol Phys 2011;80:1045-55.
[55] Berwouts D, Madani I, Duprez F, et al. Long-term outcome of 18 F-fluorodeoxyglucose-positron emission tomography-guided dose painting for head and neck cancer: Matched case-control study. Head Neck 2017.
[56] Beltran M, Ramos M, Rovira JJ, et al. Dose variations in tumor volumes and organs at risk during IMRT for head-and-neck cancer. J Appl Clin Med Phys 2012;13:101-111.
[57] Height R, Khoo V, Lawford C, et al. The dosimetric consequences of anatomic changes in head and neck radiotherapy patients. J Med Imaging Radiat Oncol 2010;54:497-504.
[58] Ho KF, Marchant T, Moore C, et al. Monitoring dosimetric impact of weight loss with kilovoltage (kV) cone beam CT (CBCT) during parotid-sparing IMRT and concurrent chemotherapy. Int J Radiat Oncol Biol Phys 2012;82:e375-82.

[59] Marzi S, Pinnaro P, D'Alessio D, et al. Anatomical and dose changes of gross tumour volume and parotid glands for head and neck cancer patients during intensity-modulated radiotherapy: effect on the probability of xerostomia incidence. Clin Oncol (R Coll Radiol) 2012;24:e54-62.
[60] O'Daniel JC, Garden AS, Schwartz DL, et al. Parotid gland dose in intensity-modulated radiotherapy for head and neck cancer: is what you plan what you get? Int J Radiat Oncol Biol Phys 2007;69:1290-6.
[61] Orban de Xivry J, Castadot P, Janssens G, et al. Evaluation of the radiobiological impact of anatomic modifications during radiation therapy for head and neck cancer: can we simply summate the dose? Radiother Oncol 2010;96:131-8.
[62] Robar JL, Day A, Clancey J, et al. Spatial and dosimetric variability of organs at risk in head-and-neck intensity-modulated radiotherapy. Int J Radiat Oncol Biol Phys 2007;68:1121-30.
[63] Yip C, Thomas C, Michaelidou A, et al. Co-registration of cone beam CT and planning CT in head and neck IMRT dose estimation: a feasible adaptive radiotherapy strategy. Br J Radiol 2014;87:20130532.

Au total, la radiothérapie adaptative semble apporter un bénéfice en termes de contrôle local (qui pourrait s'expliquer par l'amélioration de la couverture tumorale comme décrit précédemment) et en termes de diminution de la toxicité. Cependant il apparait clairement que tous les patients ne bénéficient pas d'une telle approche. Des outils d'aide à la décision de replanification [69, 91], ou de prédiction du risque de déviation de la dose délivrée par rapport à la dose planifiée [92] sont donc indispensables.

Même si le processus optimal de replanification n'a pas été clairement défini, il peut se définir selon le schéma suivant : la première étape est l'acquisition d'une imagerie 3D sous l'appareil de traitement (actuellement CBCT ou MVCT, prochainement l'IRM). Après propagation des contours par un algorithme de recalage élastique depuis le scanner de planification vers l'imagerie du jour, une approche de radiothérapie guidée par la dose serait proposée en comparant la dose cumulée par rapport à la dose planifiée. En cas de décision de replanification, une nouvelle distribution de dose serait alors calculée, en prenant en compte la dose précédemment délivrée. Afin de maximiser le bénéfice de la radiothérapie adaptative, cette replanification serait réalisée en direct, avec l'aide d'outils de planification automatiques [93, 94]. Afin de tendre vers ce schéma, plusieurs optimisations restent nécessaires, notamment pour le calcul de dose sur l'imagerie embarquée, l'amélioration des algorithmes de recalage élastique pour la propagation de contours et le cumul de dose et enfin l'utilisation d'outils de planification automatique.

5.1.2 Radiothérapie adaptative guidée par la dose

L'approche de replanification systématique, même si elle ciblée sur les patients pour lequel le bénéfice potentiel est le plus élevé, ne prend pas en compte les spécificités individuelles. Il est donc également possible d'envisager une approche plus personnalisée, reposant sur un suivi (*monitoring*) de la dose en cours de traitement. Ce monitoring de dose peut être réalisé en utilisant les systèmes d'imagerie embarquée sur les accélérateurs de traitement. Les *Cone Beam CT* (CBCT) utilisés pour le repositionnement des patients pourraient ainsi permettre d'estimer la dose reçue par le patient. Deux problématiques limitent aujourd'hui cette utilisation. La 1ière concerne la qualité d'image médiocre du CBCT, avec une résolution spatiale, un champ de vue et un contraste inférieurs à celui d'un scanner. La 2ième est en lien avec le calcul de dose, qui nécessite l'information de densité électronique (basé sur les unités Hounsfield (UH)). Les CBCT ne permettent pas d'obtenir directement les UH, rendant impossible le calcul direct de la dose. Plusieurs méthodes ont cependant été décrites pour permettre le calcul de dose sur CBCT. La 1ière méthode consiste à réaliser une calibration du CBCT. Cette méthode donne des résultats corrects, avec une différence de dose de moins de 3% entre le CBCT et le scanner pour des cancers des VADS [95-99]. Cependant pour certains patients, la différence peut être beaucoup plus marquée (jusqu'à 15% [100]), et la calibration doit être ajustée en fonction de la localisation tumorale et de l'anatomie du patient. Afin de pallier à ces inconvénients, une autre approche consiste à attribuer des densités électroniques aux structures anatomiques suivant des classes de tissus (air, eau, os). Cette approche semble permettre une précision de calcul de dose satisfaisante mais a seulement été évaluée dans un petit nombre d'études ayant inclus moins de 10 patients [95, 98]. Les premiers résultats de notre équipe sur 15 patients montrent que le calcul de dose en 3 classes de densités est faisable, avec de faibles écarts dosimétriques par rapport au calcul sur CT pour la dose moyenne aux parotides (0,2 %), la dose reçue par 2% de la moelle (0,6 %) et la couverture des PTV (0,15 %). La Figure 16 illustre un exemple des incertitudes de dose pour un patient.

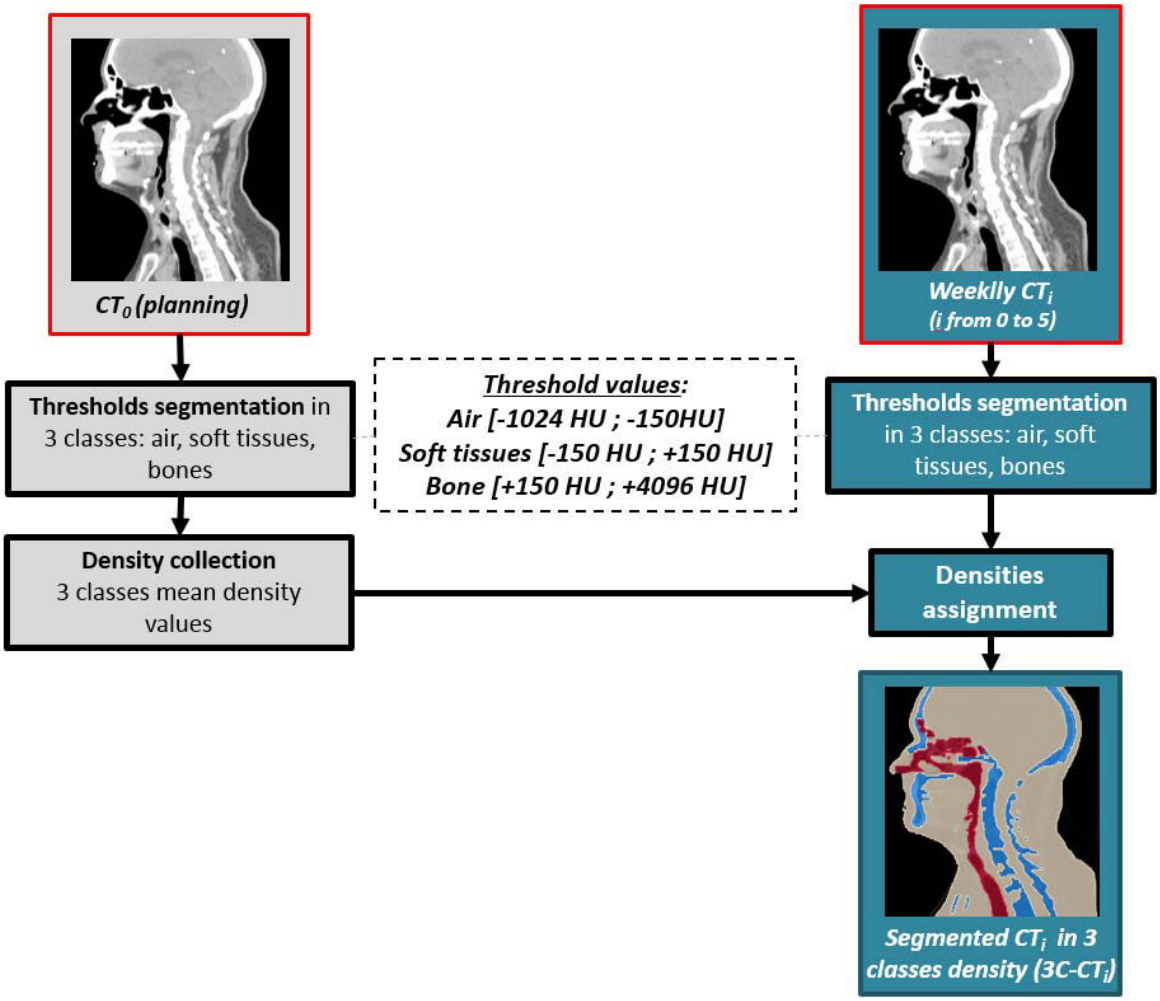

Figure 15 : Description de la méthode de densité 3 classes

L'indice I correspond au moment de la replanification, depuis (scanner initial) jusqu'à 5 (replanification à la 5eme semaine de traitement). Chaque scanner (CT_0 et CT_i, i de1 à 5) est segmenté en 3 classes (air, tissus mous et os), chacun avec un seuillage spécifique. Les densités moyennes pour chacune des 3 classes sont ensuite assignées dans le logiciel de planification en utilisation les valeurs moyennes issues du scanner de planification. Le calcul de dose est ensuite réalisé avec ces densités.

(From A. Barateau, N. Perichon, **J. Castelli** *et al*. Submitted Acta Oncologica 2017 Oct.)

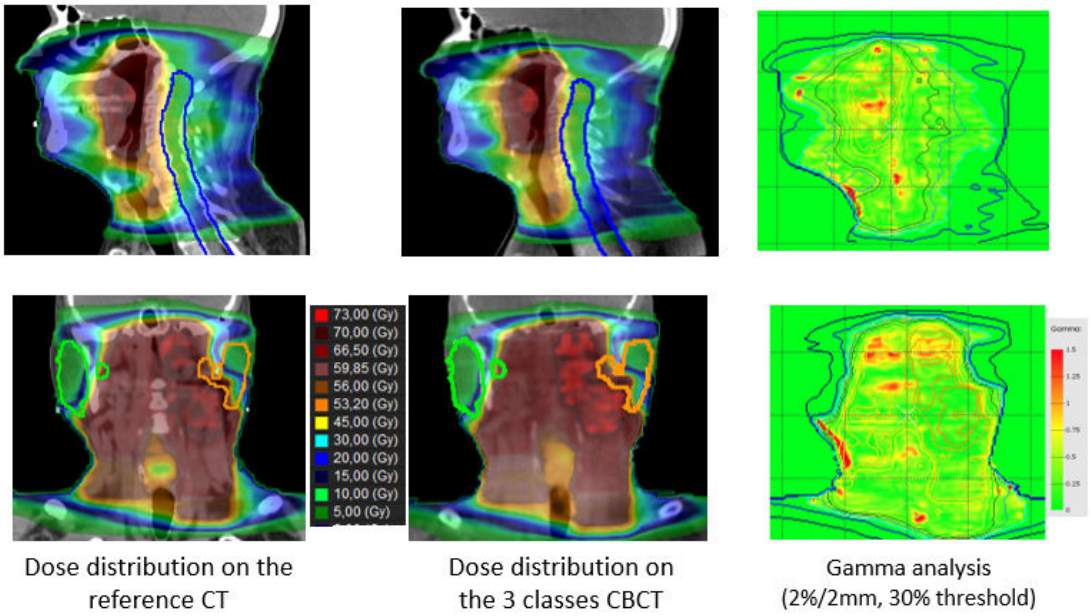

Figure 16 : Example of spatial dose uncertainties using the density assignment method on CBCT images

A gamma analysis was performed between dose distributions calculated on CT and dose distributions calculated from a three density class CBCT image. Both images (CT and CBCT) have been acquired the same day. The ipsilateral parotid gland is delineated in orange, the contralateral parotid gland in green and the spinal cord in blue.

(From A. Barateau, N. Perichon, **J. Castelli** *et al*. Submitted Acta Oncologica 2017 Oct.)

Un monitoring de la dose reposant sur cette approche semble donc acceptable, pouvant ainsi permettre une approche de radiothérapie adaptative guidée par la dose et plus précisément par la différence de dose entre la dose moyenne planifiée et la dose délivrée aux parotides (Figure 17).

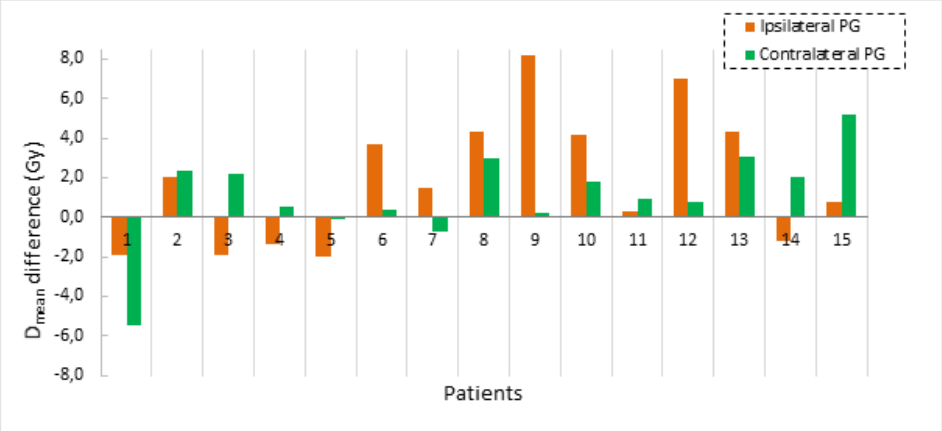

Figure 17 : Parotid gland dose difference between cumulated dose and planning dose (without replanning) The mean dose (D_{mean}) are considered. Positive difference means a parotid gland (PG) overdosage. (From A. Barateau, N. Perichon, **J. Castelli** *et al*. Submitted Acta Oncologica 2017 Oct.)

La visualisation des volumes d'intérêt sur CBCT reste cependant un facteur limitant. Suite au récent développement d'une IRM couplée avec un accélérateur [101], l'IRM peut aussi être considérée pour une approche de radiothérapie adaptative guidée par la dose. Si le problème de visualisation des volumes d'intérêt ne se pose pas sur l'IRM du fait de sa résolution spatiale et de son bon contraste, l'absence de densité électronique rend actuellement impossible le calcul direct de la dose. Comme pour le CBCT, plusieurs techniques, résumée dans la Table 6, ont été décrites pour rendre possible la réalisation d'une dosimétrie sur IRM. Deux grandes approches ont été développées, d'une part la génération d'une image de substitution tomodensitométrique à partir de l'IRM sur laquelle est finalement réalisée la planification, et d'autre part le calcul direct de dose à partir d'IRM en se basant sur des hypothèses physiques. La première méthode semble la plus réaliste à l'heure actuelle.

Table 6 : Planification d'une radiothérapie à partir d'IRM : principe, avantages et inconvénients des différentes méthodes de calcul de dose.

Méthodes de calcul de dose à partir d'IRM	Principe	Avantages	Inconvénients
Segmentation et assignation de densité	Délinéation de volumes d'intérêt sur l'IRM du patient manuelle ou automatique, puis attribution d'une valeur de densité (électronique ou physique) à chaque région définissant une pseudo-tomodensitométrie	Simplicité de la méthodologie	Forte dépendance à l'opérateur (délinéation manuelle) Temps de calcul long (délinéation automatique)
			Erreurs de segmentation Homogénéité de la densité des tissus Dose moins précise Restreint à certaines localisations
Atlas	Mise en correspondance par paires d'une base d'apprentissage d'images de tomodensitométrie et remnographiques avec l'IRM du patient, suivie d'une fusion des tomodensitométries pour générer une pseudo tomodensitométrie spécifique du patient. Les principales opérations concernent le recalage dans une approche multi-atlas	Méthode totalement automatisée	Temps de calcul long
		Bonne précision de la dose calculée Hétérogénéité de la densité tissulaire Délinéation automatique des volumes d'intérêt Génération de radiographies bidimensionnelles numériquement reconstruites précises Généricité anatomique	Sensible aux dissimilarités anatomiques Incertitude causée par les erreurs de recalage Lissage des intensités de la pseudo tomodensitométrie
Apprentissage statistique (*machine learning*)	Dans une base d'images, modélisation des relations liant les intensités des voxels des IRM et des scanographies à l'aide d'outils de *machine learning*, puis application du modèle sur l'IRM du patient définissant une pseudo tomodensitométrie. Le modèle est établi en deux temps : apprentissage (générer le modèle) et validation (application au patient)	Rapidité d'exécution	Nombre de classes déterminé empiriquement
		Bonne précision de la dose estimée	Pas de délinéation automatique des volumes d'intérêt
		Une seule étape de recalage Génération des radiographies bidimensionnelles numériquement reconstruites précises Hétérogénéité de la densité tissulaire	Erreur de classification
Physique	Estimation de la dose par un algorithme Monte-Carlo basé sur la concentration d'hydrogène quantifiée à partir de l'IRM du patient	Pas de détermination de pseudo tomodensitométrie	Spécificité de l'algorithme de calcul de dose Monte-Carlo
		Pas d'erreur de recalage	Quantification de la concentration d'hydrogène tissulaire Mesure incertaine de la densité de protons de certains tissus (collagène et cortical osseuse)

(Source : Planification à partir d'imagerie par résonance magnétique en radiothérapie. A. Largent, J.C. nunes, C. Lafond, N. Perichon, J. Castelli, *et al*. Cancer. Radiother. 2017)

5.1.4 Questions méthodologiques tenant à l'évaluation de la dose cumulée

Une des difficultés majeures lors de l'évaluation du bénéfice d'une stratégie de radiothérapie adaptative tient en effet à l'estimation de la dose cumulée sans ou avec replanification. Au vu de l'impossibilité de sommer les HDV, il est nécessaire d'utiliser des techniques de recalage élastique afin de réaliser cette estimation. Cependant la dose cumulée ainsi estimée est fortement dépendante de la précision des algorithmes de recalage élastique. Ceci est d'autant plus problématique dans les zones avec un fort gradient de dose, notamment à proximité des parotides. Nous avons ainsi évalué la précision de 10 méthodes de recalage élastique pour 15 patients, chacun avec 6 scanners. Quatorze repères anatomiques ont été utilisés. Les résultats montrent que si la précision spatiale était très bonne (1 à 2 mm), l'impact sur l'erreur d'estimation de la dose pouvait être important (2 à 5 Gy pour les parotides) (Table 7).

Table 7 : Average cumulated dose (Gy) error by landmarks and by registration methods with the first observer as anatomical reference.

	Landmark dose (Gy)															
	Bones						Soft tissues								Precision (AVG)	Accuracy (AVG SD)
	1	2	3	4	5	6	7	8	9	10	11	12	13	14		
Planned dose	44.47	35.13	54.87	64.91	63.64	8.84	44.50	64.74	21.60	66.87	66.91	63.95	39.71	41.37	48.68	10.35
Cumulated dose difference*	1.95	1.96	1.68	1.96	1.71	3.09	2.87	2.55	2.52	1.93	0.69	1.12	5.17	4.25	2.39	2.40
	Landmark Cumulated Dose Error (Gy)															
Interobserver variability	0.41	0.23	0.29	0.38	0.67	0.26	0.28	0.31	0.41	0.77	0.14	0.61	1.68	3.14	0.68	0.75
FFD MI filtered CTs	0.36	0.60	0.43	0.58	0.69	0.43	0.41	0.59	0.63	0.74	0.91	0.48	2.63	2.41	0.85	0.93
Demons MI filtered CTs	0.40	0.39	0.60	0.57	0.71	0.33	0.45	0.41	1.09	0.75	0.69	0.78	2.74	2.46	0.88	0.95
Demons MI	0.33	0.39	0.57	0.54	0.69	0.38	0.48	0.47	1.11	0.90	0.73	0.80	2.56	2.33	0.88	0.92
Demons MSE	0.41	0.52	0.42	0.48	0.88	0.40	0.43	0.56	0.85	1.38	0.74	0.75	3.15	2.96	0.99	1.22
FFD MSE filtered CTs	0.49	0.69	0.52	0.59	0.86	0.55	0.38	0.83	0.95	0.83	0.98	0.57	2.37	3.09	0.98	1.09
FFD MI	0.31	0.63	0.47	0.53	0.53	0.48	0.61	0.82	1.09	0.84	0.85	0.85	2.45	2.68	0.94	1.02
Demons MSE filtered CTs	0.41	0.52	0.42	0.48	0.88	0.40	0.43	0.56	0.85	1.38	0.74	0.75	3.15	2.96	0.99	1.25
FFD MSE	0.34	1.16	1.13	1.27	1.02	0.45	0.92	1.34	1.88	1.26	1.06	1.86	2.75	3.91	1.45	1.60
Demons D. maps	0.99	1.29	3.11	1.19	1.24	0.53	0.94	1.28	1.76	2.39	1.29	2.22	3.05	5.14	1.89	2.14
FFD D. maps	0.95	1.56	1.24	0.94	1.53	0.53	1.00	1.54	2.66	2.90	1.32	2.54	2.99	4.87	1.90	2.18
Rigid MSE	0.94	1.67	1.20	2.78	1.80	0.59	1.02	1.71	3.35	3.99	1.35	2.61	3.44	4.27	2.19	2.60

AVG: average, AVG SD: average standard deviation, FFD: free form deformation, MSE: mean squared error, MI: mutual information, and CT: computed tomography (scan).
Methods are classified by their performance order. The performance is defined by the accuracy (average of the cumulated dose error) and the precision (average of the standard deviation cumulated dose error).
The cumulated dose difference (∗) represents the reference difference between planned and cumulated doses from the first observer. A second observer allows quantifying the interobserver variability.
The "FFD with MI on filtered CTs" errors are inferior to all the methods errors ($P < 0.03$), except for the "demons with MI on filtered CTs" and "demons with MI on original CTs" methods and for the "demons with MSE on original CTs" ($P = 0.06$). The "demons with MI on filtered CTs" errors are inferior to the "delineation maps based method" errors, the "demons with MSE on filtered CTs" errors, and the "FFD MSE on original CTs" errors (respectively, $P < 0.01$, $P \leq 0.03$ and $P < 0.01$).

(Source : B.Rigaud, A.Simon, **J.Castelli**, *et al.* Biomed. Res. Int. 2015)

Cette différence de précision peut ainsi conduire à des différences de dose estimée de plusieurs Gy entre les différents algorithmes comme illustré dans la Figure 18.

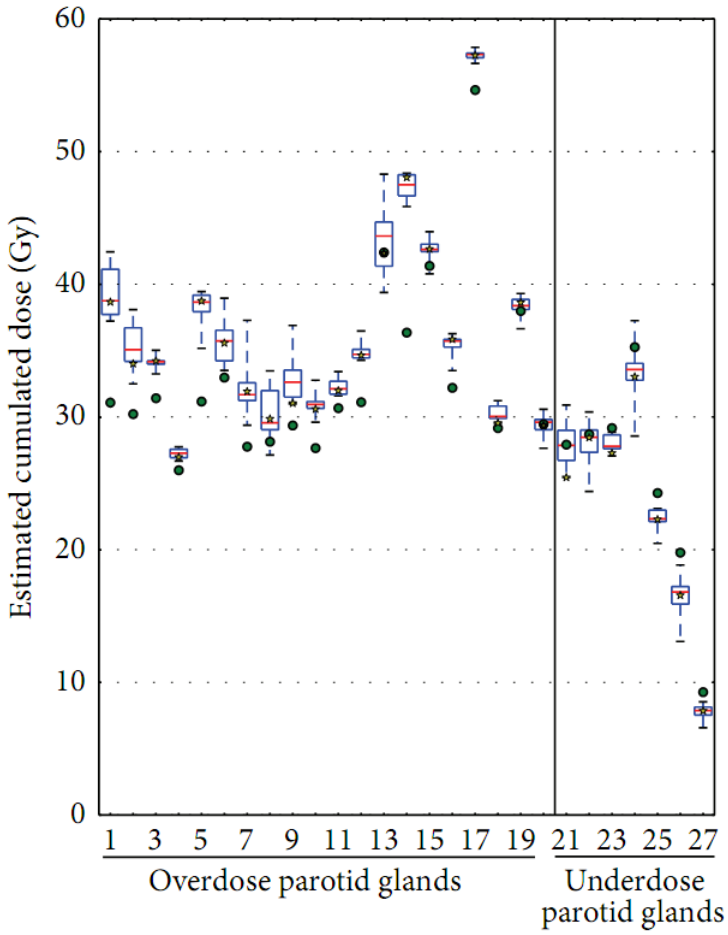

Figure 18 : Variability between estimated cumulated dose by method for the same organ with the mean dose in the parotid gland (overdose and underdose).

The green points represent the planned dose and the yellow stars represent the value returned by the free form deformation with mutual information metric on filtered CT-scans method. The limits of each box represent the 25th and 75th percentiles, the whisker represents the min and the max value, and the red line represents the median (50% of the total values). Each boxplot is represented without the outliers.

(Source : B.Rigaud, A.Simon, **J.Castelli**, *et al.* Biomed. Res. Int. 2015)

5.1.5 Limites de nos travaux

Plusieurs limites sont à souligner au regard des travaux que nous avons mené dans le domaine de la radiothérapie adaptative morphologique. Tout d'abord, il s'agit d'études de modélisation ayant portées sur un nombre restreint de patients (15 à 37 patients). Nous avons fait le choix de réaliser un cumul de dose par recalage élastique pour les parotides. Au vu des résultats d'évaluation de la précision de ces méthodes, une imprécision de l'autre du Gy demeure pour la dose cumulée. La prudence voudrait donc de ne considérer comme significatif que les patients présentant un surdosage d'au moins 1 Gy dans la parotide. La pertinence clinique d'un tel surdosage reste imprécise, car même si nous avons utilisé un modèle NTCP pour estimer une diminution de 10% du risque de xérostomie, ces modèles ont été construits en considérant la dose planifiée et non pas la dose délivrée. Concernant le volume cible, il n'est pas été possible de réaliser un cumul de dose par recalage élastique du fait de la fonte tumorale. Nous avons choisi de représenter la dose cumulée par la moyenne de la dose moyenne et de la dose reçue par 98 % et 2% du volume. La pertinence clinique de ces paramètres reste cependant à démontrer. Une autre limite tient à la fréquence d'échantillonnage du scanner réalisé une fois par semaine, qui ne permet que d'avoir une estimation de l'impact des variations anatomiques. Cependant, pour les cancers des VADS, du fait de l'apparition progressive des variations anatomiques, cet échantillonnage hebdomadaire peut être suffisant. Pour le calcul de la dose délivrée sans replanification, l'estimation a été faite à partir d'un recalage sur l'isocentre, ce qui ne correspond pas à une véritable approche de radiothérapie guidée par l'image. Cette différence pourrait entrainer une majoration des variations dosimétriques observées en lien avec une erreur de positionnement [67]. Enfin nous avons simulé une approche de radiothérapie adaptative en temps réel, difficile à mettre en place en routine clinique. Une approche en temps différé, plus réaliste, pourrait avoir un bénéfice moins important. La dernière limite majeure tient au fait qu'il s'agit d'études *in silico*, sans validation externe et surtout sans résultat clinique pour le moment. Au vu de la lourdeur de la technique,

seul un bénéfice clinique franc permettra l'adoption de la radiothérapie adaptative en routine quotidienne.

Au total, au vu de nos résultats et des limites de nos travaux, il apparait nécessaire de poursuivre les modélisations sur un plus grand nombre de patients. Idéalement, ces outils devraient reposer sur des critères anatomiques simples, ne nécessitant pas de recalculer la dose à la première semaine. Une validation prospective des outils de prédiction de surdosage des parotides et de sous dosage de la tumeur est par ailleurs indispensable. Il sera également nécessaire d'évaluer la différence de dose estimée entre un recalage sur l'isocentre et une approche de radiothérapie guidée par l'image. Enfin les algorithmes de recalage élastique doivent être améliorés et leur précision doit être évaluée, idéalement sur fantômes [102, 103], afin d'améliorer les résultats de cumul de dose. Cette étape d'évaluation sera clairement indispensable avant leur utilisation en routine clinique.

5.2 Radiothérapie adaptative métabolique

Nos travaux avaient pour but de déterminer des paramètres issus de l'imagerie métabolique permettant d'affiner le pronostic des patients à l'échelle individuelle. Nous avons confirmé la valeur pronostique indépendante de paramètres quantitatifs issus de la TEP pré-thérapeutique. Ces résultats ont été validés sur deux cohortes distinctes, issues de 2 centres différents. Nous avons ainsi pu réaliser une validation externe de notre modèle de prédiction de survie, et nous affranchir du caractère « centre dépendant » des paramètres proposés auparavant dans la littérature.

Plusieurs limites demeurent cependant dans l'utilisation de ces paramètres. Tout d'abord, même si les paramètres métaboliques ont été acquis sur 2 machines TEP différentes, il est nécessaire de réaliser une validation plus large avec des patients issus d'autres centres avec des TEP différentes. Ensuite, notre modèle de prédiction n'a été réalisé que sur des patients ayant une tumeur de l'oropharynx, et n'est basé que sur une analyse d'intensité de l'imagerie TEP. Il est possible que les paramètres soient différents pour les autres tumeurs des VADS. Par ailleurs nous n'avons pas

exploré l'utilisation d'une TEP acquise en cours de traitement. Les quelques études disponibles semblent montrer un intérêt à l'évaluation de la réponse métabolique en cours de traitement [104]. La question du meilleur moment pour réaliser cette TEP en cours de traitement est également cruciale. Cette évaluation doit être réalisée suffisamment tôt pour laisser le temps d'adapter le traitement tout en laissant le temps au traitement de commencer à agir. Si les alentours de la 2^{ième} semaine de traitement semblent être le meilleur choix [90, 104], la question reste entière actuellement. Certaines équipes ont aussi réalisé une escalade de dose guidée par l'information métabolique acquise en cours de traitement [43, 66, 105, 106]. Une des limites de cette approche reste l'absence de corrélation franche entre les paramètres métaboliques et le site de la récidive. En effet, si la récidive survient majoritairement dans le volume tumoral macroscopique [107, 108], aucune corrélation franche avec l'intensité du signal TEP n'a pu être établie pour le moment.

Au total, le développement de modèle TEP issu de cohorte multicentrique et intégrant différentes localisations au sein des VADS doit être poursuivi. La valeur prédictive de la TEP en cours de traitement doit être confirmée. L'analyse des sites de récidives et leurs relations avec l'information métabolique doit être réalisée afin de pouvoir développer une intensification thérapeutique ciblée sur les sous volumes à haut risque de récidive. Enfin une analyse de la texture du signal TEP nous semble nécessaire afin de mieux caractériser les sous volumes à risque de récidive.

6 Conclusion

La contribution de notre travail de thèse par rapport aux données de la littérature se situe sur les points suivants :

- Quantification de la dose délivrée aux parotides sans et avec radiothérapie adaptative : Nous avons montré qu'environ 2/3 des parotides présentaient un surdosage de plus de 2 Gy au cours d'une RCMI sans replanification. La réalisation d'une radiothérapie hebdomadaire systématique permettait de corriger ce surdosage dans tous les cas, permettant d'espérer une diminution en valeur absolue de 10 % du risque estimé de xérostomie.
- Identification des patients à risque de surdosage des parotides : en utilisant les données issues de 20 patients, nous avons pu développer un modèle de prédiction du risque de surdosage des parotides, permettant ainsi d'identifier les patients candidats à une radiothérapie adaptative.

- Stratégie optimale de radiothérapie adaptative pour épargner les parotides : chaque replanification supplémentaire apporte un bénéfice en termes d'épargne des parotides. Cependant la majeure partie de ce bénéfice est atteint après 3 replanifications. Dans le cas où une seule replanification est réalisée, elle doit être réalisée de façon précoce (dans les 2 premières semaines de traitement)

- Quantification de la dose délivrée à la tumeur : nous avons montré l'existence d'un sous dosage de la tumeur pour 50 % des patients en l'absence de radiothérapie adaptative. L'utilisation d'une stratégie de radiothérapie adaptative permet de corriger ce sous dosage et pourrait permettre d'augmenter le taux de contrôle local.

- Recalage élastique : le recalage élastique est une étape incontournable pour réaliser un cumul de dose. Nous avons montré que toutes les méthodes de recalage élastique comportent une incertitude de 2 à 3 Gy en fonction de l'organe considéré. Cette

incertitude doit être prise en compte lors de l'analyse des résultats de la radiothérapie adaptative.

- Radiothérapie adaptative métabolique : nous avons montré que la TEP pouvait être utilisée pour identifier les patients à haut risque de récidive et/ou de décès. Ces patients sont de bons candidats à une approche de radiothérapie adaptative pour maintenir la couverture tumorale, voire à une escalade de dose guidée par la TEP.

Au-delà des travaux de modélisation, le critère de jugement optimal reste le bénéfice clinique, idéalement observé au cours d'étude de phase III. Deux essais sont en cours dans cette optique. Le premier essai (ARTIX) compare une radiothérapie adaptative à une radiothérapie standard sans replanification. L'objectif principal est une diminution du taux de xérostomie à 1 an. J'interviens dans cet essai en tant que co-investigateur. Le deuxième essai (TEMPORAL, dont je suis coordonnateur) évalue la valeur prédictive de la TEP réalisée en cours de traitement (à la deuxième et quatrième semaine de traitement). Ces deux essais devraient terminer prochainement leurs recrutements.

7 Valorisations scientifiques

7.1 Publications en 1er auteur

- **A PET-based nomogram for oropharyngeal cancer**

  J. Castelli; A. Depeursinge; V. Ndoh; J. O. Prior; M. Ozsahin; A. Devillers; H. Bouchaab **;** E. Chajon **;** R. de Crevoisier; N. Scher ; F. Jegoux; B. Laguerre; B. De Bari; J. Bourhis

  Eur J Cancer, *2017 Apr, Vol 75(IF 6.16, Rang A)*

- **Metabolic Tumor Volume and Total Lesion Glycolysis in Oropharyngeal Cancer treated with definitive radiotherapy: Which threshold is the best predictor of local control ?**

  J.Castelli; A. Depeursinge; B. De Bari; A. Devillers; R. de Crevoisier; J. Bourhis; J.O. Prior

  Clin Nucl Med, *2017 Mar 10. doi: 10.1097 (IF 4.26, Rang B)*

- **Overview of the predictive value of quantitative 18 FDG PET in head and neck cancer treated with chemoradiotherapy**

  J.Castelli; B. De Bari; A. Depeursinge; A. Simon; A. Devillers; G. Roman Jimenez; J.O. Prior; M. Ozsahin; R. de Crevoisier; J. Bourhis

  Crit Rev Oncol Hematol, *2016 Dec;108:40-51. doi: 10.1016 (IF 5.03, Rang B)*

- **Nomogram to predict parotid gland overdose in Head & Neck IMRT**

  J.Castelli; A.Simon; B.Rigaud; C.Lafond; E.Chajon; J.D. Ospina; P.Haigron; B.Laguerre; K.Benezery; R. de Crevoisier

  Radiat. Oncol *2016 Jun 8;11(1):79 (IF 2.57, Rang D)*

- **Impact of head and neck cancer adaptive radiotherapy to spare the parotid glands and decrease the risk of xerostomia**

  J.Castelli, A.Simon, G.Louvel, O.Henry, E.Chajon, M.Nassef, P.Haigron, G.Cazoulat, J.D. Ospina, F.Jegoux, K.Benezery, R. de Crevoisier

  Radiat Oncol. *2015 Jan 9;10(1):6. (IF 2.46, Rang D)*

- **The role of imaging in adaptive radiotherapy for head and neck cancer**

  J. Castelli, A. Simon, O. Acosta, P. Haigron, M. Nassef, O. Henry, E. Chajon, R. de Crevoisier

  IRBM, *Volume 35, Issue 1, February 2014, Pages 33-40 (IF 0.62)*

7.2 Publications en tant que co-auteur

- **Optimal adaptive radiotherapy strategy in head and neck to spare the parotid gland**
  P.Zhang, A.Simon, B.Rigaud, **J.Castelli**, JD.Ospina, M.Nassef, O.Henry, P.Haigron, B.Li, H.Shu, R. de Crevoisier
  Radiother Oncol. *2016 Jun Jul;120(1):41-7 (IF 4.81, Rang B)*

- **La radiothérapie adaptative en routine ? Etat de l'art : point de vue du physicien médical**
  C.Lafond, A.Simon, O.Henry, N.Perichon, **J. Castelli**, O. Acosta, R. de Crevoisier
  Cancer Radiother. *Volume 19, Issues 6–7*, *October 2015*, *Pages 450-457 (IF 1.29, Rang E)*

- **Evaluation of deformable image registration methods for dose monitoring in head and neck radiotherapy**
  B.Rigaud, A.Simon, **J.Castelli**, M.Gobeli, J.D. Ospina, G.Cazoulat, O.Henry, P.Haigron, R. de Crevoisier
  BioMed Research International, *vol. 2015, Article ID 726268, 16 pages, 2015 (IF 2.13, Rang D)*

7.3 Article soumis

- **Adaptive radiotherapy for head and neck cancer**
  J.Castelli *et al*.

  Acta Oncol (IF 3.2) En revision

- **A density assignment method for dose monitoring in head-and-neck adaptive radiotherapy**
  A.Barateau, N. Perichon, **J. Castelli**, *et al*.
  Acta Oncol, soumis (Octobre 2017)

- **Adaptive radiotherapy in head and neck cancer to correct tumor underdose and parotid gland overdose**
  J.Castelli *et al***.**
  ***Radiother Oncol*.** (IF 4.3) Soumis (Octobre 2017)

- **Deformable image registration for radiation therapy: principle, methods, applications and evaluation**
  B. Rigaud, A. Simon, **J.Castelli** et al.
  Radiat Oncol (IF 2.5) Soumis (Octobre 2017)

7.4 Communications dans des congrès

- **A PET-based nomogram to predict survival in oropharyngeal cancers radiotherapy**
  ESTRO 36th, Vienne, Autriche, Mai 2017
  J.Castelli ; *et al.*

- **A 3-class density method to monitor the dose in the parotid gland and the spinal cord in oropharynx cancer IMRT**
  ESTRO 36th, Vienne, Autriche, Avril 2017
  N.Perichon, O.Henry, C.Lafond, **J.Castelli**, *et al.*

- **Optimale adaptive radiotherapy strategy in head and neck to spare the parotid glands**
  ESTRO 35th, Turin, Italie, Avril 2016
  J.Castelli, *et al.*

- **Evaluation of deformable image registration methods for dose monitoring in head and neck adaptive radiotherapy**
  ESTRO 3rd Forum, Barcelone, Espagne, Avril 2015
  B. Rigaud; A. Simon, **J. Castelli**, *et al.*

- **Nomograms to assess the parotid gland dose in head and neck IMRT based on anatomical markers**
  ESTRO 3rd Forum, Barcelone, Espagne, Avril 2015
  J. Castelli, *et al.*

- **Impact of weekly re-planning to spare the parotid glands in head and neck cancer radiotherapy**
  ASTRO 56th, San Francisco, USA, Septembre 2014
  J.Castelli, *et al.*

- **Anatomical markers of parotid overdosage within the course of locally advanced head and neck IMRT guiding an adaptive RT strategy**
  ESTRO 33th, Vienne, Autriche, Avril 2014
  J.Castelli; *et al.*

- **Does adaptive radiotherapy in head and neck cancer decrease xerostomia?**
  ESMO - ECCO – ESTRO, Amsterdam, Hollande, Septembre 2013
  J.Castelli; *et al.*

- **Valeur de la TEP au 18-FDG pour prédire la récidive dans les cancers ORL non oropharyngé pris en charge par chimioradiothérapie**
  28 éme congrès de la SFRO, Paris, France, Octobre 2017
  Castelli J., *et al.*

- **Quantification de la dose cumulée délivrée aux parotides, avec ou sans replanification, à partir de tomographies coniques**
  28 éme congrès de la SFRO, Paris, France, Octobre 2017
  Barateau A., Perichon N., Couespel S., **Castelli J**., *et al.*

- **Peut-on calculer une distribution de dose à partir de tomographies coniques pour monitorer la dose délivrée en cours de radiothérapie ORL ?**
  28 éme congrès de la SFRO, Paris, France, Octobre 2017
  Barateau A., Perichon N., Couespel S., **Castelli J**., *et al.*

- **Radiothérapie adaptive des cancers ORL : bénéfice sur la couverture du volume tumoral**
  28 éme congrès de la SFRO, Paris, France, Octobre 2017
  Castelli J., *et al.*

- **Stratégie optimale de radiothérapie adaptative dans les cancers ORL localement avancés**
  26 éme congrès de la SFRO, Paris, France, Octobre 2015
  J.Castelli; *et al.*

- **Nomogramme pour prédire le surdosage parotidien au cours d'une RCMI pour cancers ORL**
  26 éme congrès de la SFRO, Paris, France, Octobre 2015
  J.Castelli; *et al.*

8 Références

1. Kam, M.K., et al., *Prospective randomized study of intensity-modulated radiotherapy on salivary gland function in early-stage nasopharyngeal carcinoma patients.* J Clin Oncol, 2007. **25**(31): p. 4873-9.
2. Nutting, C.M., et al., *Parotid-sparing intensity modulated versus conventional radiotherapy in head and neck cancer (PARSPORT): a phase 3 multicentre randomised controlled trial.* Lancet Oncol, 2011. **12**(2): p. 127-36.
3. Pow, E.H., et al., *Xerostomia and quality of life after intensity-modulated radiotherapy vs. conventional radiotherapy for early-stage nasopharyngeal carcinoma: initial report on a randomized controlled clinical trial.* Int J Radiat Oncol Biol Phys, 2006. **66**(4): p. 981-91.
4. Feng, F.Y., et al., *Intensity-modulated chemoradiotherapy aiming to reduce dysphagia in patients with oropharyngeal cancer: clinical and functional results.* J Clin Oncol, 2010. **28**(16): p. 2732-8.
5. Chajon, E., et al., *Salivary gland-sparing other than parotid-sparing in definitive head-and-neck intensity-modulated radiotherapy does not seem to jeopardize local control.* Radiat Oncol, 2013. **8**: p. 132.
6. Torre, L.A., et al., *Global cancer statistics, 2012.* CA Cancer J Clin, 2015. **65**(2): p. 87-108.
7. Hashibe, M., et al., *Interaction between Tobacco and Alcohol Use and the Risk of Head and Neck Cancer: Pooled Analysis in the International Head and Neck Cancer Epidemiology Consortium.* Cancer Epidemiology Biomarkers & Prevention, 2009. **18**(2): p. 541-550.
8. Psyrri, A., P. Gouveris, and J.B. Vermorken, *Human papillomavirus-related head and neck tumors: clinical and research implication.* Curr Opin Oncol, 2009. **21**(3): p. 201-5.
9. Karim-Kos, H.E., et al., *Recent trends of cancer in Europe: a combined approach of incidence, survival and mortality for 17 cancer sites since the 1990s.* Eur J Cancer, 2008. **44**(10): p. 1345-89.
10. Corvo, R., *Evidence-based radiation oncology in head and neck squamous cell carcinoma.* Radiother Oncol, 2007. **85**(1): p. 156-70.
11. Seiwert, T.Y. and E.E. Cohen, *State-of-the-art management of locally advanced head and neck cancer.* Br J Cancer, 2005. **92**(8): p. 1341-8.
12. Pignon, J.P., et al., *Chemotherapy added to locoregional treatment for head and neck squamous-cell carcinoma: three meta-analyses of updated individual data. MACH-NC Collaborative Group. Meta-Analysis of Chemotherapy on Head and Neck Cancer.* Lancet, 2000. **355**(9208): p. 949-55.
13. Bernier, J., et al., *Postoperative irradiation with or without concomitant chemotherapy for locally advanced head and neck cancer.* N Engl J Med, 2004. **350**(19): p. 1945-52.
14. Bourhis, J., et al., *Concomitant chemoradiotherapy versus acceleration of radiotherapy with or without concomitant chemotherapy in locally advanced head and neck carcinoma (GORTEC 99-02): an open-label phase 3 randomised trial.* Lancet Oncol, 2012. **13**(2): p. 145-53.

15. Bourhis, J., et al., *Hyperfractionated or accelerated radiotherapy in head and neck cancer: a meta-analysis.* The Lancet, 2006. **368**(9538): p. 843-854.
16. de Almeida Pdel, V., et al., *Saliva composition and functions: a comprehensive review.* J Contemp Dent Pract, 2008. **9**(3): p. 72-80.
17. Blanco, A.I., et al., *Dose-volume modeling of salivary function in patients with head-and-neck cancer receiving radiotherapy.* Int J Radiat Oncol Biol Phys, 2005. **62**(4): p. 1055-69.
18. Xing, L., et al., *Dosimetric effects of patient displacement and collimator and gantry angle misalignment on intensity modulated radiation therapy.* Radiother Oncol, 2000. **56**(1): p. 97-108.
19. Hurkmans, C.W., et al., *Set-up verification using portal imaging; review of current clinical practice.* Radiother Oncol, 2001. **58**(2): p. 105-20.
20. van Lin, E.N.J.T., et al., *Set-up improvement in head and neck radiotherapy using a 3D off-line EPID-based correction protocol and a customised head and neck support.* Radiotherapy and Oncology, 2003. **68**(2): p. 137-148.
21. Houghton, F., et al., *An assessment of action levels in imaging strategies in head and neck cancer using TomoTherapy. Are our margins adequate in the absence of image guidance?* Clin Oncol (R Coll Radiol), 2009. **21**(9): p. 720-7.
22. van Kranen, S., et al., *Setup uncertainties of anatomical sub-regions in head-and-neck cancer patients after offline CBCT guidance.* Int J Radiat Oncol Biol Phys, 2009. **73**(5): p. 1566-73.
23. Graff, P., et al., *The residual setup errors of different IGRT alignment procedures for head and neck IMRT and the resulting dosimetric impact.* Int J Radiat Oncol Biol Phys, 2013. **86**(1): p. 170-6.
24. de Boer, H.C., et al., *Electronic portal image assisted reduction of systematic set-up errors in head and neck irradiation.* Radiother Oncol, 2001. **61**(3): p. 299-308.
25. Han, C., et al., *Actual dose variation of parotid glands and spinal cord for nasopharyngeal cancer patients during radiotherapy.* Int J Radiat Oncol Biol Phys, 2008. **70**(4): p. 1256-62.
26. O'Daniel, J.C., et al., *Parotid gland dose in intensity-modulated radiotherapy for head and neck cancer: is what you plan what you get?* Int J Radiat Oncol Biol Phys, 2007. **69**(4): p. 1290-6.
27. Voordeckers, M., et al., *Parotid gland sparing with helical tomotherapy in head-and-neck cancer.* Int J Radiat Oncol Biol Phys, 2012. **84**(2): p. 443-8.
28. Nguyen, N.P., et al., *Feasibility of image-guided radiotherapy based on helical tomotherapy to reduce contralateral parotid dose in head and neck cancer.* BMC Cancer, 2012. **12**: p. 175.
29. Nguyen, N.P., et al., *Feasibility of Tomotherapy to spare the cochlea from excessive radiation in head and neck cancer.* Oral Oncol, 2011. **47**(5): p. 414-9.
30. Nguyen, N.P., et al., *Feasibility of Tomotherapy-based image-guided radiotherapy to reduce aspiration risk in patients with non-laryngeal and non-pharyngeal head and neck cancer.* PLoS One, 2013. **8**(3): p. e56290.
31. Pehlivan, B., et al., *Interfractional set-up errors evaluation by daily electronic portal imaging of IMRT in head and neck cancer patients.* Acta Oncol, 2009. **48**(3): p. 440-5.

32. Djordjevic, M., et al., *Assessment of residual setup errors for anatomical sub-structures in image-guided head-and-neck cancer radiotherapy.* Acta Oncol, 2014. **53**(5): p. 646-53.
33. Rudat, V., et al., *Impact of the frequency of online verifications on the patient set-up accuracy and set-up margins.* Radiat Oncol, 2011. **6**: p. 101.
34. Den, R.B., et al., *Daily image guidance with cone-beam computed tomography for head-and-neck cancer intensity-modulated radiotherapy: a prospective study.* Int J Radiat Oncol Biol Phys, 2010. **76**(5): p. 1353-9.
35. Zeidan, O.A., et al., *Evaluation of image-guidance protocols in the treatment of head and neck cancers.* Int J Radiat Oncol Biol Phys, 2007. **67**(3): p. 670-7.
36. *National Cancer Action Team: National radiotherapy implementation group report. Image guided radiotherapy (IGRT): Guidance for implementation and use.* 2012 [cited 2017 10-27-2017]; Available from: http://www.sor.org/sites/default/files/document-versions/National%20Radiotherapy%20Implementation%20Group%20Report%20IGRT%20Final.pdf.
37. van Kranen, S., et al., *Correction strategies to manage deformations in head-and-neck radiotherapy.* Radiother Oncol, 2010. **94**(2): p. 199-205.
38. Castadot, P., et al., *Assessment by a deformable registration method of the volumetric and positional changes of target volumes and organs at risk in pharyngo-laryngeal tumors treated with concomitant chemo-radiation.* Radiother Oncol, 2010. **95**(2): p. 209-17.
39. Barker, J.L., Jr., et al., *Quantification of volumetric and geometric changes occurring during fractionated radiotherapy for head-and-neck cancer using an integrated CT/linear accelerator system.* Int J Radiat Oncol Biol Phys, 2004. **59**(4): p. 960-70.
40. Ahn, P.H., et al., *Adaptive planning in intensity-modulated radiation therapy for head and neck cancers: single-institution experience and clinical implications.* Int J Radiat Oncol Biol Phys, 2011. **80**(3): p. 677-85.
41. Ajani, A.A., et al., *A quantitative assessment of volumetric and anatomic changes of the parotid gland during intensity-modulated radiotherapy for head and neck cancer using serial computed tomography.* Med Dosim, 2013. **38**(3): p. 238-42.
42. Beltran, M., et al., *Dose variations in tumor volumes and organs at risk during IMRT for head-and-neck cancer.* J Appl Clin Med Phys, 2012. **13**(6): p. 101-111.
43. Berwouts, D., et al., *Three-phase adaptive dose-painting-by-numbers for head-and-neck cancer: initial results of the phase I clinical trial.* Radiother Oncol, 2013. **107**(3): p. 310-6.
44. Bhide, S.A., et al., *Weekly volume and dosimetric changes during chemoradiotherapy with intensity-modulated radiation therapy for head and neck cancer: a prospective observational study.* Int J Radiat Oncol Biol Phys, 2010. **76**(5): p. 1360-8.
45. Broggi, S., et al., *A two-variable linear model of parotid shrinkage during IMRT for head and neck cancer.* Radiother Oncol, 2010. **94**(2): p. 206-12.
46. Capelle, L., et al., *Adaptive radiotherapy using helical tomotherapy for head and neck cancer in definitive and postoperative settings: initial results.* Clin Oncol (R Coll Radiol), 2012. **24**(3): p. 208-15.

47. Dewan, A., et al., *Impact of Adaptive Radiotherapy on Locally Advanced Head and Neck Cancer - A Dosimetric and Volumetric Study.* Asian Pac J Cancer Prev, 2016. **17**(3): p. 985-92.
48. Duprez, F., et al., *Adaptive dose painting by numbers for head-and-neck cancer.* Int J Radiat Oncol Biol Phys, 2011. **80**(4): p. 1045-55.
49. Hansen, E.K., et al., *Repeat CT imaging and replanning during the course of IMRT for head-and-neck cancer.* Int J Radiat Oncol Biol Phys, 2006. **64**(2): p. 355-62.
50. Height, R., et al., *The dosimetric consequences of anatomic changes in head and neck radiotherapy patients.* J Med Imaging Radiat Oncol, 2010. **54**(5): p. 497-504.
51. Ho, K.F., et al., *Monitoring dosimetric impact of weight loss with kilovoltage (kV) cone beam CT (CBCT) during parotid-sparing IMRT and concurrent chemotherapy.* Int J Radiat Oncol Biol Phys, 2012. **82**(3): p. e375-82.
52. Jensen, A.D., et al., *A clinical concept for interfractional adaptive radiation therapy in the treatment of head and neck cancer.* Int J Radiat Oncol Biol Phys, 2012. **82**(2): p. 590-6.
53. Loo, H., et al., *Tumour shrinkage and contour change during radiotherapy increase the dose to organs at risk but not the target volumes for head and neck cancer patients treated on the TomoTherapy HiArt system.* Clin Oncol (R Coll Radiol), 2011. **23**(1): p. 40-7.
54. Marzi, S., et al., *Anatomical and dose changes of gross tumour volume and parotid glands for head and neck cancer patients during intensity-modulated radiotherapy: effect on the probability of xerostomia incidence.* Clin Oncol (R Coll Radiol), 2012. **24**(3): p. e54-62.
55. Nishi, T., et al., *Volume and dosimetric changes and initial clinical experience of a two-step adaptive intensity modulated radiation therapy (IMRT) scheme for head and neck cancer.* Radiother Oncol, 2013. **106**(1): p. 85-9.
56. Reali, A., et al., *Volumetric and positional changes of planning target volumes and organs at risk using computed tomography imaging during intensity-modulated radiation therapy for head-neck cancer: an "old" adaptive radiation therapy approach.* Radiol Med, 2014. **119**(9): p. 714-20.
57. Robar, J.L., et al., *Spatial and dosimetric variability of organs at risk in head-and-neck intensity-modulated radiotherapy.* Int J Radiat Oncol Biol Phys, 2007. **68**(4): p. 1121-30.
58. Sanguineti, G., et al., *Pattern and predictors of volumetric change of parotid glands during intensity modulated radiotherapy.* British Journal Of Radiology, 2013(1748-880X (Electronic)).
59. Schwartz, D.L., et al., *Adaptive radiotherapy for head-and-neck cancer: initial clinical outcomes from a prospective trial.* Int J Radiat Oncol Biol Phys, 2012. **83**(3): p. 986-93.
60. Vasquez Osorio, E.M., et al., *Local anatomic changes in parotid and submandibular glands during radiotherapy for oropharynx cancer and correlation with dose, studied in detail with nonrigid registration.* Int J Radiat Oncol Biol Phys, 2008. **70**(3): p. 875-82.
61. Wu, Q., et al., *Adaptive replanning strategies accounting for shrinkage in head and neck IMRT.* Int J Radiat Oncol Biol Phys, 2009. **75**(3): p. 924-32.
62. Yip, C., et al., *Co-registration of cone beam CT and planning CT in head and neck IMRT dose estimation: a feasible adaptive radiotherapy strategy.* Br J Radiol, 2014. **87**(1034): p. 20130532.

63. Bando, R., et al., *Changes of tumor and normal structures of the neck during radiation therapy for head and neck cancer requires adaptive strategy.* J Med Invest, 2013. **60**(1-2): p. 46-51.
64. Belli, M.L., et al., *Characterization of volume and shape modifications of PET-positive nodes during Tomotherapy for head and neck cancer as assessed by MVCTs.* Radiother Oncol, 2015. **115**(1): p. 50-5.
65. Kataria, T., et al., *Clinical outcomes of adaptive radiotherapy in head and neck cancers.* Br J Radiol, 2016. **89**(1062): p. 20160085.
66. Olteanu, L.A., et al., *Comparative dosimetry of three-phase adaptive and non-adaptive dose-painting IMRT for head-and-neck cancer.* Radiother Oncol, 2014. **111**(3): p. 348-53.
67. Schwartz, D.L., et al., *Adaptive radiotherapy for head and neck cancer--dosimetric results from a prospective clinical trial.* Radiother Oncol, 2013. **106**(1): p. 80-4.
68. Simone, C.B., 2nd, et al., *Comparison of intensity-modulated radiotherapy, adaptive radiotherapy, proton radiotherapy, and adaptive proton radiotherapy for treatment of locally advanced head and neck cancer.* Radiother Oncol, 2011. **101**(3): p. 376-82.
69. Surucu, M., et al., *Decision Trees Predicting Tumor Shrinkage for Head and Neck Cancer: Implications for Adaptive Radiotherapy.* Technol Cancer Res Treat, 2016. **15**(1): p. 139-45.
70. Schwartz, D.L., *Current progress in adaptive radiation therapy for head and neck cancer.* Curr Oncol Rep, 2012. **14**(2): p. 139-47.
71. Schwartz, D.L. and L. Dong, *Adaptive radiation therapy for head and neck cancer-can an old goal evolve into a new standard?* J Oncol, 2011. **2011**.
72. Gregoire, V., et al., *Radiotherapy for head and neck tumours in 2012 and beyond: conformal, tailored, and adaptive?* Lancet Oncol, 2012. **13**(7): p. e292-300.
73. Lim-Reinders, S., et al., *Online Adaptive Radiation Therapy.* Int J Radiat Oncol Biol Phys, 2017. **99**(4): p. 994-1003.
74. Gobeli, M., et al., *[Benefit of a pretreatment planning library-based adaptive radiotherapy for cervix carcinoma?].* Cancer Radiother, 2015. **19**(6-7): p. 471-8.
75. Nassef, M., et al., *Quantification of dose uncertainties in cumulated dose estimation compared to planned dose in prostate IMRT.* Radiother Oncol, 2016. **119**(1): p. 129-36.
76. Zhao, L., et al., *The role of replanning in fractionated intensity modulated radiotherapy for nasopharyngeal carcinoma.* Radiother Oncol, 2011. **98**(1): p. 23-7.
77. Chen, C., et al., *Will weight loss cause significant dosimetric changes of target volumes and organs at risk in nasopharyngeal carcinoma treated with intensity-modulated radiation therapy?* Med Dosim, 2014. **39**(1): p. 34-7.
78. Hunter, K.U., et al., *Parotid glands dose-effect relationships based on their actually delivered doses: implications for adaptive replanning in radiation therapy of head-and-neck cancer.* Int J Radiat Oncol Biol Phys, 2013. **87**(4): p. 676-82.
79. Orban de Xivry, J., et al., *Evaluation of the radiobiological impact of anatomic modifications during radiation therapy for head and neck cancer: can we simply summate the dose?* Radiother Oncol, 2010. **96**(1): p. 131-8.

80. Yoo, J., S. Henderson, and C. Walker-Dilks, *Evidence-based guideline recommendations on the use of positron emission tomography imaging in head and neck cancer.* Clin Oncol (R Coll Radiol), 2013. **25**(4): p. e33-66.
81. Kyzas, P.A., et al., *18F-fluorodeoxyglucose positron emission tomography to evaluate cervical node metastases in patients with head and neck squamous cell carcinoma: a meta-analysis.* J Natl Cancer Inst, 2008. **100**(10): p. 712-20.
82. Lonneux, M., et al., *Positron emission tomography with [18F]fluorodeoxyglucose improves staging and patient management in patients with head and neck squamous cell carcinoma: a multicenter prospective study.* J Clin Oncol, 2010. **28**(7): p. 1190-5.
83. Zhu, L. and N. Wang, *18F-fluorodeoxyglucose positron emission tomography-computed tomography as a diagnostic tool in patients with cervical nodal metastases of unknown primary site: a meta-analysis.* Surg Oncol, 2013. **22**(3): p. 190-4.
84. Wong, W.L., et al., *18F-fluorodeoxyglucose positron emission tomography/computed tomography in the assessment of occult primary head and neck cancers--an audit and review of published studies.* Clin Oncol (R Coll Radiol), 2012. **24**(3): p. 190-5.
85. Rudmik, L., et al., *Clinical utility of PET/CT in the evaluation of head and neck squamous cell carcinoma with an unknown primary: a prospective clinical trial.* Head Neck, 2011. **33**(7): p. 935-40.
86. Nutting, C.M., et al., *Parotid-sparing intensity modulated versus conventional radiotherapy in head and neck cancer (PARSPORT): a phase 3 multicentre randomised controlled trial.* The Lancet Oncology, 2011. **12**(2): p. 127-136.
87. Wang, Z.H., et al., *Radiation-induced volume changes in parotid and submandibular glands in patients with head and neck cancer receiving postoperative radiotherapy: a longitudinal study.* Laryngoscope, 2009. **119**(10): p. 1966-74.
88. Castadot, P., et al., *Adaptive functional image-guided IMRT in pharyngo-laryngeal squamous cell carcinoma: is the gain in dose distribution worth the effort?* Radiother Oncol, 2011. **101**(3): p. 343-50.
89. Duma, M.N., et al., *Adaptive radiotherapy for soft tissue changes during helical tomotherapy for head and neck cancer.* Strahlenther Onkol, 2012. **188**(3): p. 243-7.
90. Castelli, J., et al., *Overview of the predictive value of quantitative 18 FDG PET in head and neck cancer treated with chemoradiotherapy.* Crit Rev Oncol Hematol, 2016. **108**: p. 40-51.
91. Brown, E., et al., *Predicting the need for adaptive radiotherapy in head and neck cancer.* Radiother Oncol, 2015. **116**(1): p. 57-63.
92. Castelli, J., et al., *A Nomogram to predict parotid gland overdose in head and neck IMRT.* Radiat Oncol, 2016. **11**: p. 79.
93. Mohan, R., et al., *Use of deformed intensity distributions for on-line modification of image-guided IMRT to account for interfractional anatomic changes.* Int J Radiat Oncol Biol Phys, 2005. **61**(4): p. 1258-66.
94. Ahunbay, E.E., et al., *An on-line replanning method for head and neck adaptive radiotherapy.* Med Phys, 2009. **36**(10): p. 4776-90.

95. Fotina, I., et al., *Feasibility of CBCT-based dose calculation: comparative analysis of HU adjustment techniques.* Radiother Oncol, 2012. **104**(2): p. 249-56.
96. Elstrom, U.V., et al., *Daily kV cone-beam CT and deformable image registration as a method for studying dosimetric consequences of anatomic changes in adaptive IMRT of head and neck cancer.* Acta Oncol, 2010. **49**(7): p. 1101-8.
97. Cheung, J., et al., *Dose recalculation and the Dose-Guided Radiation Therapy (DGRT) process using megavoltage cone-beam CT.* Int J Radiat Oncol Biol Phys, 2009. **74**(2): p. 583-92.
98. Dunlop, A., et al., *Comparison of CT number calibration techniques for CBCT-based dose calculation.* Strahlenther Onkol, 2015. **191**(12): p. 970-8.
99. Kurz, C., et al., *Comparing cone-beam CT intensity correction methods for dose recalculation in adaptive intensity-modulated photon and proton therapy for head and neck cancer.* Acta Oncol, 2015. **54**(9): p. 1651-7.
100. Hatton, J., B. McCurdy, and P.B. Greer, *Cone beam computerized tomography: the effect of calibration of the Hounsfield unit number to electron density on dose calculation accuracy for adaptive radiation therapy.* Phys Med Biol, 2009. **54**(15): p. N329-46.
101. Lagendijk, J.J., M. van Vulpen, and B.W. Raaymakers, *The development of the MRI linac system for online MRI-guided radiotherapy: a clinical update.* J Intern Med, 2016. **280**(2): p. 203-8.
102. Graves, Y.J., et al., *A deformable head and neck phantom with in-vivo dosimetry for adaptive radiotherapy quality assurance.* Med Phys, 2015. **42**(4): p. 1490-7.
103. Kirby, N., C. Chuang, and J. Pouliot, *A two-dimensional deformable phantom for quantitatively verifying deformation algorithms.* Med Phys, 2011. **38**(8): p. 4583-6.
104. Garibaldi, C., et al., *Interim 18F-FDG PET/CT During Chemoradiation Therapy in the Management of Head and Neck Cancer Patients: A Systematic Review.* Int J Radiat Oncol Biol Phys, 2017. **98**(3): p. 555-573.
105. Berwouts, D., et al., *Biological 18[F]-FDG-PET image-guided dose painting by numbers for painful uncomplicated bone metastases: A 3-arm randomized phase II trial.* Radiother Oncol, 2015. **115**(2): p. 272-8.
106. Duprez, F., et al., *High-dose reirradiation with intensity-modulated radiotherapy for recurrent head-and-neck cancer: disease control, survival and toxicity.* Radiother Oncol, 2014. **111**(3): p. 388-92.
107. Chajon, E., et al., *Salivary gland-sparing other than parotid-sparing in definitive head-and-neck intensity-modulated radiotherapy does not seem to jeopardize local control.* Radiat Oncol, 2013. **8**: p. 132.
108. Mohamed, A.S.R., et al., *Patterns-of-failure guided biological target volume definition for head and neck cancer patients: FDG-PET and dosimetric analysis of dose escalation candidate subregions.* Radiother Oncol, 2017. **124**(2): p. 248-255.

ANNEXE 1

Evaluation of deformable image registration methods for dose monitoring in head and neck radiotherapy

Biomed Research International 2015

Hindawi Publishing Corporation
BioMed Research International
Volume 2015, Article ID 726268, 16 pages
http://dx.doi.org/10.1155/2015/726268

Hindawi

Research Article

Evaluation of Deformable Image Registration Methods for Dose Monitoring in Head and Neck Radiotherapy

Bastien Rigaud,[1,2] Antoine Simon,[1,2] Joël Castelli,[1,2,3] Maxime Gobeli,[3] Juan-David Ospina Arango,[1,2] Guillaume Cazoulat,[1,2] Olivier Henry,[3] Pascal Haigron,[1,2] and Renaud De Crevoisier[1,2,3]

[1] *Université de Rennes 1, LTSI, Campus de Beaulieu, 35000 Rennes, France*
[2] *INSERM, U1099, Campus de Beaulieu, 35000 Rennes, France*
[3] *Centre Eugene Marquis, Radiotherapy Department, 35000 Rennes, France*

ANNEXE 2

Optimal adaptive IMRT to spare the parotid glands in oropharyngeal cancer

Radiother Oncol. 2016 Jun Jul;120(1):41-7

Radiotherapy and Oncology 120 (2016) 41–47

Contents lists available at ScienceDirect

Radiotherapy and Oncology

journal homepage: www.thegreenjournal.com

Head and neck radiotherapy

Optimal adaptive IMRT strategy to spare the parotid glands in oropharyngeal cancer

Pengcheng Zhang [a,b,c,d], Antoine Simon [b,c,d], Bastien Rigaud [b,c,*], Joël Castelli [b,c,e], Juan David Ospina Arango [b,c], Mohamed Nassef [b,c], Olivier Henry [e], Jian Zhu [f,g], Pascal Haigron [b,c,d], Baosheng Li [f,g], Huazhong Shu [d,g], Renaud De Crevoisier [b,c,d,e,*]

ANNEXE 3

MRI-based radiotherapy planning

Cancer Radiother. 2017 Jul 6

Disponible en ligne sur
ScienceDirect
www.sciencedirect.com

Elsevier Masson France
EM|consulte
www.em-consulte.com

Mise au point

Planification à partir d'imagerie par résonance magnétique en radiothérapie

MRI-based radiotherapy planning

A. Largent[a,d], J.-C. Nunes[a,d], C. Lafond[b], N. Périchon[b], J. Castelli[a,b,d], Y. Rolland[a,c], O. Acosta[a,d], R. de Crevoisier[a,*,b,d]

Résumé

Objectifs : Notre travail avait pour objectifs (i) d'évaluer le bénéfice dosimétrique et de prédire le bénéfice clinique d'une radiothérapie adaptative pour des cancers des voies aéro-digestives supérieures, à la fois en termes de toxicité et de contrôle local, (ii) d'identifier les patients bons candidats à une stratégie de radiothérapie adaptative, et (iii) d'identifier le meilleur schéma de radiothérapie adaptative pour épargner les parotides

Matériels et méthodes : Le bénéfice dosimétrique a été évalué en utilisant les données de patients inclus dans une étude de phase III évaluant le bénéfice clinique d'une radiothérapie adaptative. La dose cumulée sans et avec radiothérapie adaptative a été estimée par des méthodes de recalage élastique. Une évaluation des différents algorithmes de recalage a été faite à la fois en termes de précision spatiale et d'impact sur la dose estimée. Des modèles de prédiction du risque de surdosage ont été développés en utilisant des modèles linéaires généralisées mixtes et une validation croisée par *leave-one-out*. L'évaluation de différents schémas de radiothérapie adaptative (en termes de fréquence et de nombre) a été réalisée en se basant sur l'épargne des parotides. La valeur prédictive de paramètres quantitatifs issus de la TEP a été évaluée à travers une revue systématique de la littérature. La valeur prédictive de paramètres intensité issue de la TEP a été analysée dans 2 cohortes indépendantes.

Résultats : Nos travaux ont confirmé qu'en l'absence de radiothérapie adaptative pour des cancers des VADS, il existe un risque de surdosage des parotides de plus de 2 Gy pour les 2/3 des patients. Il s'y associe un risque de sous dosage de la tumeur de plus de 1 Gy pour 50 % des patients. Une radiothérapie adaptative permet de corriger à la fois le surdosage des parotides (bénéfice clinique estimée de 10 % de diminution du risque de xérostomie) et le sous dosage de la tumeur. Basés sur des paramètres issus de la planification et de la première semaine de traitement, des modèles de prédiction du risque de sur dosage des parotides ou de sous dosage de la tumeur ont été développés. Les paramètres TEP prédictifs du risque de récidive ont été identifiés. Un nomogramme a pu être développé et validé dans une 2nd cohorte de patients.

Conclusion : Nos travaux confirment le bénéfice d'une radiothérapie adaptative pour épargner les parotides et maintenir la couverture tumorale. Ce bénéfice dosimétrique devrait permettre une diminution de la toxicité et une amélioration du contrôle local. Des paramètres anatomiques et dosimétriques simples permettent l'identification des patients à risque de surdosage des parotides ou de sous dosage de la tumeur. L'utilisation de la TEP permet d'identifier précocement les patients à haut risque de récidive, candidats potentiels à une intensification thérapeutique. Ces résultats justifient la poursuite des travaux sur une cohorte de patients plus importante, idéalement dans le cadre d'études cliniques de phase III.